Summer 2010

Recombinant Factors for Hemostasis

Jennifer Calcaterra
University of Nebraska at Lincoln, jenncalc2@aol.com

Recombinant Factors for Hemostasis

by

Jennifer Calcaterra

A DISSERTATION

Presented to the Faculty of

The Graduate College at the University of Nebraska

In Partial Fulfillment of Requirements

For the Degree of Doctor of Philosophy

Major: Interdepartmental Area of Engineering

(Chemical & Biomolecular Engineering)

Under the Supervision of Professor William H. Velander

Lincoln, Nebraska

August, 2010

Recombinant Factors for Hemostasis

Jennifer Calcaterra, Ph.D.

University of Nebraska, 2010

Adviser: William H. Velander

Trauma deaths are a result of hemorrhage in 37% of civilians and 47% military personnel and are the primary cause of death for individuals under 44 years of age. Current techniques used to treat hemorrhage are inadequate for severe bleeding. Preliminary research indicates that fibrin sealants (FS) alone or in combination with a dressing may be more effective; however, it has not been economically feasible for widespread use because of prohibitive costs related to procuring the proteins. To meet future demands for hemostatic therapies, FS will likely include recombinant human fibrinogen (rFI) and recombinant human Factor XIII (rFXIII). The underlying hypothesis of the research presented in this dissertation is that a liquid fibrin sealant (LFS) composed of recombinant FI, FXIII and FIIa in optimized proportions can assist hemostasis in the presence and absence of a bioresorbable bandage while using considerably fewer biologics than commercial products currently available. This dissertation characterized rFI produced in the milk of transgenic cows, plasma-derived thrombin (pdFIIa) activated by sodium citrate and rFXIIIa expressed in genetically engineered *Pichia pastoris* with respect to their capacity to serve as components in a LFS. The ratios of these factors were optimized to yield a LFS with a rapid clot formation rate and high viscoelastic strength. This optimized LFS was preliminarily tested *ex vivo* and *in vivo.* The clotting kinetics and viscoelastic strength of our optimized LFS was equivalent to those of a commercially available LFS; however, it uses approximately 75% less fibrinogen and thrombin. Our optimal LFS successfully achieved hemostasis in a significant number of the wounds that included extensive tissue and vascular damage. LFS applied without the assistance of a dressing was able

to stop bleeding of oozing wounds or those with small vessels; however, a scaffold was needed when wounds contained large vasculature.

Dedicated to my parents

Kathryn and Robert Calcaterra

Author's Acknowledgements

I want to thank Dr. Velander for providing me with the opportunity to participate in his groundbreaking research and for his mentorship, guidance and moral support. I appreciate the generous advice of Dr. Anuradha Subramanian. I would also like to thank Mostafa Fatemi for introducing me to the analytical techniques used in blood chemistry. Leonard Akert's assistance was crucial in overcoming numerous technical hurdles. I will be forever grateful to my family for their support, advice, encouragement, inspiration and proofreading.

Table of Contents

	Page
List of Tables	ix
List of Figures	x
Chapter 1. Introduction	1
Hemostasis	2
Fibrinogen	4
Hemorrhage treatment	8
Fibrin sealants	9
Recobinant alternatives for fibrin sealants	10
Hemophilia A	11
Dissertation objectives	12
References	14
Chapter 2. Sequence of Activation of Prothrombin by Sodium Citrate	20
Abstract	21
Introduction	23
Materials and Methods	29
Results	36
rFXIIIa characterization	36
Prothrombin activation by ecarin, rFIIa, FXa and sodium citrate	36
N-terminal sequencing of activated samples	44
Thrombin activity by chromogenic assay	46
Thrombin activity by SDS-PAGE	47
Thrombin activity by thromboelastography	48
Discussion	49
Acknowledgements	57
References	58
Chapter 3. Characterization of Recombinant Factor XIII Expressed in *Pichia pastoris.*	61
Abstract	62
Introduction	63
Materials and Methods	69
Results	78
rFI and pdFIIa characterization	78
Expression and purification of rFXIII	78
Comparison of pdFXIII and rFXIII by SDS-PAGE and Western blot	79
Molecular weight estimates of expressed protein	80
Aggregation/molecular weight analysis (SDS-PAGE, DLS, AUC, SEC)	81
Activation and inactivation of rFXIII by thrombin	83
Chromogenic activity assay	85
γ-γ crosslinking of fibrin(ogen) by FXIIIa	86
Clot formation by thromboelastography	88
Discussion	89
Acknowledgements	93
References	95
Chapter 4. Optimization of a Liquid Fibrin Sealant to Achieve its Maximal Strength and Activation Speed	103
Abstract	104
Introduction	106
Materials and Methods	110
Results	116
rFXIIIa and pdFIIa characterization	116
γ-γ crosslinking of FI by FXIIIa	116
Thromboelastography analysis of fibrin clot formation	117

Clot lysis by thromboelastography 125
Discussion 126
Acknowledgements 130
References 131
Chapter 5. *Ex vivo* Evaluation of the Liquid Fibrin Sealant Components 135
Abstract 136
Introduction 138
Materials and Methods 139
Results 143
rFXIIIa and pdFIIa characterization 143
Donor data 144
TEG analysis of haemodilution 144
TEG analysis of protein doping into NHB, PRP and PPP 149
TEG analysis of time to clot initiation 150
TEG analysis of coagulation time 153
TEG analysis of maximal clot strength 155
TEG analysis of lysis 158
Discussion 160
Acknowledgements 164
References 165
Chapter 6. Preliminary *in vivo* Testing of the Optimized Liquid Fibrin Sealant 167
Abstract 168
Introduction 169
Materials and Methods 172
Results 184
Evaluation of swine clotting factors 184
LFS on hepatic wedge resections 186
rLFS on hepatic stelate laceration 189
rLFS dressing on femoral arteriotomy model 190
rLFS dressing on hepatic resections 192
Discussion 195
Acknowledgements 200
References 202
Chapter 7. Biologically Active Single Chain Recombinant Human FVIII:von Willebrand Factor Complexes Made Abundantly in Transgenic Milk 205
Abstract 206
Introduction 207
Materials and Methods 209
Results 214
Identification and expansion of transgenic lineages 214
Coexpression of 226/N6-tg, vWF-tg and AAT-tg in trigenic mouse milk 217
Presence of FVIII-vWF complexes in trigenic mouse milk 219
Coexpression of AAT 221
Quantitative analysis of rFVIII biological activity 222
In vivo tail clip assay in the hemophilia A mouse 224
Discussion 226
Authorship 232
Acknowledgements 232
References 233
Chapter 8. Future Works 236
Citrate activation of prothrombin 237
Recombinant factor XIIIa 238
Optimization of a liquid fibrin sealant 239
In vivo testing of rLFS 242
References 244

List of Tables

	Page
Table 2.1. N-terminal amino acid sequences of prothrombin and its fragments following activation by FXa (2%) and sodium citrate (35%). ……..	45
Table 2.2. Specific activity of activated prothrombin by chromogenic assay ……..	47
Table 3.1. Structure, function and genetic differences between the A- and B-chains of FXIII. ……..	63
Table 3.2. FXIII substrates, crosslinking sites, crosslinking molecules and function. ……..	67
Table 3.3. Molecular weight estimations of expressed rFXIII and rFXIIIa. ……..	81
Table 3.4. Molecular weight estimates of rFXIII in solution by multiple techniques. ……..	82
Table 3.5. N-terminal amino acid sequences of purified FXIII expressed by yeast. ……..	85
Table 4.1. Effects of plasmin on clotting parameters of Tisseel®, pdFI- and rFI-based clots by TEG. ……..	126
Table 5.1. p values from t test comparisons of normal human blood (NHB), platelet rich plasma (PRP) and platelet poor plasma (PPP) on time to clot initiation (R), time to reach clot firmness of 20 mm (K) and maximal clot strength (MA). ……..	149
Table 5.2. p values from ANOVA analyses on time to clot initiation (R), time to reach clot firmness of 20 mm (K) and maximal clot strength (MA) due to treatement with biologics. ……..	150
Table 5.3. p values from t test analyses on time to clot initiation (R) comparing diluted normal human blood (NHB), platelet rich plasma (PRP) and platelet poor plasma (PPP) to samples containing biologics. ……..	150
Table 5.4. p values from t test analyses on coagulation time (K) comparing diluted normal human blood (NHB), platelet rich plasma (PRP) and platelet poor plasma (PPP) to samples containing biologics. ……..	153
Table 5.5. p values from t test analyses on maximal clot strength (MA) comparing diluted normal human blood (NHB), platelet rich plasma (PRP) and platelet poor plasma (PPP) to samples containing biologics. ……..	156
Table 6.1. Average time to clot initiation (R), coagulation time (K) and maximum amplitude of pre-surgical and post-surgical blood samples and the subsequent percent change. ……..	184
Table 6.2. Average hemostasis scores for excision depths. ……..	188
Table 6.3. Estimated areas of the wound created by the wedge excisions. ……..	188
Table 6.3. Average hemostasis scores for number X-shaped wounds. ……..	190
Table 6.4. Hemostatic results of PLA treated with Ringer's or various components of LFS applied to femoral arteriotomies. ……..	192
Table 6.5. Hemostatic results of PLA treated with LFS applied to hepatic resections. ……..	193
Table 7.1. A comparison of expression levels and activity of WT-FVIII made in plasma, cell culture and milk of transgenic animals. ……..	208
Table 7.2. ELISA, 2-stage activity assay, and specific activity data on mono-, bi- and trigenic mice. ……..	219
Table 7.3. Potential volumes of source materials needed for current global FVIII consumption. ……..	231

List of Figures

Page

Figure 1.1. Schematic of the cascade of protein activation reactions that occur to create a fibrin clot. ……. 3

Figure 1.2. Schematic of the fibrinogen and fibrin molecules and protofibril formation. ……. 5

Figure 1.3. Schematic of aggregation and γ-γ crosslinking of fibrin. ……. 6

Figure 1.4. Biochemistry of ε-(γ-glutamyl)lysine crosslinking of fibrin molecules by FXIIIa. ……. 7

Figure 2.1. Schematic of the amino acid sequence of prepro-prothrombin. ……. 25

Figure 2.2. Activation of prothrombin. ……. 26

Figure 2.3. Autolytic inactivation of thrombin. ……. 29

Figure 2.4. Evaluation of the activation of prothrombin without added activators in the presence and absence of FIIa and FXa inhibitors by nonreduced SDS-PAGE. ……. 37

Figure 2.5. Evaluation of prothrombin activation over 28 days after being treated with FIIa and FXa inhibitors by nonreduced SDS-PAGE. ……. 37

Figure 2.6. Evaluation of the activation of prothrombin by rFIIa in the presence and absence of FXa inhibitor by nonreduced SDS-PAGE. ……. 38

Figure 2.7. Evaluation of the activation of prothrombin by FX and FXa by nonreduced SDS-PAGE ……. 39

Figure 2.8. Evaluation of the activation of prothrombin by ecarin by nonreduced SDS-PAGE. ……. 40

Figure 2.9. Evaluation of the activation of prothrombin by 25% and 35% sodium citrate by nonreduced SDS-PAGE. ……. 41

Figure 2.10. Evaluation of the activation of prothrombin by 35% sodium citrate in the presence and absence of FXa inhibitor by nonreduced SDS-PAGE. ……. 42

Figure 2.11. Evaluation of the activation of prothrombin by 35% sodium citrate in combination with FXa or FIIa in the presence of FXa inhibitor by nonreduced SDS-PAGE. ……. 43

Figure 2.12. Evaluation of the activation of prothrombin by FIIa and sodium citrate by nonreduced SDS-PAGE. ……. 44

Figure 2.13. Identification of the fragments of prothrombin activated by 35% sodium citrate suggested by N-terminal sequencing. ……. 46

Figure 2.14. Fibrinopeptide release and Factor XIIIa molecular weight shift by prothrombin samples activated by rFIIa, FXa, ecarin and 35% sodium citrate. ……. 48

Figure 2.15: Comparison of clotting activity of rFIIa and citrate activated pdFIIa clotting analysis by thromboelastography. ……. 49

Figure 2.16. Suggested primary pathway of activation of prothrombin by sodium citrate. ……. 55

Figure 3.1. Schematic representation of thrombin activation of plasma FXIII. ……. 64

Figure 3.2. Biochemistry of ε-(γ-glutamyl)lysine crosslinking of fibrin molecules by FXIIIa. ……. 66

Figure 3.3. Schematic of vector pPICZA-FXIIIA. ……. 71

Figure 3.4. Purification of rFXIII as analyzed by reducing SDS-PAGE and immunoblot. ……. 79

Figure 3.5. Plasma-derived and recombinant Factor XIII by SDS-PAGE. ……. 80

Figure 3.6. Overlaid tracing of proteins analyzed by size exclusion chromatography and individual tracing of rFXIII. ……. 83

Figure 3.7. Recombinant Factor XIII cleavage by thrombin. ……. 84

Figure 3.8. Linear model of the expected and actual molecules expressed by yeast and the subsequent degradation products. ……. 85

Figure 3.9. Ability of rFXIIIa to crosslink fibrin and fibrinogen γ-chain by reducing SDS-PAGE. ……. 87

Figure 3.10. Ability of rFXIIIa to covalently crosslink A2AP to rFI by SDS-PAGE and immunoblot. ……. 88
Figure 3.11. Analysis of the effect of rFXIIIa on clot strength by thromboelastography. ……. 89
Figure 4.1. Uses for fibrin sealant. ……..……. 108
Figure 4.2. Formation of fibrin γ-chain crosslinks as analyzed by reducing SDS-PAGE. ……. 117
Figure 4.3. Effect of increasing rFI concentration on clot parameters by thromboelastography. ……. 118
Figure 4.4. FIIa dependent maximal clot strength (MA) and clot initiation time (R) with constant FI and rFXIIIa. ……. 119
Figure 4.5. rFXIIIa dependent maximal clot strength (MA) and clot initiation time (R) with constant FI and pdFIIa concentrations. ……. 120
Figure 4.6. $CaCl_2$ dependent maximal clot strength (MA) with constant rFI, rFXIIIa and pdFIIa concentrations. ……. 121
Figure 4.7. Effect of increasing rFI while maintaining stoichiometric molar ratios of rFXIIIa/rFI and pdFIIa/rFI of 0.16 and 0.18, respectively. ……. 122
Figure 4.8. Effect of increasing rFXIIIa concentration. ……..……. 123
Figure 4.9. Thromboelastograhic properties of NHB and tri-component mixtures of rFI, pdFIIa and rFXIIIa. ……. 124
Figure 4.10. Thromboelastograhic properties of the optimized tri-component rLFS and a pdLFS (Tisseel®). ……. 125
Figure 5.1. Percent change in time to clot initiation (R), clot coagulation time (K) and maximal clot strength (MA) when normal human blood (NHB) is diluted 30% with Ringer's solution. ……. 146
Figure 5.2. Percent change in time to clot initiation (R), clot coagulation time (K) and maximal clot strength (MA) when platelet rich plasma (PRP) is diluted 30% with Ringer's solution. ……. 147
Figure 5.3. Percent change in time to clot initiation (R), clot coagulation time (K) and maximal clot strength (MA) when platelet poor plasma (PPP) is diluted 30% with Ringer's solution. ……. 148
Figure 5.4. Percent change in time to clot initiation (R) with the addition of recombinant fibrinogen (rFI), plasma-derived thrombin (pdFIIa) and/or recombinant FXIIIa (rFXIIIa) to normal human blood (NHB), platelet rich plasma (PRP) and platelet poor plasma (PPP). ……. 152
Figure 5.5. Percent change in coagulation time (K) with the addition of recombinant fibrinogen (rFI), plasma-derived thrombin (pdFIIa) and/or recombinant FXIIIa (rFXIIIa) to normal human blood (NHB), platelet rich plasma (PRP) and platelet poor plasma (PPP). ……. 155
Figure 5.6. Percent change in maximal clot strength (MA) with the addition of recombinant fibrinogen (rFI), plasma-derived thrombin (pdFIIa) and/or recombinant FXIIIa (rFXIIIa) to normal human blood (NHB), platelet rich plasma (PRP) and platelet poor plasma (PPP). ……. 158
Figure 5.7. Percent lysis 60 minutes after reaching maximum clot strength of undiluted or diluted normal human blood (NHB), platelet rich plasma (PRP) and platelet poor plasma (PPP) alone or with the addition of recombinant fibrinogen (rFI), plasma-derived thrombin (pdFIIa) and/or recombinant FXIIIa (rFXIIIa). ……. 160
Figure 6.1. Device and method for perforating the PLA dressing. ……..……. 175
Figure 6.2. Plates and method employed to corrugate PLA. ……. 176
Figure 6.3. Final PLA bandage format. ……..……. 176
Figure 6.4. LFS application device used during *in vivo* experiments. ……..……. 177
Figure 6.5. Wedges marked on a liver lobe by a cauterization tool. ……..……. 180
Figure 6.6. Device used to create stelate liver laceration. ……. 182
Figure 6.7. Representative TEG tracings of blood samples from a pig before, ……. 185

during and at the conclusion of the surgery.
Figure 6.8. Wedge resection treated with rLFS applied by spray-device. ……. 186
Figure 6.9. Wedge resection treated with rLFS applied by double barrel syringe. ……. 186
Figure 6.10. Frequency of hemostasis scores at each excision depth. ……. 187
Figure 6.11. Sizeable vessel transected in larger wedge resections. ……..……. 189
Figure 6.12. Grade 5 stelate liver injury treated with LFS. ……..……. 190
Figure 6.13. 4 mm arteriotomy treated with bandages soaked in LFS. ……. 191
Figure 6.14. Treatment of large hepatic resection with gauze coated with rLFS. ……. 193
Figure 6.15. Treatment of a large hepatic resection with nanofiberous PLA coated with rLFS. ……. 194
Figure 7.1. Transgene construction schematics and Southern analysis for 226/N6, vWF, and AAT. ……. 216
Figure 7.2. 226/N6-tg is complexed with vWF-tg in transgenic mouse milk. Assessment of vWF binding by analyzing (A) reduced anti-FVIII, (B) reduced anti-vWF, (C) non-reduced anti-FVIII, and (D) non-reduced anti-vWF Western Blots. ……. 218
Figure 7.3. AAT is coexpressed in transgenic mouse milk. ……. 221
Figure 7.4. 226/N6-tg binds pd-vWF similarly to rFVIII. ……..……. 224
Figure 7.5. Hemostatic efficacy *in* vivo of 226/N6-tg and 226/N6–CHO within the hemophilia A mouse model. ……. 226

Chapter 1

Introduction

Hemostasis

Hemostasis is a delicate balance between pro- and anticoagulant forces which require numerous proteins in the proper concentrations to activate, function and inactivate correctly to stop bleeding after tissue injury and avert inappropriate clotting events.[1, 2] Hemostasis has three phases: the primary and secondary phases occur quickly to stop bleeding while the final stage breaks down the clot once the blood vessel is repaired. Primary hemostasis is instigated by tissue injury which exposes collagen fibers from the injured vascular endothelium to blood. When exposed to the collagen, platelets are activated initiating the release of numerous signaling molecules and coagulation factors which results in their adherence to each other and the vessel wall. Once activated, negatively charged phospholipids are transported to the external membrane of platelets to serve as a catalytic surface for binding of coagulation factors.[1] During this initial phase, the platelet plug minimizes blood loss[1, 3] but only a miniscule amount of prothrombin (1 to 5 nM) is activated to thrombin (FIIa) by activated Factor X (FXa) attached to the phospholipid membrane.[4, 5] While the enzyme FXa can convert prothrombin, it has insufficient catalytic efficiency to activate the necessary proteins to stop bleeding.[6]

Secondary hemostasis is initiated by the exposure of tissue factor (TF) to blood resulting in a cascade of activation of numerous serine proteases and several nonenzymatic cofactors (Figure 1.1).

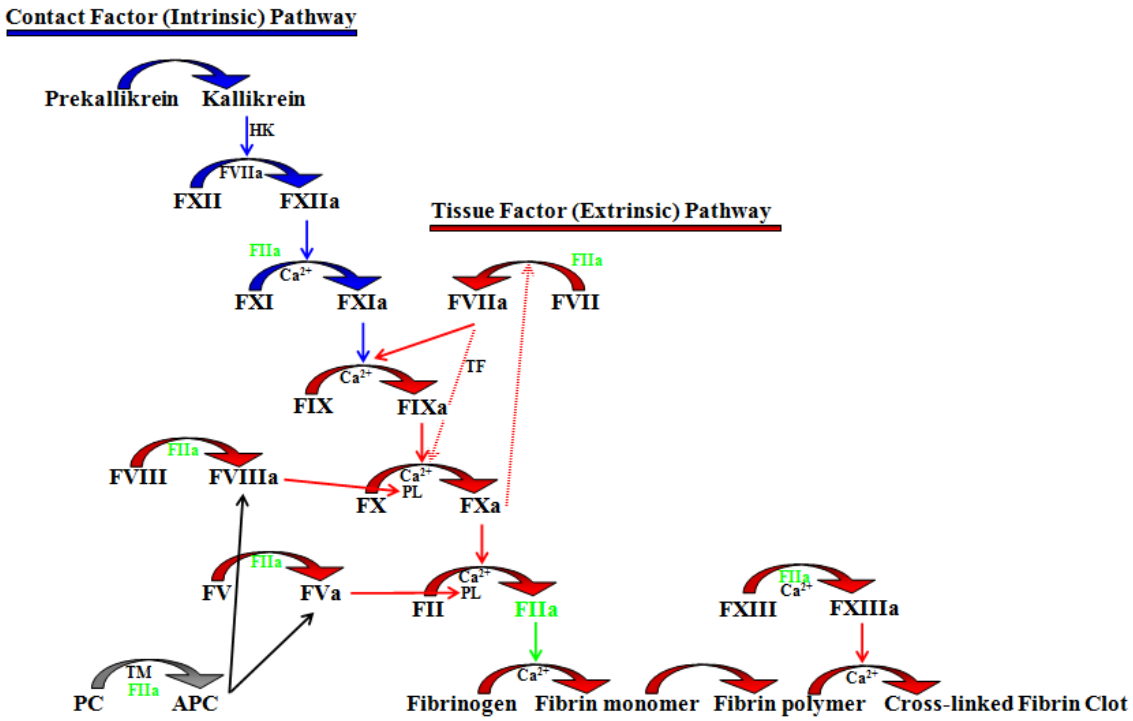

Figure 1.1. Schematic of the cascade of protein activation reactions that occur to create a fibrin clot. Red arrows indicate steps within the procoagulation pathway. Blue arrows are steps initiated within the intrinsic pathway. Black arrows indicate inactivation of FVIIIa and FVa by APC (one of the components of the anticoagulant pathway) resulting in the down-regulation of thrombin.

TF activates Factor VII (FVII) which activates Factor IX (FIX). FIX can also be activated without tissue injury by activated Factor XI (FXIa) through the intrinsic coagulation pathway. In both pathways, activated Factor IX (FIXa) binds with activated Factor VIII (FVIIIa), a nonenzymatic cofactor, and the negatively charged phospholipid surface of platelets to form the tenase complex which activates Factor X (FX) to FXa. FXa and thrombin proteolyze Factor V (FV) to activated Factor V (FVa), another nonenzymatic cofactor that serves as a catalyst for FXa's generation of thrombin. Finally, thrombin cleaves fibrinogen into soluble fibrin fibers which polymerize into a fibrin clot[1, 3] which is subsequently cross-linked and made insoluble by thrombin activated Factor XIII (FXIIIa).[3, 7, 8] This fibrin clot is critical in the cessation of bleeding.

Fibrinogen

Fibrinogen (FI) is the penultimate protein in hemostasis. In addition to assisting in the initial platelet aggregation following vascular injury,[9, 10] during the last step of the clotting cascade FI is activated to fibrin which aggregates and is crosslinked to form the fibrin clot. In clot form, the fibrin stops bleeding and provides a scaffold for cellular migration and proliferation required for tissue regeneration.[11-14]

FI, a 340,000 Da (450 Å) protein, is synthesized by hepatocytes and circulates in plasma at 2-4 mg/ml (6-12 μM).[5, 15] FI consists of two Aα (66 kDa), two Bβ (52 kDa) and two γ-chains (46.5 kDa)[16] held together by 29 disulfide bonds.[5, 15] Each chain is synthesized by hepatocytes and each undergoes posttranslational modifications: Aα-chain phosphorylation[17] (Ser3 and Ser345),[18] Bβ- and γ-chain N-glycosylation[19] and γ'-chain tyrosine sulfation.[20] Following modification, hexameric FI is assembled in the endoplasmic reticulum (ER)[21] creating a trinodal structure[22] with a central "E" nodule, containing the N-terminals of the six chains, and two "D" nodules linked by α-helical, coiled-coil segments (Figure 1.2A).[22]

FI is activated into fibrin monomer by thrombin which binds to the E nodule and cleaves the 16 residue N-terminal peptide of the Aα chain (fibrinopeptide A, FpA) at Arg16-Gly17 and then the 14 residue N-terminal peptide of the Bβ chain (fibrinopeptide B, FpB) at Arg14-Gly15 (Figure 1.2B). The release of FpA exposes the new N-terminal sequence of the α-chain ("A" site) which is involved in noncovalent interactions with the C-terminal γ-chain in the D nodule ("a" pocket, blue triangles in Figure 1.2) of an adjacent FI molecule resulting in protofibril formation.[5, 23] Subsequent release of FpB yields a similar interaction between the newly formed N-terminal of the β-chain ("B"

site) with the D nodule β chain ("b" pocket, pink triangles in Figure 1.2) of another molecule.[5, 24] Activated fibrin molecules combine to make double-stranded protofibrils (Figure 1.2C). These double-stranded protofibrils subsequently aggregate laterally producing a soluble fibrin clot composed of thick fibers (Figure 1.3).[25]

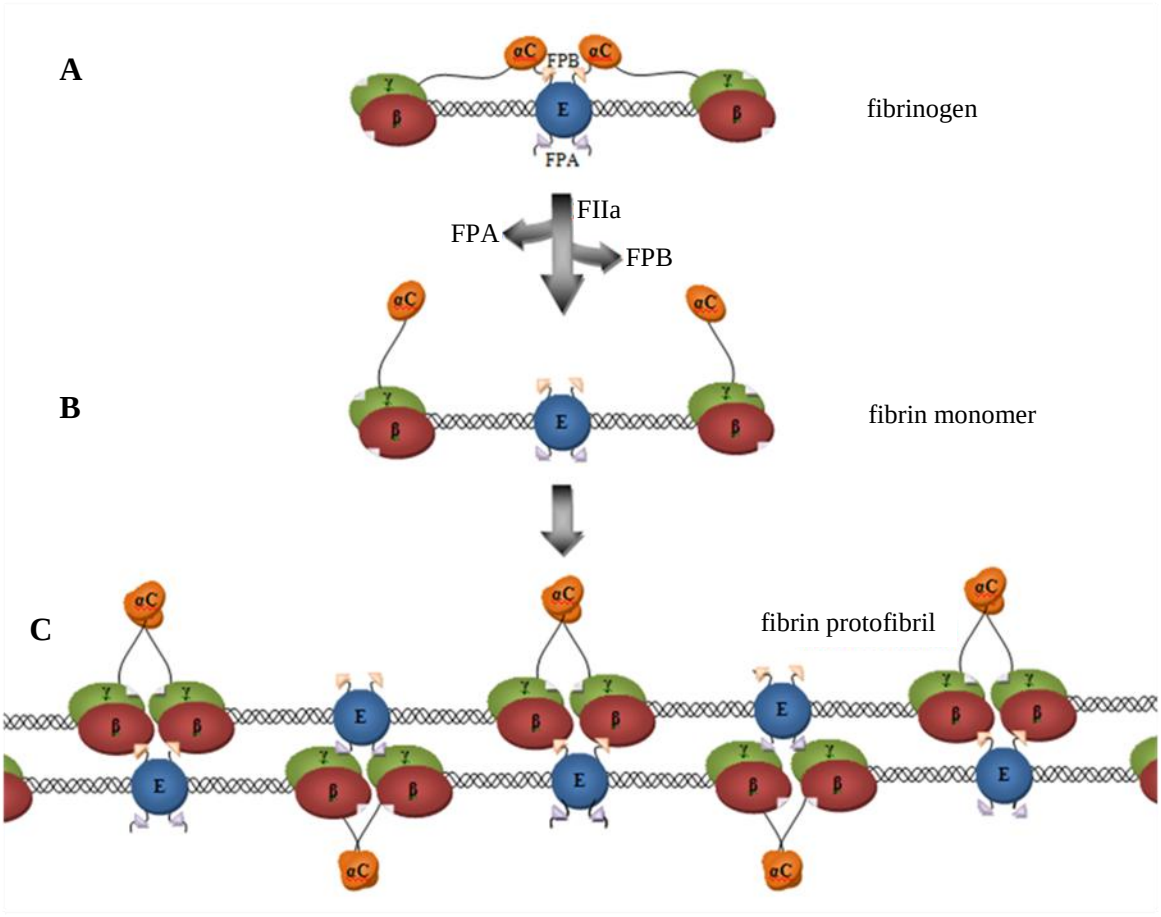

Figure 1.2. Schematic of the fibrinogen and fibrin molecules and protofibril formation.[22, 25, 26] Fibrinogen consists of an E nodule (blue circles) and two D nodules (green and red ovals) connected by coiled-coils. The αC-domains (orange ovals) extend out from the D nodule and curl around and bind to the E nodule in fibrinogen (A). When activated by thrombin, fibrin monomer is formed when fibrinopeptide A and B are released resulting in the freeing of the αC-domains (B). These activated fibrin monomers aggregate into protofibrils (C).

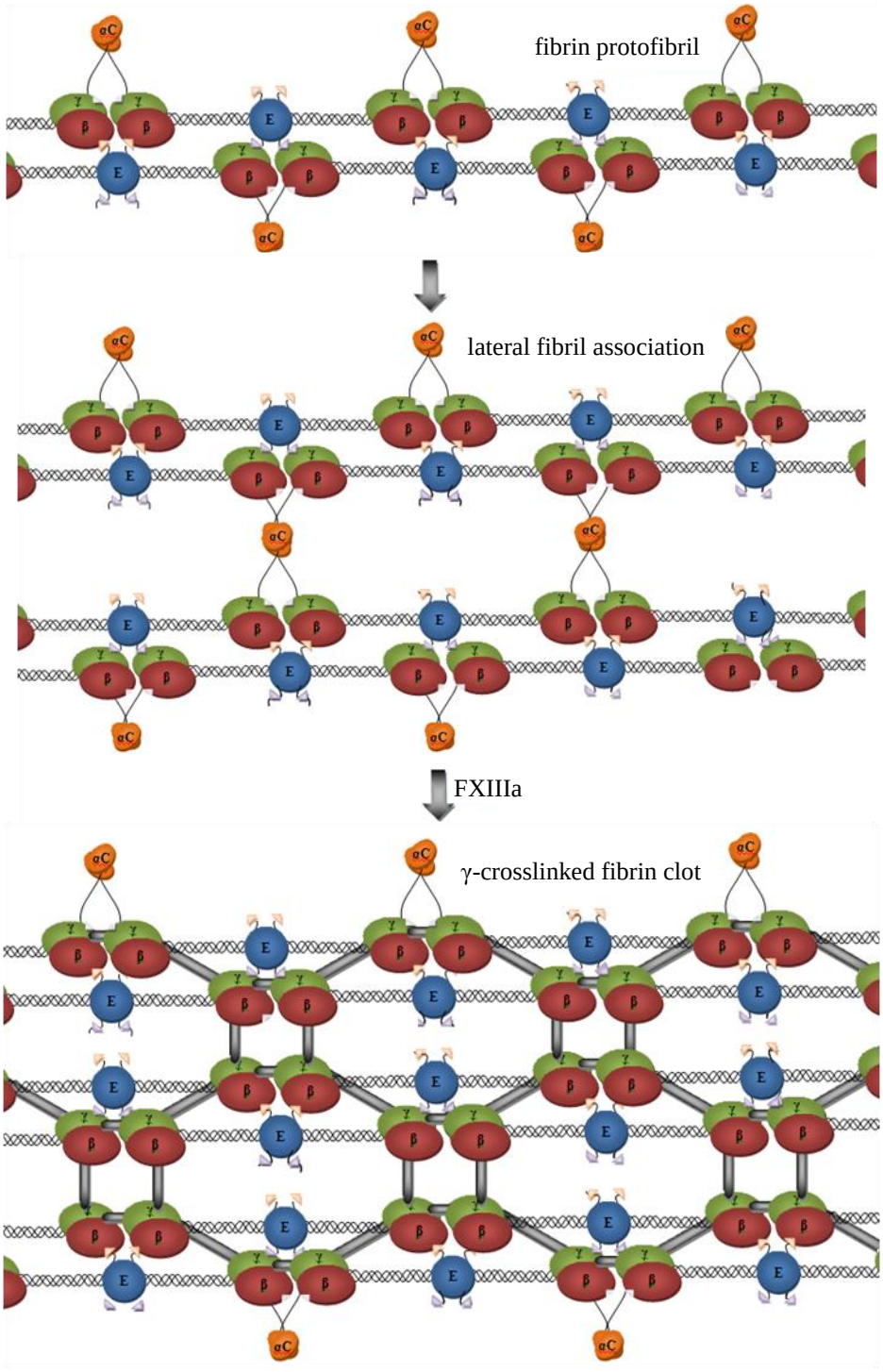

Figure 1.3. Schematic of aggregation and γ-γ crosslinking of fibrin.[27-29] The αC-domains of the fibrin protofibrils interact resulting in lateral association creating thicker fibrin polymers. FXIIIa creates a stiffer clot by γ-γ crosslinking (represented by gray bars). Longitudinal (end-to-end) crosslinking occurs between "D:D" sites located at the outside of the D nodule.[27, 28] Transverse crosslinking occurs between γ_{XL} sites located on γ_A and γ' chains protruding out from the D nodule.[27, 28] γ chains can also be linked laterally.[30]

Factor XIII (FXIII) and its activated form (FXIIIa) crosslinks FI[31] and fibrin protofibrils by a calcium-dependent reaction[32, 33] transforming the soluble clot to a stiffer[26, 34] insoluble clot[35] with resistance to fibrinolysis.[34] Once activated, FXIIIa binds to residues 241 to 476 in the αC-domain of fibrin[36] which brings fibrin protofibrils into close proximity. Aggregation of fibrin monomers aligns the proteins easing the crosslinking process.[37, 38] Crosslinks are constructed by FXIII's catalytic triad (Cys314, His373 and Asp396)[39] which creates an intermolecular γ-glutamyl-ε-lysine bridge between the side-chains of two aligned fibrin molecules (Figure 1.4).[40-45]

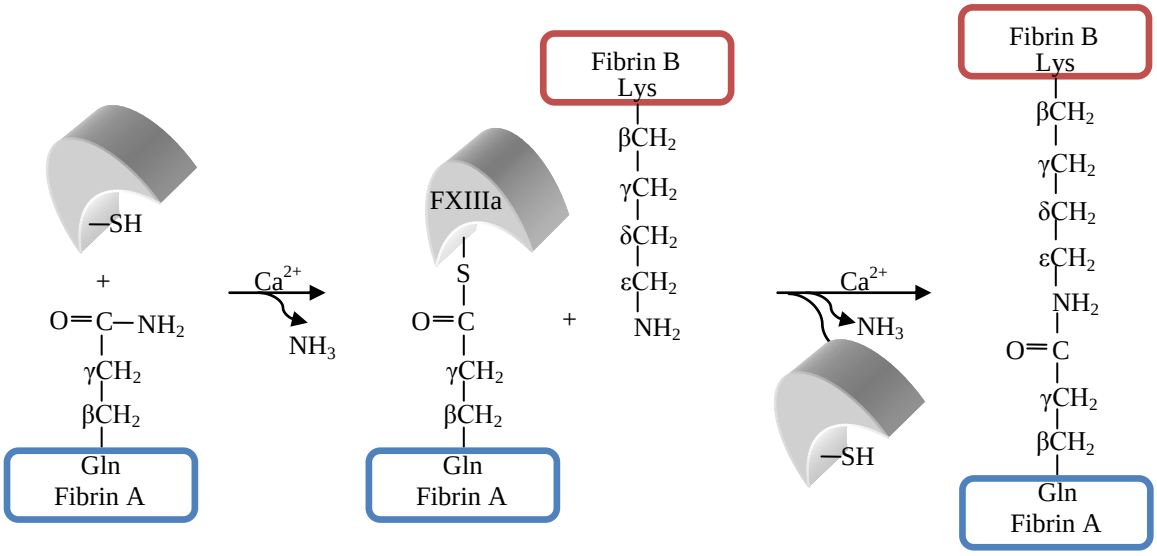

Figure 1.4. Biochemistry of ε-(γ-glutamyl)lysine crosslinking of fibrin molecules by FXIIIa.[32, 42, 45, 46] FXIIIa, a transglutaminase, forms a thioester bond to a specific glutamine residue of the bound molecule, releasing ammonia.[47] This thioester reacts with the primary amine of a lysine residue of another molecule near the catalytic site creating an amide bond.[43, 48]

FXIIIa crosslinks antiparallel[49] fibrin α- and γ-chains with the γ-γ formation proceeding at a much faster rate than the α-α crosslinking.[46, 50, 51] Gln398 or 399 on one fibrin γ-chain crosslinks to Lys406 on an adjacent fibrin γ-chain within 10 minutes.[52, 53] In addition to contributing to viscoelastic strength,[54, 55] γ-γ crosslinking holds the fibrin aggregates in the proper orientation allowing α-α crosslinking to occur.[8] α-chain

crosslinking can take up to 24 hours to form[56] but is important in resisting plasminolysis[57-60] because it yields high viscoelastic strength[46, 50] and insolubility.[50] α- and γ-chains can also be crosslinked; however, this does not greatly affect clot strength.[55]

Hemorrhage treatment

Hemorrhage occurs when primary and secondary hemostasis fails to stop blood loss. Trauma deaths are a result of hemorrhage in 37% of civilians[61] and 47% military[62] and is the primary cause of death for individuals under 44 years of age.[63] For the past 2000 years, the same techniques have been used to stop hemorrhage: packing with gauze, direct pressure and tourniquet.[64] This method is inadequate for treating severe hemorrhage. The Department of Defense Combat Casualty Care Research Program is focused on developing more effective options for treating hemorrhage.[65]

Several hemostatic products are currently used or under development. Cyanoacrylates are utilized as hemostatic aides in oral surgery but can cause inflammation and necrosis.[66] Gelatin-resorcinol-formaldehyde (GRF) glue is frequently used as a sealant and yields excellent tensile strength but has less clotting ability, inferior clots to other sealants and results in fibroblast infiltration.[67] QuikClot speeds clot formation by creating an exothermic reaction when absorbing water; however, it is not biodegradable requiring its removal post-treatment.[68, 69] Compared to other treatment options, fibrin sealants (FS), also known as fibrin glues, are viewed as the best sealant[70] because they are biocompatible,[66, 71, 72] biodegradable[66] and safe[71] and are not linked to excessive inflammation, immune responses or necrosis.[66, 72]

Fibrin sealants

Fibrin sealants (FS) which are composed of fibrinogen (FI), thrombin (FIIa), calcium chloride and occasionally Factor XIII (FXIII) are designed to mimic the final stage of the coagulation cascade by forming a fibrin clot. When applied to a wound, these exogenous components can assist the same endogenous proteins in achieving hemostasis. Because they mimic natural clotting mechanisms, FS are biocompatible,[66, 71, 72] biodegradable[66] and safe[71] and are not linked to excessive inflammation, immune responses or necrosis[66, 72] and provide similar functions as endogenous plasma components.[73]

FS is used as a hemostatic agent,[74] matrix for wound healing,[72, 74] adherence for tissues[74] and drug delivery[74] in a variety of procedures. With respect to hemostasis, FS can be used alone or in combination with a dressing to stop blood oozing from holes, incisions and raw surfaces which cannot be stopped by suturing.[67] The use of FS has been shown to reduce blood loss,[74, 75] fluid loss,[74] transfusion occurrence,[76] operative time,[75] mortality,[75] hospital stay[77] and treatment costs.[74]

Despite its usefulness, FS have drawbacks. Current FS are relatively expensive making it economically infeasible for use as a dressing coating or for widespread uses in the field. In addition, commercial sealants contain plasma-derived proteins which are purified from limited blood sources and have associated risks of pathogen contamination[77] that can withstand current treatments.[66, 74] Some FS use bovine proteins which can initiate immune responses.[74, 77] Consequently, a safer, more abundant source of materials for FS is needed.

Recombinant alternatives for fibrin sealants

A hallmark of hypocoagulopathic states (disseminated intravascular coagulation (DIC),[78-81] liver disease,[81, 82] surgery,[79, 83, 84] acute haemorrhagic injury[79, 85] and haemodilution due to fluid resuscitation,[79, 81, 83, 86]) is depletion of FI which plays a primary role in the formation of blood clots. Consequently, FI may be helpful as topical and systemic therapies for treatment of severe haemorrhagic injury.[81, 87] Because of its utility, fibrin(ogen) is the key and prominent protein in fibrin sealants (FS) which are used for hemostasis in various surgical procedures and treatments for wound healing. Both topical[88, 89] and systemic administrations of FI may require gram dosings as normal plasma concentrations range from 2 to 5 grams per liter.[5, 32, 46, 71, 83] As a result, the therapeutic use of fibrin(ogen) will continue to increase, requiring a source to provide an abundant amount of medical-grade material.

Current products contain plasma-derived fibrinogen (pdFI) which is purified from limited blood sources and has associated risks of pathogen contamination. These risks and limitations could be minimized by producing a recombinant version of human fibrinogen (rFI). Recombinant versions of the α-, β- and γ-chains have been individually expressed in *Escherichia coli*;[90-92] however, they were not biologically functional.[20] Active recombinant human fibrinogen has been expressed by baby hamster kidney (BHK),[20] monkey kidney COS-1 cells[93] and Chinese hamster ovary (CHO) cells which closely mimics its plasma-derived counterpart.[94] Unfortunately, these systems produce less than 4 μg/ml and are therefore unable to meet therapeutic demands.[95]

Another option for producing an ample amount of rFI is production in transgenic animals. Functional human fibrinogen has been expressed and assembled in the milk of transgenic mice at expression levels up to 2 mg/ml.[95] This proved the feasibility of producing ample amounts of fibrinogen in transgenic animals. The work in this dissertation uses a rFI expressed in the milk of transgenic cows. Cows were chosen because they can produce amounts necessary to meet therapeutic demands. Each transgenic cow can produce 25 liters of milk per day for 300 days per year allowing the production of significant amounts of protein per transgenic animal.

Fibrinogen is a complex protein requiring multiple post-translational modifications; therefore, to produce a functional protein, it must be produced by mammalian cells. Unlike fibrinogen, an active A-chain of FXIII can be produced in abundance by yeast.[96-98]

Hemophilia A

Hemophilia A is an X-linked, inherited disorder of blood coagulation primarily caused by deficiency or dysfunction of factor VIII (FVIII) that affects approximately one in every 5,000-10,000 males.[99-101] Currently, hemophilic patients are treated with intravenous infusion of highly purified FVIII concentrates derived from donor human plasma or a variety of recombinantly-derived FVIII (rFVIII) produced by animal cells in large scale bioreactors.[102-104] Despite the clear benefits of prophylactic therapy in this population, 80% of the world hemophilia population does not receive adequate access to replacement therapy. Many factors contribute to this, but a lack of abundance and associated costs of current production of plasma-derived FVIII and rFVIII concentrates

preclude the application of universal prophylactic treatment of hemophilia A in even the most economically developed countries and routine access in developing countries.[99, 102, 103] Thus, another system must be developed that can economically produce an abundant quantity of therapeutic-grade FVIII. FVIII is complex and requires numerous post-translational modifications necessitating the production by mammalian cells. While cell culture has thus far not been economically viable for unlimited production, expressing therapeutic proteins in the milk of transgenic animals has yielded ample amounts more economically.[105]

Dissertation objectives

The underlying hypothesis of the research presented in this dissertation is that a LFS composed of recombinant FI, FXIII and FIIa in optimized proportions can assist hemostasis in the presence and absence of a bioresorbable bandage while using considerably less biologics than commercial products currently available. To test this hypothesis, each of the components of the LFS need to be evaluated. This dissertation has multiple specific aims:

1. *Identify the mechanism of activation of pdFII by sodium citrate*: Recombinant thrombin was not available for initial LFS experiments; therefore, plasma-derived thrombin (pdFIIa) was used. pdFIIa for these experiments was activated from plasma-derived prothrombin (pdFII) by 35% sodium citrate. The research presented in this chapter was designed to identify the intermediates produced when activating plasma-derived prothrombin (pdFII) with 35% sodium citrate.

The time course of intermediate formations was evaluated and a mechanism of activation suggested.

2. *Characterize rFXIII*: Recombinant Factor XIII (rFXIII) produced in *Pichia pastoris* was evaluated with respect to the hypothesis that recombinant FXIII A-chain expressed in *Pichia pastoris* has the same structure, function and activity as its plasma-derived counterpart. It was evaluated as a future component of an LFS.
3. *Optimize LFS components*: Research was designed to test the hypotheses that (1) the addition of rFXIIIa will increase clot strength thereby reducing the amount of FI need in FS; and (2) our LFS containing optimized ratios of rFI, rFXIIIa and FIIa will yield equivalent clot kinetics and strengths as plasma-derived LFS.
4. *Test optimal LFS ex vivo*: Interactions of normal human blood, platelet rich plasma and platelet poor plasma with each LFS component alone or in combination with others were evaluated to anticipate *in vivo* success.
5. *Evaluate efficacy of LFS in multiple surgical models*: FS function is based on complicated interactions between other pro- and anticoagulant proteins, blood cells and vessel surface under flow and viscosity conditions;[67] therefore, the optimized LFS was tested *in vivo* in liver and femoral artery models.
6. *Characterize partially B-domain deleted rFVIII*: rFVIII (226/N6-tg) was produced in the milk of transgenic mice with both von Willebrand Factor (vWF) and α_1-antitrypsin (A1AT). The milk was evaluated for the presence of all three recombinant proteins and was tested by several techniques to determine whether the mammary gland could produce a functional FVIII molecule in abundance.

References

1. Segers, K., Dahlbaeck, B. & Nicolaes, G.A.F. Coagulation factor V and thrombophilia: background and mechanisms. *Thromb Haemost* **98**, 530-542 (2007).
2. Pecheniuk, N.M., Walsh, T.P. & Marsh, N.A. DNA technology for the detection of common genetic variants that predispose to thrombophilia. *Blood Coagul Fibrinolysis* **11**, 683-700 (2000).
3. Dahlback, B. & Villoutreix, B.O. The anticoagulant protein C pathway. *FEBS Lett* **579**, 3310-3316 (2005).
4. Mann, K.G. & Kalafatis, M. Factor V: a combination of Dr Jekyll and Mr Hyde. *Blood* **101**, 20-30 (2003).
5. Wolberg, A.S. Thrombin generation and fibrin clot structure. *Blood Rev.* **21**, 131 (2007).
6. Bukys, M.A. et al. The structural integrity of anion binding exosite I of thrombin is required and sufficient for timely cleavage and activation of factor V and factor VIII. *J Biol Chem* **281**, 18569-18580 (2006).
7. Ariens, R.A., Lai, T.S., Weisel, J.W., Greenberg, C.S. & Grant, P.J. Role of factor XIII in fibrin clot formation and effects of genetic polymorphisms. *Blood* **100**, 743-754 (2002).
8. McDonagh, J.M. in Hemostasis and Thrombosis: Basic Principles and Clinical Practice. (eds. R.W. Colman, J. Hirsh, V.J. Marder & E.W. Salzman) 301-313 (J.B. Lippincott Company, Philadelphia; 1994).
9. Remijn, J.A. et al. Mutations on fibrinogen (g316-322) are associated with reduction in platelet adhesion under flow conditions. *Ann.N.Y.Acad.Sci.* **936**, 444 (2001).
10. Podolnikova, N.P. et al. A cluster of basic amino acid residues in the gamma370-381 sequence of fibrinogen comprises a binding site for platelet integrin alpha(IIb)beta3 (glycoprotein IIb/IIIa). *Biochemistry (N.Y.)* **44**, 16920-16930 (2005).
11. Lord, S.T. Fibrinogen and fibrin: scaffold proteins in hemostasis. *Curr.Opin.Hematol.* **14**, 236 (2007).
12. Clark, R.A. Fibrin and wound healing. *Ann N Y Acad Sci* **936**, 355-367 (2001).
13. Greiling, D. & Clark, R.A. Fibronectin provides a conduit for fibroblast transmigration from collagenous stroma into fibrin clot provisional matrix. *J Cell Sci* **110 (Pt 7)**, 861-870 (1997).
14. Geer, D.J. & Andreadis, S.T. A novel role of fibrin in epidermal healing: plasminogen-mediated migration and selective detachment of differentiated keratinocytes. *J Invest Dermatol* **121**, 1210-1216 (2003).
15. Medved, L.V., Gorkun, O.V. & Privalov, P.L. Structural organization of C-terminal parts of fibrinogen A alpha-chains. *FEBS Lett* **160**, 291-295 (1983).
16. McKee, P.A., Rogers, L.A., Marler, E. & Hill, R.L. The subunit polypeptides of human fibrinogen. *Arch Biochem Biophys* **116**, 271-279 (1966).
17. Kudryk, B., Okada, M., Redman, C.M. & Blomback, B. Biosynthesis of dog fibrinogen. Characterization of nascent fibrinogen in the rough endoplasmic reticulum. *Eur J Biochem* **125**, 673-682 (1982).

18. Seydewitz, H.H., Kaiser, C., Rothweiler, H. & Witt, I. The location of a second in vivo phosphorylation site in the A alpha-chain of human fibrinogen. *Thromb Res* **33**, 487-498 (1984).
19. Nickerson, J.M. & Fuller, G.M. Modification of fibrinogen chains during synthesis: glycosylation of B beta and gamma chains. *Biochemistry* **20**, 2818-2821 (1981).
20. Farrell, D.H., Mulvihill, E.R., Huang, S.M., Chung, D.W. & Davie, E.W. Recombinant human fibrinogen and sulfation of the gamma' chain. *Biochemistry* **30**, 9414-9420 (1991).
21. Redman, C.M. & Xia, H. Fibrinogen biosynthesis. Assembly, intracellular degradation, and association with lipid synthesis and secretion. *Ann N Y Acad Sci* **936**, 480-495 (2001).
22. Clark, R.A. Fibrin is a many splendored thing. *J Invest Dermatol* **121**, xxi-xxii (2003).
23. Ferry, J.D. & Morrison, P.R. Preparation and properties of serum and plasma proteins. VIII. The conversion of human fibrinogen to fibrin under various conditions. *J Am Chem Soc* **69**, 388-400 (1947).
24. Betts, L., Merenbloom, B.K. & Lord, S.T. The structure of fibrinogen fragment D with the 'A' knob peptide GPRVVE. *J Thromb Haemost* **4**, 1139-1141 (2006).
25. Weisel, J.W. Fibrinogen and fibrin. *Adv.Protein Chem.* **70**, 247 (2005).
26. Burton, R.A., Tsurupa, G., Medved, L. & Tjandra, N. Identification of an ordered compact structure within the recombinant bovine fibrinogen alphaC-domain fragment by NMR. *Biochemistry (N.Y.)* **45**, 2257-2266 (2006).
27. Mosesson, M.W., Siebenlist, K.R. & Meh, D.A. The structure and biological features of fibrinogen and fibrin. *Ann N Y Acad Sci* **936**, 11-30 (2001).
28. Mosesson, M.W. Fibrinogen and fibrin structure and functions. *J Thromb Haemost* **3**, 1894-1904 (2005).
29. Mosesson, M.W., DiOrio, J.P., Siebenlist, K.R., Wall, J.S. & Hainfeld, J.F. Evidence for a second type of fibril branch point in fibrin polymer networks, the trimolecular junction. *Blood* **82**, 1517-1521 (1993).
30. Hantgan, R., McDonagh, J. & Hermans, J. Fibrin assembly. *Ann.N.Y.Acad.Sci.* **408**, 344-366 (1983).
31. Siebenlist, K.R., Meh, D.A. & Mosesson, M.W. Protransglutaminase (factor XIII) mediated crosslinking of fibrinogen and fibrin. *Thromb.Haemost.* **86**, 1221-1228 (2001).
32. Lorand, L., Losowsky, M.S. & Miloszewski, K.J. Human factor XIII: fibrin-stabilizing factor. *Prog.Hemost.Thromb.* **5**, 245 (1980).
33. Folk, J.E. Mechanism and basis for specificity of transglutaminase-catalyzed epsilon-(gamma-glutamyl) lysine bond formation. *Adv Enzymol Relat Areas Mol Biol* **54**, 1-56 (1983).
34. Collet, J.P. et al. The alphaC domains of fibrinogen affect the structure of the fibrin clot, its physical properties, and its susceptibility to fibrinolysis. *Blood* **106**, 3824-3830 (2005).
35. Lorand, L. Fibrin clots. *Nature* **166**, 694-695 (1950).
36. Procyk, R., Bishop, P.D. & Kudryk, B. Fibrin--recombinant human factor XIII a-subunit association. *Thromb Res* **71**, 127-138 (1993).

37. Achyuthan, K.E., Dobson, J.V. & Greenberg, C.S. Gly-Pro-Arg-Pro modifies the glutamine residues in the alpha- and gamma-chains of fibrinogen: inhibition of transglutaminase cross-linking. *Biochim Biophys Acta* **872**, 261-268 (1986).
38. Lorand, L., Parameswaran, K.N. & Murthy, S.N. A double-headed Gly-Pro-Arg-Pro ligand mimics the functions of the E domain of fibrin for promoting the end-to-end crosslinking of gamma chains by factor XIIIa. *Proc Natl Acad Sci U S A* **95**, 537-541 (1998).
39. Yee, V.C. et al. Three-dimensional structure of a transglutaminase: human blood coagulation factor XIII. *Proc Natl Acad Sci U S A* **91**, 7296-7300 (1994).
40. Lorand, L. Fibrinoligase: the fibrin-stabilizing factor system of blood plasma. *Ann.N.Y.Acad.Sci.* **202**, 6-30 (1972).
41. Lorand, L., Downey, J., Gotoh, T., Jacobsen, A. & Tokura, S. The transpeptidase system which crosslinks fibrin by gamma-glutamyle-episilon-lysine bonds. *Biochem Biophys Res Commun* **31**, 222-230 (1968).
42. Pisano, J.J., Finlayson, J.S. & Peyton, M.P. [Cross-link in fibrin polymerized by factor 13: epsilon-(gamma-glutamyl)lysine.]. *Science* **160**, 892-893 (1968).
43. Matacic, S. & Loewy, A.G. The identification of isopeptide crosslinks in insoluble fibrin. *Biochem Biophys Res Commun* **30**, 356-362 (1968).
44. Chen, R. & Doolittle, R.F. Isolation, characterization, and location of a donor-acceptor unit from cross-linked fibrin. *Proc Natl Acad Sci U S A* **66**, 472-479 (1970).
45. Folk, J.E. & Finlayson, J.S. The epsilon-(gamma-glutamyl)lysine crosslink and the catalytic role of transglutaminases. *Adv Protein Chem* **31**, 1-133 (1977).
46. Ariens, R.A., Lai, T.S., Weisel, J.W., Greenberg, C.S. & Grant, P.J. Role of factor XIII in fibrin clot formation and effects of genetic polymorphisms. *Blood* **100**, 743 (2002).
47. Loewy, A.G., Dunathan, K., Kriel, R. & Wolfinger, H.L., Jr. Fibrinase. I. Purification of substrate and enzyme. *J Biol Chem* **236**, 2625-2633 (1961).
48. Lorand, L. et al. Lysine as amine donor in fibrin crosslinking. *Biochem Biophys Res Commun* **25**, 629-637 (1966).
49. Doolittle, R.F., Chen, R. & Lau, F. Hybrid fibrin: proof of the intermolecular nature of - crosslinking units. *Biochem Biophys Res Commun* **44**, 94-100 (1971).
50. Schwartz, M.L., Pizzo, S.V., Hill, R.L. & McKee, P.A. The effect of fibrin-stabilizing factor on the subunit structure of human fibrin. *J Clin Invest* **50**, 1506-1513 (1971).
51. Shen, L.L., Hermans, J., McDonagh, J., McDonagh, R.P. & Carr, M. Effects of calcium ion and covalent crosslinking on formation and elasticity of fibrin cells. *Thromb Res* **6**, 255-265 (1975).
52. Purves, L., Purves, M. & Brandt, W. Cleavage of fibrin-derived D-dimer into monomers by endopeptidase from puff adder venom (Bitis arietans) acting at cross-linked sites of the gamma-chain. Sequence of carboxy-terminal cyanogen bromide gamma-chain fragments. *Biochemistry* **26**, 4640-4646 (1987).
53. Spraggon, G., Everse, S.J. & Doolittle, R.F. Crystal structures of fragment D from human fibrinogen and its crosslinked counterpart from fibrin. *Nature* **389**, 455-462 (1997).

54. Standeven, K.F. et al. Functional analysis of fibrin {gamma}-chain cross-linking by activated factor XIII: determination of a cross-linking pattern that maximizes clot stiffness. *Blood* **110**, 902-907 (2007).
55. Standeven, K.F. et al. Functional analysis of fibrin g-chain cross-linking by activated factor XIII: determination of a cross-linking pattern that maximizes clot stiffness. *Blood* **110**, 902 (2007).
56. Gaffney, P.J. et al. Fibrin subunits in venous and arterial thromboembolism. *Cardiovasc Res* **10**, 421-426 (1976).
57. McDonagh, R.P., Jr., McDonagh, J. & Duckert, F. The influence of fibrin crosslinking on the kinetics of urokinase-induced clot lysis. *Br J Haematol* **21**, 323-332 (1971).
58. Gaffney, P.J. & Whitaker, A.N. Fibrin crosslinks and lysis rates. *Thromb Res* **14**, 85-94 (1979).
59. Francis, C.W., Marder, V.J. & Barlow, G.H. Plasmic degradation of crosslinked fibrin. Characterization of new macromolecular soluble complexes and a model of their structure. *J Clin Invest* **66**, 1033-1043 (1980).
60. Muller, M.F., Ris, H. & Ferry, J.D. Electron microscopy of fine fibrin clots and fine and coarse fibrin films. Observations of fibers in cross-section and in deformed states. *J Mol Biol* **174**, 369-384 (1984).
61. Stewart, R.M. et al. Seven hundred fifty-three consecutive deaths in a level I trauma center: the argument for injury prevention. *J Trauma* **54**, 66-70; discussion 70-61 (2003).
62. Bellamy, R.F., Maningas, P.A. & Vayer, J.S. Epidemiology of trauma: military experience. *Ann Emerg Med* **15**, 1384-1388 (1986).
63. Anderson, R.N. & Smith, B.L. Deaths: leading causes for 2001. *Natl Vital Stat Rep* **52**, 1-85 (2003).
64. Holcomb, J. et al. Efficacy of a dry fibrin sealant dressing for hemorrhage control after ballistic injury. *Arch.Surg.* **133**, 32-35 (1998).
65. Pusateri, A.E. et al. Effect of a chitosan-based hemostatic dressing on blood loss and survival in a model of severe venous hemorrhage and hepatic injury in swine. *J Trauma* **54**, 177-182 (2003).
66. Jackson, M.R. Fibrin sealants in surgical practice: An overview. *Am.J.Surg.* **182**, 1S (2001).
67. Mankad, P.S. & Codispoti, M. The role of fibrin sealants in hemostasis. *Am.J.Surg.* **182**, 21S (2001).
68. Alam, H.B. et al. Application of a zeolite hemostatic agent achieves 100% survival in a lethal model of complex groin injury in Swine. *J Trauma* **56**, 974-983 (2004).
69. Rhee, P. et al. QuikClot use in trauma for hemorrhage control: case series of 103 documented uses. *J Trauma* **64**, 1093-1099 (2008).
70. Gibble, J.W. & Ness, P.M. Fibrin glue: the perfect operative sealant? *Transfusion* **30**, 741-747 (1990).
71. Sierra, D.H. Fibrin sealant adhesive systems: a review of their chemistry, material properties and clinical applications. *J.Biomater.Appl.* **7**, 309 (1993).
72. Amrani, D.L., Diorio, J.P. & Delmotte, Y. Wound healing: Role of commercial fibrin sealants. *Ann.N.Y.Acad.Sci.* **936**, 566 (2001).

73. Laurens, N., Koolwijk, P. & De Maat, M.P.M. Fibrin structure and wound healing. *Journal of Thrombosis and Haemostasis* **4**, 932 (2006).
74. Spotnitz, W.D. & Prabhu, R. Fibrin sealant tissue adhesive--review and update. *J.Long.Term.Eff.Med.* **15**, 245 (2005).
75. MacGillivray, T.E. Fibrin sealants and glues. *J.Card.Surg.* **18**, 480 (2003).
76. Carless, P.A., Henry, D.A. & Anthony, D.M. Fibrin sealant use for minimising peri-operative allogeneic blood transfusion. *Cochrane Database Syst Rev*, CD004171 (2003).
77. Jackson, M.R. Tissue sealants: current status, future potential. *Nat Med* **2**, 637-638 (1996).
78. Semeraro, N. & Colucci, M. Changes in the coagulation-fibrinolysis balance of endothelial cells and mononuclear phagocytes: role in disseminated intravascular coagulation associated with infectious diseases. *Int.J.Clin.Lab.Res.* **21**, 214 (1992).
79. Hardy, J.-F., de, M.P. & Samama, C.M. Massive transfusion and coagulopathy: pathophysiology and implications for clinical management. *Can.J.Anaesth.* **53**, S40 (2006).
80. Ponce, R.A. et al. Preclinical safety and pharmacokinetics of recombinant human factor XIII. *Toxicol.Pathol.* **33**, 495 (2005).
81. Key, N.S. & Negrier, C. Coagulation factor concentrates: past, present, and future. *Lancet* **370**, 439-448 (2007).
82. O'Shaughnessy, D.F. et al. Guidelines for the use of fresh-frozen plasma, cryoprecipitate and cryosupernatant. *Br.J.Haematol.* **126**, 11 (2004).
83. Hiippala, S.T., Myllyla, G.J. & Vahtera, E.M. Hemostatic factors and replacement of major blood loss with plasma-poor red cell concentrates. *Anesth.Analg.* **81**, 360 (1995).
84. Blome, M. et al. Relationship between factor XIII activity, fibrinogen, hemostasis screening tests and postoperative bleeding in cardiopulmonary bypass surgery. *Thromb.Haemost.* **93**, 1101 (2005).
85. Velik-Salchner, C. et al. The effect of fibrinogen concentrate on thrombocytopenia. *Journal of Thrombosis and Haemostasis* **5**, 1019 (2007).
86. Fenger-Eriksen, C., Anker-Moller, E., Heslop, J., Ingerslev, J. & Sorensen, B. Thrombelastographic whole blood clot formation after ex vivo addition of plasma substitutes: improvements of the induced coagulopathy with fibrinogen concentrate. *Br.J.Anaesth.* **94**, 324 (2005).
87. Bishop, P. & Lawson, J. Recombinant biologics for treatment of bleeding disorders. *Nature Reviews Drug Discovery* **3**, 684 (2004).
88. Larson, M.J., Bowersox, J.C., Lim, R.C., Jr. & Hess, J.R. Efficacy of a fibrin hemostatic bandage in controlling hemorrhage from experimental arterial injuries. *Arch.Surg.* **130**, 420 (1995).
89. Jackson, M.R. et al. Hemostatic efficacy of a fibrin sealant-based topical agent in a femoral artery injury model: a randomized, blinded, placebo-controlled study. *J.Vasc.Surg.* **26**, 274 (1997).
90. Lord, S.T. Expression of a cloned human fibrinogen cDNA in Escherichia coli: synthesis of an A alpha polypeptide. *DNA* **4**, 33-38 (1985).

91. Bolyard, M.G. & Lord, S.T. High-level expression of a functional human fibrinogen gamma chain in Escherichia coli. *Gene* **66**, 183-192 (1988).
92. Bolyard, M.G. & Lord, S.T. Expression in Escherichia coli of the human fibrinogen B beta chain and its cleavage by thrombin. *Blood* **73**, 1202-1206 (1989).
93. Hartwig, R. & Danishefsky, K.J. Studies on the assembly and secretion of fibrinogen. *J.Biol.Chem.* **266**, 6578 (1991).
94. Gorkun, O.V., Veklich, Y.I., Weisel, J.W. & Lord, S.T. The conversion of fibrinogen to fibrin: recombinant fibrinogen typifies plasma fibrinogen. *Blood* **89**, 4407-4414 (1997).
95. Prunkard, D. et al. High-level expression of recombinant human fibrinogen in the milk of transgenic mice. *Nat.Biotechnol.* **14**, 867 (1996).
96. Bishop, P.D. et al. Expression, purification, and characterization of human factor XIII in Saccharomyces cerevisiae. *Biochemistry* **29**, 1861 (1990).
97. Bishop, P.D., Lasser, G.W., Le Trong, I., Stenkamp, R.E. & Teller, D.C. Human recombinant factor XIII from Saccharomyces cerevisiae. Crystallization and preliminary x-ray data. *J.Biol.Chem.* **265**, 13888 (1990).
98. Lewis, K.B., Teller, D.C., Fry, J., Lasser, G.W. & Bishop, P.D. Crosslinking kinetics of the human transglutaminase, factor XIII A2 , acting on fibrin gels and gamma-chain peptides. *Biochemistry* **36**, 995 (1997).
99. Kasper, C.K. et al. Haemophilia in the 1990s: report of a joint meeting of the World Health Organization and World Federation of Hemophilia. *Vox Sang* **61**, 221-224 (1991).
100. Rosendaal, F.R. & Briet, E. The increasing prevalence of haemophilia. *Thromb Haemost* **63**, 145 (1990).
101. Hoyer, L.W. Hemophilia A. *N Engl J Med* **330**, 38-47 (1994).
102. Pipe, S.W., Saint-Remy, J.-M. & Walsh, C.E. New High-technology Products for the Treatment of Haemophilia. *Haemophilia* **10**, 55-63 (2004).
103. Pipe, S.W., High, K.A., Ohashi, K., Ural, A.U. & Lillicrap, D. Progress in the molecular biology of inherited bleeding disorders. *Haemophilia* **14 Suppl 3**, 130-137 (2008).
104. Jankowski, M.A. et al. Defining 'full-length' recombinant factor VIII: a comparative structural analysis. *Haemophilia* **13**, 30-37 (2007).
105. Echelard, Y., Ziomek, C.A. & Meade, H.M. Production of recombinant therapeutic proteins in the milk of transgenic animals. *BioPharm Int.* **19**, 36-40, 42, 44, 46 (2006).

Chapter 2

Sequence of Activation of Prothrombin by Sodium Citrate

Abstract

Thrombin is the key serine protease in hemostasis because it is responsible for activating both procoagulant proteins critical for creating fibrin clots and anticoagulant proteins needed to return the system to balance. Prothrombin is converted to thrombin in primary hemostasis by activated Factor X (FXa) attached to the phospholipid membrane and secondary hemostasis by the prothrombinase complex which consists of FXa, activated Factor V (FVa), calcium ions complexed on the phospholipid surface of activated platelets. In the laboratory, prothrombin can be activated to thrombin in solutions containing high sodium citrate concentrations; however, the mechanism is not well understood. The work presented in this chapter focuses on identifying intermediates and fragments derived from prothrombin activation by sodium citrate using SDS-PAGE and N-terminal sequencing analyses. The activity of the citrate activated thrombin was analyzed by chromogenic assay and functionality evaluated by ability to cleave FXIIIa and activate fibrinogen. This research found that prothrombin could be activated in the absence of added activators. This activation was not due to autocatalytic degradation but is due to contaminating FX which alone or activated to FXa proteolyzed prothrombin. Incubating prothrombin in 25% or 35% sodium citrate also resulted in activation of prothrombin. Activation by citrate may be autocatalytic or a result of FX; however, FXa and thrombin did not play a role in citrate activation. Analysis of activation fragments indicates that the sequence of activation does not follow the primary or secondary hemostasis pathways; rather, it follows an alternative pathway with a prethrombin-1 intermediate that is subsequently proteolyzed into prethrombin-2, prethrombin-2a, thrombin, α-thrombin and β-thrombin. The activity of citrate activated thrombin was 368

± 173 U/mg (mean ± standard deviation) which is significantly lower than previous reports probably due to the presence of less active thrombin forms. Thrombin formed by 35% sodium citrate appeared to release all of fibrinopeptide B but only a portion of fibrinopeptide A; however, it was able to cleave FXIIIa in the same manner as recombinant thrombin. When evaluated by thromboelastography, citrate activated thrombin created a fibrin clot at equivalent kinetics as the highly purified recombinant thrombin. Although activation of prothrombin by sodium citrate is different than physiological mechanisms, the thrombin produced is functional.

Introduction

Thrombin (FIIa) is the key serine protease in hemostasis because it is responsible for activating both procoagulant proteins critical for creating fibrin clots and anticoagulant proteins needed to return the system to balance.[1] With regard to procoagulation, FIIa activates many of the proteins in the clotting cascade including fibrinogen (FI), factor V (FV), factor VIII (FVIII), factor XI (FXI), factor XIII (FXIII), and can convert additional prothrombin to FIIa.[1, 2] FIIa also activates platelets and vascular endothelial cells[3] and is integral in initiating cellular responses including production and secretion of cytokines, growth factors and cellular adhesion molecules.[1, 2] With regard to its anticoagulant function, FIIa activates anti-fibrinolytic components such as protein C and FIIa-activated fibrinolysis inhibitor (TAFI).[4]

Thrombin's precursor, prepro-prothrombin (Figure 2.1), is synthesized in hepatocytes where it undergoes posttranslational modifications. After entering the endoplasmic reticulum (ER), the signal peptide is removed and 10 glutamate residues adjacent to the propeptide are converted to γ-carboxyglutamate (Gla) residues.[5-7] This Gla domain interacts with calcium ions and is critical for creating the conformation required to bind to negatively-charged phospholipid surfaces of injured vascular tissue and activated platelets[1] which concentrates this key enzyme at the injury site. Following alteration of the Gla residues, the propeptide is removed followed by the attachment of three N-linked oligosaccharide chains, two in the first kringle domain and the last in the B-domain. Thrombin's zymogen, prothrombin (70 kDa), is then secreted into blood at a concentration of 1.2 μM.[1]

Prothrombin is converted to FIIa during primary and secondary hemostasis by slightly different mechanisms (Figure 2.2). During primary hemostasis (the formation of a platelet plug) a miniscule amount of prothrombin (1 to 5 nM) is activated by activated Factor X (FXa) attached to the phospholipid membrane (Figure 2.2, left side).[8] FXa activates prothrombin by cleaving Arg273-Thr274 creating the intermediate prethrombin-2 consisting of combined A- and B-chains and releasing fragment 1.2.[9] This intermediate is subsequently converted to FIIa by cleavage at Arg322-Ile323 to separate the A- and B-chains[9] which remain attached by a disulfide bridge.[10] While the enzyme FXa can convert prothrombin, it has insufficient catalytic efficiency to activate the necessary proteins to stop bleeding.[11] Formation by FXa alone is significantly slower than conversion during secondary hemostasis.[8, 9, 12] During secondary hemostasis, exposed tissue factor (TF) initiates a cascade of activation of numerous serine proteases and several nonenzymatic cofactors. Once the coagulation cascade is activated, prothrombin is converted to FIIa by the prothrombinase complex which consists of FXa, activated Factor V (FVa), and calcium ions complexed on the phospholipid surface of activated platelets.[9, 13, 14] This complex converts prothrombin to meizothrombin by cleaving Arg322-Ile323[9, 15] resulting in the B-chain held to the rest of the molecule by a disulfide bridge (Figure 2.2, right side). Subsequent cleavage at Arg273-Thr274 results in FIIa and the release of fragment 1.2.[9, 12] During this second, critical phase, the prothrombinase complex activates prothrombin to FIIa five-fold faster than FXa alone[15] propagating the formation of FIIa (700 to 900 nM)[10] by FXa and its cofactor FVa in close proximity.[16] FXa[17] or FIIa[9] can then cleave Arg155-Ser156 to separate the kringle domains into

Fragments 1 and 2 from fragment 1.2. FIIa can also cleave Arg286-Thr287 creating prothrombin-2a from prethrombin-2 and α-thrombin from meizothrombin or FIIa.[9]

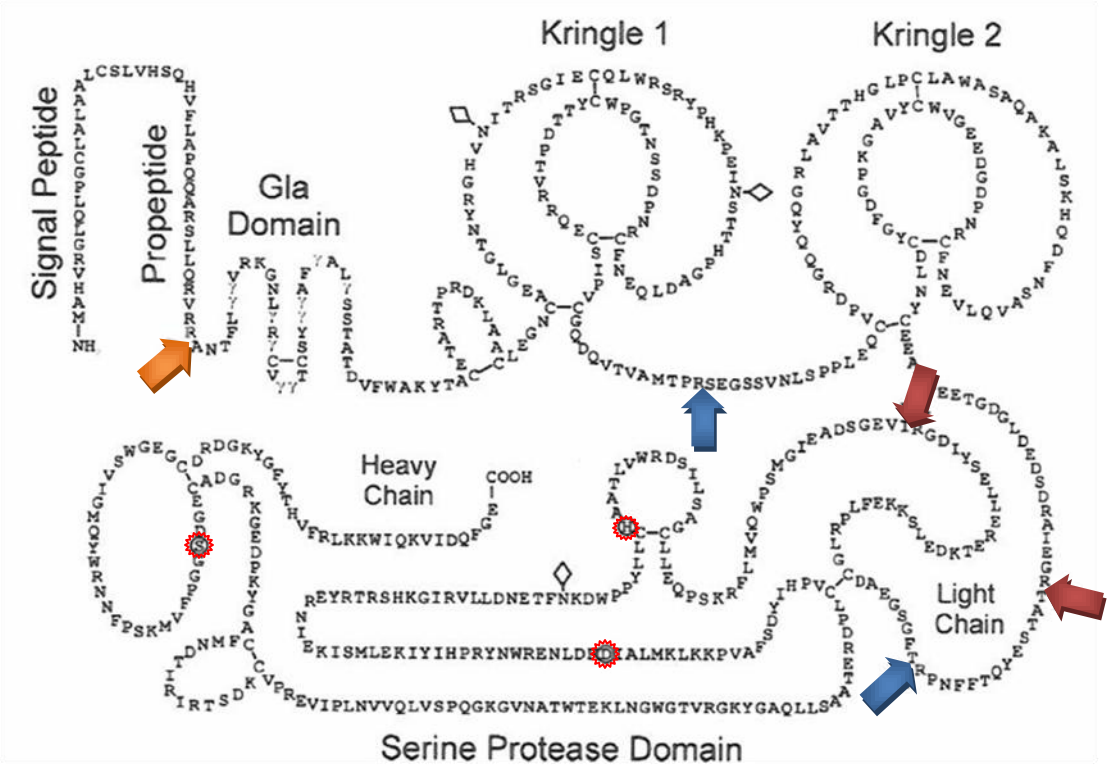

Figure 2.1. Schematic of the amino acid sequence of prepro-prothrombin. Prepro-prothrombin contains a signal peptide, propeptide, Gla domain, two Kringle domains and a light (A-chain) and heavy (B-chain) chain.[1] The N-terminal sequence of prothrombin is indicated by an orange arrow. Gla residues are in the sequence as γ and the three ◊ indicated N-linked carbohydrates. FXa cuts that occur during activation are marked with red arrows and blue arrows indicate sites cleaved by FIIa. The serine protease catalytic triad (His, Asp and Ser) are circled in red. This figure minus a few additions is adapted from Davie and Kulman.[1]

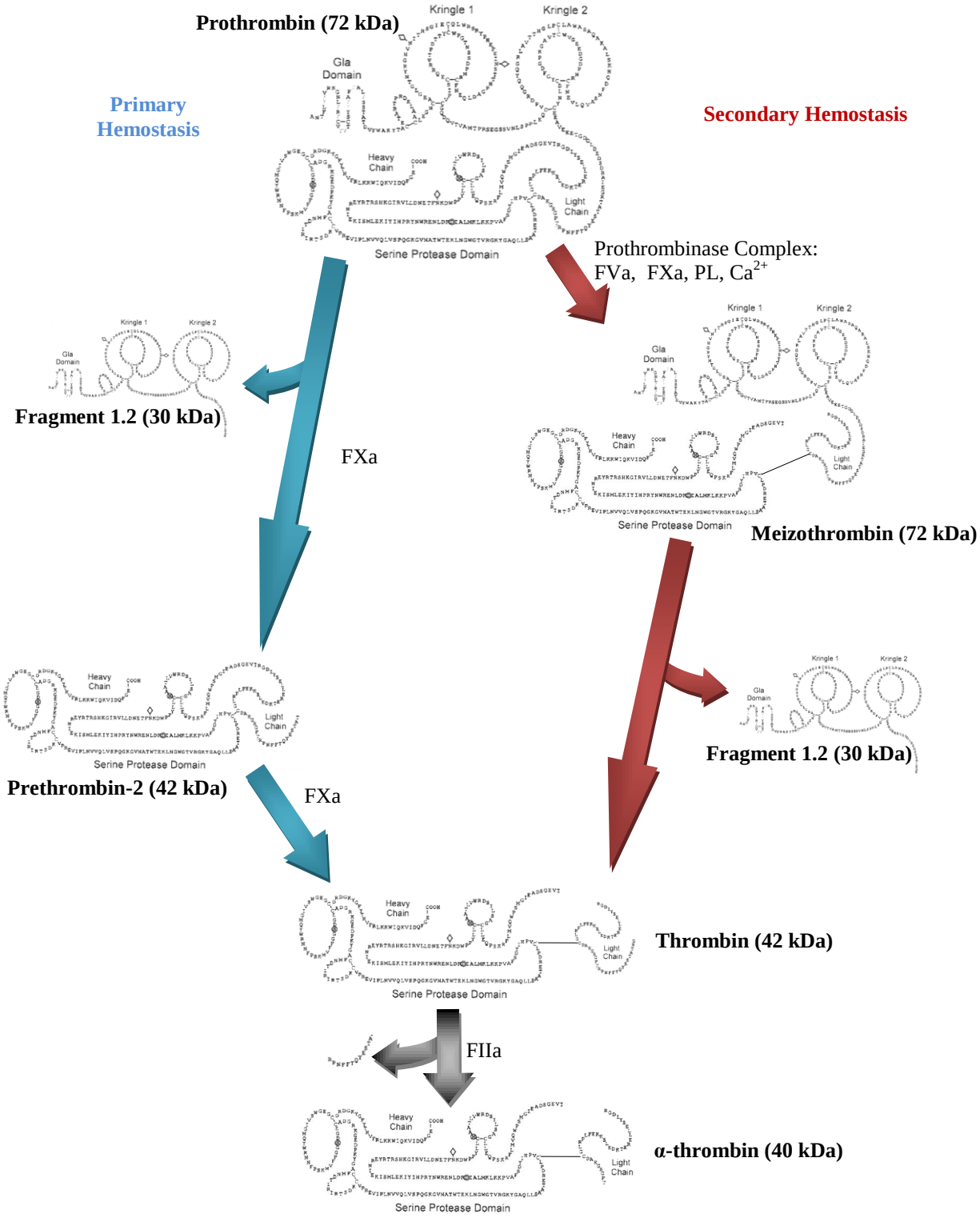

Figure 2.2. Activation of prothrombin. Prothrombin is activated by two mechanisms *in vivo* during primary and secondary hemostasis. This figure modifies the prothrombin schematic published by Davie and Kulman.[1] Note: Prethrombin-2a is equivalent to prethrombin-2 minus the 13 amino acid N-terminal of the A-chain.

The serine protease, FIIa, consists of the 49 residue A-chain linked to the 259 residue B-chain by a disulfide bond (Figure 2.2). α-thrombin is formed when FIIa is cleaved after Arg284 releasing a 13 residue peptide (Figure 2.3). Both FIIa and α-thrombin (α-FIIa) are active serine proteases; however, which species acts at the injury site *in vivo* is unknown.[1] FIIa is homologous to and has the same catalytic triad as other serine proteases. The catalytic triad consists of His43, Asp99 and Ser205 which is located in a cleft within the B-domain[18, 19] and brought into close proximity by salt bridges following activation.[19] The active site is surrounded by three surface loops[19-21] and two charged surface areas (exosites)[11] that create specificity for certain substrates.

FIIa is removed quickly from the blood stream *in vivo*; however, *in vitro*, FIIa can be degraded into less active products: β- and γ-thrombin (Figure 2.3).[1] These degraded species result from proteolysis of the B-chain by plasmin, trypsin,[22] FXa[23] or FIIa itself.[22] β-thrombin is formed when FIIa cleaves the B-chain after Arg380 and Arg391 (prothrombin numbering, Arg62 and Arg73 in FIIa numbering) releasing a small 11 residue peptide important for recognizing fibrinogen thereby creating the B1 and B2 fragments.[22] γ-thrombin is subsequently formed with the cleavage after Arg442 and Lys472 (prothrombin numbering, Arg123 and Arg154 in FIIa numbering) resulting in the creation of the B3 and B4 fragments.[1, 22] The B-chain in β- and γ-thrombin are held together by noncovalent interactions[22] and because they still contain the catalytic triad they retain some activity.[23]

In the laboratory, prothrombin is frequently activated to FIIa by venom. Ecarin, the venom from Indian saw-scale vipers (*Echis carinatus*), activates prothrombin to FIIa with the meizothrombin intermediate.[24, 25] Other venoms, like that from the Taipan snake

(*Oxyuranus scutellatus*), activates prothrombin with both meizothrombin and prethrombin-1 intermediates.[26] Prothrombin can also be activated to FIIa in solutions containing high sodium citrate concentrations;[27-31] however, the mechanism is not well understood.[32] Prothrombin was initially thought to auto-activate under high citrate conditions;[29, 30] however, other researchers assert that impurities, such as FX, play key roles in the activation.[28, 32] While low concentrations of sodium citrate yield minimal activation of prothrombin, concentrations of 25% (weight/volume) is much more effective.[30]

Like Lanchantin, Friedmann and Hart (1965),[28] this work focuses on identifying species derived from prothrombin activation and evaluating the functionality of the resulting FIIa with respect to fibrinogen and Factor XIII (FXIII) activation and fibrin clot formation. To our knowledge, this work is the first detailed analysis of the time course of activation of prothrombin by sodium citrate and first attempt at identifying the intermediates and fragments created during the process. This information was used to suggest a sequence of activation.

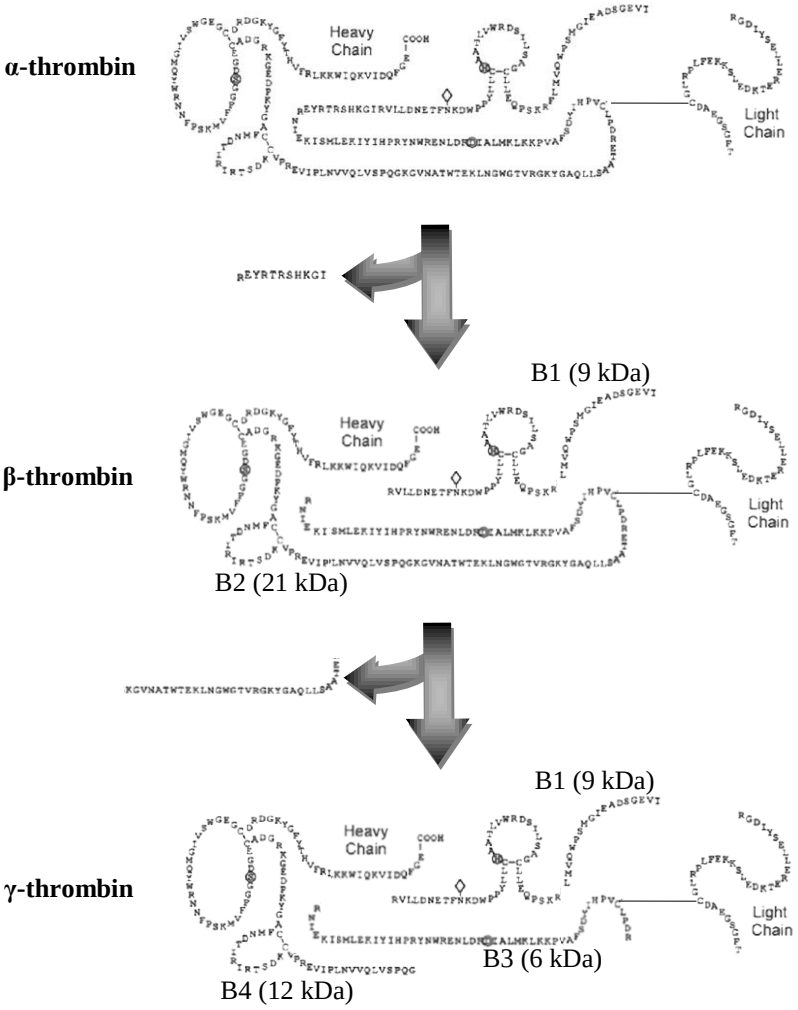

Figure 2.3. Autolytic inactivation of thrombin. α-thrombin can be autolytically degraded to β- and γ-thrombin.[22] This figure modifies the prothrombin schematic published by Davie and Kulman.[1]

Materials and Methods

Materials

Purified, plasma-derived prothrombin was bought from Enzyme Research Laboratories (South Bend, IN) with a specific activity of 11.11 U/mg. Recombinant thrombin (Recothrom®) (rFIIa) was purchased from Zymogenetics. Purified recombinant fibrinogen, expressed in the milk of transgenic cows, was obtained from Pharming Group

NV (Leiden, Netherlands). Phe-Pro-Arg-chloromethylketone (PPACK) and Glu-Gly-Arg-chloromethylketone (GGACK), specific and irreversible inhibitors of FIIa[33, 34] and FXa,[33, 35] respectively, were purchased from Haematologic Technologies (Essex Junction, VT). Materials for the thromboelastograph were purchased from Haemoscope (Niles, IL). Ecarin, sodium citrate and all other reagents were purchased from Sigma (St. Louis, MO) unless otherwise specified.

Vector construction, expression and purification of FXIIIA in Pichia pastoris

The human Ultimate ORF clone containing the human coagulation factor FXIIIA1 cDNA in the pENTR^{TM}221 vector was purchased from Invitrogen (Carlsbad CA). The following primers were used to obtain FXIIIa gene to subclone in pPICZA intracellular Pichia expression vector. (Forward, 5'-CCAATTGATGCATCATCATCATCATTCAGAAACTTCCAGGACCGC-3'; Reverse, 5'-GCGGCCGCTCACATGGAAGGTCGTCTTTGAATC-3'). The forward primer introduced a methionine and 6 histidine amino acids at the N-terminus of mature FXIIIa peptide. The PCR product was digested with MfeI and NotI and subcloned into pPICZA which was digested with the same enzymes. The DNA sequence of the FXIIIA was confirmed by sequencing the insert fragment. One of the confirming plasmid pPICZAFXIIIa was linearized with PmeI and transformed into P. pastoris X-33 host strain and copy number of the clones was determined as described.[36] Varying copy number clones were screened in shake flask culture to confirm intracellular production of FXIIIa protein. The highest producing clone was scaled up to 5 L bench scale. A fed-batch fermentation protocol was followed to optimize FXIIIa production as described by

Zhang et al., (2007).[37] At the end of fermentation process the cells were separated by centrifugation (6,000g) and pellet was stored at -80^{o}C.

Frozen cell paste was processed in 300 gram batches. Cells were lysed in three sets of 100 gram batches. 100 grams of cell paste was resuspended in 100 ml of cold lysis buffer (50 mM Tris-HCL, 10 mM $MgSO_4$, 1 mM EDTA, 10 mM potassium acetate, 1 mM DTT (DL-Dithiothreitol), 2 mM PMSF (phenylmethanesulphonylfluoride) in methanol, pH 9.5). 100 ml (250 g) of 0.5 mm glass beads (Biospec, Bartlesville, OK) were added to the cells. Surrounded by an ice bath, cells were lysed using a BeadBeater Blender (Biospec, Bartlesville, OK) with twenty 20 second on/off cycles. The cell lysate mixture was then centrifuged to remove cellular debris. The lysate from 300 grams of cell paste was combined and purified using the HisBind Purification Kit (EMD Chemicals, Inc., San Diego, CA) with 40 ml of resin slurry. Following purification, rFXIII was dialyzed in 10 mM Tris-HCl, 0.1 mM EDTA, 60 µM polysorbate-20, pH 8.0 in snake-like dialysis membranes and the protein samples were filter-sterilized and concentrated using the Amicon tubes (Millipore, Billerica, MA). The purity of the sample was tested by SDS-PAGE (NuPAGE 12% Bis-Tris) (Invitrogen, Carlsbad, CA) and immunoblot. The concentration of rFXIII was determined by standard Bicinconic Acid (BCA) methods.

Prothrombin activation by ecarin, rFIIa, FXa and sodium citrate

Plasma-derived human prothrombin (Enzyme Research Laboratories, South Bend, IN) was treated with PPACK (final concentration: 60 µM) and GGACK (final concentration: 60 µM) (Haemotologic Technologies, Essex Junction, VT) to eliminate FIIa and FXa activity, respectively. Following a 24 hour incubation period at 37^{o}C on a

rotating mixer, the PPACK and GGACK was removed by ultracentrifugation with Amicon tubes with a 10,000 Da molecular weight cut-off membrane (Millipore, Billerica, MA). Prothrombin was subsequently activated by several methods: rFIIa, FXa, ecarin and sodium citrate in the presence and absence of 60 µM GGACK.

Prothrombin (final concentration: 1 mg/ml) was incubated at 37^{o}C with 0.2% rFIIa (0.002 mg/ml, 4.65 U/ml) (Zymogenetics, Seattle, WA) or 2% FXa (0.02 mg/ml) (Enzyme Research Laboratories, South Bend, IN), 20 U/ml of ecarin (*Echis carinatus*) (Sigma, St. Louis, MO), or 25% or 35% (weight/volume) sodium citrate (0.25 or 0.35 grams of sodium citrate per milliliter of solution). Ecarin samples were incubated for 0, 5, 15, 30, 60, 120, 180, 240, 360 and 480 minutes. Sodium citrate treated samples were incubated for 0, 6, 12, 18, 24, 36 and 48 hours while samples activated by FIIa and/or FXa were incubated for 0, 24, 48 and 72 hours. Control samples were also run: prothrombin in the presence and absence of PPACK and GGACK were incubated for 0, 24, 48 and 72 hours under the same conditions as the activated samples. At the proper time periods, 10 µl of unactivated samples and those activated by ecarin, rFIIa and FXa were removed and the reaction stopped by adding it to 8.75 µl NuPage® LDS sample buffer (Invitrogen, Carlsbad, CA) and storing it at -20^{o}C. Sodium citrate samples were removed and stored at -80^{o}C. Sodium citrate was removed with PD-10 desalting columns (GE Healthcare, Giles, United Kingdom).

For identifying the role FIIa plays during citrate activation and to determine the efficacy of the FXa inhibitor under harsh conditions created by 35% sodium citrate, prothrombin (final concentration: 1 mg/ml) was incubated at 37^{o}C with 35% sodium citrate (0.35 grams of sodium citrate per milliliter of solution) alone or with 0.2% rFIIa

(0.0002 mg/ml) or 0.2% FXa (0.0002 mg/ml) (Enzyme Research Laboratories, South Bend, IN) in the presence of 60 µM GGACK. Samples were incubated for 6, 24 and 72 hours horizontally on a shaker maintained at 37^{o}C. Sodium citrate samples were removed and stored at -80^{o}C. Sodium citrate was removed with PD-10 desalting columns (GE Healthcare, Giles, United Kingdom).

Activation of prothrombin was evaluated by SDS-PAGE on 12% NuPage® Bis-Tris gels (Invitrogen, Carlsbad, CA) under nonreducing conditions with 2-(N-morpholino)ethanesulfonic acid (MES) running buffer and NuPage® LDS sample buffer which were purchased from Invitrogen (Carlsbad, CA). Samples were incubated at 74^{o}C for 10 minutes before loading on the gels which were run at 200 volts for one hour. Gels were stained with Colloidal Blue (Invitrogen).

N-terminal sequencing of activated samples

Fragments produced by rFIIa, FXa, ecarin and 35% sodium citrate activation of prothrombin (see above) were evaluated by N-terminal sequencing. Bands were separated by sodium dodecylsulfate-polyacrylamide (SDS-PAGE) gel electrophoresis on 4-12% NuPage® Bis-Tris gels with 2-(N-morpholino)ethanesulfonic acid (MES) running buffer, NuPage® LDS sample buffer (Invitrogen, Carlsbad, CA). Samples were incubated at 74^{o}C for 10 minutes before loading on the gels and then electroblotted onto polyvinylidene fluoride (PVDF) membrane (Millipore, Billerica, MA) by applying 30 volts for one hour. The blot was stained with Colloidal Blue (Invitrogen, Carlsbad, CA). Each band was excised and the first ten amino acids in the N-terminal were sequenced by Edman degradation with an Applied Biosystems 494 Procise automated sequencer. N-

terminal N-terminal sequencing was performed by the University of Nebraska Medical Center's Protein Structure Core Facility.

Thrombin activity by chromogenic assay

The specific activity of the FIIa produced by FXa and 35% sodium citrate activation was determined by a chromogenic assay. 50 µl of standard and samples were added in triplicate to wells of a 96-well plate. Recothrom® was used to create an eight-interval standard curve ranging from 1.8 mU to 293.6 mU. Based on BCA concentration results, rFIIa was diluted so that wells would contain 1, 20 and 80 ng. The plate was incubated at 37°C for two minutes. 50 µl Tris-buffered saline (TBS) were added to each well followed by three minute incubation at 37°C. 50 µl Chromogenix S-2238 (DiaPharma Group, West Chester, OH) were added to each well followed by two minute incubation at 37°C. 50 µl 20% acetic acid was added to stop the reaction. The absorbance was then read on a Beckman Coulter AD340 Microplate Reader (Brea, CA) at 405 and 495 nm wavelengths. Data was imported into Microsoft Excel and the 495 nm absorbance was subtracted from that at 405 nm. The standard curve was established and the sample activity calculated.

Thrombin activity by SDS-PAGE

The ability of the activated prothrombin samples were evaluated by monitoring the activation of fibrinogen to fibrin and FXIII to FXIIIa by SDS-PAGE. rFI or rFXIII (final concentrations: 0.4 mg/ml) were incubated with FIIa (0.10 mg/ml) in Ringers solution (155 mM NaCl, 5 mM KCl, 2 mM $CaCl_2$, 1 mM $MgCl_2$) for 60 minutes at 37°C. The activation reactions were halted by the addition of NuPage® LDS sample buffer and

NuPage® Sample Reducing buffer (β-mercaptoethanol) (Invitrogen, Carlsbad, CA). Samples were evaluated by sodium dodecylsulfate-polyacrylamide (SDS-PAGE) gel electrophoresis on 4-12% NuPage® Bis-Tris gels with 2-(N-morpholino)ethanesulfonic acid (MES) running buffer. Samples were incubated at 74°C for 10 minutes before loading on the gels which were run at 200 volts for one hour and were stained with Colloidal Blue (Invitrogen, Carlsbad, CA).

Thrombin activity by thromboelastography

The kinetics of the FIIa initiation of a fibrin clot was determined by thromboelastography (TEG) which was performed on solutions containing purified rFI and rFXIII with a Thromboelastograph® (TEG®) Hemostasis System 5000 series (Haemoscope Corp., Niles, IL). rFI (final concentration: 8.56 mg/ml) was transferred to a single-use TEG cup maintained at 37°C by the instrument. rFXIII (final concentration: 0.35 mg/ml) was added. $CaCl_2$ (final concentration: 11 mM) and Ringers solution (155 mM NaCl, 5 mM KCl, 2 mM $CaCl_2$, 1 mM $MgCl_2$, was added to standardize the volumes in the cups) was added followed quickly by FIIa (final concentration: 52.8 U/ml) to initiate clot formation. Data was collected every five seconds for 30 minutes by the TEG interfaced with a computer. The TEG Analytical Software (version 4.2.2, Haemoscope, Niles, IL) collected the time to clot initiation (R), the time to achieve a clot firmness of 20mm (K) and the maximal clot strength (MA). The instrument was calibrated each day of use. Each sample was run in triplicate so means and standard deviations could be calculated. The data was exported and analyzed in Microsoft® Excel.

Results

rFXIIIa characterization

SDS-PAGE and N-terminal sequencing indicated that the purified protein from the yeast was rFXIIIa rather than rFXIII. These and immunoblots indicated rFXIIIa had a purity of greater than 98% (data not shown). The Pefakit® Factor XIII Incorporation Assay (Pentapharm, CT) yielded a specific activity of almost 7,000 U/mg for rFXIII compared to the theoretical specific activity of approximately 100 U/mg of plasma-derived FXIII.

Prothrombin activation by ecarin, rFIIa, FXa and sodium citrate

Plasma-derived prothrombin was incubated at 37^{o}C in the presence and absence of FXa (GGACK) and FIIa (PPACK) inhibitors (Figure 2.4). Over a 72 hour incubation period, there was a gradual decrease in the main 72 kDa band which corresponded to a gradual increase in bands at approximately 50 and 22 kDa. When GGACK and PPACK were added, prothrombin consists of a main band at approximately 72 kDa and a minor band at 50 kDa at all time periods (Figure 2.4B). If incubated for a month at 37^{o}C, prothrombin was gradually activated even in the presence of FXa and FIIa inhibitors (Figure 2.5). The starting material for this experiment started with a major band at approximately 72 kDa and minor bands at 50 and 30 kDa (Figure 2.5, lane 2). The bands were not significantly changed at 26 hours of incubation; however, over the next month, the 72 and 50 kDa bands gradually decreased while the band at approximately 42 increases.

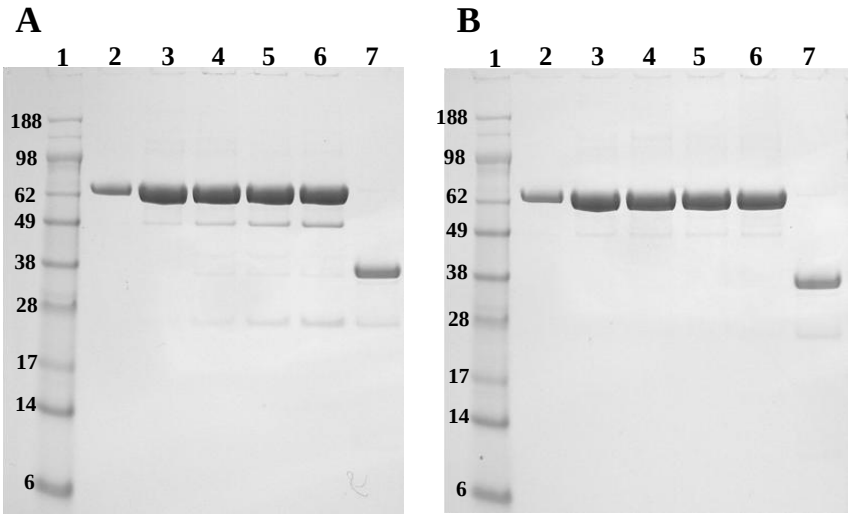

Figure 2.4. Evaluation of the activation of prothrombin without added activators in the presence and absence of FIIa and FXa inhibitors by nonreduced SDS-PAGE. Prothrombin was incubated at 37°C in the absence (A) and presence of 60 µM FIIa and 60 µM FXa inhibitors, PPACK and GGACK respectively (B). Lane 1: molecular weight marker. Lane 2: starting prothrombin. Lanes 3 through 6: prothrombin incubated for 0, 24, 48 and 72 hours. Lane 7 of each contains rFIIa.

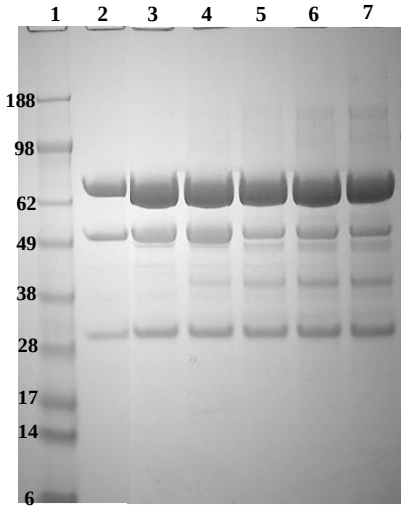

Figure 2.5. Evaluation of prothrombin activation over 28 days after being treated with FIIa and FXa inhibitors by nonreduced SDS-PAGE. Prothrombin was incubated at 37°C in the presence of 60 µM FIIa and 60 µM FXa inhibitors for 28 days. Lane 1: molecular weight marker. Lane 2: starting prothrombin. Lanes 3 through 7: prothrombin incubated for 1.1, 7, 14, 21 and 28 days.

Prothrombin was activated by several methods in order to compare and characterize the mechanism employed by sodium citrate. Activation was evaluated by

nonreduced SDS-PAGE. When treated with 0.2% rFIIa, prothrombin (~72 kDa) was gradually activated resulting in the appearance of bands at approximately 50 kDa, 38 kDa (doublet), 25 kDa and 13 kDa (Figure 2.6A). As the 72 kDa band faded, the bands at 50 kDa, 38 kDa and 28 kDa darken. After 72 hours incubation, most of the prothrombin was degraded; however, there is still a significant band at 50 kDa. If added FIIa was increased or the reaction was allowed to incubate longer, all of the prothrombin was degraded into FIIa and other fragments. If incubated too long, FIIa was degraded (data not shown). If GGACK was added prior to rFIIa addition, the band at ~72 kDa is maintained over the 72 hour incubation period (Figure 2.6B).

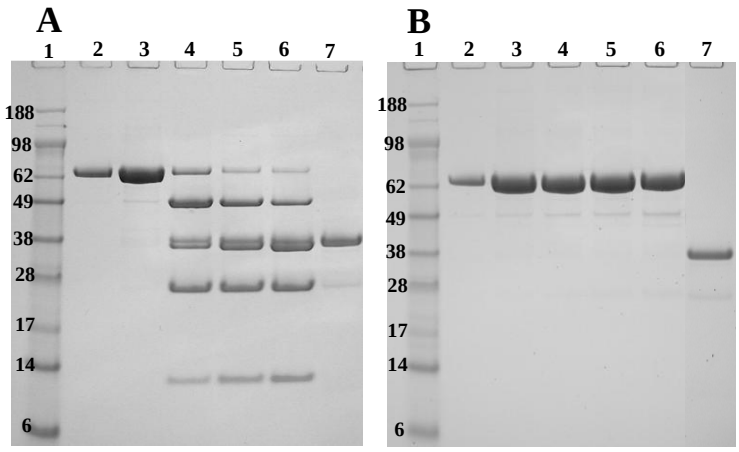

Figure 2.6. Evaluation of the activation of prothrombin by rFIIa in the presence and absence of FXa inhibitor by nonreduced SDS-PAGE. Prothrombin was activated by 0.2% rFIIa in the absence (A) and presence of 60 µM GGACK (B). Lane 1: molecular weight marker. Lane 2: starting prothrombin. Lanes 3 through 6: prothrombin with rFIIa incubated for 0, 24, 48 and 72 hours. Lane 7: rFIIa.

Activation by FX resulted in gradual proteolysis of the band at approximately 72 kDa (Figure 2.7A). At the initial time point, prothrombin remained at 72 kDa. At 24 hours, there were minor bands at 72 and 46 kDa with heavier bands at approximately 36, 22 and 10 kDa (Figure 2.7A, lane 4). At 48 and 72 hours, the same bands were present; however, the 72 kDa band density decreased with increases in low molecular weight

degradation bands. When incubated with 2% FXa, prothrombin (~72 kDa) immediately started degrading. Just after addition, FXa had formed a light band at approximately 40 kDa (Figure 2.7B, lane 3). Within 24 hours, the 72 kDa band was gone leaving bands at approximately 40, 26, and 13 kDa (Figure 2.7B, lane 4). Incubation for an additional 24 or 48 hours did not result in further activation or degradation (Figure 2.7B, lanes 5 and 6, respectively).

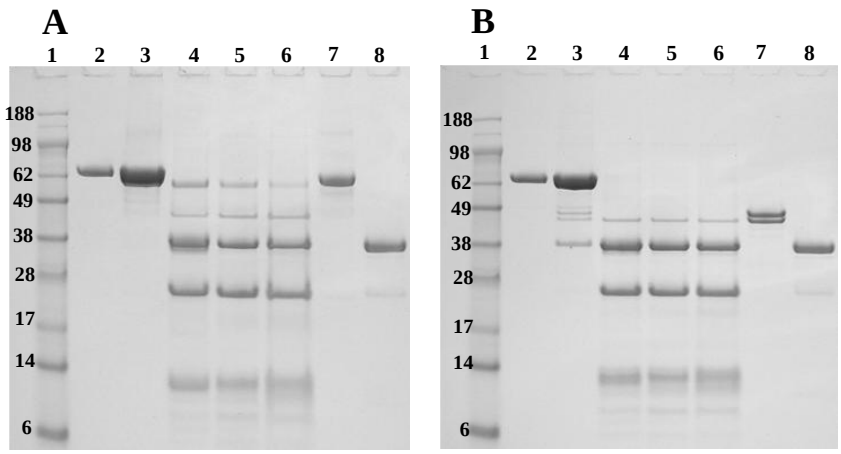

Figure 2.7. Evaluation of the activation of prothrombin by FX and FXa by nonreduced SDS-PAGE. pdFII was activated by 10% FX (A) and 2% FXa (B). Lane 1: molecular weight marker. Lane 2: starting prothrombin. Lanes 3 through 6: prothrombin with rFIIa incubated for 0, 24, 48 and 72 hours. Lane 7 of the FX and FXa activation gels contains FX and FXa, respectively. Lane 8: rFIIa.

Prothrombin was also activated by ecarin (Figure 2.8). Within 5 minutes, the addition of ecarin resulted in the reduction of the prothrombin band (~72 kDa) and the formation of bands at approximately 50 and 26 kDa (Figure 2.8A, lane 4). After 15 minutes, most of the 72 kDa band had disappeared resulting in the darkening of the 50 kDa band and the appearance of a doublet band at approximately 40 kDa (Figure 2.8A, lane 5). After 30 minutes, most of the 50 kDa band had disappeared resulting in the darkening of the 40 kDa band and the appearance of a band at approximately 13 kDa

(Figure 2.8A, lane 6). Incubation for 60 minutes, yielded only three bands at approximately 40, 26 and 13 kDa (Figure 2.8A, lane 7). Incubation for 240 or 480 minutes did not result in further activation or degradation (Figure 2.8A, lanes 8 and 9, respectively). If GGACK is added prior to the addition of ecarin, the band at ~72 kDa gradually disappeared with the appearance and darkening of bands at approximately 50 and 26 kDa. By 30 minutes, the entirety of the 72 kDa band was gone replaced by primarily the band at 50 kDa and 26 kDa with a doublet at ~40 kDa. The following 60 minutes of incubation did not significantly alter the band ratio (Figure 2.8B).

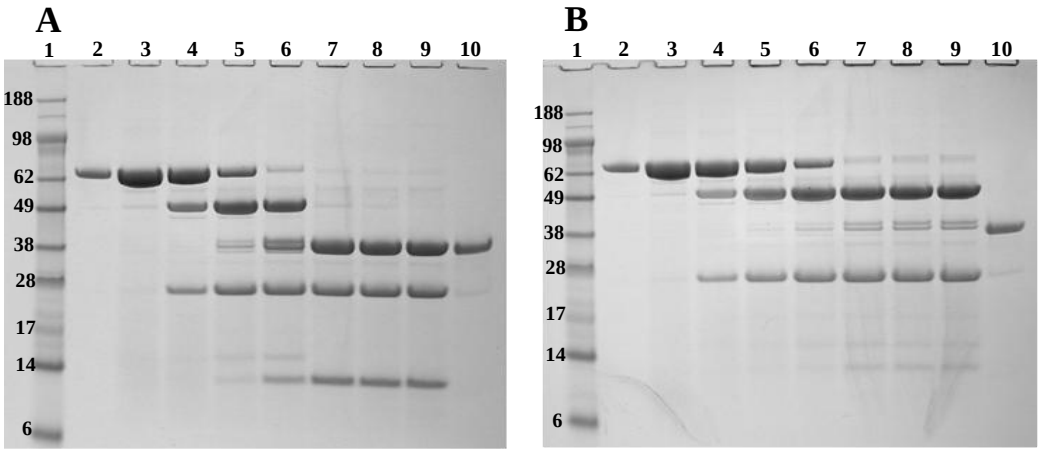

Figure 2.8. Evaluation of the activation of prothrombin by ecarin by nonreduced SDS-PAGE. pdFII was activated by 20 U/ml ecarin in the absence (A) and presence of 60 µM GGACK (B). Lane 1: molecular weight marker. Lane 2: starting prothrombin. For the gel in the absence of GGACK (A), lanes 3 through 9: prothrombin incubated with ecarin for 0, 5, 15, 30, 60, 240 and 480 minutes. For the gel in the presence of GGACK (B), lanes 3 through 9: prothrombin incubated with ecarin for 0, 5, 10, 15, 30, 45 and 60 minutes. Lane 10 of each gel contains rFIIa.

Activation by 25% sodium citrate resulted in a slow lightening of the 72 kDa band and gradual appearance of bands at approximately 50 and 26 kDa starting after incubation for 24 hours (Figure 2.9A). If the reaction was allowed to incubate longer, all of the prothrombin was degraded into FIIa and other fragments. If incubated too long, FIIa was degraded (data not shown). Increasing sodium citrate to 35% resulted in the

appearance of the 50 and 26 kDa bands within 12 hours (Figure 2.9B, lane 5). At 36 hours, the 72 kDa band was almost gone; however, the 50 kDa band has not darkened. Bands have appeared at approximately 40, 26, 24, 13 and 10 kDa (Figure 2.9B, lane 7). After 72 hours incubation, only a light band was visible at 40 kDa (Figure 2.9B, lane 9). 35% sodium citrate activation follows the same activation time course and sequence in the presence or absence of 60 µM GGACK (Figure 2.10).

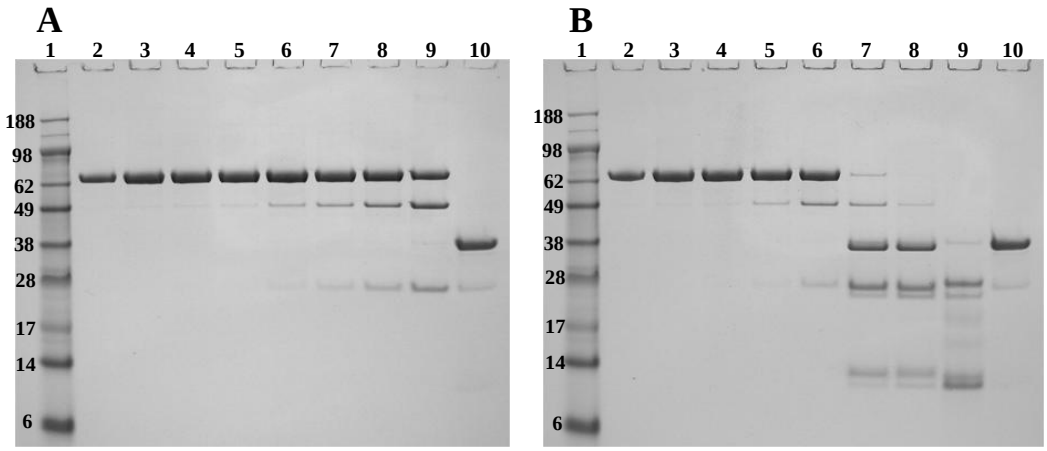

Figure 2.9. Evaluation of the activation of prothrombin by 25% and 35% sodium citrate by nonreduced SDS-PAGE. Prothrombin was activated by 25% (A) and 35% (B) sodium citrate. Lane 1: molecular weight marker. Lane 2: starting prothrombin. Lanes 3 through 9: samples incubated for 0, 6, 12, 24, 36, 48 and 72 hours. Lane 10 contains rFIIa.

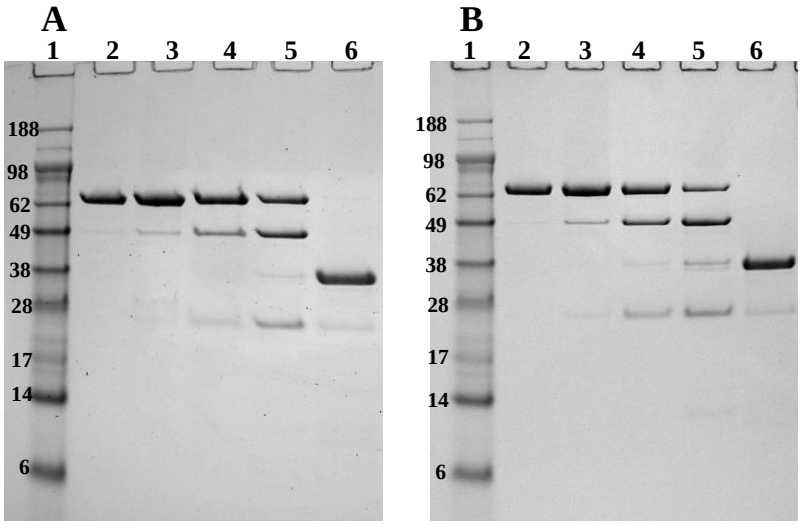

Figure 2.10. Evaluation of the activation of prothrombin by 35% sodium citrate in the presence and absence of FXa inhibitor by nonreduced SDS-PAGE. Prothrombin was activated by 35% sodium citrate in the absence (A) and presence (B) of 60 µM GGACK. Lane 1: molecular weight marker. Lane 2: starting prothrombin. Lanes 3 through 5: samples incubated for 24, 48 and 72 hours. Lane 6: rFIIa.

Prothrombin was incubated with 35% sodium citrate alone, with FXa or with FIIa in the presence of FXa inhibitor (Figure 2.11). All three samples showed equivalent activation rates and fragments.

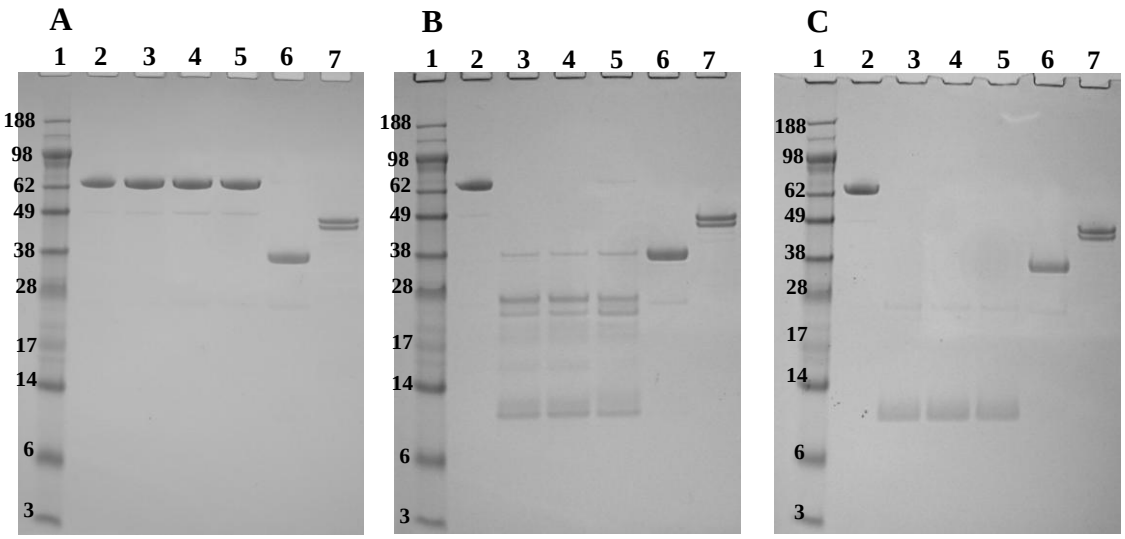

Figure 2.11. Evaluation of the activation of prothrombin by 35% sodium citrate in combination with FXa or FIIa in the presence of FXa inhibitor by nonreduced SDS-PAGE. Prothrombin was activated by 35% sodium citrate alone or in combination with rFIIa or FXa. Samples were incubated for 8 (A), 24 (B) and 72 (C) hours. Lane 1: molecular weight marker. Lane 2: starting prothrombin. Lanes 3: prothrombin incubated with 35% citrate alone. Lane 4: prothrombin incubated with 35% citrate and 0.02% FXa. Lane 5: prothrombin incubated with 35% citrate and 0.02% rFIIa. Lane 6: rFIIa. Lane 7: FXa.

Prothrombin was also activated by a combination of 0.2% FIIa and 35% sodium citrate (Figure 2.12). At 0 and 1 minutes, the major band is at approximately 72 kDa. Over the following hour, the band at 72 kDa decreased with an increase in the bands at 50, 42, 28 and 14 kDa.

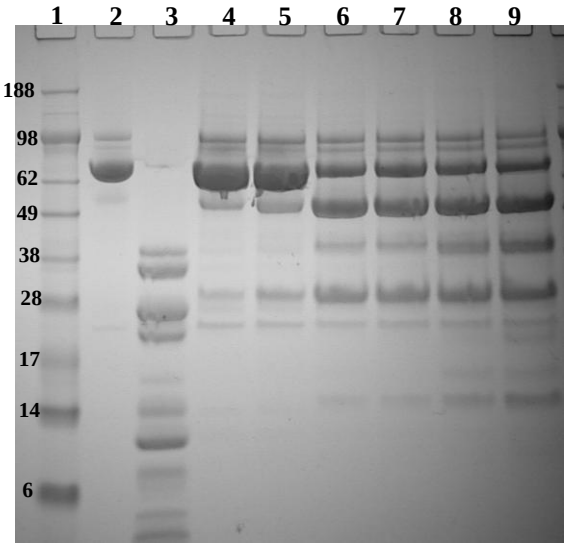

Figure 2.12. Evaluation of the activation of prothrombin by FIIa and sodium citrate by nonreduced SDS-PAGE. Prothrombin was activated by 0.2% plasma-derived FIIa and 35% sodium citrate. Lane 1: molecular weight marker. Lane 2: starting prothrombin. Lane 3: plasma-derived FIIa used for activation. Lanes 4 through 9: samples incubated for 0, 1, 5, 15, 30 and 60 minutes.

N-terminal sequencing of activated samples

The first five to ten amino acids of the N-terminal were determined for each of the main fragments resulting from activation by 2% FXa and 35% sodium citrate (Table 2.1). Activation by FXa resulted in fragments with molecular weights of ~45 kDa (FXa), ~40 kDa (IVESGEADIG), ~22 kDa (ANTFLEAVVK) and ~13 kDa (SEGNXVA). Several prothrombin fragments activated by 35% sodium citrate alone or with 0.2% FIIa were analyzed by N-terminal sequencing. These fragments included bands at ~50 kDa (N-terminal sequence: ANTFLXLVVX), ~42 kDa (N-terminal sequence: TATSEYQTFF), ~40 kDa (N-terminal sequence: TFGSGEADIG), ~26 kDa (N-terminal sequence: ANTFLXXVXK), ~25 kDa (N-terminal sequence: TFGSGEADIG), ~22 kDa (N-terminal sequence: IVEGSDAEIG), ~13 kDa (N-terminal sequence: TFXXX) and various degradation bands with lower molecular weights. Based on these sequences,

molecular weights and presence or absence of other bands at certain time points, each sequenced band was identified as a particular prothrombin/thrombin species (Table 2.1, Figure 2.13).

Table 2.1. N-terminal amino acid sequences of prothrombin and its fragments following activation by FXa (2%) and sodium citrate (35%).

Activation Enzyme	Approximate Molecular Weight (kDa)	Amino Acid Sequence	Identity
None (starting material)	72	ANTFLXLVVX	Prothrombin
Activated Factor X (FXa)	40	IVESGEADIG	B-chain
	22	ANTFLEAVVK	Fragment 1
	13	SEGNXVA	Fragment 2
35% Sodium Citrate	50	SEGSSVNLSP	Prethrombin-1
	42	TATSEYQTFF	Prethrombina-2 or FIIa
	40	TFGSGEADIG	Prethrombina-2a or αFIIa
	26	ANTFLXXVXK	Fragment 1
	25	TFGSGEADIG	βFIIa
	22	IVEGSDAEIG	B-chain from βFIIa
	13	TFXXX	Fragment 2

Notations: Prethrombin-1 (PreFIIa-1), Prethrombin-2 (PreFIIa-2), Prethrombin-2a (PreFIIa-2a), Thrombin (FIIa), α-thrombin (αFIIa), β-thrombin (βFIIa), γ-thrombin (γFIIa).

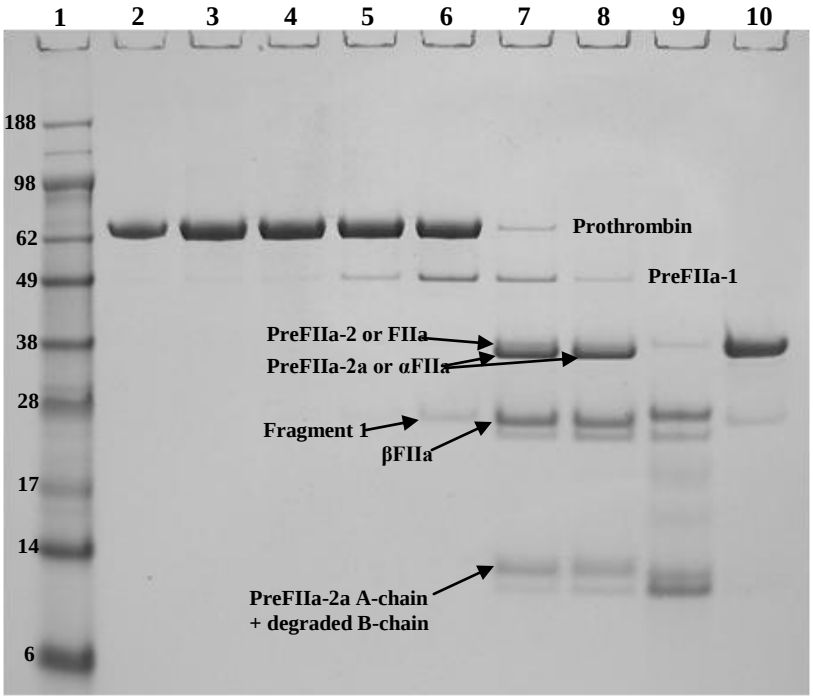

Figure 2.13. Identification of the fragments of prothrombin activated by 35% sodium citrate suggested by N-terminal sequencing. Results from several N-terminal sequencing analyses of multiple prothrombin samples activated by 35% sodium citrate with or without thrombin were compiled and shown overlaying an equivalent time course activation by citrate. Lane 1: molecular weight marker. Lane 2: starting prothrombin. Lanes 3 through 9: samples incubated for 0, 6, 12, 24, 36, 48 and 72 hours. Lane 10: rFIIa.

Thrombin activity by chromogenic assay

The activity of plasma-derived thrombin (pdFIIa) prepared by FXa and citrate activation were determined by chromogenic assay. Positive and negative controls yielded specific activities similar to those reported by the manufacturer (Table 2.2). The specific activity of the FXa activated prothrombin sample was 293 U/mg. The mean specific activity of citrate activated prothrombin was 368 ± 173 U/mg (mean and standard deviation of four samples activated by 35% sodium citrate).

Table 2.2. Specific activity of activated prothrombin by chromogenic assay.

	Estimated Specific Activity (U/mg)	Specific Activity, as per manufacturer (U/mg)
Prothrombin (Enzyme Research)	0	11
Prothrombin (Enzyme Research)	2,805	3,230
rFIIa (Zymogenetics)	2,618	2,370
Prothrombin activated by 2% FXa	293	
Prothrombin activated by 35% sodium citrate	368 ± 173	

Note: Each sample was measured in triplicate at three dilutions. Intra-sample standard deviations were 0 for prothrombin, 874 for plasma-derived FIIa (Enzyme Research), 625 for rFIIa (Zymogenetics), 1 for FXa activated and between 12 and 38 for citrate activated samples. Four samples from different 35% sodium citrate activations were measured in three assays to yield a mean ± standard deviation.

Thrombin activity by SDS-PAGE

The functions of the samples activated by 0.2% rFIIa (72 hours), 2% FXa (72 hours), 20 U/ml ecarin (480 minutes), 35% sodium citrate (48 hours) were evaluated by a 60 minute incubation with rFI (Figure 2.14A) and rFXIII (Figure 2.14B). rFI incubated with a commercial recombinant thrombin (rFIIa) is activated into fibrin with the release of fibrinopeptide A (FpA) and fibrinopeptide B (FpB) as seen by the decrease in molecular weight of the 66 and 52 kDa bands (Figure 2.14A, lane 3). Prothrombin samples activated to pdFIIa by 2% FXa (Figure 2.14A, lane 5) and 20 U/ml ecarin (Figure 2.14A, lane 6) resulted in identical shifts. Prothrombin samples activated to pdFIIa by 0.2% rFIIa resulted in a shift of the 52 kDa band but not the 66 kDa band (Figure 2.14A, lane 4). The sample activated by 35% sodium citrate resulted in a partial shift in the 66 kDa band and full shift in the 52 kDa band (Figure 2.14A, lane 7).

When incubated with a commercial thrombin (rFIIa), the molecular weight of rFXIIIa shifted down slightly from ~84 kDa to ~80 kDa (Figure 2.14B, lane 3). The molecular weight shift of rFXIIIa was fully achieved by pdFIIa activated by 2% FXa

(Figure 2.14B, lane 5) and 20 U/ml ecarin (Figure 2.14B, lane 6). pdFIIa activated by 0.2% rFIIa and 35% sodium citrate shifted most of the rFXIIIa; however, a minor band at the original molecular weight was visible (Figure 2.14B, lanes 4 and 7, respectively). The proper thrombin-mediated FXIIIa inactivation fragments (~25 and ~54 kDa) were also seen for rFIIa, FXa and ecarin activated pdFIIa.

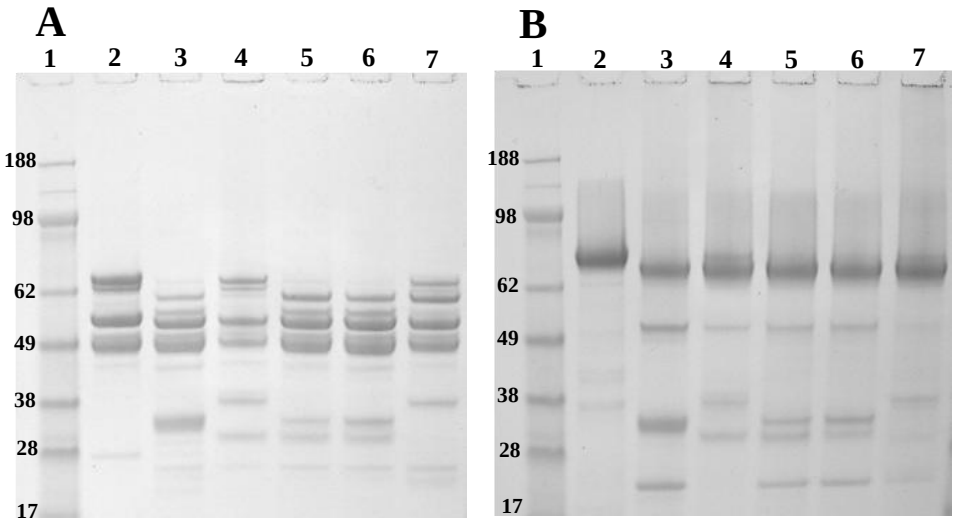

Figure 2.14. Fibrinopeptide release and Factor XIIIa molecular weight shift by prothrombin samples activated by rFIIa, FXa, ecarin and 35% sodium citrate. Prothrombin (0.10 mg/ml) activated by rFIIa, FXa, ecarin and 35% sodium citrate were evaluated by incubation with 0.4 mg/ml rFI (A) or 0.4 mg/ml rFXIII (B). Lane 1: molecular weight marker. Lane 2: rFI (A) or rFXIII (B) alone. The remaining lanes contain rFI (A) or rFXIII (B) incubated for 60 minutes rFIIa (lane 3) or with prothrombin activated by 0.2% rFIIa (lane 4), 2% FXa (lane 5), 20 U/ml ecarin (lane 6) or 35% sodium citrate (lane 7).

Thrombin activity by thromboelastography

The kinetics and strength of clots formed by 8.56 mg/ml rFI, 0.35 mg/ml rFXIII and 52.8 U/ml rFIIa or prothrombin activated by 35% sodium citrate (pdFIIa) were evaluated by thromboelastography (TEG) (Figure 2.15). The time to clot initiation (R) and clotting kinetics (K) catalyzed by pdFIIa (11.86 ± 2.89 and 50.0 ± 0 seconds, respectively) were equivalent to that catalyzed by rFIIa (10.00 ± 0 and 50.0 ± 0 seconds, respectively). Maximal clot strengths for the pdFIIa catalyzed reaction (10,585.97 ±

1,670.88 dynes/sec) were comparable to that created by rFIIa (12,865.60 ± 1,688.44 dynes/sec).

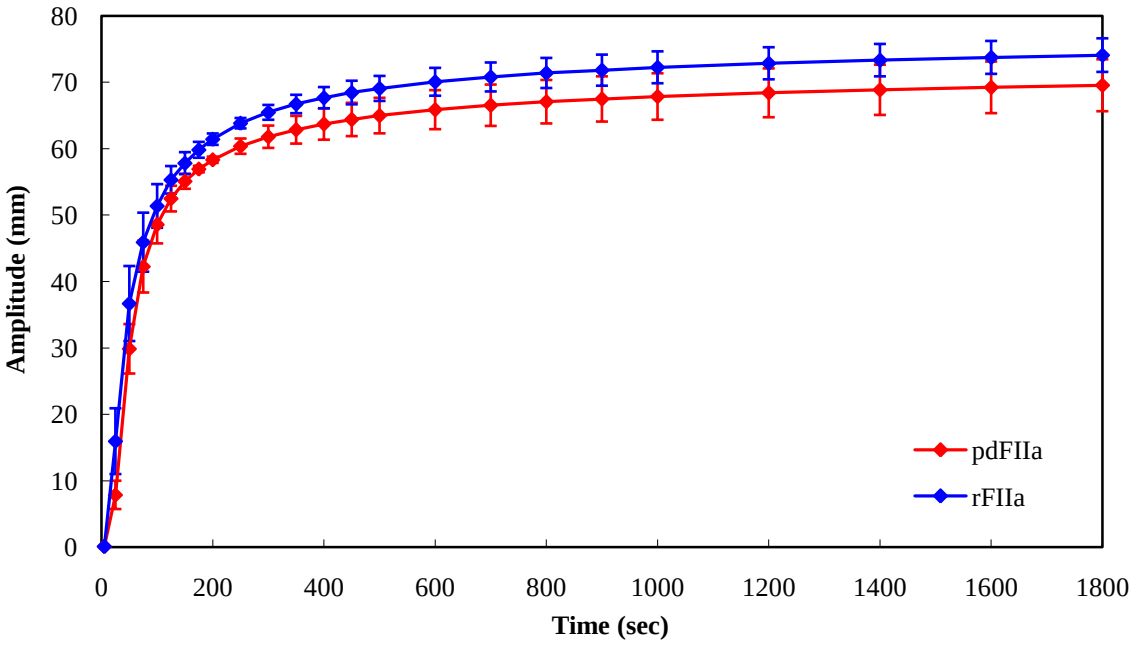

Figure 2.15: Comparison of clotting activity of rFIIa and citrate activated pdFIIa clotting analysis by thromboelastography. TEG monitored the initiation of clot formation, clotting kinetics and change in clot strength over time of rFI (8.56 mg/ml) and rFXIII (0.35 mg/ml) activated by pdFIIa (red) or rFIIa (blue) (52.8 U/ml).

Discussion

Detailed analysis of the activation of prothrombin by sodium citrate has not previously been accomplished and only limited evaluations have been completed on the fragments produced. The mechanism of activation by citrate is unknown. The research presented in this chapter focused on identifying the sequence of activation of prothrombin by sodium citrate. This was accomplished by analyzing molecular weight changes by SDS-PAGE, N-terminal sequencing and comparison to activations with known sequences. The activity of the subsequently activated thrombin samples was also determined.

Research has been complicated by the presence of trace amounts of other plasma proteins in purified prothrombin samples which can activate it into thrombin.[32] These results support that assertion. When purified prothrombin with a >95% purity is incubated over 72 hours, a portion of prothrombin is activated into prethrombin-1 (Figure 2.4A). If the same prothrombin sample is pre-treated with FXa and FIIa inhibitors which are subsequently removed, prothrombin is not activated over a 72 hour incubation period (Figure 2.4B). These results indicate that trace amounts of FXa and/or FIIa are responsible for activating prothrombin. Even if pretreated, prothrombin is slowly activated when incubated at 37^{o}C for 28 days (Figure 2.5). If incubated for over five and a half months, most of the prothrombin is proteolyzed into small molecular weight pieces (data not shown). The activation of prothrombin after pre-treatment with FIIa and FXa inhibitors indicates that some component in the sample is activating the zymogen. Some researchers believe prothrombin can autoactivate[27] while others assert that FX is responsible for activating prothrombin.[32]

Research presented in this chapter indicates that trace amounts of FIIa in the prothrombin sample are not responsible for activation of prothrombin. When thrombin was added to prothrombin pretreated with FXa and FIIa inhibitors, prothrombin was activated within 24 hours (Figure 2.6A); however, when FXa inhibitor was added with the FIIa, prothrombin was not activated (Figure 2.6B). Thus, rather than activating prothrombin, FIIa is activating the trace amount of FX into FXa which is subsequently activating prothrombin.

When FX is added to prothrombin, FX (~59 kDa) is activated into FXa (~46 kDa) and prothrombin is activated into thrombin and other fragments within 24 hours (Figure

2.7A). Activating with FXa similarly transformed all of the prothrombin to thrombin within 24 hours (Figure 2.7B). This activation of FX occurs in the absence of thrombin; therefore, this research supports assertions that FX can be autocatalytically activated or activated by prothrombin.[32] It is still unclear whether FX can activate prothrombin or whether prothrombin is activated once FXa is created.

Research has been mixed with regard to the success of citrate activation. Early research indicated that prothrombin could auto-activate to thrombin in the presence of 25% sodium citrate;[29, 30] however, Teng and Seegers (1981) found that prothrombin, prethrombin-1 nor prethrombin-2 were activated by 25% sodium citrate with or without activated thrombin.[32] Teng and Seegers asserted that contaminating traces of other plasma proteins are necessary to activate prothrombin to thrombin.[32] They stated that citrate activation of prothrombin was a result of "reciprocal proenzyme activation" where FX and prothrombin activate each other; however, while FX can auto-activate, prothrombin requires the presence of FX.[32]

While we know our prothrombin sample is contaminated with other plasma proteins, pretreatment with FXa and FIIa inhibitors cease activation over 72 hours; however, the addition of sodium citrate initiates prothrombin activation and as seen previously[27] activation proceeded at a faster rate at the higher citrate level. We have shown that FIIa is not responsible for this activation. It is unclear whether trace amounts of FX are responsible but FXa is not. Incubation with 35% citrate alone or with added FXa inhibitor yielded equivalent activation profiles (Figure 2.10); therefore, FXa does not appear to play a role in this activation. When FXa was added to prothrombin in combination with FXa inhibitor and 35% sodium citrate, activation rates and fragments

were equivalent indicating that the FXa inhibitor is still functional in the harsh sodium citrate environment. Activation by sodium citrate could be due to FX, autocatalytic or non-enzymatic activation. Autolytic degradation of thrombin has been reported in the literature. α-thrombin in the presence of 0.4 M NaCl will autolytically degrade into β- and γ-thrombin.[22] Future research needs to include studies designed answer this question.

Whatever the activator, previous research found that in the presence of 25% citrate, thrombin was formed within five hours as measured by thrombin activity.[27, 28, 32] In our studies, it typically took more than 72 hours and between 24 and 36 hours for prothrombin to be activated to FIIa by 25% and 35% sodium citrate, respectively (Figure 2.9); however, activation times were occasionally more than 72 hours (Figure 2.10). Our erratic activation times in the presence of citrate have been previously observed in prothrombin samples that are not highly pure; however, the causes for these inconsistencies are unknown.[27]

In 1950, Seegers, McClaughry and Fahey, using electrophoretic mobility and activity assays, tentatively asserted that a minimum of three different molecular weight species were derived following activation by 25% sodium citrate.[27] Lanchantin, Friedmann and Hart (1965), using sedimentation velocity techniques, identified a molecular weight decrease from approximately 70 kDa to 35 kDa with subsequent fragments with approximate weights of 25 and 10 kDa after incubation with 25% sodium citrate.[28] This work identifies several more intermediates and fragments produced by citrate activation of prothrombin. Both 25% and 35% sodium citrate followed identical pathways with 25% citrate activating at a slower rate (Figure 2.9 and other data not shown).

Initially, prothrombin is activated into two species at approximately 50 and 26 kDa (Figure 2.9B, lane 5 and 6). N-terminal sequencing indicates that the band at ~26 kDa has the same amino terminal as prothrombin; therefore, the band is either fragment 1 or fragment 1.2. The molecular weight is more consistent with fragment 1.2 which should be approximately 30 kDa which would indicate a meizothrombin intermediate. However, if it were fragment 1.2, a band should also exist at approximately 42 kDa for FIIa which is the other fragment formed with meizothrombin. Since there is no corresponding band at 42 kDa but only bands at 72 and 50, then the 26 kDa band must be fragment 1. This conclusion is supported by the N-terminal sequencing of the 50 kDa band which indicates it is prethrombin-1 indicating that the 26 kDa band is the released of fragment 1.

After further incubation, prothrombin and prethrombin-1 are activated into a band at approximately 42 and 40 kDa (Figure 2.9B, lane 7). N-terminal sequencing indicates that the 42 kDa band corresponds to thrombin and/or prethrombin-2 and the 40 kDa band is α-thrombin and/or prethrombin-2a. A proteolyzed thrombin, β-thrombin (~25 kDa), is also formed. This proteolysis results in fragments at 13 kDa which is α-thrombin or prethrombin-2a degraded on the C-terminal and multiple lower molecular weight degradation bands. It is possible that prethrombin-2a is directly activated from prethrombin-1; however, after all of the prothrombin and most of the prethrombin-1 has been proteolyzed, the band at 42 kDa is no longer present replaced by only the 40 kDa band corresponding to prethrombin-2a and/or α-thrombin. Therefore, it appears that prethrombin-2 is converted to prethrombin-2a. Under reducing conditions, the 40 kDa band splits into a doublet of bands at approximately 40 and 36 kDa exist which N-

terminal sequencing indicates as prethrombin-2a and the B-chain, respectively. These results indicate that under nonreducing conditions, the band at 40 kDa includes both α-thrombin and prethrombin-2a.

This sequence of activation by sodium citrate does not follow the primary or secondary hemostasis pathways (Figure 2.1); rather, it follows an alternative pathway similar to that of primary hemostasis (Figure 2.16). Activation with prethrombin-1 as an intermediate has been reported for bovine and human prothrombin when treated with thrombin.[38] It is interesting to note that activation by ecarin resulted in a similar sequence of activation with a prethrombin-1 intermediate although it should have yielded a fragment 1.2 intermediate instead.

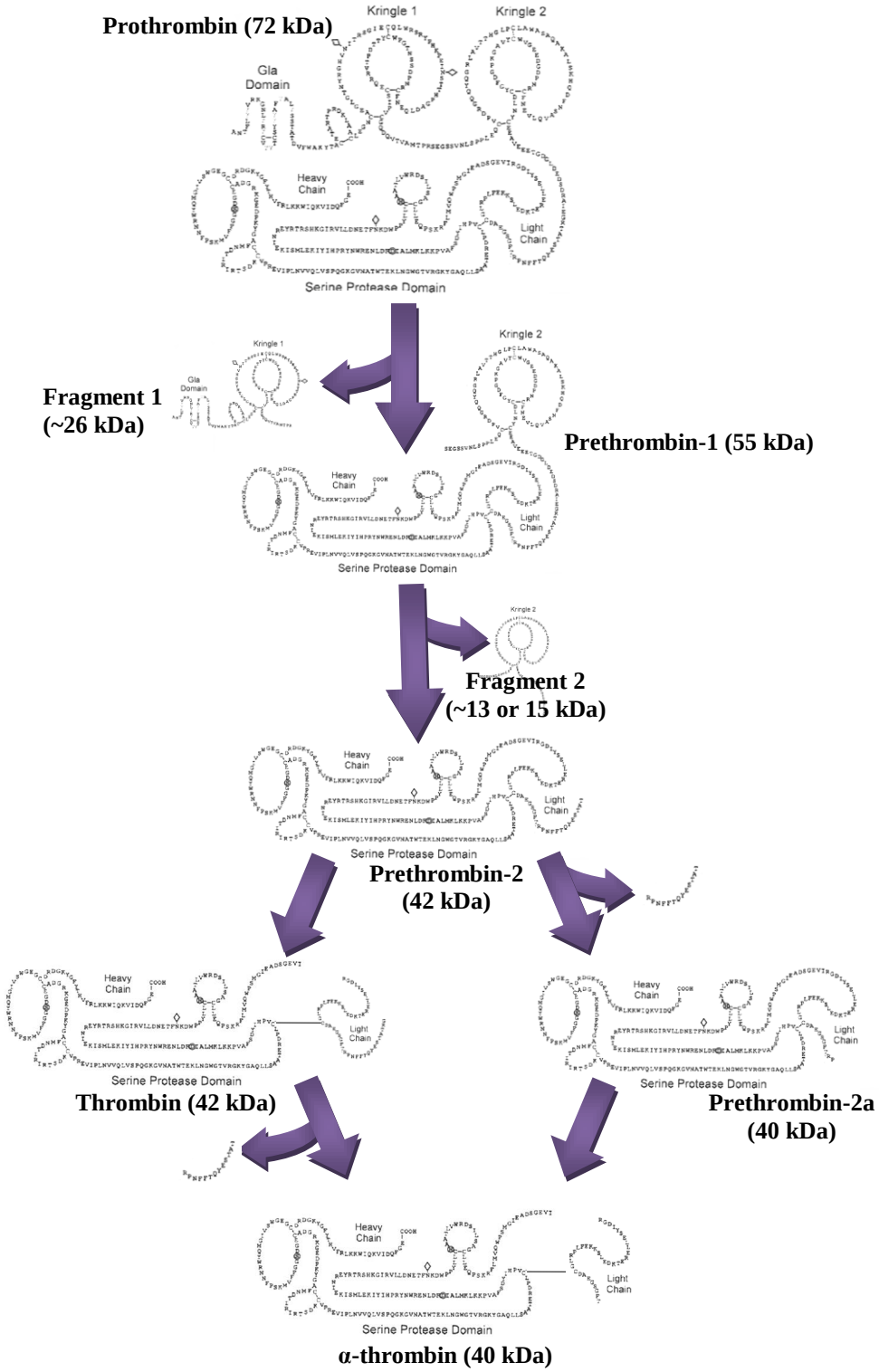

Figure 2.16. Suggested primary pathway of activation of prothrombin by sodium citrate. When activated by sodium citrate, prothrombin is proteolyzed into prethrombin-1 then to prethrombin-2, FIIa, prethrombin-2a or αFIIa. The order of activation after formation of prethrombin-1 is uncertain. This figure modifies the prothrombin schematic published by Davie and Kulman.[1]

The activity of four thrombin solutions, activated by 35% sodium citrate and 0.2% FIIa, containing primarily prethrombin-2a and α-thrombin but also β-thrombin (Figure 2.12, lane 3) was determined by chromogenic assay. The activity was 368 ± 173 U/mg (mean ± standard deviation) which is significantly lower than earlier specific activity reports of 1,400[27] to 4,000 U/mg.[28] Our activities are probably lower than other reports and purchased thrombin references because it contains thrombin, α-thrombin, and the less active β-thrombin rather than a pure thrombin as is in Recothrom.

The activity of citrate activated thrombin was also measured by SDS-PAGE and thromboelastography. Activity was evaluated with regard to the ability of the citrate activated thrombin sample to activate fibrinogen to fibrin and factor XIIIa to its lower molecular weight form. Thrombin formed by 35% sodium citrate appeared to release all of fibrinopeptide B but only a portion of fibrinopeptide A (Figure 2.14A). However, it was able to cleave FXIIIa in the same manner as recombinant thrombin (Figure 2.14B). The lower efficiency of citrate activated thrombin in releasing fibrinopeptide A compared to recombinant thrombin may be due to high number of degradation bands. When evaluated by thromboelastography, citrate activated thrombin created a fibrin clot at equivalent kinetics as the highly purified recombinant thrombin (Figure 2.15). For the SDS-PAGE analysis, thrombin was added by mass; therefore, the recombinant thrombin reactions contained approximately 7-fold more units per ml than the citrate activated thrombin reactions. When dosed at equivalent activity levels as rFIIa in the thromboelastographic analysis, pdFIIa activated by sodium citrate yielded equivalent clotting kinetics and clot strength.

This research examined the activation of prothrombin in the presence and absence of sodium citrate. Thrombin is not responsible for activation of prothrombin in the absence of high salts; rather, thrombin activates trace amount of FX to FXa which subsequently activates prothrombin. FX did result in prothrombin proteolysis; however, it is unclear whether FX directly proteolyzed prothrombin or autocatalytically produced FXa which subsequently activated prothrombin. Despite remaining questions regarding the activation of prothrombin in the absence of sodium citrate, prothrombin activation in the presence of citrate does not appear to be related to FXa. The sequence of activation of prothrombin by sodium citrate did not follow the primary or secondary hemostasis pathways; rather, it followed an alternative pathway with prethrombin-1 as an intermediate. Although activation of prothrombin by sodium citrate is different than physiological mechanisms, the thrombin produced is functional. Further research with a recombinant prothrombin will eliminate contamination of other plasma proteins and thereby allow further elucidation of activation sequences and intermediates.

Acknowledgements

I would like to thank Zurima Zaldua for her observations of the activation of prothrombin in the absence of sodium citrate. UNMC's Protein Structure Core Facility completed all of the N-terminal sequencing. This work was supported by a grant from the Department of Defense titled "Production and Purification of Fibrinogen Components for the Production of a Fibrin Sealant Hemostatic Dressing."

References

1. Davie, E.W. & Kulman, J.D. An overview of the structure and function of thrombin. *Semin.Thromb.Hemost.* **32**, 3 (2006).
2. Crawley, J.T.B., Zanardelli, S., Chion, C.K.N.K. & Lane, D.A. The central role of thrombin in hemostasis. *Journal of Thrombosis and Haemostasis* **5**, 95-101 (2007).
3. Bahou, W.F. Attacked from within, blood thins. *Nature Medicine (New York, NY, United States)* **8**, 1082 (2002).
4. Wolberg, A.S. Thrombin generation and fibrin clot structure. *Blood Rev* **21**, 131-142 (2007).
5. Stenflo, J., Fernlund, P., Egan, W. & Roepstorff, P. Vitamin K dependent modifications of glutamic acid residues in prothrombin. *Proc Natl Acad Sci U S A* **71**, 2730-2733 (1974).
6. Nelsestuen, G.L., Zytkovicz, T.H. & Howard, J.B. The mode of action of vitamin K. Identification of gamma-carboxyglutamic acid as a component of prothrombin. *J Biol Chem* **249**, 6347-6350 (1974).
7. Wu, S.M., Cheung, W.F., Frazier, D. & Stafford, D.W. Cloning and expression of the cDNA for human gamma-glutamyl carboxylase. *Science* **254**, 1634-1636 (1991).
8. Mann, K.G. & Kalafatis, M. Factor V: a combination of Dr Jekyll and Mr Hyde. *Blood* **101**, 20-30 (2003).
9. Krishnaswamy, S., Church, W.R., Nesheim, M.E. & Mann, K.G. Activation of human prothrombin by human prothrombinase. Influence of factor Va on the reaction mechanism. *J.Biol.Chem.* **262**, 3291 (1987).
10. Bishop, P.D., Lewis, K.B., Schultz, J. & Walker, K.M. Comparison of recombinant human thrombin and plasma-derived human a-thrombin. *Semin.Thromb.Hemost.* **32**, 86 (2006).
11. Bukys, M.A. et al. The structural integrity of anion binding exosite I of thrombin is required and sufficient for timely cleavage and activation of factor V and factor VIII. *J.Biol.Chem.* **281**, 18569 (2006).
12. Bukys, M.A. et al. Incorporation of Factor Va into prothrombinase is required for coordinated cleavage of prothrombin by factor Xa. *J Biol Chem* **280**, 27393-27401 (2005).
13. Miletich, J.P., Jackson, C.M. & Majerus, P.W. Properties of the factor Xa binding site on human platelets. *J Biol Chem* **253**, 6908-6916 (1978).
14. Dahlback, B. & Stenflo, J. Binding of bovine coagulation factor Xa to platelets. *Biochemistry (N.Y.)* **17**, 4938-4945 (1978).
15. Nesheim, M.E., Taswell, J.B. & Mann, K.G. The contribution of bovine Factor V and Factor Va to the activity of prothrombinase. *J Biol Chem* **254**, 10952-10962 (1979).
16. Nesheim, M.E., Eid, S. & Mann, K.G. Assembly of the prothrombinase complex in the absence of prothrombin. *J Biol Chem* **256**, 9874-9882 (1981).
17. Kamath, P. & Krishnaswamy, S. Fate of Membrane-bound Reactants and Products during the Activation of Human Prothrombin by Prothrombinase. *J.Biol.Chem.* **283**, 30164 (2008).

18. Fehlhammer, H., Bode, W. & Huber, R. Crystal structure of bovine trypsinogen at 1-8 A resolution. II. Crystallographic refinement, refined crystal structure and comparison with bovine trypsin. *J Mol Biol* **111**, 415-438 (1977).
19. Bode, W., Turk, D. & Karshikov, A. The refined 1.9-A X-ray crystal structure of D-Phe-Pro-Arg chloromethylketone-inhibited human alpha-thrombin: structure analysis, overall structure, electrostatic properties, detailed active-site geometry, and structure-function relationships. *Protein Sci* **1**, 426-471 (1992).
20. Di Cera, E. et al. The Na+ binding site of thrombin. *J Biol Chem* **270**, 22089-22092 (1995).
21. Dang, Q.D., Sabetta, M. & Di Cera, E. Selective loss of fibrinogen clotting in a loop-less thrombin. *J Biol Chem* **272**, 19649-19651 (1997).
22. Boissel, J.P., Le Bonniec, B., Rabiet, M.J., Labie, D. & Elion, J. Covalent structures of beta and gamma autolytic derivatives of human alpha -thrombin. *J.Biol.Chem.* **259**, 5691-5697 (1984).
23. Soslau, G., Goldenberg, S.J., Class, R. & Jameson, B. Differential activation and inhibition of human platelet thrombin receptors by structurally distinct a-, b- and g-thrombin. *Platelets* **15**, 155 (2004).
24. Kornalik, F. & Blomback, B. Prothrombin activation induced by Ecarin - a prothrombin converting enzyme from Echis carinatus venom. *Thromb Res* **6**, 57-63 (1975).
25. Morita, T., Iwanaga, S. & Suzuki, T. The mechanism of activation of bovine prothrombin by an activator isolated from Echis carinatus venon and characterization of the new active intermediates. *J Biochem* **79**, 1089-1108 (1976).
26. Speijer, H., Govers-Riemslag, J.W., Zwaal, R.F. & Rosing, J. Prothrombin activation by an activator from the venom of Oxyuranus scutellatus (Taipan snake). *J Biol Chem* **261**, 13258-13267 (1986).
27. Seegers, W.H., Mc, C.R.I. & Fahey, J.L. Some properties of purified prothrombin and its activation with sodium citrate. *Blood* **5**, 421-433 (1950).
28. Lanchantin, G.F., Friedmann, J.A. & Hart, D.W. The conversion of human prothrombin to thrombin by sodium citrate. Analysis of the activation mixture. *J.Biol.Chem.* **240**, 3276 (1965).
29. Seegers, W.H. Activation of purified prothrombin. *Proc Soc Exp Biol Med* **72**, 677-680 (1949).
30. Seegers, W.H., Mc, C.R. & Fahey, J.L. Some properties of purified prothrombin and its activation with sodium citrate. *Blood* **5**, 421-433 (1950).
31. Lanchantin, G.F., Friedmann, J.A. & Hart, D.W. Esterase and clotting activities derived from citrate activation of human prothrombin. *J.Biol.Chem.* **242**, 2491 (1967).
32. Teng, C.-M. & Seegers, W.H. Activation of factor X and thrombin zymogens in 25% sodium citrate solution. *Thromb.Res.* **22**, 203-212 (1981).
33. Kettner, C. & Shaw, E. Inactivation of trypsin-like enzymes with peptides of arginine chloromethyl ketone. *Methods Enzymol* **80 Pt C**, 826-842 (1981).
34. Mann, K.G. et al. Active site-specific immunoassays. *Blood* **76**, 755-766 (1990).
35. Kettner, C. & Shaw, E. The selective affinity labeling of factor Xa by peptides of arginine chloromethyl ketone. *Thromb Res* **22**, 645-652 (1981).

36. Inan, M. et al. Saturation of the secretory pathway by overexpression of a hookworm (Necator americanus) protein (Na-ASP1). *Methods in Molecular Biology (Totowa, NJ, United States)* **389**, 65 (2007).
37. Zhang, W., Inan, M. & Meagher, M.M. Rational design and optimization of fed-batch and continuous fermentations. *Methods in Molecular Biology (Totowa, NJ, United States)* **389**, 43 (2007).
38. Mann, K.G. Prothrombin. *Methods Enzymol* **45**, 123-156 (1976).

Chapter 3

Characterization of Recombinant Factor XIII Expressed in *Pichia pastoris*

Abstract

Factor XIII A-chain (FXIII), also known as fibrin-stabilizing factor, is important in establishing hemostasis because it crosslinks fibrin during clot formation imparting viscoelastic strength and resistance to lysis. Consequently, FXIII deficiency results in a hemophilia characterized by recurrent bleeding. Its importance in producing a resilient clot indicates that it would be a valuable component in liquid fibrin sealants; therefore, FXIII was produced in *Pichia pastoris.* Rather than producing FXIII, N-terminal sequencing indicated that the yeast expressed FXIIIa which is the active form of the enzyme. This recombinant protein was produced at approximately 0.24 mg per gram of cell mass and purified by His-tag affinity chromatography. While SDS-PAGE and size exclusion chromatography indicate that FXIIIa primarily exists in monomer form with small amounts of aggregates, dynamic light scattering and analytical ultracentrifuge suggest that FXIIIa exists as a trimer in solution. The expressed FXIIIa had a molecular weight of approximately 82 kDa but was rapidly cleaved by thrombin to the 79 kDa. After further incubation, thrombin proteolyzed the expressed FXIIIa into two bands at approximately 25 and 54 kDa which is equivalent to degradation products of plasma-derived material. The recombinant FXIIIa (rFXIIIa) had a specific activity of almost 7,000 U/mg and successfully crosslinked fibrin(ogen) in the presence and absence of thrombin and α_2-antiplasmin (A2AP) to fibrinogen. Thromboelastography showed that the addition of rFXIIIa to fibrinogen and thrombin significantly increased clot strength. These results indicate that rFXIIIa expressed in *Pichia pastoris* successfully functions as a transglutaminase closely mimicking plasma-derived FXIII and may be a good alternative for therapeutic uses.

Introduction

Factor XIII (FXIII) is a coagulation protein located in plasma and on platelets at a ratio between 1:1[1] and 5:1;[2] however, FXIII activity is split evenly between plasma and platelets.[3, 4] Platelet FXIII is a 166 kDa homodimer consisting of two A-chains[3] linked by strong noncovalent bonding.[5] Plasma FXIII is a 326 kDa noncovalently-bound heterogeneous tetramer consisting of two A-chains (82 kDa) and two B-chains (76 kDa)[6-8] held together by strong noncovalent bonds.[5] The A- and B-chains of FXIII are different in structure and function (Table 3.1).

Table 3.1. Structure, function and genetic differences between the A- and B-chains of FXIII.

	A-chain	B-chain
Molecular weight (kDa)[6-8]	82	76.5
Amino acids[9, 10]	731	641
Location[8]	Plasma, platelets, placenta	Plasma
Structure[11]	Globular	Kinked, thin, flexible strand
Carbohydrate[12-14]	None	~8.5% total weight
Disulfide Bridges[7, 10, 14]	None	20
Synthesized by[4, 15-17]	hepatocytes, monocytes, megakaryocytes	hepatocytes
Function[5, 18]	Enzyme: transglutaminase	Stabilization and transport
Domains[14, 19-21]	β-sandwich, catalytic core and two barrels	Ten β glycoprotein-1
Chromosome location[22, 23]	6p24-p25	1q32-q32.1
Kilobases (kb)[9, 10]	160	28
Exons[9, 10]	15	12

Plasma and platelet FXIII A-chains are identical in structure and function.[2, 24, 25] Although the A-chain has six possible asparagine-linked glycosylation sites, none contain carbohydrates.[12, 13] Synthesized by hepatocytes, monocytes and megakaryocytes,[15-17] the A-chain contains four domains: a β-sandwich, catalytic core and two barrels.[20, 21] The B-chain is secreted as a single chain into plasma by hepatocytes where some form complexes with the A-chain[17] and others circulate freely.[5] FXIII tetramer circulates in plasma at approximately 0.07 μM[18] while the B-chain circulates at a concentration

between 14 and 0.24 µM.[26, 27] The A-chain is the catalytic component of the enzyme;[15-17] while the B-chain surrounds the hydrophobic A-chain and is thought to stabilize the enzyme during transport.[5, 18] While A-chain is intertwined into the fibrin clot during its formation,[18] the B-chain is absent.[28]

When plasma FXIII is in the tetramer form, the 36 amino acid[29] activation peptide of one A-chain protects the cysteine in the active site of the other A-chain. This conformation is secured by hydrogen bonds and salt bridges.[20] Plasma and platelet FXIII can be activated by trypsin,[24] papain,[24] platelet acid protease[30] or calpain;[31] however, it is primarily activated into active FXIII (FXIIIa) by thrombin which binds to the A-chains' 4.5 kDa activation peptide[32] and cleaves at Arg37-Gly38 by hydrolysis.[29] During this cleavage, the activation peptide is released.[33] Fibrin and calcium ions then initiate the dissociation of the B-chain to form FXIIIa (Figure 3.1).

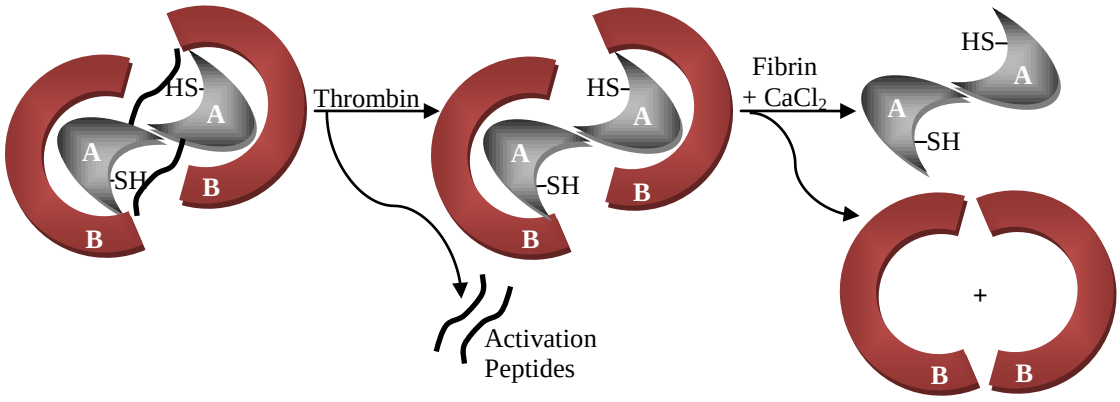

Figure 3.1. Schematic representation of thrombin activation of plasma FXIII. Plasma FXIII is a heterogeneous tetramer of two A- and two B-chains. The activation peptide of each A-chain covers the active site of the other A-chain. Thrombin cleaves the activation peptide exposing the enzymes' active sites. Calcium and fibrin initiate dissociation of the B-chains leaving activated FXIII (FXIIIa).[18]

The presence of calcium greater than 10 mM is critical for activation of FXIII after cleavage by thrombin[34, 35] because it initiates conformational changes resulting in

dissociation of the B-chains[19] and exposure of the active site.[34, 36, 37] The activation to FXIIIa by thrombin is hastened by the presence of fibrin polymers[24, 33, 38-41] which apparently changes its conformation, altering the calcium binding site[42] lowering the calcium requirement to 1.5 mM which is the calcium content in plasma[37, 41] and promoting the dissociation of the B-chain.[40, 43] Both the B-chain of the heterotetramer plasma FXIII[44] and thrombin[45] bind to the γ-chain of fibrinogen which localizes the three integral proteins required to form a fibrin clot in close proximity and disperses FXIII throughout the forming clot.[18] Unlike the fast thrombin activation of platelet FXIII,[46] plasma FXIII activation is significantly slower because the rate is limited by B-chain dissociation.[40, 46-49] This is thought to regulate the activation of FXIII in plasma.[42]

FXIII also known as fibrin-stabilizing factor, is important in establishing hemostasis because it plays a key role in the final stage of coagulation. During this stage, thrombin cleaves fibrinogen into fibrin which polymerizes into a soluble fibrin clot. Thrombin activated Factor XIII (FXIIIa) creates an insoluble clot by crosslinking fibrin polymers.[50] The manner in which FXIIIa recognizes its substrate is unknown;[18] however, once activated, FXIIIa binds to residues 241 to 476 in the αC-domain of fibrin.[51] Fibrin polymers in close proximity are crosslinked by the catalytic triad (Cys314, His373 and Asp396)[21] of FXIIIa which creates an intermolecular γ-glutamyl-ε-lysine bridge between the side-chains of two aligned fibrin molecules (Figure 3.2).[25, 52-56]

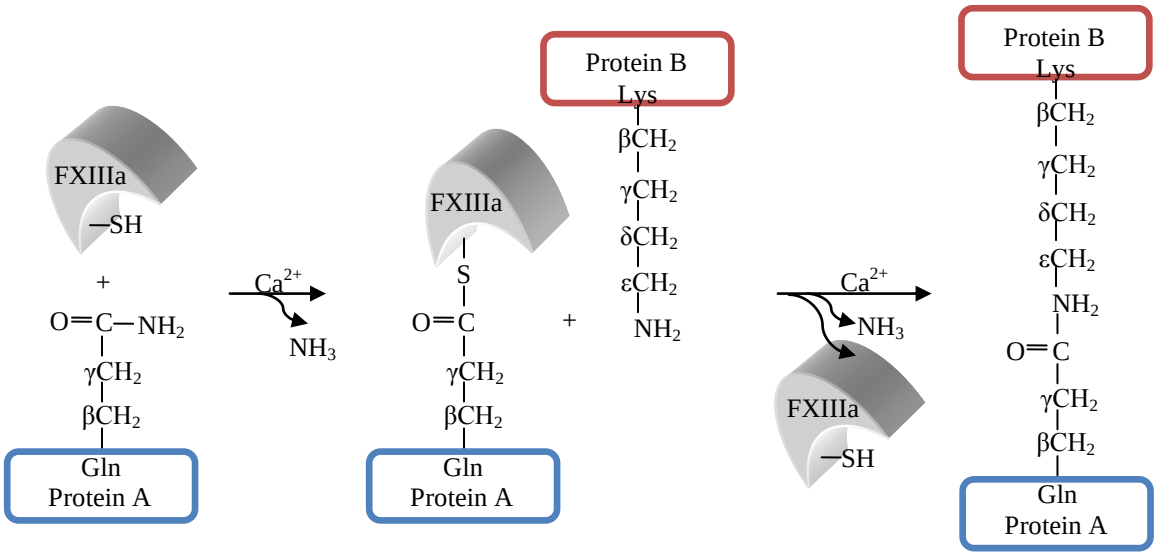

Figure 3.2. Biochemistry of ε-(γ-glutamyl)lysine crosslinking of fibrin molecules by FXIIIa.[18, 25, 37, 54] FXIIIa forms a thioester bond to a specific glutamine residue of the bound molecule, releasing ammonia.[57] This thioester reacts with the primary amine of a lysine residue of another molecule near the catalytic site creating an amide bond.[55, 58]

Aggregation of fibrin monomers aligns the proteins easing the crosslinking process.[59, 60] FXIIIa crosslinks antiparallel[61] fibrin α- and γ-chains with the γ-γ formation proceeding at a much faster rate than the α-α crosslinking.[18, 62, 63] Gln398 or 399 on one fibrin γ-chain crosslinks to Lys406 on an adjacent fibrin γ-chain within 10 minutes[64, 65] which significantly increases clot stiffness."[66, 67] One of four glutamine residues[68-70] and one of 15 lysine residues[71, 72] can be involved in α-chain crosslinking which can take up to 24 hours to form[73] but is important in resisting plasminolysis[74-77] because it yields high viscoelastic strength[18, 62] and insolubility.[62] α- and γ-chains can also be crosslinked; however, this does not greatly affect clot strength.[67] FXIIIa can also crosslink the same sites of fibrinogen but at a slower rate.[24, 78]

In addition to fibrin and fibrinogen, FXIIIa is important in crosslinking α2-antiplasmin,[79] fibronectin,[80, 81] collagen,[80, 82] von Willebrand factor,[83, 84] Factor V[85, 86] and numerous other substrates necessary for clot stabilization, adhering clot to vessel wall,[42]

resistance to lysis and wound healing (Table 3.2).[18] FXIIIa also binds directly to platelets.[87] Platelet FXIII appears to play the key role with respect to creating resistance to lysis.[88]

Table 3.2. FXIII substrates, crosslinking sites, crosslinking molecules and function.[18]

Substrate	Cross-linking Site	Crosslinked with	Function
Fibrin(ogen) γ-chain[64, 65, 89]	Gln398, Gln399 and Lys406	Itself and α-chain	Clot stabilization
Fibrin(ogen) α-chain[68-72]	Gln221, Gln237, Gln328, Gln366 and 15 potential lysines from Lys208 to Lys606	Itself and α-chain	Clot stabilization
α2-Antiplasmin[79]	Gln2	Fibrin α-chain Lys303	Resistance to fibrinolysis
TAFI[79]	Gln2, Gln5, Gln292	Fibrin, itself	Resistance to fibrinolysis
PAI-2[90, 91]	-	Fibrin α-chain Lys148, Lys230, Lys413	Resistance to fibrinolysis
Fibronectin[80, 81]	Gln3	Itself, fibrin, collagen	Migration of cells into the clot; wound healing
Collagen[80, 82]	-	Fibronectin, fibrin	Stabilization of extracellular matrix
Von Willebrand factor[83, 84]	-	Fibrin, collagen	Platelet adhesion to clot
Vitronectin[92, 93]	Gln93	-	-
Thrombospondin[94]	-	Fibrin	-
Factor V[85, 86]	-	Fibrin, platelets	Increased thrombin generation at the clot surface
Actin[95, 96]	-	Fibrin	Clot retraction, stabilization of platelet cytoskeleton
Myosin[97]	-	Itself	
Vinculin[98]	-	Fibrin	
$\alpha_{IIb}\beta_3$[99]	-	Fibrin	Stabilization of platelet and fibrin clot

The depletion of calcium is the only known inhibitor of FXIIIa in physiology;[100] however, there are synthetic inhibitors.[101] FXIIIa is inactivated by thrombin cleaving the A-chain at Lys513 or Arg515[42] resulting in two fragments of 25 and 54 kDa.[8]

The importance of FXIII in the formation of a blood clot is best characterized by the description of issues seen with individuals with FXIII deficiency. Individuals with this disease typically show normal clot formation; however, the fibrin polymers are not crosslinked and are consequently still soluble resulting in short-lived clots in which bleeding recurs 24 to 48 hours after injury.[37, 42, 102] This bleeding and clotting cycle may recur for months.[102] These patients also suffer from other related issues including death from intracranial hemorrhage and atypical wound healing.[42] FXIIIa appears to have several functions:

1. Crosslink the fibrin clot to yield a clot with high viscoelastic strength.[18, 103]
2. Reduce the rate of clot lysis[74-77] by forming the strong clot and crosslinking lysis inhibitors into the clot. Clot lysis is directly and inversely related to the amount of fibrin α-α crosslinking.[24]
3. Weave cell signaling molecules into the clot to encourage wound healing.[104]
4. Crosslink the clot to the vessel wall.[80, 82]

Thromboelastography indicates that FXIIIa prolongs fibrinolysis,[105] reduces time to clot initiation, speeds clotting kinetics and increases viscoelastic strength.[106, 107] Platelets dispersed throughout the clot probably hasten[108] and further stabilize the clot[109] by releasing additional FXIII. Research indicates that FXIII in the platelets is necessary to obtain optimal crosslinking.[110]

A recombinant version of FXIII's A-chain (rFXIIIA) has been expressed in *Saccharomyces cerevisiae*[111-113] as a nonglycosylated homodimer[114] that functions in the same manner as platelet FXIII.[46] This rFXIIIA has been used to examine the kinetic details of fibrin γ-chain crosslinking[113] and evaluated as a drug for treating FXIII

deficiency.[115-117] In clinical trials, the rFXIIIA produced in *Saccharomyces cerevisiae* did not result in serious adverse events or have immunological repercussions after single[115, 116] or multiple[117] intravenous doses. Clinical studies indicate that rFXIIIA infusion into patients with FXIII deficiency restores clot strength and lysis resistance.[116] Preclinical studies also indicate that rFXIII infusion is a beneficial treatment to combat depletion of coagulation proteins following cardiopulmonary bypass surgery.[118] In addition to functioning like native FXIII, after injection, rFXIIIA appears to bind to free-circulating plasma-derived FXIII (pdFXIII) B-chain and circulates as A_2B_2 like native pdFXIII.[115-117]

The research presented in this chapter was designed to test the hypothesis that recombinant FXIII A-chain expressed in *Pichia pastoris* has the same structure, function and activity as its plasma-derived counterpart and rFXIIIA expressed by *Saccharomyces cerevisiae*. Rather than producing FXIII, N-terminal sequencing indicated that the yeast expressed FXIIIa which successfully crosslinked fibrin(ogen) yielding a clot with increased viscoelastic strength.

Materials and Methods

Materials

Purified, plasma-derived prothrombin and plasma-derived FXIII was bought from Enzyme Research Laboratories (South Bend, IN). Recombinant thrombin (Recothrom®) was purchased from Zymogenetics. Materials for the thromboelastograph were purchased from Haemoscope (Niles, IL). Purified recombinant fibrinogen, expressed in the milk of transgenic cows, was obtained from Pharming Group NV (Leiden,

Netherlands). PPACK was purchased from Haematologic Technologies (Essex Junction, VT). Unless otherwise specified, reagents were purchased from Sigma (St. Louis, MO).

Vector construction, expression and purification of FXIIIA in Pichia pastoris

The human Ultimate ORF clone containing the human coagulation factor FXIIIA1 cDNA in the pENTR^{TM}221 vector was purchased from Invitrogen (Clone ID: IOH11901, Carlsbad CA). The following primers were used to obtain FXIIIA gene to subclone in pPICZA intracellular Pichia expression vector. (Forward, 5'-CCAATTGATGCATCATCATCATCATCATTCAGAAACTTCCAGGACCGC-3'; Reverse, 5'-GCGGCCGCTCACATGGAAGGTCGTCTTTGAATC-3'). The forward primer introduced a methionine and six histidine amino acids at the N-terminal of mature FXIIIA peptide. The PCR product was digested with MfeI and NotI and subcloned into pPICZA which was digested with the same enzymes. The DNA sequence of the FXIIIA was confirmed by sequencing the insert fragment. One of the confirming plasmid pPICZA-FXIIIA was linearized with PmeI and transformed into *Pichia pastoris* X-33 host strain and copy number of the clones was determined as described.[119] Varying copy number clones were screened in shake flask culture to confirm intracellular production of FXIIIA protein. The highest producing clone was scaled up to 5 L bench scale. A fed-batch fermentation protocol was followed to optimize FXIIIa production as described by Zhang et al., (2007).[120] At the end of fermentation process the cells were separated by centrifugation (6,000xg) and pellet was stored at -80^{o}C.

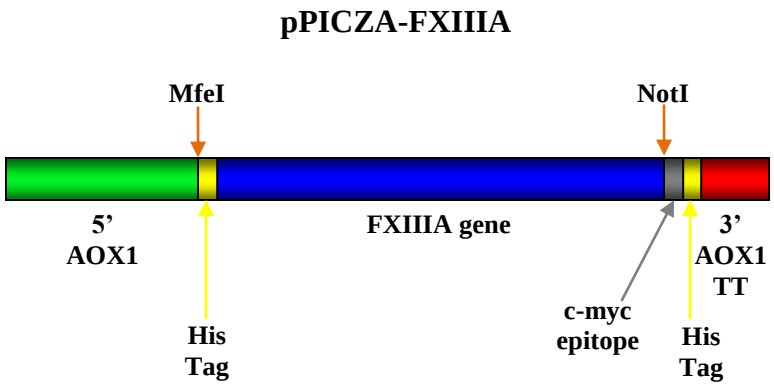

Figure 3.3. Schematic of vector pPICZA-FXIIIA. FXIIIA cDNA (2199 bases) with a six histidine tag (17 bases) on the N-terminal was inserted into the pPICZA vector containing a 5' AOX1 promoter (941 bases), multiple cloning site (79 bases), c-myc epitope (32 bases), six histidine tag (17 bases) and 3' AOX1 transcription termination region (341 bases). The restriction enzyme sites utilized are shown with orange arrows.

Frozen cell paste was processed in 300 gram batches. Cells were lysed in three sets of 100 gram batches. 100 grams of cell paste was resuspended in 100 ml of cold lysis buffer (50 mM Tris-HCL, 10 mM $MgSO_4$, 1 mM EDTA, 10 mM potassium acetate, 1 mM DTT (DL-Dithiothreitol), 2 mM PMSF (phenylmethanesulphonylfluoride) in methanol, pH 9.5). 100 ml (250 g) of 0.5 mm glass beads (Biospec, Bartlesville, OK) were added and the cells. Surrounded by an ice bath, cells were lysed using a BeadBeater Blender (Biospec, Bartlesville, OK) with twenty 20 second on/off cycles. The cell lysate mixture was then centrifuged to remove cellular debris. The lysate from 300 grams of cell paste was combined and purified using the HisBind Purification Kit (EMD Chemicals, Inc., San Diego, CA) with 40 ml of resin slurry. Following purification, rFXIII was dialyzed in 10 mM Tris-HCl, 0.1 mM EDTA, 60 µM polysorbate-20, pH 8.0 in snake-like dialysis membranes and the protein samples were filter-sterilized and concentrated using the Amicon tubes (Millipore, Billerica, MA). The purity of the sample was tested by SDS-PAGE (NuPAGE 12% Bis-Tris) (Invitrogen, Carlsbad, CA)

and immunoblot. The concentration of rFXIII was determined by standard Bicinconic Acid (BCA) methods. The molecular weights of the rFXIII expressed by the yeast and the activated rFXIIIa were calculated based on the amino acid sequence[8] and molecular weights of the amino acids (Table 3.3).

Plasma-derived thrombin preparation

Plasma-derived human prothrombin (Enzyme Research Laboratories, South Bend, IN), was thawed at 37^{o}C. Plasma-derived thrombin (Enzyme Research Laboratories, South Bend, IN) was added at a 1/10 mass to mass thrombin/prothrombin ratio. 0.35 grams of sodium citrate per milliliter of solution was added and then incubated at 37^{o}C on a rotating mixer for five hours. Sodium citrate was removed with PD-10 desalting columns (GE Healthcare, Giles, United Kingdom). Activation of prothrombin to thrombin was confirmed by reducing and nonreducing SDS-PAGE (12% Bis-Tris NuPAGE) (Invitrogen, Carlsbad, CA) stained with Colloidal Blue (Invitrogen, Carlsbad, CA) and Western blot analysis. The concentration of the thrombin solution was determined by standard Bicinconic Acid (BCA) methods. The specific activity was determined by aPTT analysis.

Comparison of pdFXIII and rFXIII by SDS-PAGE and Western blot

Reduced FXIII samples were evaluated by sodium dodecylsulfate-polyacrylamide (SDS-PAGE) gel electrophoresis on 4-12% NuPage® Bis-Tris gels with 2-(N-morpholino)ethanesulfonic acid (MES) running buffer and NuPage® LDS sample buffer which were purchased from Invitrogen (Carlsbad, CA). Reduced samples were treated with NuPage® Sample Reducing buffer (β-mercaptoethanol) (Invitrogen). Samples were

incubated at 74^{o}C for 10 minutes before loading on the gels which were run at 200 volts for one hour. Gels were stained with Colloidal Blue (Invitrogen) or electroblotted onto polyvinylidene fluoride (PVDF) membrane (Millipore, Billerica, MA). Blots were subsequently developed with an anti-human factor XIII subunit A polyclonal antibody made in sheep (US Biologicals, Swampscott, MA) and then an anti-sheep IgG peroxidase conjugate antibody (Sigma, St. Louis, MO).

Dynamic light scattering

Dynamic light scattering was used to identify the radius of gyration of the recombinant FXIII and estimate polydispersity of molecular weights in solution. pdFXIII and rFXIII samples were diluted with 10 mM Tris-HCl, 0.1 mM EDTA, 60 µM polysorbate-20, pH 8.0 to various dilutions. Data were collected at 24^{o}C by a DynaPro^{TM} (Protein Solutions^{TM}) Titan (Wyatt Technologies, Santa Barbara, CA) dynamic light scattering instrument and analyzed by DYNAMICS software (Wyatt Technologies, Santa Barbara, CA) which provided data regarding radius of gyrations and estimated molecular weights of the particles in solution. Four measurements were collected for each sample.

Analytical ultracentrifuge

Sedimentation velocity experiments were performed using a ProteomeLab XL-I analytical ultracentrifuge (Beckman Coulter, Brea, CA) to estimate molecular weights and evaluate aggregation of rFXIII in solution. rFXIII sample, in 10 mM Tris-HCl, 50 mM NaCl, 60 µM polysorbate-20, pH 8.0, was tested at 0.1, 0.3 and 0.5 mg/ml and three speeds (8,000, 10,000 and 12,000 rpm) and three wave lengths (275, 280 and 285 nm) at 20^{o}C. 110 µl rFXIII and 125 µl of the corresponding buffer were loaded in triplicate into

cells with sapphire windows and a 6-channel equilibrium centerpiece. Cells were spun in an An-50 Ti 8-hole rotor and run for 22 hours at each speed collecting data at 20 and 22 hours. The partial specific volume of 0.73 ml/g was calculated for the A subunit of FXIII was calculated from the amino acid sequence as described by Perkins (1986).[121] Data was analyzed using Microcal Origin 6.0 software.

Size exclusion chromatography

Size exclusion chromatography (SEC) was also utilized to estimate molecular weight and possible aggregation of rFXIII. Bovine serum albumin (Sigma, St. Louis, MO), immunoglobulin A (IgA) (Sigma, St. Louis, MO) and immunoglobulin G (IgG) (Green Mountain Antibodies, Burlington, VT) were exchanged into 20 mM Tris-HCl, 200 mM NaCl, 60 μM Tween 20, pH 7.0 and rendered 1.94 mg/ml by ultracentrifugation. After being passed through a 0.20 μm nylon filter (Millipore, Billerica, MA), 0.5 ml of each sample were sequentially passed through a TSK-G3000SW_{xL} (Tosoh Biosciences, South San Francisco, CA) column (14 ml, 30 cm length, 7.8 mm ID) attached to a Knauer HPLC System at 0.5 ml/min for 45 minutes and data were collected by a photodiode array (PDA) with a 1 mm flow cell and analyzed by EZChrom Elite software. rFXIII (0.5 ml at 1.94 mg/ml) in 20 mM Tris-HCl, 200 mM NaCl, 60 μM Tween 20, pH 7.0 was also subsequently passed through the column using the same method. The EZChrom Elite software was used to overlay the tracings and match the heights of the primary peaks. Retention times of the primary peaks of the known samples were obtained from the EZChrom Elite software and plotted in Excel. A linear trend line was fit and rFXIII molecular weights estimated from resultant retention times. Purification products were analyzed by SDS/PAGE and Western blot with an anti-FXIII antibody (US Biologicals,

Swampscott, MA). The percentage of rFXIII at different molecular weights was estimated by determining the mass of rFXIII in each peak by SDS-PAGE.

Activation and inactivation of rFXIII by rFIIa

The ability of the recombinant FXIII to be activated and inactivated by rFIIa was evaluated by SDS-PAGE by a similar procedure previously described.[111] rFXIII (final concentration: 0.67 mg/ml) was incubated with rFIIa (60 U/ml) in Ringers solution (155 mM NaCl, 5 mM KCl, 2 mM $CaCl_2$, 1 mM $MgCl_2$) for 0, 5, 15, 30, 60, 120, 180, 240 and 360 minutes at 37^{o}C. The activation/inactivation reaction was halted by the addition of PPACK (final concentration: 5 μM). For the zero time point, rFIIa and PPACK were added at the same time. Samples were evaluated by sodium dodecylsulfate-polyacrylamide (SDS-PAGE) gel electrophoresis on 4-12% NuPage® Bis-Tris gels with 2-(N-morpholino)ethanesulfonic acid (MES) running buffer, NuPage® LDS sample buffer and NuPage® Sample Reducing buffer (β-mercaptoethanol) (Invitrogen, Carlsbad, CA). Samples were incubated at 74^{o}C for 10 minutes before loading on the gels which were run at 200 volts for one hour and stained with Colloidal Blue (Invitrogen, Carlsbad, CA) or electroblotted onto polyvinylidene fluoride (PVDF) membrane (Millipore, Billerica, MA) by applying 30 volts for one hour and stained with Colloidal Blue. Each band was excised and the first ten amino acids in the N-terminal were sequenced by Edman degradation with an Applied Biosystems 494 Procise automated sequencer. N-terminal sequencing was performed by the University of Nebraska Medical Center's Protein Structure Core Facility.

Chromogenic activity assay

The activity of rFXIII was determined using a Pefakit® Factor XIII Incorporation Assay (Pentapharm, CT) by comparing rFXIII to a plasma-derived reference FXIII (Enzyme Research Laboratories, South Bend, IN). rFXIII was diluted to 0.055, 0.55, 5.5, 55 and 550 ng/ml with Tris buffered saline included in the kit. FXIII is activated to FXIIIa by thrombin in wells coated with fibrinogen in the presence of 5-biotinamidopentylamin (BAPA). FXIIIa crosslinks BAPA to fibrin(ogen) which is subsequently bound by streptavidine-alkaline phosphatase conjugate (Strept-AP). Finally, addition of alkaline phosphatase produces p-nitrophenol and phosphate from p-nitro phenyl phosphate (pNPP) which can be detected at 405 nm.

FXIIIa crosslinking ability

The ability of the recombinant FXIII to catalyze γ-γ crosslinking of fibrinogen and fibrin was analyzed by a similar procedure previously described.[122] Briefly, rFI (final concentration: 0.38 mg/ml) was incubated with pdFXIII or rFXIII (final concentration: 0.01 mg/ml) and pdFIIa (5 U/ml) in Ringers solution (155 mM NaCl, 5 mM KCl, 2 mM $CaCl_2$, 1 mM $MgCl_2$) for 0, 5, 15, 30 and 60 minutes at 37^{o}C. rFI was also incubated with pdFIIa without FXIII. Crosslinking of fibrinogen was also tested by incubating rFI (0.38 mg/ml) and rFXIIIa (0.014 mg/ml) in Ringers solution for 0, 5, 15, 30, 60, 120 and 240 minutes. The reactions were halted by the addition of NuPage® Sample Reducing Buffer (β-mercaptoethanol) (Invitrogen, Carlsbad, CA) and NuPage® LDS buffer and incubation at 74^{o}C for 10 minutes. For the zero time point, the reaction buffers were added immediately after the addition of thrombin. Crosslinking was studied

by reducing SDS-PAGE (12% Bis-Tris NuPAGE) which were run at 200 volts for one hour and stained with Colloidal Blue (Invitrogen, Carlsbad, CA).

The ability of FXIIIa to covalently crosslink α_2-antiplasmin (A2AP) to rFI was analyzed by SDS-PAGE and immunoblot. rFI (0.38 mg/ml) was incubated with rFXIIIa (98 U/ml, 0.014 mg/ml) in the presence and absence of A2AP (0.51 mg/ml, 1 mol A2AP per mol rFI) in Ringers solution (155 mM NaCl, 5 mM KCl, 2 mM $CaCl_2$, 1 mM $MgCl_2$) for 90 minutes at 37^{o}C. The crosslinking reaction was halted by the addition of NuPage® Sample Reducing Buffer (β-mercaptoethanol) (Invitrogen, Carlsbad, CA) and NuPage® LDS buffer and incubation at 74^{o}C for 10 minutes. Crosslinking was studied by reducing SDS-PAGE (4-12% Bis-Tris NuPAGE) stained with Colloidal Blue (Invitrogen, Carlsbad, CA) and immunoblot with an anti-A2AP antibody (US Biologicals, Swampscott, MA).

Clot formation by thromboelastography

The ability of the recombinant FXIII to catalyze crosslinks and thereby increasing clot stiffness was evaluated by thromboelastography (TEG) which was performed on solutions containing purified rFXIII, rFI and pdFIIa with a Thromboelastograph® (TEG®) Hemostasis System 5000 series (Haemoscope Corp., Niles, IL). Clotting strength and kinetics of purified rFXIII with rFI and pdFIIa were evaluated. rFI (final concentration: 8.56 mg/ml) was transferred to a single-use TEG cup maintained at 37^{o}C by the instrument. rFXIII (final concentration: 2,429 U/ml, 0.35 mg/ml) was added. $CaCl_2$ (final concentration: 11 mM) and Ringers solution (155 mM NaCl, 5 mM KCl, 2 mM $CaCl_2$, 1 mM $MgCl_2$, added to standardize volume in cup) was added followed quickly by pdFIIa (final concentration: 52.8 U/ml) to initiate clot formation. Data were collected

every five seconds for 30 minutes by the TEG interfaced with a computer. The TEG Analytical Software (version 4.2.2, Haemoscope, Niles, IL) collected the time to clot initiation (R), the time to achieve a clot firmness of 20mm (K) and the maximal clot strength (MA). The instrument was calibrated each day of use. Each sample was run in triplicate so means and standard deviations could be calculated. The data was exported and analyzed in Microsoft® Excel.

Results

rFI and pdFIIa characterization

SDS-PAGE and immunoblots indicated rFI had a purity of greater than 98% (data not shown). The pdFIIa prepared by citrate activation was comprised of α-thrombin and fragments as per SDS-PAGE. Chromogenic assay yielded a specific activity of 528 U per mg.

Expression and purification of rFXIII

DNA sequencing indicated that the gene of the FXIII A-chain was successfully inserted into the cassette prior to transformation into *Pichia pastoris*. Clones had between one and five gene copies. rFXIII was produced at greater than 0.24 mg per gram of cell mass by clones with four gene copies. rFXIII was located in the cell inclusion body and could be successfully extracted and purified by His-tag with affinity chromatography. Typical purification products are shown in Figure 3.4. When grown in a flask, the yeast produced a 36 kDa protein that is also purified (Figure 3.4, lane 9); however, this protein did not alter rFXIII's activity and could be removed by size

exclusion chromatography. This protein was not present when the yeast was grown in a fermentor (data not shown) yielding a greater than 98% purity. The final yield following purification, dialysis and concentration steps were approximately 0.24 mg rFXIII per gram cell paste.

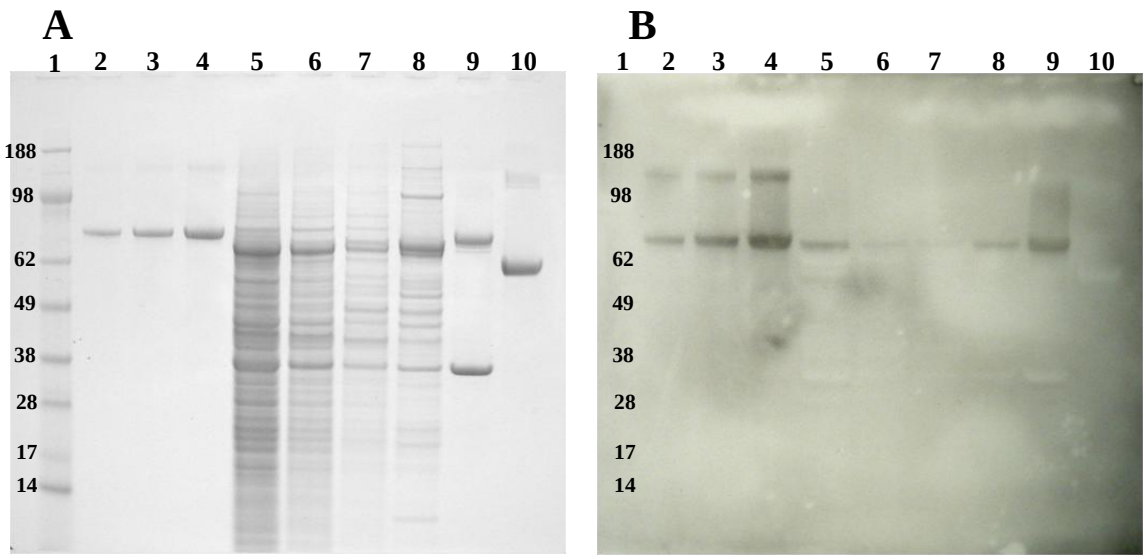

Figure 3.4. Purification of rFXIII as analyzed by reducing SDS-PAGE and immunoblot. SDS-PAGE (A) and immunoblot (B) under reducing conditions. Lane 1: molecular weight marker. Lanes 2, 3 and 4: 0.5, 1, and 2 µg purified rFXIII. Lane 5: cell lysate. Lane 6: loading flow through. Lanes 7 and 8: wash 1 and 2. Lane 9: elution. Lane 10: bovine serum albumin.

Comparison of pdFXIII and rFXIII by SDS-PAGE and western blot

The rFXIII A-chain is almost identical to the A-chain of plasma-derived FXIII (pdFXIIIA) by SDS-PAGE analysis. Under nonreducing (Figure 3.5A) and reducing (Figure 3.5B) conditions, rFXIII is at the same molecular weight (~82,000 Da) as pdFXIIIA. pdFXIII also has a B-chain that is visible at a molecular weight of approximately 60 kDa under nonreducing conditions but is approximately 80 kDa under reducing conditions due to the numerous disulfide bridges. Only the A-chain is expressed in the yeast.

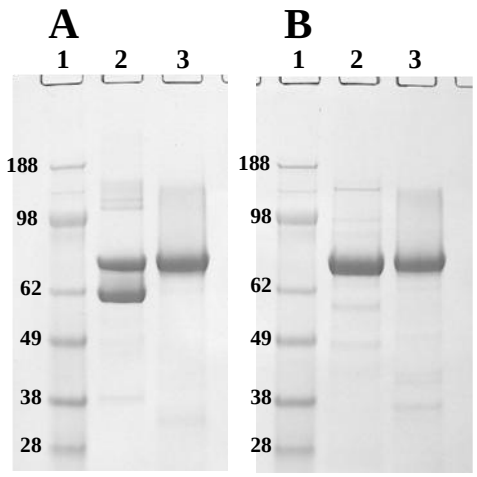

Figure 3.5. Plasma-derived and recombinant Factor XIII by SDS-PAGE. SDS-PAGE gels under nonreducing (A) and reducing (B) conditions. Lane 1: molecular weight marker. Lane 2: pdFXIII. Lanes 3: rFXIII.

Molecular weight estimates of expressed protein

The recombinant protein expressed by the yeast should be FXIII with the His-tag designed into the gene and the myc epitope and His-tag from the yeast vector (Figure 3.3). When the activation peptide of FXIII is cleaved by thrombin, the resulting protein should contain FXIIIa with the myc epitope and His-tag from the yeast vector. The molecular weights of these two products were calculated based on the amino acid sequence[8] and molecular weights of the amino acids (Table 3.3). The expressed rFXIII should have an approximate molecular weight of 85 kDa. The pPICZA vector does not contain any known thrombin cleavage sites; therefore, once cleaved by thrombin, the molecular weight should drop to 82 kDa.

Table 3.3. Molecular weight estimations of expressed rFXIII and rFXIIIa.

Amino Acids	Molar Mass (g/mol)	rFXIII*	rFXIIIa*	myc epitope + His-tag	rFXIIIa without myc epitope + His-tag
Alanine	71.08	38	34	1	33
Arginine	156.19	45	41	0	41
Asparagine	114.10	41	38	1	37
Aspartic Acid	115.09	49	47	2	45
Cysteine	103.14	9	9	0	9
Glutamic Acid	129.12	52	49	3	46
Glutamine	128.13	27	26	1	25
Glycine	57.05	50	47	0	47
Histidine	137.14	20	20	6	14
Isoleucine	113.16	39	39	1	38
Leucine	113.16	50	48	2	46
Lysine	128.17	39	39	1	38
Methionine	131.20	18	18	0	18
Phenylalanine	147.18	32	31	0	31
Proline	97.12	33	29	0	29
Serine	87.08	48	45	2	43
Threonine	101.11	45	42	0	42
Tryptophan	186.21	15	15	0	15
Tyrosine	163.18	29	29	0	29
Valine	99.13	72	68	1	67
Estimated Molecular Weights (Da)		**85,483**	**81,591**	**2,495**	**79,097**

* The expressed rFXIII should contain two His-tags and the myc epitope. rFXIIIa should contain one His-tag and the myc epitope.

Aggregation/molecular weight analysis (SDS-PAGE, DLS, AUC, SEC)

SDS-PAGE, dynamic light scattering (DLS), analytical ultracentrifuge (AUC) sedimentation equilibrium and size exclusion chromatography were utilized to identify different molecular weight species of rFXIII in solution (Table 3.3). Dynamic light scattering indicated that rFXIII existed in solution as a single molecular weight species with a mean molecular weight estimate of 228.75 ± 18.39 kDa for rFXIII compared to 381.20 ± 110.63 for pdFXIII. Analytical ultracentrifuge estimated FXIII in solution at 241.0 ± 48.6 kDa. SDS-PAGE and SEC suggested rFXIII exists primarily as a monomer with some aggregates (Table 3.4). SDS-PAGE shows rFXIII with a molecular weight of approximately 80 and 160 kDa (Figure 3.4B, Lanes 2, 3 and 4).

Table 3.4. Molecular weight estimates of rFXIII in solution by multiple techniques.

Technique	Estimated MW Mean ± Standard Deviation (kDa)	Primary Species	Secondary Species
SDS-PAGE	~80 and ~160	Monomer	Dimer
Dynamic Light Scattering	229 ± 18	Trimer	
Analytical Ultracentrifuge	241 ± 49	Trimer	
Size Exclusion Chromatography	58, 183, 255, 365	Monomer	Trimer, Tetramer, Hexamer

The retention time of rFXIII in a size exclusion column was compared to retention times of three proteins with known molecular weights: BSA (~66 kDa monomer), IgG (~150 kDa) and IgA (~300 kDa) (Figure 3.6). IgA (blue) yielded a single peak while IgG (green) yielded one primary peak and two small peaks. BSA (black) yielded a primary monomer peak and a secondary peak which appears to be aggregation of two molecules. The retention times of the primary peaks of BSA, IgG and IgA were plotted against their molecular weights and a linear trend line (R^2 = 0.9992) was fit. rFXIII molecular weights estimated from resultant retention times of peaks seen in the SEC tracing (Figure 3.6 inset) were calculated using the equation for the trend line. SEC suggests multiple molecular weights. 61.0% of the rFXIII exited the column at 18.10 minutes (~58 kDa), 36.6% at 15.28 minutes (~183 kDa), 1.7% at 13.68 minutes (~255 kDa) and 0.7% at 11.22 minutes (~365 kDa).

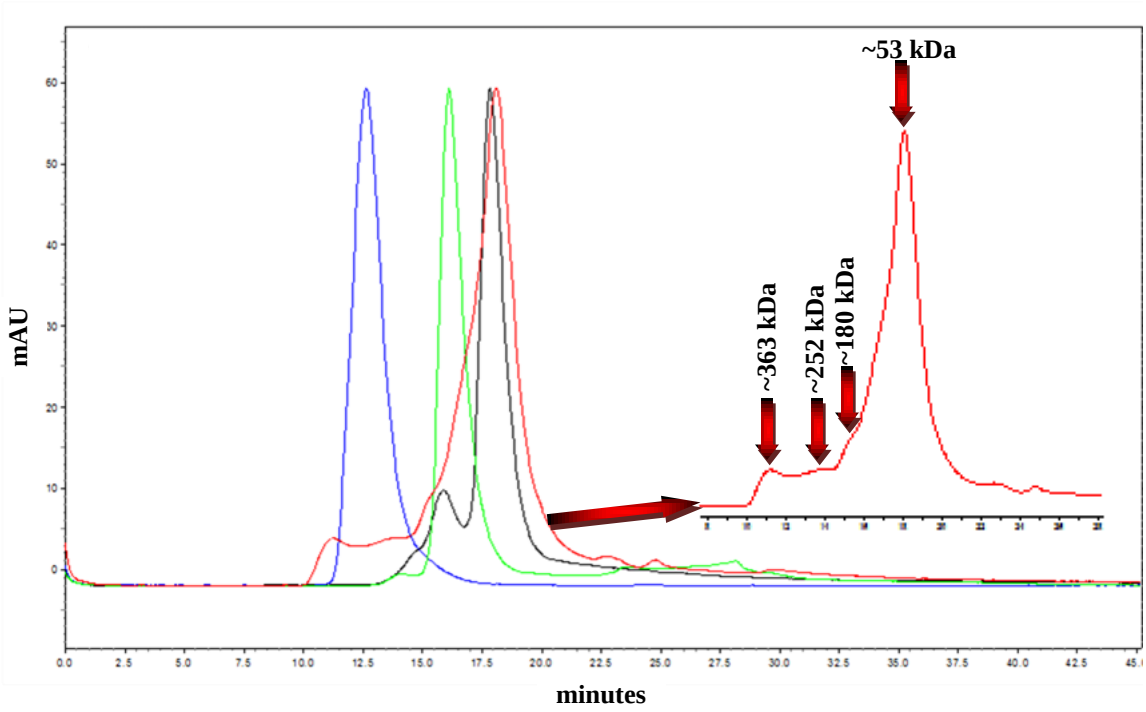

Figure 3.6. Overlaid tracing of proteins analyzed by size exclusion chromatography and individual tracing of rFXIII (insert). BSA (~66 kDa monomer, black), IgG (~150 kDa, green) and IgA (~300 kDa, blue) were passed through an SEC column to yield tracings of known molecular weights. rFXIII was then passed through the column (red) and estimated molecular weights calculated from a linear trend line (R^2 = 0.9992) produced with results from the known samples.

Activation and inactivation of rFXIII by thrombin

The activation and inactivation of rFXIII by thrombin was evaluated by SDS-PAGE by a similar procedure previously described and yielded similar results (Figure 3.7).[111] Before being treated with rFIIa, rFXIII consisted of a single band at approximately 82 kDa. Within five minutes of incubation with thrombin, a second band appears with a molecular weight approximately 3 kDa lower than the original band. By 15 minutes, a majority of the protein is approximately 79 kDa; however, very little has been inactivated. Between 30 and 360 minutes incubation, the protein is degraded into two fragments visible at approximately 25 and 54 kDa.

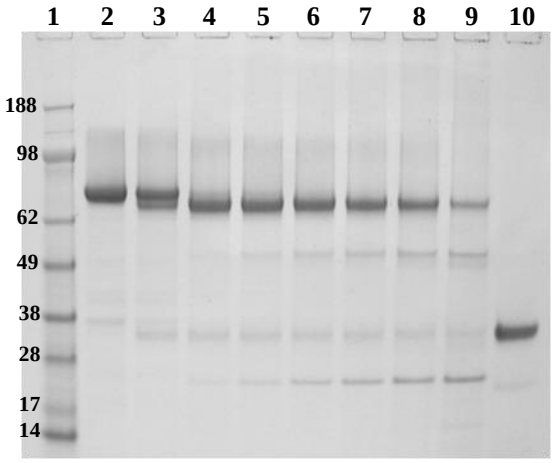

Figure 3.7. Recombinant Factor XIII cleavage by thrombin. SDS-PAGE gel analysis of rFXIII (0.67 mg/ml) and rFIIa (60 IU/ml) under reducing conditions. Lane 1: molecular weight marker; Lanes 2 through 9: Time periods 0, 5, 15, 30, 60, 120, 240 and 360 minutes. Lane 10: rFIIa.

The N-terminal amino acids of the bands at ~82, ~79, ~54 and ~25 kDa were sequenced (Table 3.5 and Figure 3.8). The first 10 residues of the bands at approximately 54 and 79 kDa are consistent with the primary FIIa cleavage site that yields FXIIIa and the first fragment. The first 10 residues of the 25 kDa band is consistent with the second FIIa cleavage site. N-terminal amino acid sequence analysis of the 82 kDa band, however, indicates the presence of multiple proteins. The most abundant protein in that band has a 10 residue sequence consistent with FXIIIa. The other possible sequences do not match the zymogen or any other expected sequence.

Table 3.5. N-terminal amino acid sequences of purified FXIII expressed by yeast.

Approximate Molecular Weight by SDS-PAGE (kDa)	Amino Acid Sequence	Identity
~82	GVNLQEFLNVTI	FXIIIa + c-myc epitope and His tag?
~79	GVNLQEFLNV	FXIIIa
~54	GVNLQEFLNV	FXIIIa N-terminal after FIIa clip (K513-S514)
~25	SPSNVDMXFE	FXIIIa C-terminal after FIIa clip (K513-S514)

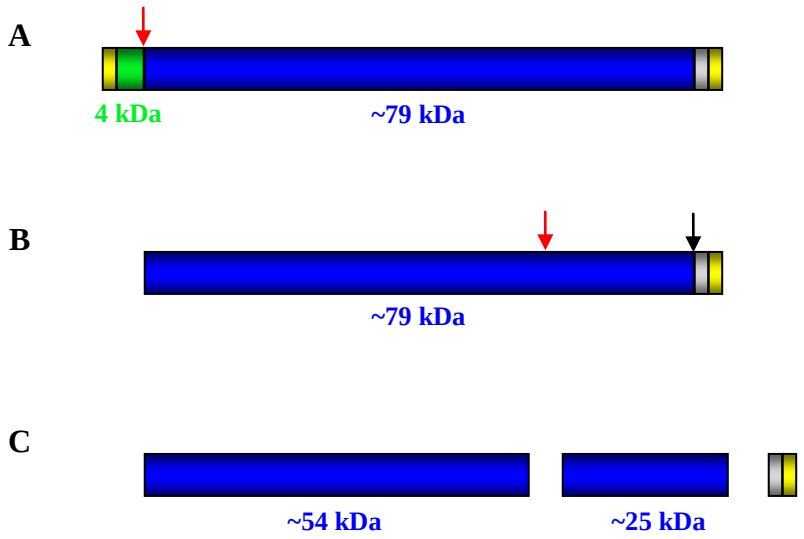

Figure 3.8. Linear model of the expected and actual molecules expressed by yeast and the subsequent degradation products. Schematic of the expected FXIII expressed by yeast (A), FXIIIa molecule purified from yeast (B), and degradation products of FXIIIa (C). FXIII is composed of an activation peptide (green) and the remainder of the molecule (blue) which is designated FXIIIa in the absence of the activation peptide. His-tags are designated in yellow and the c-myc epitope in grey. The known thrombin cleavage sites are indicated by red arrows and the suspected site by a black arrow.

Chromogenic activity assay

The activity of rFXIIIa was determined using a Pefakit® Factor XIII Incorporation Assay. The activity of rFXIIIa purified within two months of the activity test yielded a specific activity of 6,940 ± 2,272 U/mg.

γ-γ crosslinking of fibrin(ogen) by FXIIIa

γ-γ crosslinking of fibrinogen by FXIIIa was analyzed by SDS-PAGE as previously described.[122] γ-chain dimers begin forming within a couple of seconds when catalyzed by either pdFXIII (Figure 3.9A) or rFXIIIa (Figure 3.9B). After 5 minutes, a majority of the γ-chains were crosslinked and the remaining chains were slowly converted to γ-γ dimers over the next 55 minutes. pdFXIII and rFXIIIa catalyze the formation of γ-γ dimers at similar rates as seen by the disappearance of the monomer and appearance of the dimer. The α-chain monomer is also disappearing for both samples resulting in higher molecular weight bands. γ-γ dimers were not formed when pdFXIII or rFXIIIa were added (Figure 3.9A and B, lane 8). When rFI and rFXIIIa are incubated in the absence of thrombin, γ-γ crosslinking is visible within seconds (Figure 3.9C, lane 3). Over the following 60 minutes, the α- (~67 kDa) and γ-chains (~47 kDa) gradually decrease while the band at ~94 kDa and smearing at the top of the wells darken.

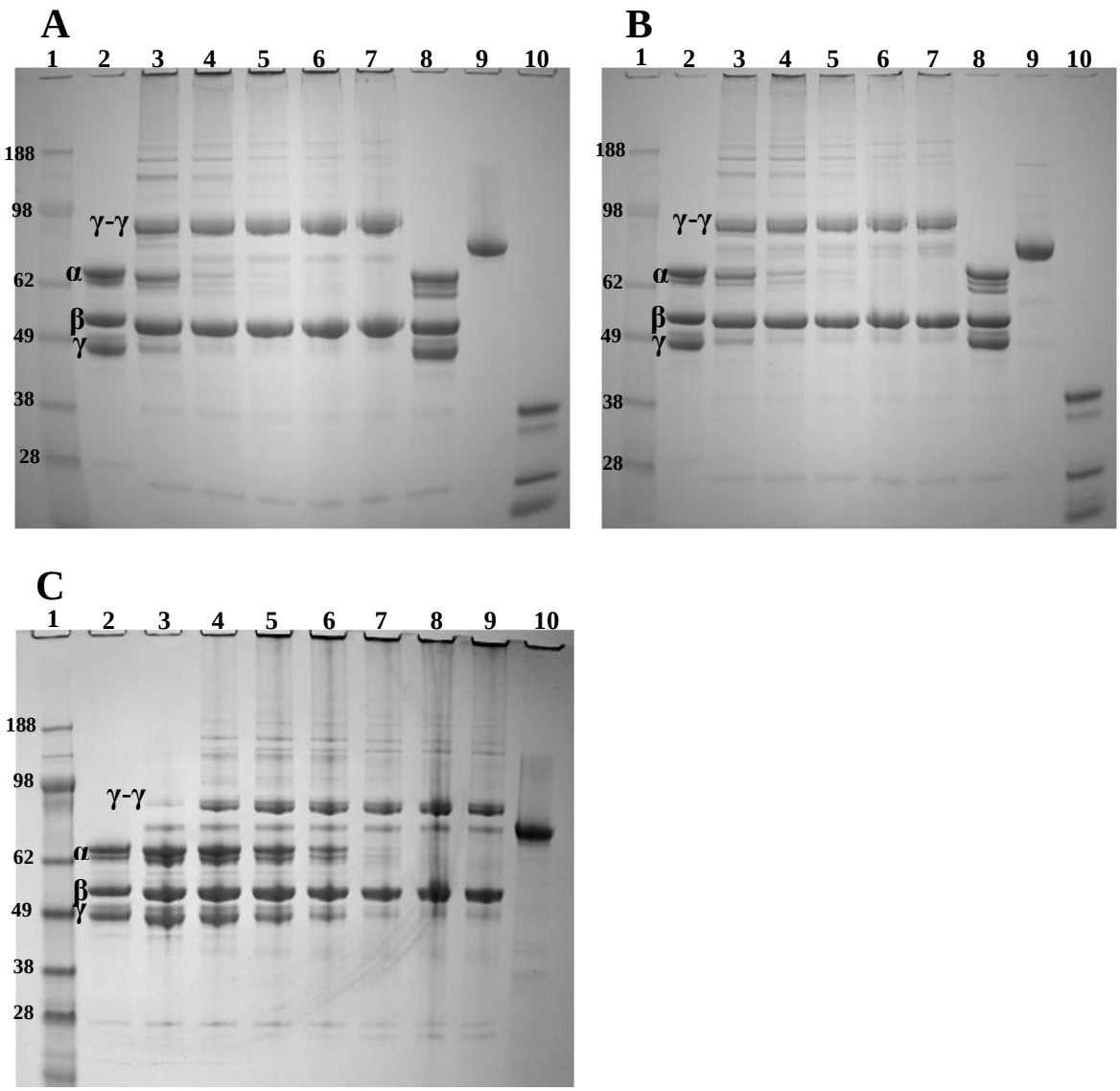

Figure 3.9. Ability of rFXIIIa to crosslink fibrin and fibrinogen γ-chain by reducing SDS-PAGE. Formation of fibrin γ-chain crosslinks was analyzed by SDS-PAGE gels under reducing conditions for clots created with rFI, pdFIIa and pdFXIII (A), rFI, pdFIIa and rFXIIIa (B), and rFI and rFXIIIa in the absence of thrombin (C). Lane 1: molecular weight marker. Lane 2: rFI sample prior to incubation with FXIII and pdFIIa. For panels A and B, Lanes 3 through 7: rFI, FXIII and pdFIIa incubated for 2 seconds, 5, 15, 30 and 60 minutes. Lane 8: rFI incubated with pdFIIa for 60 minutes. Lane 9: FXIII sample prior to incubation with rFI and pdFIIa. Lane 10: pdFIIa sample prior to incubation with FXIII and rFI. For panel C, Lanes 3 through 9: rFI and rFXIIIa incubated for 2 seconds, 5, 15, 30, 60, 120 and 240 minutes. Lane 10: FXIII sample prior to incubation with rFI and pdFIIa.

The ability of rFXIIIa to covalently crosslink α_2-antiplasmin (A2AP) to rFI was analyzed by SDS-PAGE and immunoblot (Figure 3.10). rFI incubated with A2AP in the absence of rFXIIIa have multiple bands all below approximately 70 kDa (Figure 3.10A,

lane 7) with the A2AP band at ~62 kDa (Figure 3.10B, lane 7). When rFI is incubated with rFXIIIa in the presence or absence of A2AP, bands appear above 70 kDa (Figure 3.10A, lanes 8 and 9, respectively). Incubation of rFI with rFXIIIa and A2AP results in multiple A2AP bands (Figure 3.10A, lane 9). The largest band is at approximately 62 kDa followed by bands at ~130 and ~200 kDa indicating A2AP crosslinking to fibrinogen's α-chain and α-α crosslinking.

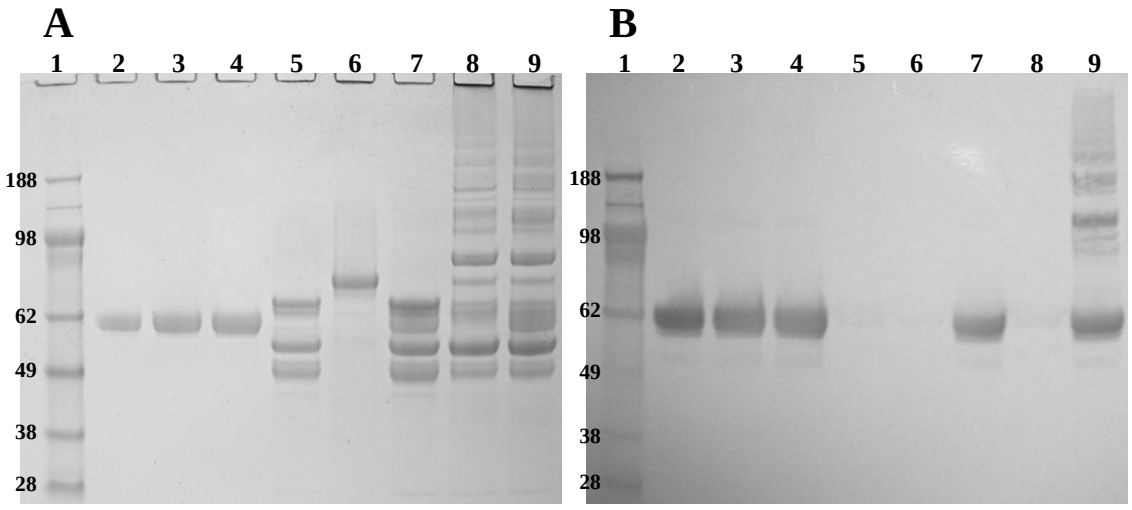

Figure 3.10. Ability of rFXIIIa to covalently crosslink A2AP to rFI by SDS-PAGE and immunoblot. The ability of A2AP to covalently bind to rFI was analyzed by SDS-PAGE (A) and an anti-A2AP immunoblot (B). Lane 1: molecular weight marker. Lanes 2, 3 and 4: 0.5, 1.0 and 1.5 µg A2AP, respectively. Lane 5: rFI. Lane 6: rFXIIIa. Lane 7: rFI incubated with A2AP. Lane 8: rFI incubated with rFXIIIa. Lane 9: rFI incubated with rFXIIIa and A2AP.

Clot formation by thromboelastography

The role FXIII plays in clot formation was evaluated by thromboelastography (TEG) (Figure 3.11). The kinetics and strength of polymerized fibrin formed by rFI and rFIIa were measured when in the presence or absence of rFXIII. The time to clot initiation of rFI treated with rFIIa in the absence of rFXIII was 21.7 ± 2.9 seconds compared to 18.3 ± 5.8 seconds in the presence of rFXIII. Maximal clot strength increased from 1,345.2 ± 298.2 to 8,637.3 ± 867.2 dynes/sec when rFXIII is added.

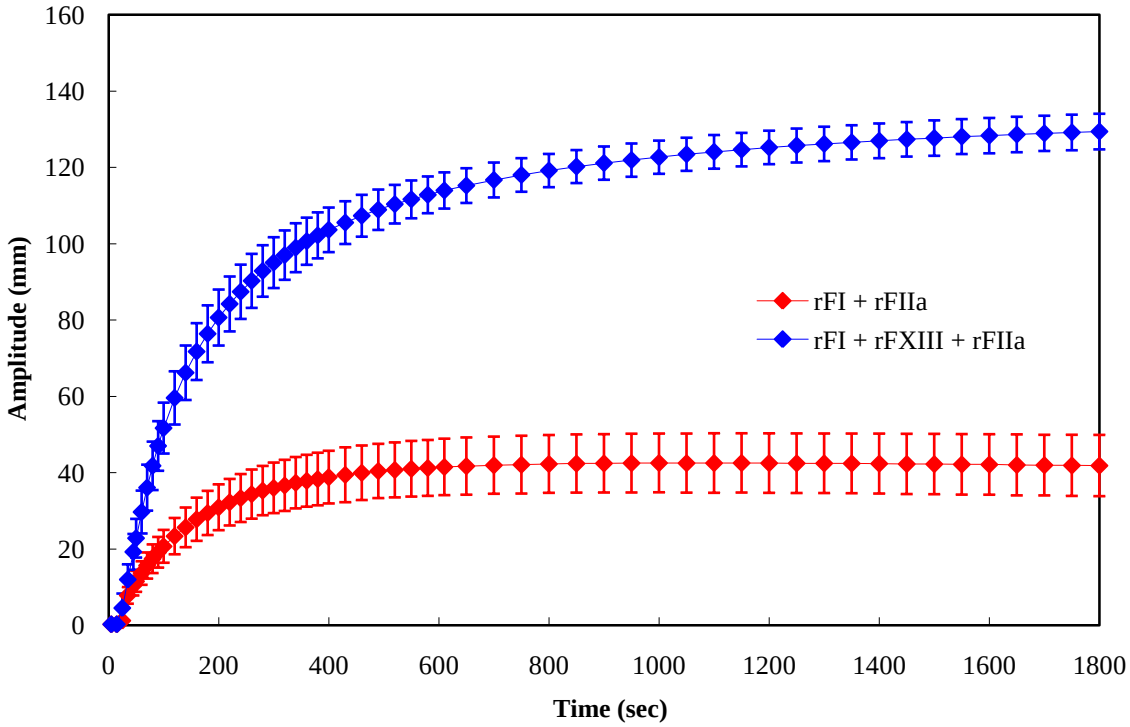

Figure 3.11. Analysis of the effect of rFXIIIa on clot strength by thromboelastography. TEG monitored the change in clot strength over time of recombinant fibrinogen (8.56 mg/ml) activated by recombinant thrombin (52.8 U/ml) with (blue) and without (red) rFXIII (0.35 mg/ml). Data are expressed as mean +/- standard deviation.

Discussion

Pichia pastoris is widely used to produce recombinant proteins for research and medical purposes because it can be cultivated to high density and efficiently secrete protein.[123, 124] The FXIII A-chain does not exhibit glycosylation; therefore, differences in glycosylation between mammalian cells and yeast is not a concern.[125] Consequently, this production system was selected as a possibility to produce abundant quantities of FXIII for use as therapeutics.

Initially, the gene to the A-chain of FXIII (FXIIIA) was inserted into yeast in a vector designed to secrete the recombinant protein into the culture medium. Numerous researchers have successfully used the same α-factor secretion signal from

Saccharomyces cerevisiae to secrete recombinant proteins from *Pichia pastoris.*[126-128] FXIII was expressed by the yeast but not secreted. This may indicate that the protein was not folded properly by the endoplasmic reticulum (ER).[127, 129, 130] Consequently, FXIIIA gene was inserted into a vector for intracellular expression. The PCR amplified DNA indicated that the full and unmutated FXIIIA gene was present when inserted into the yeast.

Initial analyses of the expressed and purified protein were consistent with naturally occurring inactivate FXIII. The molecular weight of the expressed protein was approximately 82 kDa; however, N-terminal sequencing identified this band as the activated enzyme: FXIIIa. Molecular weight estimates of the protein that should have been expressed and its active form support the identification of the purified protein as FXIIIa. The yeast should have expressed rFXIII at a molecular weight of approximately 85 kDa because of the inclusion of the myc epitope and His-tag attached by the yeast vector (Table 3.3). 82 kDa is consistent with the estimate of rFXIIIa with the added peptides. When activated by thrombin, the 85 kDa protein should have become ~82 kDa. Instead, the yeast expressed an 82 kDa which dropped to 79 kDa when cleaved by thrombin. 79 kDa is consistent with rFXIIIa after the removal of the myc epitope and His-tag. N-terminal sequencing identified both bands as FXIIIa. This was further supported by rFXIIIa's rapid crosslinking of fibrinogen's γ-chains (Figure 3.9C). While FXIII and FXIIIa both yield γ-γ and α-α crosslinks, FXIIIa crosslinks at a faster rate[131] more consistent with our results. The high specific activity of rFXIIIa of almost 7,000 U/mg compared to the activity of pdFXIII of approximately 50 U/mg also supports the data indicating that the active form of rFXIII is the protein purified from the yeast.

The yeast most likely expresses FXIII which is cleaved by a protease in the cell to FXIIIa. The protease is extremely efficient. Although multiple proteins were detected during N-terminal sequencing of the 82 kDa band, the primary sequence was FXIIIa. The tentative secondary sequence did not correspond to FXIII or any other expected sequence. The cleavage site to remove the activation peptide from FXIII to produce FXIIIa is a thrombin site as is the degradation site at K513-S514. While the activation peptide appears to be removed from a vast majority of the FXIII molecules, none have been degraded into the 54 and 25 kDa fragments. The protein purified from yeast cell lysate has a molecular weight of approximately 82 kDa which consists of the 79 kDa FXIIIa, the 1 kDa His-tag and the 1.2 kDa c-myc epitope. Since N-terminal sequencing indicates that the band at 79 kDa is the same as that of the 82 kDa band, it appears that the His-tag and c-myc epitope are cleaved very rapidly when incubated with thrombin leaving only FXIIIa; however, there is no known thrombin cleavage site. Despite the presence of the extra peptide region on the C-terminal, FXIIIa is active and functional when not treated with thrombin.

While pdFXIII exists as a heterotetramer in plasma and homodimer in platelets,[24] rFXIII produced in *Saccharomyces cerevisiae* was secreted and maintained as a dimer.[111] While SDS-PAGE and size exclusion chromatography indicate that rFXIIIa expressed in *Pichia pastoris* primarily exists as a monomer with small amounts of aggregates, dynamic light scattering and analytical ultracentrifuge indicate the existence of a trimer (Table 3.4). The harsh conditions of SDS and mechanical stress of size exclusion chromatography appears to disrupt rFXIIIa aggregation; therefore, dynamic light scattering and analytical ultracentrifuge, which analyze aggregation without significant

disturbance of the solution, may provide more accurate estimates of molecular weight species. Dynamic light scattering yielded a molecular weight estimate of approximately 381 kDa for pdFXIII which is consistent with the heterotetramer in plasma from which the reference material was derived. rFXIIIa purified from yeast does not appear to exist as a homodimer as is seen under natural conditions. This could be related to the buffer composition or improper folding which has been shown to result in abnormal aggregation due to hydrophobic interactions.[132]

When incubated with thrombin, rFXIIIa expressed and purified from *Pichia pastoris* was cleaved at K513-S514 yielding fragments of approximately 25 and 54 kDa. N-terminal sequences of these two degradation bands is consistent with the second thrombin cleavage site observed for plasma-derived FXIIIa.[8] These results were similar to those seen with a rFXIII produced in *Saccharomyces cerevisiae* that is currently in clinical trials.[115, 117]

rFXIIIa expressed by yeast was functionally active. rFXIIIa successfully catalyzed γ-dimer formation when incubated with rFI (Figure 3.9C) or fibrin (Figure 3.9B). It was also able to covalently bind A2AP to rFI (Figure 3.10). Previous research has shown that FXIII is critical for the formation of a strong, elastic clot in whole blood, platelet rich and platelet poor plasma by thromboelastography.[4, 116] rFXIIIa produced in the yeast significantly increased clot strength compared to rFI and rFIIa alone.

The production of rFXIIIa rather than FXIII may be beneficial for therapeutic uses. Expression of the A-chain alone is beneficial because it significantly increases its rate of activation by eliminating the rate limiting dissociation of the B-chain.[40, 46-49] Unlike the rFXIII produced in *Saccharomyces cerevisiae*, our rFXIIIa is already in active

form with a high specific activity of 6,940 ± 2,272 U/mg. Consequently, it does not need to be activated by thrombin before achieving optimal crosslinking potential. This could be beneficial for certain therapies such as a component for fibrin sealants because FXIIIa immediately begins crosslinking fibrin.

This research characterized rFXIII expressed in *Pichia pastoris*. Rather than producing FXIII, N-terminal sequencing indicated that the yeast expressed the active FXIIIa. This recombinant protein was produced at approximately 0.24 mg per gram of cell mass and purified by His-tag affinity chromatography. While SDS-PAGE and size exclusion chromatography indicate that FXIIIa primarily exists in monomer form with small amounts of aggregates, dynamic light scattering and analytical ultracentrifuge point toward FXIIIa in trimer form in solution. The expressed FXIIIa had a molecular weight of approximately 82 kDa but is rapidly cleaved by thrombin to the expected 79 kDa. After further incubation, thrombin proteolyzed the expressed FXIIIa into two bands at 25 and 54 kDa which is identical to degradation products of plasma-derived material. The recombinant FXIIIa had a specific activity of almost 7,000 U/mg and successfully crosslinked γ-chains of fibrin(ogen) and A2AP to fibrinogen. rFXIIIa significantly increased clot strength. These results indicate that rFXIIIa expressed in *Pichia pastoris* closely mimic plasma-derived FXIII and may be a good alternative for therapeutic uses; however, further research will further elucidate the efficacy of rFXIIIa as a therapeutic.

Acknowledgements

I would like to thank Dr. Mehmed Inan and Vijay Jain for cloning the A-chain of FXIII gene into yeast and identifying a purification process. I would also like to thank

Sarah Conrad, Weijie Xu, Mohammed Halhouli and Ayman Ismail for assisting in rFXIIIa purification. I am also very grateful to Dr. Donald Becker for allowing us the use of his analytical ultracentrifuge and assistance in analyzing the results. I would also like to thank Mostafa Fatemi for assisting me with SEC. UNMC's Protein Structure Core Facility conducted the N-terminal sequencing. This work was supported by a grant from the Department of Defense titled "Production and Purification of Fibrinogen Components for the Production of a Fibrin Sealant Hemostatic Dressing."

References

1. Loewy, A.G. [Mechanism of action of factor XIII]. *Thromb Diath Haemorrh Suppl* **28**, 1-12; discussion; 23-54 (1968).
2. Kiesselbach, T.H. & Wagner, R.H. Fibrin-stabilizing factor: a thrombin-labile platelet protein. *Am J Physiol* **211**, 1472-1476 (1966).
3. McDonagh, J.M., McDonagh, R.P., Jr., Delage, J.M. & Wagner, R.H. Factor XIII in human plasma and platelets. *J.Clin.Invest.* **48**, 940 (1969).
4. McDonagh, J., McDonagh, R.P., Jr., Delage, J.M. & Wagner, R.H. Factor XIII in human plasma and platelets. *J Clin Invest* **48**, 940-946 (1969).
5. McDonagh, J. in Hemostasis and Thrombosis: Basic Principles and Clinical Practice, Edn. Third Edition. (eds. R.W. Colman, J. Hirsh, V.J. Marder & E.W. Salzman) (J.B. Lippincott Company, Philadelphia; 1994).
6. Grundmann, U., Amann, E., Zettlmeissl, G. & Kupper, H.A. Characterization of cDNA coding for human factor XIIIa. *Proc Natl Acad Sci U S A* **83**, 8024-8028 (1986).
7. Ichinose, A., Hendrickson, L.E., Fujikawa, K. & Davie, E.W. Amino acid sequence of the a subunit of human factor XIII. *Biochemistry* **25**, 6900-6906 (1986).
8. Takahashi, N., Takahashi, Y. & Putnam, F.W. Primary structure of blood coagulation factor XIIIa (fibrinoligase, transglutaminase) from human placenta. *Proc Natl Acad Sci U S A* **83**, 8019-8023 (1986).
9. Ichinose, A. & Davie, E.W. Characterization of the gene for the a subunit of human factor XIII (plasma transglutaminase), a blood coagulation factor. *Proc Natl Acad Sci U S A* **85**, 5829-5833 (1988).
10. Bottenus, R.E., Ichinose, A. & Davie, E.W. Nucleotide sequence of the gene for the b subunit of human factor XIII. *Biochemistry* **29**, 11195-11209 (1990).
11. Carrell, N.A., Erickson, H.P. & McDonagh, J. Electron microscopy and hydrodynamic properties of factor XIII subunits. *J Biol Chem* **264**, 551-556 (1989).
12. Schwartz, M.L., Pizzo, S.V., Hill, R.L. & McKee, P.A. The subunit structures of human plasma and platelet factor XIII (fibrin-stabilizing factor). *J Biol Chem* **246**, 5851-5854 (1971).
13. Ashcroft, A.E., Grant, P.J. & Ariens, R.A. A study of human coagulation factor XIII A-subunit by electrospray ionisation mass spectrometry. *Rapid Commun Mass Spectrom* **14**, 1607-1611 (2000).
14. Bohn, H., Haupt, H. & Kranz, T. [Molecular structure of human fibrin stabilizing factors]. *Blut* **25**, 235-248 (1972).
15. Weisberg, L.J., Shiu, D.T., Conkling, P.R. & Shuman, M.A. Identification of normal human peripheral blood monocytes and liver as sites of synthesis of coagulation factor XIII a-chain. *Blood* **70**, 579-582 (1987).
16. Muszbek, L., Adany, R., Kavai, M., Boda, Z. & Lopaciuk, S. Monocytes of patients congenitally deficient in plasma factor XIII lack factor XIII subunit a antigen and transglutaminase activity. *Thromb.Haemost.* **59**, 231-235 (1988).
17. Nagy, J.A., Kradin, R.L. & McDonagh, J. Biosynthesis of factor XIII A and B subunits. *Adv Exp Med Biol* **231**, 29-49 (1988).

18. Ariens, R.A., Lai, T.S., Weisel, J.W., Greenberg, C.S. & Grant, P.J. Role of factor XIII in fibrin clot formation and effects of genetic polymorphisms. *Blood* **100**, 743 (2002).
19. Yee, V.C. et al. Structure and function studies of factor XIIIa by x-ray crystallography. *Semin Thromb Hemost* **22**, 377-384 (1996).
20. Weiss, M.S., Metzner, H.J. & Hilgenfeld, R. Two non-proline cis peptide bonds may be important for factor XIII function. *FEBS Lett* **423**, 291-296 (1998).
21. Yee, V.C. et al. Three-dimensional structure of a transglutaminase: human blood coagulation factor XIII. *Proc Natl Acad Sci U S A* **91**, 7296-7300 (1994).
22. Board, P.G., Webb, G.C., McKee, J. & Ichinose, A. Localization of the coagulation factor XIII A subunit gene (F13A) to chromosome bands 6p24----p25. *Cytogenet Cell Genet* **48**, 25-27 (1988).
23. Webb, G.C., Coggan, M., Ichinose, A. & Board, P.G. Localization of the coagulation factor XIII B subunit gene (F13B) to chromosome bands 1q31-32.1 and restriction fragment length polymorphism at the locus. *Hum Genet* **81**, 157-160 (1989).
24. Schwartz, M.L., Pizzo, S.V., Hill, R.L. & McKee, P.A. Human Factor XIII from plasma and platelets. Molecular weights, subunit structures, proteolytic activation, and cross-linking of fibrinogen and fibrin. *J Biol Chem* **248**, 1395-1407 (1973).
25. Folk, J.E. & Finlayson, J.S. The epsilon-(gamma-glutamyl)lysine crosslink and the catalytic role of transglutaminases. *Adv Protein Chem* **31**, 1-133 (1977).
26. Yorifuji, H., Anderson, K., Lynch, G.W., Van de Water, L. & McDonagh, J. B protein of factor XIII: differentiation between free B and complexed B. *Blood* **72**, 1645-1650 (1988).
27. Kroll, J. The subunit composition of factor XIII proteins in normal and factor XIII deficient plasma and serum analysed by line immunoelectrophoresis. *Clin Chim Acta* **179**, 279-284 (1989).
28. Greenberg, C.S., Dobson, J.V. & Miraglia, C.C. Regulation of plasma factor XIII binding to fibrin in vitro. *Blood* **66**, 1028 (1985).
29. Takagi, T. & Doolittle, R.F. Amino acid sequence studies on factor XIII and the peptide released during its activation by thrombin. *Biochemistry (N.Y.)* **13**, 750-756 (1974).
30. Lynch, G.W. & Pfueller, S.L. Thrombin-independent activation of platelet factor XIII by endogenous platelet acid protease. *Thromb.Haemost.* **59**, 372-377 (1988).
31. Ando, Y. et al. Platelet factor XIII is activated by calpain. *Biochem Biophys Res Commun* **144**, 484-490 (1987).
32. Freyssinet, J.M., Lewis, B.A., Holbrook, J.J. & Shore, J.D. Protein-protein interactions in blood clotting. The use of polarization of fluorescence to measure the dissociation of plasma factor XIIIa. *Biochem J* **169**, 403-410 (1978).
33. Lewis, S.D., Janus, T.J., Lorand, L. & Shafer, J.A. Regulation of formation of factor XIIIa by its fibrin substrates. *Biochemistry* **24**, 6772-6777 (1985).
34. Curtis, C.G. et al. Calcium-dependent unmasking of active center cysteine during activation of fibrin stabilizing factor. *Biochemistry (N.Y.)* **13**, 3774-3780 (1974).
35. Hornyak, T.J. & Shafer, J.A. Role of calcium ion in the generation of factor XIII activity. *Biochemistry* **30**, 6175-6182 (1991).

36. Lewis, B.A., Freyssinet, J.M. & Holbrook, J.J. An equilibrium study of metal ion binding to human plasma coagulation factor XIII. *Biochem J* **169**, 397-402 (1978).
37. Lorand, L., Losowsky, M.S. & Miloszewski, K.J. Human factor XIII: fibrin-stabilizing factor. *Prog.Hemost.Thromb.* **5**, 245 (1980).
38. Janus, T.J., Lewis, S.D., Lorand, L. & Shafer, J.A. Promotion of thrombin-catalyzed activation of factor XIII by fibrinogen. *Biochemistry* **22**, 6269-6272 (1983).
39. Greenberg, C.S., Miraglia, C.C., Rickles, F.R. & Shuman, M.A. Cleavage of blood coagulation factor XIII and fibrinogen by thrombin during in vitro clotting. *J.Clin.Invest.* **75**, 1463 (1985).
40. Greenberg, C.S., Achyuthan, K.E. & Fenton, J.W., II Factor XIIIa formation promoted by complexing of a-thrombin, fibrin, and plasma factor XIII. *Blood* **69**, 867 (1987).
41. Credo, R.B., Curtis, C.G. & Lorand, L. Ca2+-related regulatory function of fibrinogen. *Proc Natl Acad Sci U S A* **75**, 4234-4237 (1978).
42. McDonagh, J.M. in Hemostasis and Thrombosis: Basic Principles and Clinical Practice. (eds. R.W. Colman, J. Hirsh, V.J. Marder & E.W. Salzman) 301-313 (J.B. Lippincott Company, Philadelphia; 1994).
43. Credo, R.B., Curtis, C.G. & Lorand, L. Alpha-chain domain of fibrinogen controls generation of fibrinoligase (coagulation factor XIIIa). Calcium ion regulatory aspects. *Biochemistry* **20**, 3770-3778 (1981).
44. Siebenlist, K.R., Meh, D.A. & Mosesson, M.W. Plasma factor XIII binds specifically to fibrinogen molecules containing gamma chains. *Biochemistry* **35**, 10448-10453 (1996).
45. Meh, D.A., Siebenlist, K.R. & Mosesson, M.W. Identification and characterization of the thrombin binding sites on fibrin. *J Biol Chem* **271**, 23121-23125 (1996).
46. Hornyak, T.J., Bishop, P.D. & Shafer, J.A. Alpha-thrombin-catalyzed activation of human platelet factor XIII: relationship between proteolysis and factor XIIIa activity. *Biochemistry* **28**, 7326-7332 (1989).
47. Lorand, L. et al. Dissociation of the subunit structure of fibrin stabilizing factor during activation of the zymogen. *Biochem Biophys Res Commun* **56**, 914-922 (1974).
48. Chung, S.I. & Folk, J.E. Kinetic studies with transglutaminases. The human blood enzymes (activated coagulation factor 13 and the guinea pig hair follicle enzyme. *J Biol Chem* **247**, 2798-2807 (1972).
49. Chung, S.I., Lewis, M.S. & Folk, J.E. Relationships of the catalytic properties of human plasma and platelet transglutaminases (activated blood coagulation factor XIII) to their subunit structures. *J Biol Chem* **249**, 940-950 (1974).
50. Lorand, L. Fibrin clots. *Nature* **166**, 694-695 (1950).
51. Procyk, R., Bishop, P.D. & Kudryk, B. Fibrin--recombinant human factor XIII a-subunit association. *Thromb Res* **71**, 127-138 (1993).
52. Lorand, L. Fibrinoligase: the fibrin-stabilizing factor system of blood plasma. *Ann.N.Y.Acad.Sci.* **202**, 6-30 (1972).

53. Lorand, L., Downey, J., Gotoh, T., Jacobsen, A. & Tokura, S. The transpeptidase system which crosslinks fibrin by gamma-glutamyle-episilon-lysine bonds. *Biochem Biophys Res Commun* **31**, 222-230 (1968).
54. Pisano, J.J., Finlayson, J.S. & Peyton, M.P. [Cross-link in fibrin polymerized by factor 13: epsilon-(gamma-glutamyl)lysine.]. *Science* **160**, 892-893 (1968).
55. Matacic, S. & Loewy, A.G. The identification of isopeptide crosslinks in insoluble fibrin. *Biochem Biophys Res Commun* **30**, 356-362 (1968).
56. Chen, R. & Doolittle, R.F. Isolation, characterization, and location of a donor-acceptor unit from cross-linked fibrin. *Proc Natl Acad Sci U S A* **66**, 472-479 (1970).
57. Loewy, A.G., Dunathan, K., Kriel, R. & Wolfinger, H.L., Jr. Fibrinase. I. Purification of substrate and enzyme. *J Biol Chem* **236**, 2625-2633 (1961).
58. Lorand, L. et al. Lysine as amine donor in fibrin crosslinking. *Biochem Biophys Res Commun* **25**, 629-637 (1966).
59. Achyuthan, K.E., Dobson, J.V. & Greenberg, C.S. Gly-Pro-Arg-Pro modifies the glutamine residues in the alpha- and gamma-chains of fibrinogen: inhibition of transglutaminase cross-linking. *Biochim Biophys Acta* **872**, 261-268 (1986).
60. Lorand, L., Parameswaran, K.N. & Murthy, S.N. A double-headed Gly-Pro-Arg-Pro ligand mimics the functions of the E domain of fibrin for promoting the end-to-end crosslinking of gamma chains by factor XIIIa. *Proc Natl Acad Sci U S A* **95**, 537-541 (1998).
61. Doolittle, R.F., Chen, R. & Lau, F. Hybrid fibrin: proof of the intermolecular nature of - crosslinking units. *Biochem Biophys Res Commun* **44**, 94-100 (1971).
62. Schwartz, M.L., Pizzo, S.V., Hill, R.L. & McKee, P.A. The effect of fibrin-stabilizing factor on the subunit structure of human fibrin. *J Clin Invest* **50**, 1506-1513 (1971).
63. Shen, L.L., Hermans, J., McDonagh, J., McDonagh, R.P. & Carr, M. Effects of calcium ion and covalent crosslinking on formation and elasticity of fibrin cells. *Thromb Res* **6**, 255-265 (1975).
64. Purves, L., Purves, M. & Brandt, W. Cleavage of fibrin-derived D-dimer into monomers by endopeptidase from puff adder venom (Bitis arietans) acting at cross-linked sites of the gamma-chain. Sequence of carboxy-terminal cyanogen bromide gamma-chain fragments. *Biochemistry* **26**, 4640-4646 (1987).
65. Spraggon, G., Everse, S.J. & Doolittle, R.F. Crystal structures of fragment D from human fibrinogen and its crosslinked counterpart from fibrin. *Nature* **389**, 455-462 (1997).
66. Standeven, K.F. et al. Functional analysis of fibrin {gamma}-chain cross-linking by activated factor XIII: determination of a cross-linking pattern that maximizes clot stiffness. *Blood* **110**, 902-907 (2007).
67. Standeven, K.F. et al. Functional analysis of fibrin g-chain cross-linking by activated factor XIII: determination of a cross-linking pattern that maximizes clot stiffness. *Blood* **110**, 902 (2007).
68. Cottrell, B.A., Strong, D.D., Watt, K.W. & Doolittle, R.F. Amino acid sequence studies on the alpha chain of human fibrinogen. Exact location of cross-linking acceptor sites. *Biochemistry* **18**, 5405-5410 (1979).

69. Fretto, L.J., Ferguson, E.W., Steinman, H.M. & McKee, P.A. Localization of the alpha-chain cross-link acceptor sites of human fibrin. *J Biol Chem* **253**, 2184-2195 (1978).
70. Matsuka, Y.V., Medved, L.V., Migliorini, M.M. & Ingham, K.C. Factor XIIIa-catalyzed cross-linking of recombinant alpha C fragments of human fibrinogen. *Biochemistry* **35**, 5810-5816 (1996).
71. Lorand, L. Factor XIII: structure, activation, and interactions with fibrinogen and fibrin. *Ann.N.Y.Acad.Sci.* **936**, 291-311 (2001).
72. Sobel, J.H. & Gawinowicz, M.A. Identification of the alpha chain lysine donor sites involved in factor XIIIa fibrin cross-linking. *J Biol Chem* **271**, 19288-19297 (1996).
73. Gaffney, P.J. et al. Fibrin subunits in venous and arterial thromboembolism. *Cardiovasc Res* **10**, 421-426 (1976).
74. McDonagh, R.P., Jr., McDonagh, J. & Duckert, F. The influence of fibrin crosslinking on the kinetics of urokinase-induced clot lysis. *Br J Haematol* **21**, 323-332 (1971).
75. Gaffney, P.J. & Whitaker, A.N. Fibrin crosslinks and lysis rates. *Thromb Res* **14**, 85-94 (1979).
76. Francis, C.W., Marder, V.J. & Barlow, G.H. Plasmic degradation of crosslinked fibrin. Characterization of new macromolecular soluble complexes and a model of their structure. *J Clin Invest* **66**, 1033-1043 (1980).
77. Muller, M.F., Ris, H. & Ferry, J.D. Electron microscopy of fine fibrin clots and fine and coarse fibrin films. Observations of fibers in cross-section and in deformed states. *J Mol Biol* **174**, 369-384 (1984).
78. Kanaide, H. & Shainoff, J.R. Cross-linking of fibrinogen and fibrin by fibrin-stablizing factor (factor XIIIa). *J Lab Clin Med* **85**, 574-597 (1975).
79. Valnickova, Z. & Enghild, J.J. Human procarboxypeptidase U, or thrombin-activable fibrinolysis inhibitor, is a substrate for transglutaminases. Evidence for transglutaminase-catalyzed cross-linking to fibrin. *J Biol Chem* **273**, 27220-27224 (1998).
80. Mosher, D.F., Schad, P.E. & Vann, J.M. Cross-linking of collagen and fibronectin by factor XIIIa. Localization of participating glutaminyl residues to a tryptic fragment of fibronectin. *J Biol Chem* **255**, 1181-1188 (1980).
81. Procyk, R., Adamson, L., Block, M. & Blomback, B. Factor XIII catalyzed formation of fibrinogen-fibronectin oligomers--a thiol enhanced process. *Thromb Res* **40**, 833-852 (1985).
82. Mosher, D.F. & Schad, P.E. Cross-linking of fibronectin to collagen by blood coagulation Factor XIIIa. *J Clin Invest* **64**, 781-787 (1979).
83. Hada, M., Kaminski, M., Bockenstedt, P. & McDonagh, J. Covalent crosslinking of von Willebrand factor to fibrin. *Blood* **68**, 95-101 (1986).
84. Bockenstedt, P., McDonagh, J. & Handin, R.I. Binding and covalent cross-linking of purified von Willebrand factor to native monomeric collagen. *J Clin Invest* **78**, 551-556 (1986).
85. Francis, R.T., McDonagh, J. & Mann, K.G. Factor V is a substrate for the transamidase factor XIIIa. *J Biol Chem* **261**, 9787-9792 (1986).

86. Huh, M.M., Schick, B.P., Schick, P.K. & Colman, R.W. Covalent crosslinking of human coagulation factor V by activated factor XIII from guinea pig megakaryocytes and human plasma. *Blood* **71**, 1693-1702 (1988).
87. Greenberg, C.S. & Shuman, M.A. Specific binding of blood coagulation factor XIIIa to thrombin-stimulated platelets. *J.Biol.Chem.* **259**, 14721 (1984).
88. McDonagh, J., Kiesselbach, T.H. & Wagner, R.H. Factor 13 and antiplasmin activity in human platelets. *Am J Physiol* **216**, 508-513 (1969).
89. Weisel, J.W., Francis, C.W., Nagaswami, C. & Marder, V.J. Determination of the topology of factor XIIIa-induced fibrin gamma-chain cross-links by electron microscopy of ligated fragments. *J Biol Chem* **268**, 26618-26624 (1993).
90. Ritchie, H., Lawrie, L.C., Crombie, P.W., Mosesson, M.W. & Booth, N.A. Cross-linking of plasminogen activator inhibitor 2 and alpha 2-antiplasmin to fibrin(ogen). *J Biol Chem* **275**, 24915-24920 (2000).
91. Ritchie, H., Lawrie, L.C., Mosesson, M.W. & Booth, N.A. Characterization of crosslinking sites in fibrinogen for plasminogen activator inhibitor 2 (PAI-2). *Ann.N.Y.Acad.Sci.* **936**, 215-218 (2001).
92. Sane, D.C. et al. Vitronectin is a substrate for transglutaminases. *Biochem Biophys Res Commun* **157**, 115-120 (1988).
93. Skorstengaard, K., Halkier, T., Hojrup, P. & Mosher, D. Sequence location of a putative transglutaminase cross-linking site in human vitronectin. *FEBS Lett* **262**, 269-274 (1990).
94. Bale, M.D., Westrick, L.G. & Mosher, D.F. Incorporation of thrombospondin into fibrin clots. *J Biol Chem* **260**, 7502-7508 (1985).
95. Mui, P.T. & Ganguly, P. Cross-linking of actin and fibrin by fibrin-stabilizing factor. *Am J Physiol* **233**, H346-349 (1977).
96. Cohen, I., Blankenberg, T.A., Borden, D., Kahn, D.R. & Veis, A. Factor XIIIa-catalyzed cross-linking of platelet and muscle actin. Regulation by nucleotides. *Biochim Biophys Acta* **628**, 365-375 (1980).
97. Cohen, I., Young-Bandala, L., Blankenberg, T.A., Siefring, G.E., Jr. & Bruner-Lorand, J. Fibrinoligase-catalyzed cross-linking of myosin from platelet and skeletal muscle. *Arch Biochem Biophys* **192**, 100-111 (1979).
98. Asijee, G.M. et al. Platelet vinculin: a substrate of activated factor XIII. *Biochim Biophys Acta* **954**, 303-308 (1988).
99. Cohen, I. et al. Disulfide-linked and transglutaminase-catalyzed protein assemblies in platelets. *Blood* **66**, 143-151 (1985).
100. Feddersen, J.C. & Gormsen, J. gamma-dimerization, alpha-polymerization, and plasmin degradation of human fibrin. Effect of various inhibitors of factor XIII on the patterns in SDS-electrophoresis and crossed immunoelectrophoresis. *Thromb.Haemost.* **36**, 27-36 (1976).
101. Curtis, C.G. & Lorand, L. Fibrin-stabilizing factor (factor XIII). *Methods Enzymol* **45**, 177-191 (1976).
102. Gootenberg, J.E. Factor concentrates for the treatment of factor XIII deficiency. *Curr Opin Hematol* **5**, 372-375 (1998).
103. Shen, L. & Lorand, L. Contribution of fibrin stabilization to clot strength. Supplementation of factor XIII-deficient plasma with the purified zymogen. *J Clin Invest* **71**, 1336-1341 (1983).

104. Grinnell, F., Feld, M. & Minter, D. Fibroblast adhesion to fibrinogen and fibrin substrata: requirement for cold-insoluble globulin (plasma fibronectin). *Cell* **19**, 517-525 (1980).
105. Nielsen, V.G., Steenwyk, B.L. & Gurley, W.Q. Contact activation prolongs clot lysis time in human plasma: role of thrombin-activatable fibrinolysis inhibitor and Factor XIII. *J.Heart Lung Transplant.* **25**, 1247 (2006).
106. Nielsen, V.G., Gurley, W.Q., Jr. & Burch, T.M. The impact of factor XIII on coagulation kinetics and clot strength determined by thrombelastography. *Anesth.Analg.* **99**, 120 (2004).
107. Nielsen, V.G., Kirklin, J.K., Hoogendoorn, H., Ellis, T.C. & Holman, W.L. Thrombelastographic method to quantify the contribution of factor XIII to coagulation kinetics. *Blood Coagul.Fibrinolysis* **18**, 145 (2007).
108. Devine, D.V., Andestad, G., Nugent, D. & Carter, C.J. Platelet-associated factor XIII as a marker of platelet activation in patients with peripheral vascular disease. *Arterioscler Thromb* **13**, 857-862 (1993).
109. Devine, D.V. & Bishop, P.D. Platelet-associated factor XIII in platelet activation, adhesion, and clot stabilization. *Semin Thromb Hemost* **22**, 409-413 (1996).
110. Francis, C.W. & Marder, V.J. Rapid formation of large molecular weight alpha-polymers in cross-linked fibrin induced by high factor XIII concentrations. Role of platelet factor XIII. *J Clin Invest* **80**, 1459-1465 (1987).
111. Bishop, P.D. et al. Expression, purification, and characterization of human factor XIII in Saccharomyces cerevisiae. *Biochemistry* **29**, 1861 (1990).
112. Bishop, P.D., Lasser, G.W., Le Trong, I., Stenkamp, R.E. & Teller, D.C. Human recombinant factor XIII from Saccharomyces cerevisiae. Crystallization and preliminary x-ray data. *J.Biol.Chem.* **265**, 13888 (1990).
113. Lewis, K.B., Teller, D.C., Fry, J., Lasser, G.W. & Bishop, P.D. Crosslinking kinetics of the human transglutaminase, factor XIII A2 , acting on fibrin gels and gamma-chain peptides. *Biochemistry* **36**, 995 (1997).
114. Radek, J.T., Jeong, J.M., Wilson, J. & Lorand, L. Association of the A subunits of recombinant placental factor XIII with the native carrier B subunits from human plasma. *Biochemistry* **32**, 3527-3534 (1993).
115. Reynolds, T.C. et al. Safety, pharmacokinetics, and immunogenicity of single-dose rFXIII administration to healthy volunteers. *J.Thromb.Haemost.* **3**, 922 (2005).
116. Lovejoy, A.E. et al. Safety and pharmacokinetics of recombinant factor XIII-A2 administration in patients with congenital factor XIII deficiency. *Blood* **108**, 57 (2006).
117. Visich, J.E. et al. Safety and pharmacokinetics of recombinant factor XIII in healthy volunteers: a randomized, placebo-controlled, double-blind, multi-dose study. *Thromb.Haemost.* **94**, 802 (2005).
118. Ponce, R. et al. Safety of recombinant human factor XIII in a cynomolgus monkey model of extracorporeal blood circulation. *Toxicol.Pathol.* **33**, 702 (2005).
119. Inan, M. et al. Saturation of the secretory pathway by overexpression of a hookworm (Necator americanus) protein (Na-ASP1). *Methods in Molecular Biology (Totowa, NJ, United States)* **389**, 65 (2007).

120. Zhang, W., Inan, M. & Meagher, M.M. Rational design and optimization of fed-batch and continuous fermentations. *Methods in Molecular Biology (Totowa, NJ, United States)* **389**, 43 (2007).
121. Perkins, S.J. Protein volumes and hydration effects. The calculations of partial specific volumes, neutron scattering matchpoints and 280-nm absorption coefficients for proteins and glycoproteins from amino acid sequences. *Eur J Biochem* **157**, 169-180 (1986).
122. Gorkun, O.V., Veklich, Y.I., Weisel, J.W. & Lord, S.T. The conversion of fibrinogen to fibrin: recombinant fibrinogen typifies plasma fibrinogen. *Blood* **89**, 4407-4414 (1997).
123. Bretthauer, R.K. & Castellino, F.J. Glycosylation of Pichia pastoris-derived proteins. *Biotechnol Appl Biochem* **30 (Pt 3)**, 193-200 (1999).
124. De Schutter, K. et al. Genome sequence of the recombinant protein production host Pichia pastoris. *Nat Biotechnol* **27**, 561-566 (2009).
125. Hamilton, S.R. & Gerngross, T.U. Glycosylation engineering in yeast: the advent of fully humanized yeast. *Curr Opin Biotechnol* **18**, 387-392 (2007).
126. Ogunjimi, A.A., Chandler, J.M., Gooding, C.M., Recinos, A., III & Choudary, P.V. High-level secretory expression of immunologically active intact antibody from the yeast Pichia pastoris. *Biotechnol. Lett.* **21**, 561-567 (1999).
127. Inan, M., Aryasomayajula, D., Sinha, J. & Meagher, M.M. Enhancement of protein secretion in Pichia pastoris by overexpression of protein disulfide isomerase. *Biotechnol. Bioeng.* **93**, 771-778 (2006).
128. Wang, Y. et al. Expression, purification, and characterization of recombinant human keratinocyte growth factor-2 in Pichia pastoris. *J. Biotechnol.* **132**, 44-48 (2007).
129. Gething, M.J. & Sambrook, J. Protein folding in the cell. *Nature (London, U. K.)* **355**, 33-45 (1992).
130. Gilbert, H.F. Protein disulfide isomerase. *Methods Enzymol.* **290**, 26-50 (1998).
131. Siebenlist, K.R., Meh, D.A. & Mosesson, M.W. Protransglutaminase (factor XIII) mediated crosslinking of fibrinogen and fibrin. *Thromb.Haemost.* **86**, 1221-1228 (2001).
132. Lord, J.M., Davey, J., Frigerio, L. & Roberts, L.M. Endoplasmic reticulum-associated protein degradation. *Semin. Cell Dev. Biol.* **11**, 159-164 (2000).

Chapter 4

Optimization of a Liquid Fibrin Sealant to Achieve its Maximal Strength and Activation Speed

Abstract

To meet future demands for hemostatic therapies, liquid fibrin sealants (LFS) will likely include recombinant human fibrinogen (rFI) and recombinant human Factor XIII (rFXIII). The research described here optimizes the components of a LFS containing rFI produced in the milk of transgenic cows, active rFXIII (rFXIIIa) expressed in genetically engineered *Pichia pastoris*, plasma-derived thrombin (pdFIIa) and $CaCl_2$. Each component was optimized individually while maintaining the levels of other ingredients. The optimal concentration of rFXIIIa and $CaCl_2$ were selected to provide the highest viscoelastic strength. The optimal level of thrombin was selected to provide the fastest initiation of clot formation and clotting kinetics. rFI concentrations were selected to provide the necessary clot strength while minimizing material used. The molecular behavior of rFI with rFXIIIa catalyzed by FIIa was similar to the respective human plasma analogues as judged by molecular weight changes by SDS-PAGE, polymerization kinetics by turbidity, and formation of γ-γ chain crosslinked fibrin. rFXIIIa to rFI ratios greater than 0.15 yield maximal clot strength. FIIa to rFI ratios greater than 0.09 yield the fastest clot onset time and 0.14 ratio yields the greatest clot strength. rFXIIIa and FIIa ratios to FI of 0.16 and 0.18, respectively, were selected for the optimal LFS for future research. Fibrin clots made with rFI, rFXIII and FIIa yielded 5.0-fold greater shear elastic modulus strength than clots formed from NHB alone. The addition of rFXIIIa significantly increased clot strength thereby reducing the amount of FI need in the LFS. The clotting kinetics and viscoelastic strength of our optimized LFS was equivalent to those of a commercially available LFS; however, it uses approximately 75% less fibrinogen and thrombin. These results suggest that rFI and rFXIII in combination with

FIIa can be combined to create a LFS with equivalent or better kinetic and viscoelastic properties as currently available products.

Introduction

Trauma deaths are a result of hemorrhage in 37% of civilians[1] and 47% military personnel[2] and are the primary cause of death for individuals under 44 years of age.[3] For the past 2000 years, the same techniques have been used to stop hemorrhage: packing with gauze, direct pressure and tourniquet.[4] This method is inadequate for treating severe hemorrhage. The Department of Defense Combat Casualty Care Research Program is focused on developing more effective options for treating hemorrhage.[5]

Several hemostatic products are currently used or under development. Cyanoacrylates are utilized as hemostatic aides in oral surgery but can cause inflammation and necrosis.[6] Gelatin-resorcinol-formaldehyde (GRF) glue is frequently used as a sealant and yields excellent tensile strength but has less clotting ability, inferior clots to other sealants and results in fibroblast infiltration.[7] QuikClot speeds clot formation by creating an exothermic reaction when absorbing water; however, it is not biodegradable requiring its removal post-treatment.[8, 9] Compared to other treatment options, fibrin sealants (FS), also known as fibrin glues, are viewed as the best sealant[10] because they are biocompatible,[6, 11, 12] biodegradable[6] and safe[11] and are not linked to excessive inflammation, immune responses or necrosis.[6, 12] Because they mimic natural clotting mechanisms, FS provide similar functions as endogenous components: creating hemostatic clots[13] and providing a scaffold for cellular infiltration needed to regenerate tissue[13, 14] and dissolve the clot.[13]

FS reproduce the final stage of the clotting cascade to assist in hemostasis. Fibrin sealants contain fibrinogen (FI), thrombin (FIIa) and calcium chloride and on

occasion Factor XIII (FXIII) which are the elements in the last step of the cascade required to produce a fibrin clot. When applied to a wound, these exogenous components can assist the same endogenous proteins in achieving hemostasis. FIIa catalyzes the conversion of FI to soluble fibrin monomer and FXIII to activated FXIII (FXIIIa).[15-18] FXIIIa then catalyzes the formation of the cross-linked, insoluble fibrin clot that is melded with the platelet-based, primary hemostatic plug.[17, 19-21] In addition to binding other fibrin molecules and creating the fibrin clot, fibrin adheres the clot to the wound by binding to collagen exposed at the site of tissue injury in addition to platelets, endothelial and other cells.[11]

Fibrin has been utilized for 100 years for numerous biomedical therapies but was first used as an adhesive with addition of bovine thrombin[11] in the early 1940s for skin grafts for burn patients.[22] Unfortunately, the fibrin glue was a source of infection[22] and failed to provide the necessary strength required to maintain its function until tissue repair[11] resulting in a loss of interest in FS as treatment options for hemorrhage. In the early 1970s, researchers again began refining FS.[11] Today, multiple products are commercially available in the United States and Europe.[11] The first FS approved by the FDA was Baxter's Tisseel® in 1998.[23] Vitagel (Orthovita) and Crosseal (Johnson & Johnson) were subsequently approved in 2000 and 2003, respectively.[23] All of these products use plasma-derived proteins. Tisseel,® like most FS,[11] is a two-component system: one containing FI and plasminolysis inhibitor and the second containing human thrombin and calcium chloride.

FS are used as hemostatic agents,[23] matrices for wound healing,[12, 23] adherents for tissues[23] and drug deliveries[23] in a variety of settings (Figure 4.1). With respect to

hemostasis, FS can be used alone or in combination with a dressing to stop blood oozing from holes, incisions and raw surfaces which cannot be stopped by suturing.[7] Research indicates that liquid fibrin sealants (LFS) can be used as a drug delivery device for high doses of antibiotics and growth factors.[11, 24] Historically, FS were primarily used in trauma situations[24] and during cardiac[7, 24] and vascular surgeries[24] but are now frequently used in general surgery.[11, 25] FS has been shown to be useful in various surgical settings including cardiovascular,[11, 26] vascular,[27] thoracic,[28, 29] plastic,[11, 30] reconstructive,[31] oncologic,[23] ophthalmologic,[23] dental,[23] orthopedic,[11, 23] hepatic[7] and urologic surgeries,[32, 33] microsurgical procedures[11] and neurosurgery.[11, 34, 35] The use of FS has been shown to reduce blood loss,[23, 36] fluid loss,[23] transfusion occurrence,[37] operative time,[36] mortality,[36] hospital stay[24] and treatment costs.[23]

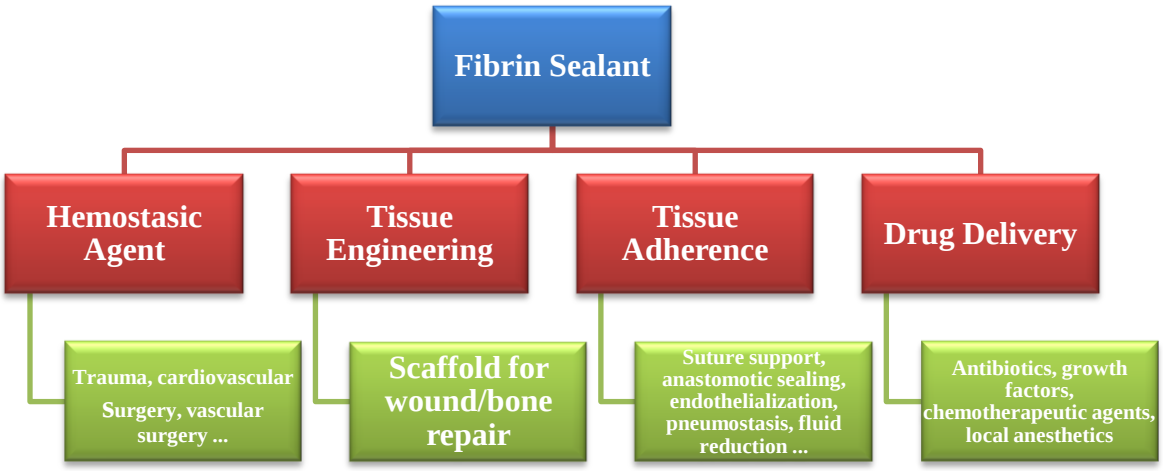

Figure 4.1. Uses for fibrin sealant. Based on the schematic published by Spotnitz and Prabhu.[23]

Despite its usefulness, FS have drawbacks. Current FS are relatively expensive. For example, Tisseel® is over $130 per ml FI[36] which makes it economically infeasible for use as a dressing coating or for widespread use in the field. In addition, commercial sealants use plasma-derived materials. In 1978, the Food and Drug Administration

(FDA) suspended the use of fibrin sealants due to contamination with hepatitis.[38] Treatments have been developed to minimized viral contaminants;[24] however, there is still some concern of contamination with viruses or prions able to withstand current treatments.[6, 23] For example, human parovirus B19 is not killed by current pasteurization processes.[23] Tisseel, Crosseal and Vitagel, the three FDA approved fibrin sealants, and frequently used "home-made" fibrin sealants each have their own issues. Vitagel[23] and the home-made FS prepared by some medical centers use bovine thrombin.[24] Although relatively rare, bovine proteins in FS can initiate immune responses.[23, 24] While Crosseal contains only human proteins, it contains tranexamic acid which has been linked to severe reactions that contraindicate its use when it may come in contact with dura matter or cerebral spinal fluid.[23, 39] Consequently, a safer, more abundant source of material for FS is needed.

The objective of this chapter is three-fold: (1) characterize the importance of FXIII in LFS; (2) optimize the concentrations of each LFS component to create the strongest clot in the fastest time; and (3) compare recombinant human fibrinogen-based to commercially available plasma-derived human fibrinogen-based LFS. Due to limitations in the availability of cost effective, safe supplies from human plasma, future FS will be more often derived from recombinant technology which can produce products more economically and in abundance.[40-45] This study utilizes recombinant human fibrinogen (rFI) purified from the milk of cloned, transgenic cows and recombinant human activate factor XIII (rFXIIIa) expressed in yeast. Initial studies used pdFIIa; however, final experiments utilized rFIIa from CHO cells. Experiments were designed to evaluate the role of FXIII in FS. Most FS on the market contain FI

and FIIa in similar amounts; however, FXIII content ranges.[46] The ratio of FXIII to FI in human plasma is approximately 0.4 U/mg; however, some commercial products contain no FXIII or 0.1 U/mg except for Beriplast P which contains approximately 0.44 to 0.89 U/mg.[46] We vary FXIII activity from 0 to 274 U rFXIIIa per mg FI. In addition to testing the efficacy of our recombinant proteins and importance of FXIII in FS, the ratios of components have never been optimized with the availability of highly active FXIIIa. This research was designed to test the hypotheses that (1) the addition of rFXIIIa will increase clot strength thereby reducing the amount of FI need in FS; and (2) our LFS containing optimized ratios of rFI, rFXIIIa and FIIa will yield equivalent clot kinetics and strengths as plasma-derived LFS.

Materials and Methods

Materials

Purified, plasma-derived prothrombin was bought from Enzyme Research Laboratories (South Bend, IN). Recombinant thrombin (Recothrom®) was purchased from Zymogenetics. Purified recombinant fibrinogen, expressed in the milk of transgenic Swiss Brown cows, was obtained from Pharming Group NV (Leiden, Netherlands). Materials for the thromboelastograph were purchased from Haemoscope (Niles, IL). Unless otherwise specified, reagents were purchased from Sigma (St. Louis, MO).

Vector construction, expression and purification of FXIIIA in Pichia pastoris

The human Ultimate ORF clone containing the human coagulation factor FXIIIA1 cDNA in the pENTR™221 vector was purchased from Invitrogen (Carlsbad

CA). The following primers were used to obtain FXIIIa gene to subclone in pPICZA intracellular Pichia expression vector. (Forward, 5'-CCAATTGATGCATCATCATCATCATTCAGAAACTTCCAGGACCGC-3'; Reverse, 5'-GCGGCCGCTCACATGGAAGGTCGTCTTTGAATC-3'). The forward primer introduced a methionine and 6 histidine amino acids at the N-terminus of mature FXIIIa peptide. The PCR product was digested with MfeI and NotI and subcloned into pPICZA which was digested with the same enzymes. The DNA sequence of the FXIIIA was confirmed by sequencing the insert fragment. One of the confirming plasmid pPICZAFXIIIa was linearized with PmeI and transformed into P. pastoris X-33 host strain and copy number of the clones was determined as described.[47] Varying copy number clones were screened in shake flask culture to confirm intracellular production of FXIIIa protein. The highest producing clone was scaled up to 5 L bench scale. A fed-batch fermentation protocol was followed to optimize FXIIIa production as described by Zhang et al., (2007).[48] At the end of fermentation process the cells were separated by centrifugation (6,000g) and pellet was stored at -80^{o}C.

Frozen cell paste was processed in 300 gram batches. Cells were lysed in three sets of 100 gram batches. 100 grams of cell paste was resuspended in 100 ml of cold lysis buffer (50 mM Tris-HCL, 10 mM $MgSO_4$, 1 mM EDTA, 10 mM potassium acetate, 1 mM DTT (DL-Dithiothreitol), 2 mM PMSF (phenylmethanesulphonylfluoride) in methanol, pH 9.5). 100 ml (250 g) of 0.5 mm glass beads (Biospec, Bartlesville, OK) were added and the cells. Surrounded by an ice bath, cells were lysed using a BeadBeater Blender (Biospec, Bartlesville, OK) with twenty 20 second on/off cycles. The cell lysate mixture was then centrifuged to remove cellular debris. The lysate from 300 grams of

cell paste was combined and purified using the HisBind Purification Kit (EMD Chemicals, Inc., San Diego, CA) with 40 ml of resin slurry. Following purification, rFXIII was dialyzed in 10 mM Tris-HCl, 0.1 mM EDTA, 60 µM polysorbate-20, pH 8.0 in snake-like dialysis membranes and the protein samples were filter-sterilized and concentrated using the Amicon tubes (Millipore, Billerica, MA). The purity of the sample was tested by SDS-PAGE (NuPAGE 12% Bis-Tris) (Invitrogen, Carlsbad, CA) and immunoblot. The concentration of rFXIII was determined by standard Bicinconic Acid (BCA) methods.

FIIa preparation

Frozen, plasma-derived human prothrombin (Enzyme Research Laboratories, South Bend, IN), was thawed at 37^{o}C. Plasma-derived thrombin (Enzyme Research Laboratories, South Bend, IN) was added at a 1/10 mass to mass thrombin/prothrombin ratio. 0.35 grams of sodium citrate per milliliter of solution was added (Lanchantin 1965). This solution was incubated at 37^{o}C on a rotating mixer for five hours. Sodium citrate was removed using PD-10 desalting columns (GE Healthcare, Giles, United Kingdom). Activation of prothrombin to thrombin was confirmed by reducing and nonreducing SDS-PAGE (12% Bis-Tris NuPAGE) (Invitrogen, Carlsbad, CA) stained with Colloidal Blue (Invitrogen, Carlsbad, CA). The concentration of the thrombin solution was determined by standard Bicinconic Acid (BCA) methods. The specific activity was determined by aPTT analysis.

γ-γ crosslinking of FI by FXIIIa

γ-γ crosslinking of FI by FXIIIa was analyzed by a similar procedure previously described.[49] Briefly, rFI (final concentration: 0.38 mg/ml) was incubated with rFXIII (final concentration: 0.01 mg/ml), pdFIIa or rFIIa (5 U/ml) in Ringer's solution (155 mM NaCl, 5 mM KCl, 2 mM $CaCl_2$, 1 mM $MgCl_2$) for 0, 5, 15, 30 and 60 minutes at 37^{o}C. rFI was also incubated with pdFIIa or rFIIa without rFXIII. The reactions were halted by the addition of NuPage® Sample Reducing Buffer (β-mercaptoethanol) (Invitrogen, Carlsbad, CA) and NuPage® LDS buffer and incubation at 74^{o}C for 10 minutes. For the zero time point, the reaction buffers were added immediately after the addition of thrombin. Crosslinking was studied by reducing SDS-PAGE (12% Bis-Tris NuPAGE) run at 200 volts for one hour and stained with Colloidal Blue (Invitrogen, Carlsbad, CA).

Thromboelastography analysis of fibrin clot formation

Clotting strength and kinetics of various tri-component mixtures of purified rFI or plasma-derived human fibrinogen (pdFI), rFXIII and pdFIIa or rFIIa were evaluated by thromboelastography (TEG) (Thromboelastograph® Hemostasis System 5000 series, Haemoscope Corp., Niles, IL). The effect of FI on clot strength and kinetics was evaluated by maintaining rFXIII (0.35 mg/ml, 2408 U/ml) and pdFIIa (0.10 mg/ml, 52.8 U/ml) levels while varying rFI concentrations (0, 3, 6, 9, 12 and 15 mg/ml). The effect of rFXIII on clot strength and kinetics was evaluated by maintaining FI (8.56 mg/ml) and pdFIIa (0.10 mg/ml, 52.8 U/ml) levels while varying rFXIII concentrations (0, 0.03, 0.13, 0.23, 0.28, 0.35 and 0.42 mg/ml). The effect of pdFIIa on clot strength and kinetics was also evaluated by maintaining FI (8.56 mg/ml) and rFXIII (0.35 mg/ml, 2408 U/ml) levels while varying pdFIIa concentrations (0, 0.03, 0.05, 0.10, 0.15, 0.20 and 0.25

mg/ml). For all experiments, FI then FXIII was transferred to a single-use TEG cup and warmed to 37^{o}C by the TEG instrument. Calcium chloride (Sigma, St. Louis, MO) was then added to the cups and clot formation was initiated by adding pdFIIa.

Using the same method, stoichiometric molar ratio based experiments were performed. Once the optimal ratio was established, experiments were also performed that maintained stoichiometric molar ratios of rFXIII/rFI (0.16) and pdFIIa/rFI (0.18) while increasing rFI concentrations (9, 12, 12.5 and 15 mg/ml) to determine the effect of increasing FI. To determine whether the rFXIII/rFI ratio of 0.16 was optimal at a higher rFI concentration (12.5 mg/ml), experiments were performed that maintained rFI and FIIa (FIIa/FI = 0.18) while increasing rFXIII/FI (0.16, 0.18 and 0.20).

Clotting parameters of several tri-component solutions consisting of different levels of rFI, pdFI (Enzyme Research, Laboratories, South Bend, IN) or pdFI (Tisseel®, Baxter, Deerfield, IL) and rFXIII were compared to human blood. Tisseel's sealant and thrombin solutions were reconstituted as per manufacturer's instructions. Tisseel's overall protein concentration was determined by standard Bicinconic Acid (BCA) methods. FI (2.9 or 8.6 mg/ml) were combined with rFXIII (0.03 or 0.35 mg/ml), pdFIIa (52.8 U/ml) and 11 mM $CaCl_2$ and analyzed by TEG. Fresh, normal whole human blood (NHB) from 22 healthy, medication-free individuals, collected in tubes containing 3.2% citrate, was obtained from Research Blood Components (Brighton, MA). 340 µl of blood was transferred to a single-use TEG cup and warmed to 37^{o}C by the TEG instrument. 20 µl of 200 mM $CaCl_2$ solution was then added to the cups to initiate clotting.

The optimized rLFS was compared to the commercially available Tisseel® which was reconstituted as per manufacturer's instructions used as intended by mixing the

sealant and thrombin solutions in equal proportions. 180 µl of Tisseel's sealant, which consists of between 67 and 106 mg/ml pdFI and 2,250 and 3,750 KIU/ml inhibitor, was transferred to a single-use TEG cup and warmed to 37°C by the TEG instrument. 180 µl of Tisseel's thrombin solution, which contains 400 to 625 U/ml pdFIIa and 36 to 44 mM $CaCl_2$, was then added to the cups containing sealant. These results were compared to clotting parameters obtained with combining rFI (15 mg/ml), rFXIII (0.59 mg/ml, 4,095 U/ml, rFXIII/rFI = 0.16), rFIIa (0.33 mg/ml, 176.7 U/ml, rFIIa/rFI = 0.18) and 12 mM $CaCl_2$ in a TEG cup as described above.

The TEG Analytical Software (version 4.2.2, Haemoscope, Niles, IL) collected time to clot initiation (R), time to achieve a clot firmness of 20mm (K) and maximal clot strength (MA). Results were compared by ANOVA and t test with an α of 0.05. The instrument was calibrated each day of use. All tests described above include a minimum of three replicate samples in each treatment group. All NHB samples were tested within 36 hours of the blood draw of each individual donor.

Clot lysis by thromboelastography

Percent lysis by added plasmin was determined by thromboelastography which was performed on solutions containing purified rFI or pdFI, rFXIII and rFIIa with a Thromboelastograph® (TEG®) Hemostasis System 5000 series (Haemoscope Corp., Niles, IL). Clotting strength and kinetics of purified rFI or pdFI with rFXIIIa and rFIIa with added plasmin was evaluated. rFI or pdFI (final concentration: 9 mg/ml) transferred to a single-use TEG cup maintained at 37°C by the instrument. rFXIIIa (final concentration: 2,429 U/ml, 0.35 mg/ml rFXIIIa/FI = 0.16) and various amounts of plasmin (final concentrations: 0, 8.4, 17, 84 and 842 mU/ml, 0.002 to 0.216 mg/ml) were

added. $CaCl_2$ (final concentration: 12 mM) and Ringers solution (155 mM NaCl, 5 mM KCl, 2 mM $CaCl_2$, 1 mM $MgCl_2$, added to standardize volume in cup) was added followed quickly by pdFIIa (final concentration: 105.6 U/ml, FIIa/FI = 0.18) to initiate clot formation. Data was collected every five seconds for 30 minutes by the TEG interfaced with a computer. Each sample was run in triplicate so means and standard deviations could be calculated. The data was exported and analyzed in Microsoft® Excel.

Results

rFXIIIa and pdFIIa characterization

SDS-PAGE and N-terminal sequencing indicated that the purified protein from the yeast was rFXIIIa rather than rFXIII. These and immunoblots indicated rFXIIIa had a purity of greater than 98% (data not shown). The Pefakit® Factor XIII Incorporation Assay (Pentapharm, CT) yielded a specific activity of almost 7,000 U/mg for rFXIIIa. The pdFIIa prepared by citrate activation was comprised of α-thrombin and fragments as per SDS-PAGE (Figure 6.2A, lane 10) and chromogenic assay yielded a specific activity of 528 U per mg.

γ-γ crosslinking of FI by FXIIIa

γ-γ crosslinking of rFI by rFXIIIa was analyzed by SDS-PAGE as previously described.[49] γ-chain dimers begin forming within a couple of seconds when rFI and rFXIII were activated by pdFIIa (Figure 4.2A) and rFIIa (Figure 4.2B) as seen by the disappearance of the monomer and appearance of the dimer. The α-chain monomer is also disappearing for both rFI samples and by 5 minutes, most of the rFI α-chain

monomer has disappeared resulting in smearing at the top of the lanes. γ-γ dimers were not observed in the rFI sample treated with pdFIIa (Figure 4.2A, lane 8) or rFIIa (Figure 4.2B, lane 8).

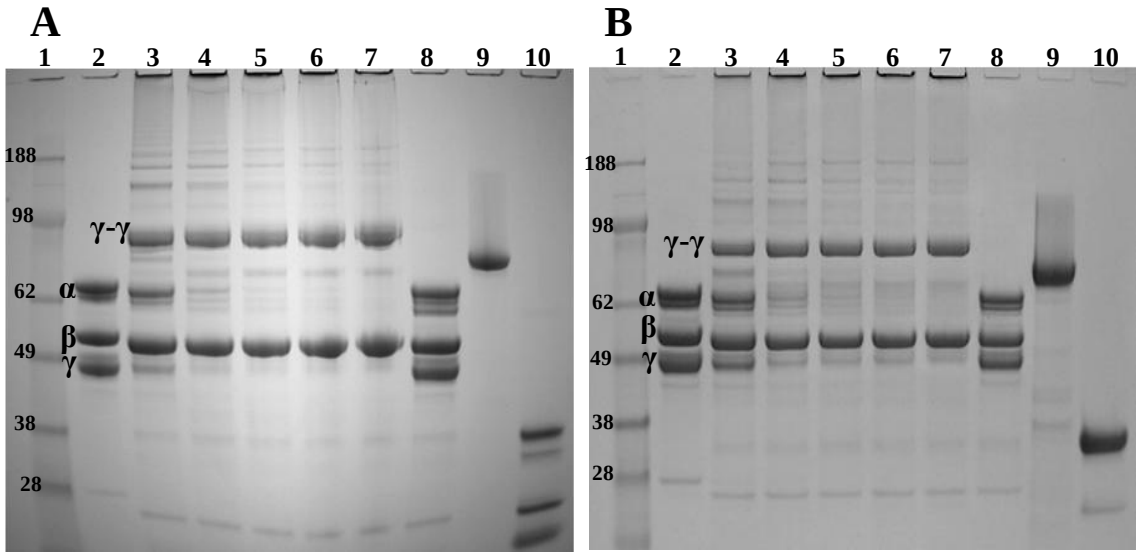

Figure 4.2. Formation of fibrin γ-chain crosslinks as analyzed by reducing SDS-PAGE. SDS-PAGE gels under reducing conditions. Formation of fibrin γ-chain cross-links was analyzed for clots created with components used to optimize the LFS: rFI, rFXIII and pdFIIa (A) or rFIIa (B). Lane 1: a molecular weight marker. Lane 2: rFI prior to incubation with rFXIII and FIIa. Lanes 3 through 7: rFI, rFXIII and FIIa incubated for 2 seconds, 5, 15, 30 and 60 minutes. Lane 8: rFI incubated with FIIa for 60 minutes. Lane 9: rFXIII sample prior to incubation with rFI and FIIa. Lane 10: FIIa sample prior to incubation with rFXIII and rFI.

Thromboelastography (TEG) analysis of fibrin clot formation

The effect of increasing FI concentration was analyzed by TEG. While rFXIIIa (0.35 mg/ml) and pdFIIa (52.8 U/ml) were held constant, rFI was increased from zero to 15 mg/ml (Figure 4.3). As expected, rFXIIIa treated with pdFIIa did not yield any change in viscosity. Increase in rFI concentration did not greatly affect time to clot initiation (R) which ranged from 16.67 ± 2.89 seconds for 6 and 12 mg/ml and 21.67 ± 2.89 mg/ml for 3 mg/ml rFI. Clotting kinetics were also relatively consistent for 6 (K = 51.67 ± 2.89, α = 79.83 ± 1.5), 9 (K = 50.00 ± 0, α = 81.90 ± 0.56), 12 (K = 50.00 ± 0, α = 82.50 ± 0.69) and 15 mg/ml (K = 50.00 ± 0, α = 83.10 ± 0.50). Maximum clot strength

increased significantly with the increase in FI concentration ($p < 0.001$). At 0, 3, 6, 9, 12, and 15 mg/ml, clot strengths increased: 0 ± 0, 1,355.9 ± 556.4, 4,610.8 ± 127.9, 9,856.0 ± 1,093.0, 19,946.8 ± 2,343.3 and 25,283.2 ± 3,861.9 dynes/sec.

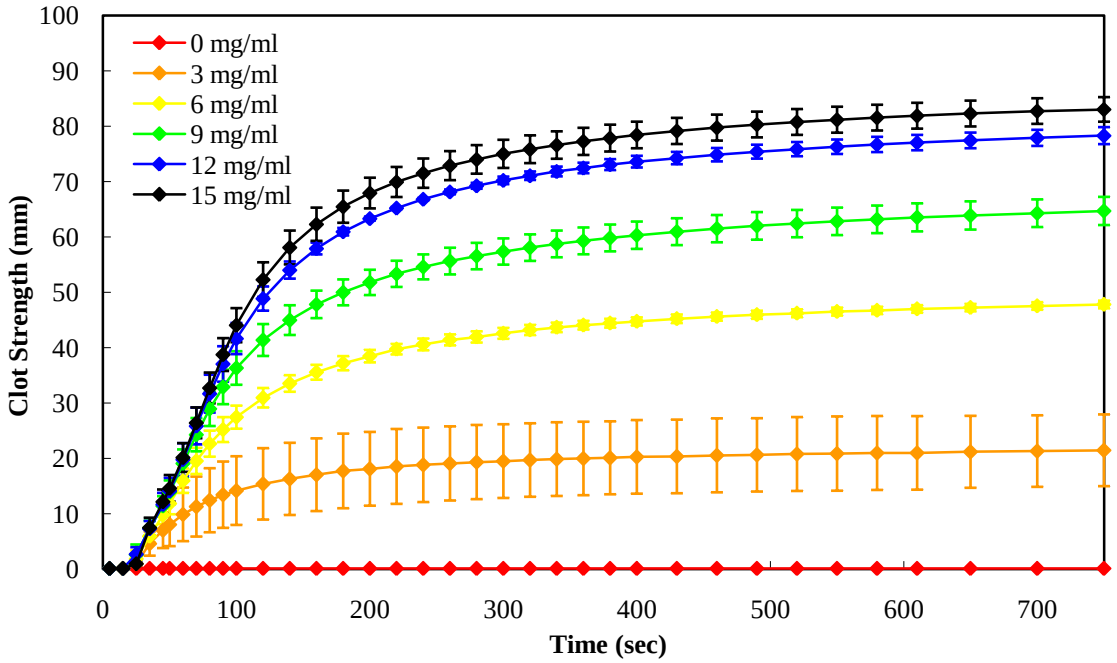

Figure 4.3. Effect of increasing rFI concentration on clot parameters by thromboelastography. Thromboelastographic data was collected on solutions containing constant concentrations of pdFIIa (52.8 U/ml) and rFXIIIa (0.35 mg/ml) with varying concentrations of rFI of 0, 3, 6, 9, 12 and 15 mg/ml. Data were expressed as mean +/- standard deviation.

Clotting strength and kinetics of various tri-component mixtures of rFI and pdFI (from Enzyme Research and Baxter- Tisseel®), rFXIIIa and pdFIIa at different concentrations were evaluated by thromboelastography. The first experiment added variable concentrations of pdFIIa (0, 0.03, 0.05, 0.10, 0.15, 0.20, and 0.25 mg/ml) while maintaining constant concentrations of rFI or pdFI (8.56 mg/ml) and rFXIII (0.35). Increasing pdFIIa significantly sped clot initiation time (R) and time to clot firmness (K) and increased clot strength (MA) for both rFI and pdFI ($p < 0.001$ for all) (Figure 4.4).

At the highest pdFIIa level, time to clot initiation was equivalent for all three FI: 10.0 ± 0 seconds.

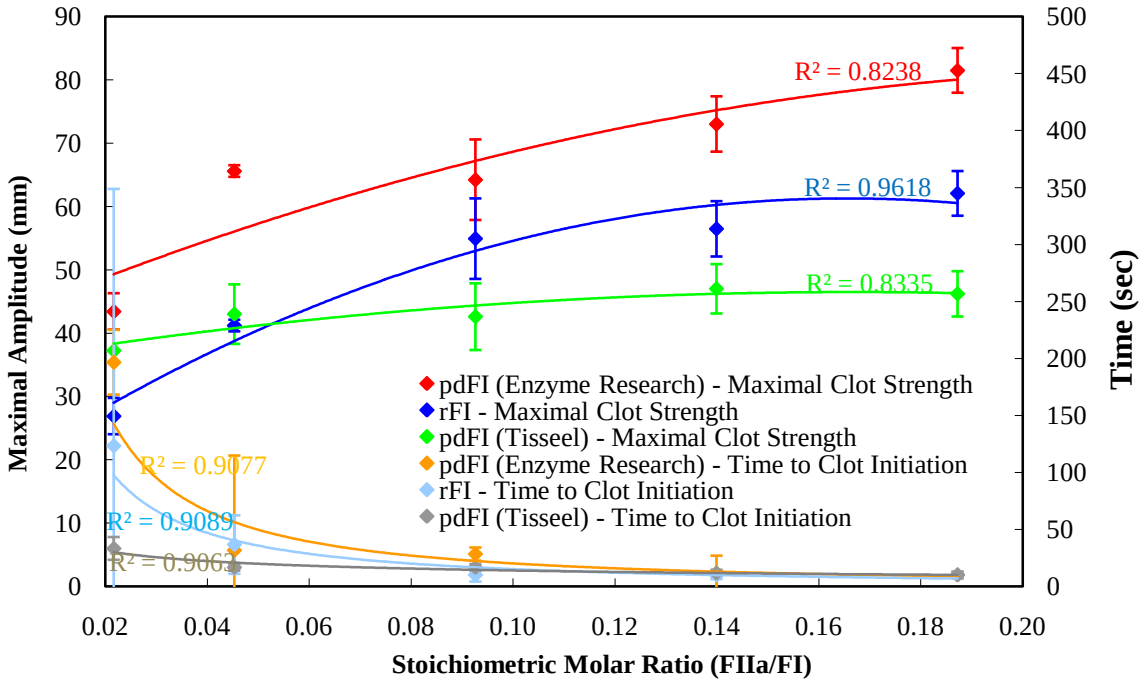

Figure 4.4. FIIa dependent maximal clot strength (MA) and clot initiation time (R) with constant FI and rFXIIIa. Thromboelastographic data was collected on solutions containing constant concentrations of pdFI or rFI (8.56 mg/ml) and rFXIIIa (0.35 mg/ml, 2,408 U/ml, stoichiometric molar ratio (rFXIIIa/FI) = 0.17) with varying concentrations of added pdFIIa of 0, 0.03, 0.05, 0.10, 0.15, 0.20 and 0.25 mg/ml (stoichiometric molar ratios: 0, 0.03, 0.06, 0.13, 0.19, 0.26 and 0.32). At the various levels of pdFIIa, pdFI from Enzyme Research result in stronger clot strengths (red, R^2 = 0.82) than pdFI (Tisseel®) from Baxter (green, R^2 = 0.83). rFI yields clot strengths lower than both pdFI samples with low pdFIIa levels but exceeds strengths of pdFI (Tisseel®) at high levels of pdFIIa (blue, R^2 = 0.96). The addition of increasing units of pdFIIa resulted in faster clot initiation times for pdFI from Enzyme Research (orange, R^2 = 0.91), pdFI from Baxter (gray, R^2 = 0.91) and rFI (pale blue, R^2 = 0.91). Data were expressed as mean +/- standard deviation.

The second experiment added variable concentrations of rFXIII (0, 0.03, 0.13, 0.23, 0.28, 0.35 and 0.42 mg/ml) while maintaining constant concentrations of rFI or pdFI (8.56 mg/ml) and pdFIIa (52.8 U/ml). Increasing rFXIIIa did not greatly alter the clot initiation time (R); however, it did significantly increase clot strength (MA) for rFI ($p < 0.001$) and both pdFI samples (Tisseel p , Enzyme Research $p < 0.001$) (Figure 4.5).

At the highest level of rFXIIIa, pdFI from Tisseel® yielded the lowest clot strength (4,367.3 ± 761.8 dynes/sec), pdFI (Enzyme Research Laboratories) yielded the highest (12,347.5 ±1,429.5 dynes/sec) and rFI fell between (6,904.8 ± 566.2 dynes/sec). Times to clot initiation were similar for the three FI samples.

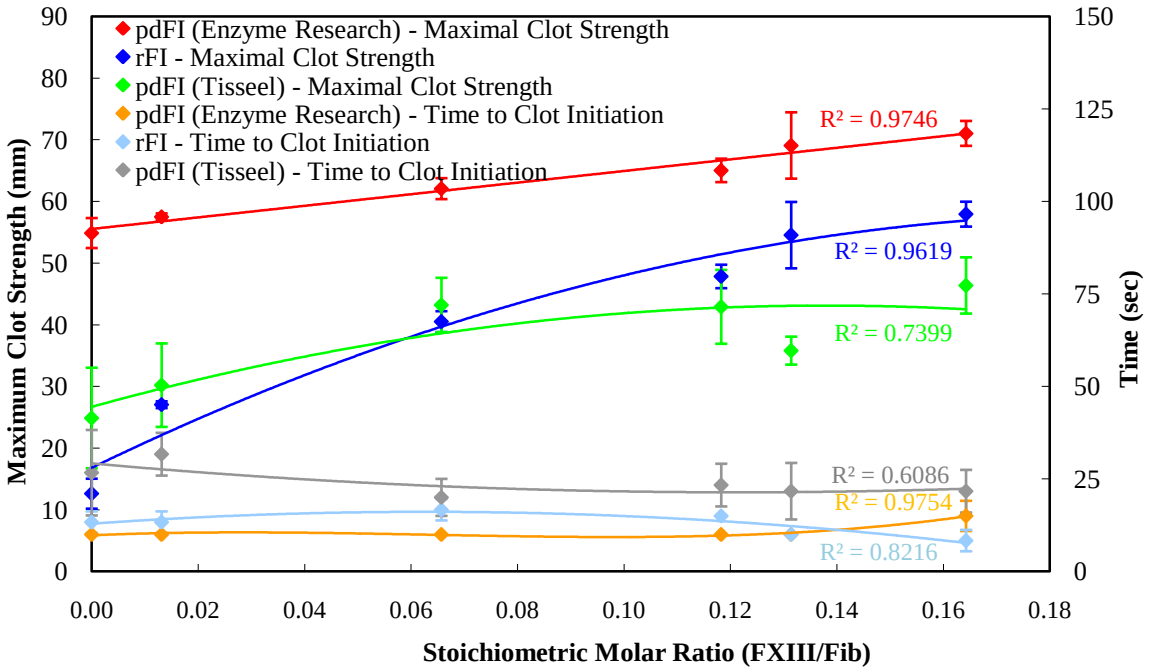

Figure 4.5. rFXIIIa dependent maximal clot strength (MA) and clot initiation time (R) with constant FI and pdFIIa concentrations. Thromboelastographic data was collected on solutions containing constant concentrations of plasma-derived or recombinant fibrinogen (8.56 mg/ml) and pdFIIa (0.10 mg/ml, stoichiometric molar ratio (FIIa/FI) = 0.13) with varying concentrations of added rFXIIIa of 0, 0.03, 0.13, 0.23, 0.28, 0.35 and 0.42 mg/ml (stoichiometric molar ratios: 0, 0.01, 0.07, 0.12, 0.14 and 0.17). At the various levels of rFXIIIa, pdFI from Enzyme Research yielded almost two-fold greater clot strengths (red, R^2 = 0.97) than pdFI (Tisseel®) from Baxter (green, R^2 = 0.74). rFI yielded clot strengths lower than both pdFI samples with low rFXIIIa exceeds strengths of pdFI (Tisseel®) at high levels of rFXIIIa (blue, R^2 = 0.96). The addition of rFXIIIa to resulted in minimal changes in clot initiation times for pdFI from Enzyme Research (orange, R^2 = 0.98), pdFI from Baxter (gray, R^2 = 0.61) and rFI (pale blue, R^2 = 0.82). Data were expressed as mean +/- standard deviation.

Increasing the concentration of rFXIIIa (Figure 4.5) and FIIa (Figure 4.4) both yielded asymptotic approaches to maximal clot strength for rFI and both FI samples. Ratios of rFXIIIa (0.16, 0.039 mg rFXIIIa per mg FI) and FIIa (0.18, 11.7 U FIIa per mg FI) with

respect to fibrinogen, located at the asymptote for clot strength, were selected for the remaining experiments.

The optimal level of calcium was also determined by maintaining rFI at 15 mg/ml and rFXIIIa and pdFIIa molar ratios to FI at 0.16 and 0.18, respectively. Calcium was added at 0, 3, 6, 9, 11, 12 and 15 mM. Calcium concentration did not alter time to clot initiation (R) or coagulation time (K); however, maximum clot strength was dependent on calcium. At 0 mM $CaCl_2$, clot strength was 3,399 dynes/sec. Maximum clot strength was not significantly different for $CaCl_2$ at 3 mM or greater ($p = 0.876$) (Figure 4.6). Further experiments used 12 mM $CaCl_2$.

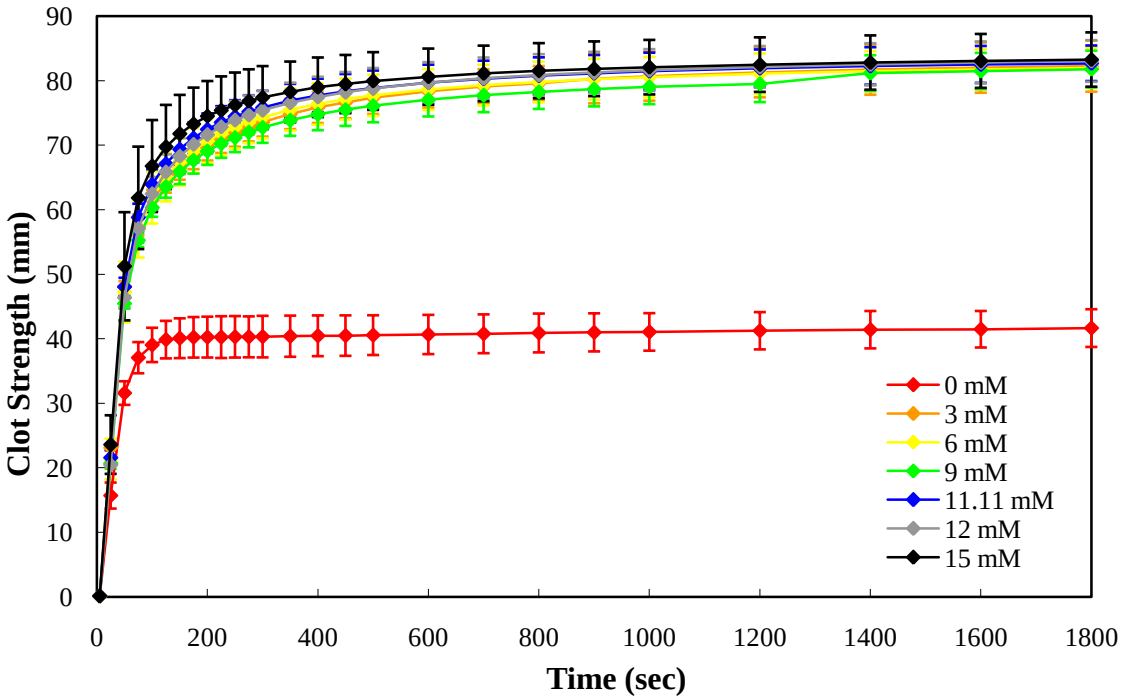

Figure 4.6. $CaCl_2$ dependent maximal clot strength (MA) with constant rFI, rFXIIIa and pdFIIa concentrations. Thromboelastographic data was collected on solutions containing constant concentrations of rFI (15 mg/ml), rFXIIIa (0.59 mg/ml, stoichiometric molar ratio (FXIIIa/FI) = 0.16) and pdFIIa (0.33 mg/ml, stoichiometric molar ratio (FIIa/FI) = 0.18) with varying concentrations of $CaCl_2$ of 0, 3, 6, 9, 11, 12, and 15 mM. Data were expressed as mean +/- standard deviation.

Once the optimal ratio was established, experiments were also performed to identify whether the ratios were optimal at higher FI concentrations and whether an

increase in rFXIIIa helped in the presence of higher rFI. The first experiment maintained stoichiometric molar ratios of rFXIIIa/rFI (0.16) and pdFIIa/rFI (0.18) while increasing rFI concentrations (9, 12, 12.5 and 15 mg/ml). Increasing FI resulted in an increase in clot strength ($p = 0.017$); however, 15 mg/ml was not significantly greater than that of 12.5 mg/ml ($p = 0.262$) (Figure 4.7). Time to clot initiation was not affected.

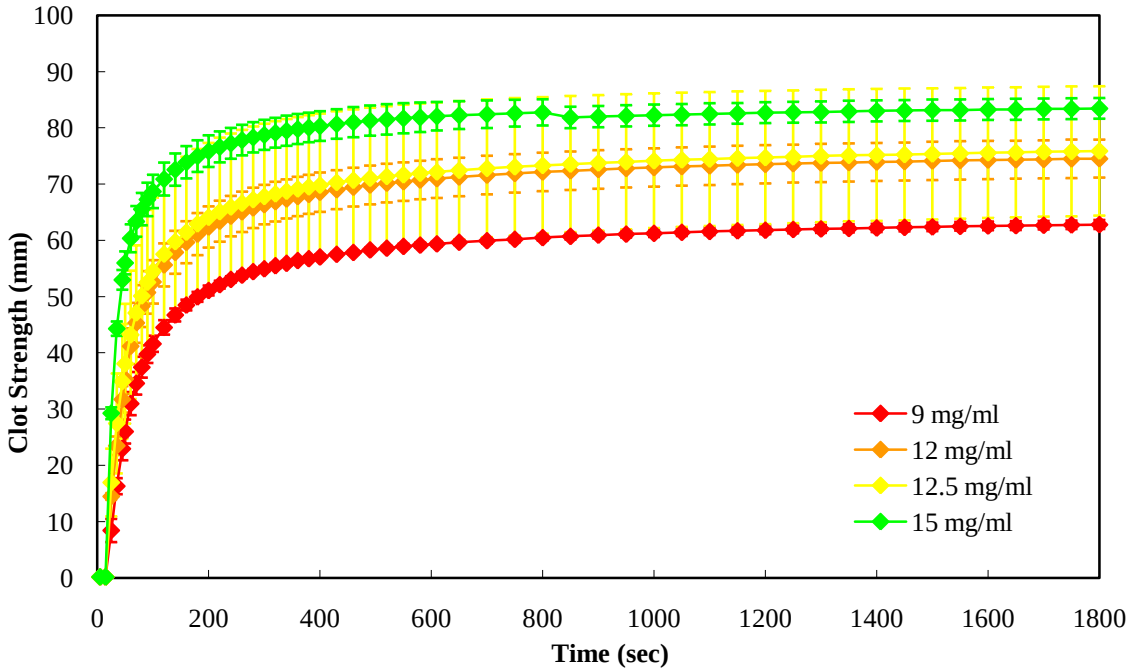

Figure 4.7. Effect of increasing rFI while maintaining stoichiometric molar ratios of rFXIIIa/rFI and pdFIIa/rFI of 0.16 and 0.18, respectively. Thromboelastographic data was collected on solutions containing increasing concentrations of rFI (9, 12, 12.5 and 15 mg/ml) while maintaining stoichiometric molar ratios of rFXIIIa/rFI and pdFIIa/rFI at 0.16 and 0.18, respectively. Data were expressed as mean +/- standard deviation.

To determine whether the rFXIIIa/rFI ratio of 0.16 was optimal at a higher rFI concentration (12.5 mg/ml), experiments were performed that maintained rFI and FIIa (FIIa/FI = 0.18) while increasing rFXIIIa/FI (0.16, 0.18 and 0.20). Increasing the ratio of rFXIII/rFI did not alter clot strength ($p = 0.292$), kinetics ($p < 0.001$) or time to clot initiation ($p < 0.001$) (Figure 4.8).

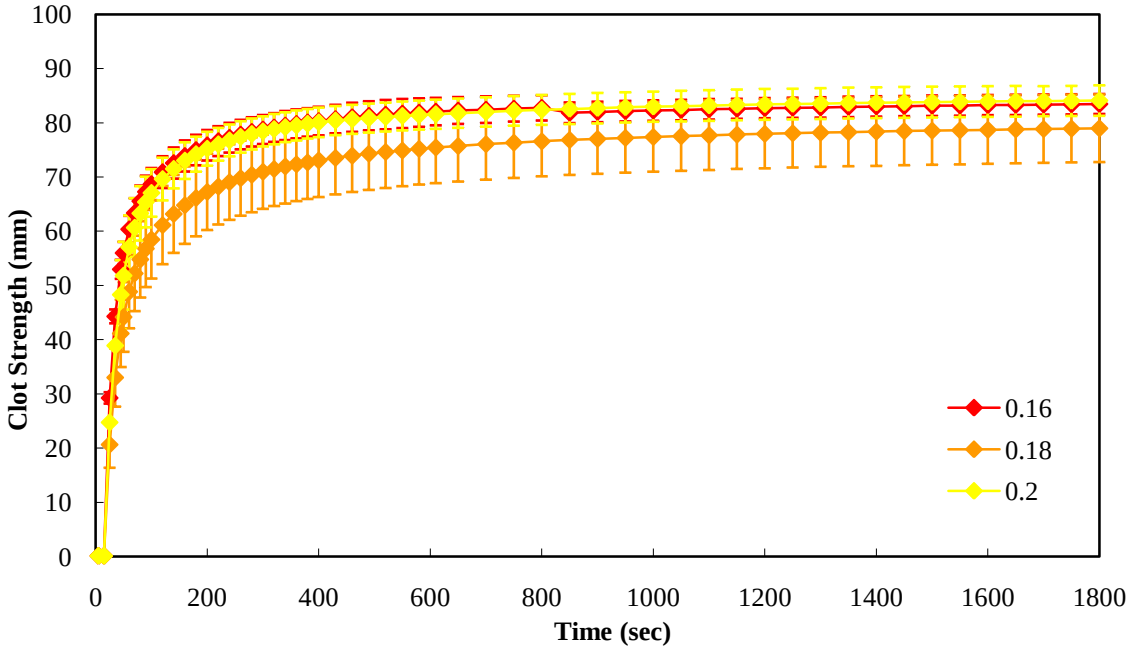

Figure 4.8. Effect of increasing rFXIIIa concentration. Thromboelastographic data was collected on solutions containing constant concentrations of rFI (12.5 mg/ml) and pdFIIa (stoichiometric molar ratio (FIIa/FI) = 0.18) with varying stoichiometric molar ratios of rFXIIIa of 0.16, 0.18 and 0.2. Data were expressed as mean +/- standard deviation.

Thromboelastographic properties of clots made by tri-component mixtures of rFI, rFXIII and pdFIIa were compared to the average values (N = 22) of clots made by fresh citrated human whole blood (Figure 4.9). Clots consisting of 8.6 mg/ml rFI, 0.35 mg/ml rFXIIIa and 52.8 U/ml pdFIIa had maximum clot strengths 3.5 ± 0.2 -fold greater (11,550 ± 560 dyne/sec) than clots formed by NHB alone (3,330 ± 810 dyne/sec). Clot onset (R) and time to clot firmness (K) were also much faster for this tri-component mixture (R = 12 ± 3 seconds, K = 50 ± 0 seconds) than NHB (R = 412 ± 68 seconds, K = 375 ± 136 seconds). A tri-component mixture that replaced 8.6 mg/ml rFI with 8.6 mg/ml FI (Tisseel®, Baxter) and contained equivalent amounts of rFXIIIa and pdFIIa yielded slower clot onset time and time to clot firmness (R = 22 ± 6 seconds, K = 60 ± 17 seconds) and significantly lower clot strength (4,367 ± 762 dyne/sec) than the rFI version.

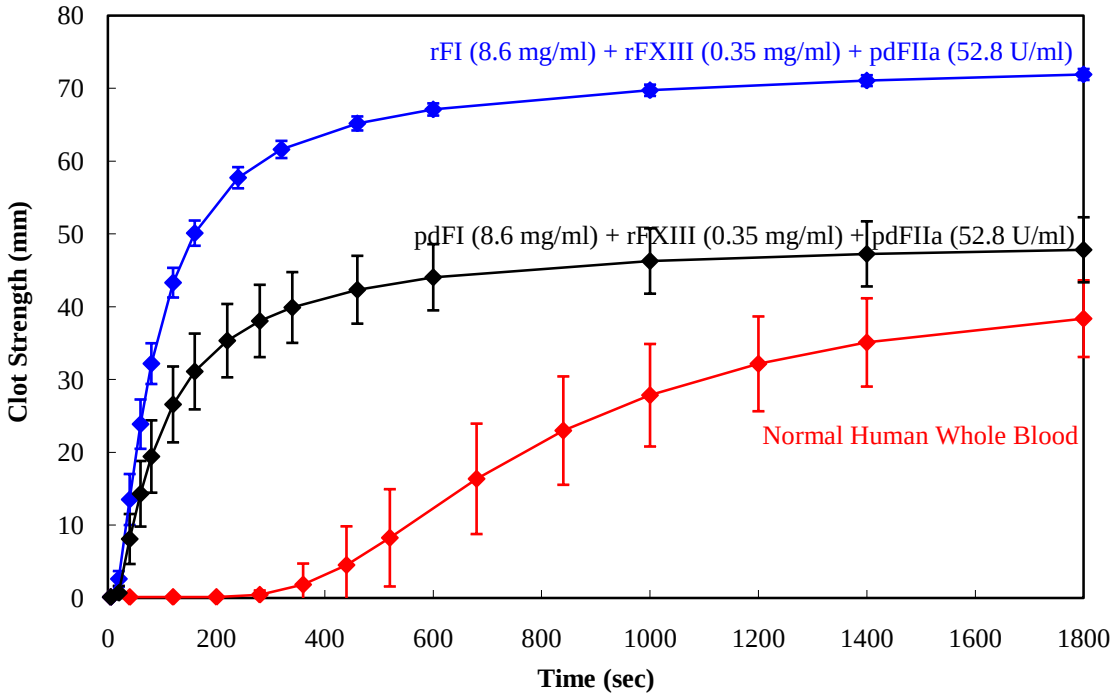

Figure 4.9. Thromboelastographic properties of NHB and tri-component mixtures of rFI, pdFIIa and rFXIIIa. Clots consisting of 8.6 mg/ml plasma-derived fibrinogen from a commercial LFS, 0.35 mg/ml rFXIII and 52.8 U/ml pdFIIa (black) have maximal clot strengths 18% greater than the average maximal strength of clots from whole blood of 22 normal donors (red). Replacing the plasma-derived fibrinogen with recombinant fibrinogen (blue) yielded clot strengths 67% greater than blood and 41% greater than that of the fibrinogen from the commercially available LFS. Data were expressed as mean +/- standard deviation.

Finally, the optimal fully-recombinant LFS was compared to a commercially available pdLFS (Tisseel,® Baxter) used as intended. The fibrin sealant and thrombin portions of Tisseel® were mixed in equal portions yielding a pdLFS containing between 67 and 106 mg/ml pdFI and 400 to 625 U/ml pdFIIa and 36 to 44 mM $CaCl_2$. These results were compared to clotting parameters obtained with combining rFI (15 mg/ml), rFXIII (0.59 mg/ml, rFXIII/rFI = 0.16), rFIIa (0.33 U/ml, rFIIa/rFI = 0.18) and 12 mM $CaCl_2$ (Figure 4.10). The time to clot initiation (R) was slightly slower for the optimized rLFS (10.0 ± 0 seconds) than Tisseel® (8.3 ± 2.89 seconds) ($p = 0.374$); however, the time to clot firmness (K) were equivalent (50.0 ± 0 seconds). Maximum clot strengths

were similar at 24,424.9 ± 3,821.9 and 26,374.6 ± 6,242.6 dynes/sec, respectively (p = 0.728).

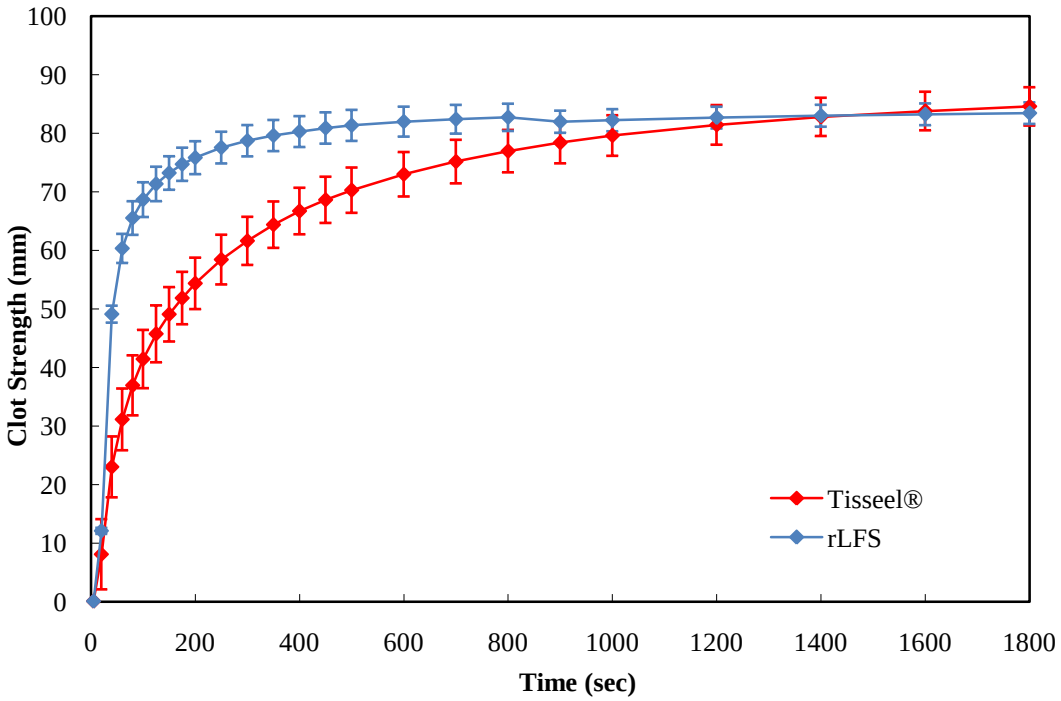

Figure 4.10. Thromboelastographic properties of the optimized tri-component rLFS and a pdLFS (Tisseel®). Clots consisting of 15 mg/ml rFI, 0.59 mg/ml (4,095 U/ml) rFXIIIa and 0.33 mg/ml (176.7 U/ml) rFIIa (FXIIIa/FI = 0.16, FIIa/FI = 0.18) (blue) have faster clot kinetics and equivalent maximal clot strengths as a pdLFS (Tisseel®) as prepared by its manufacturer's instructions (red). Tisseel contains 33.5 to 53 mg/ml pdFI and 200 to 312.5 U/ml pdFIIa. Data were expressed as mean +/- standard deviation.

Clot lysis by thromboelastography

Plasminolysis of clots formed by rFI- and pdFI-based LFS were examined by TEG. Plasmin did not greatly affect the initiation of clot onset but altered clot strength greatly for both pdFI and rFI (Table 4.1). Addition of 8.4 and 84 U/ml plasmin to Tisseel® results in no alteration in clotting kinetics and no lysis. Addition of 8.4 or 17 U/ml of plasmin to pdFI-based clots, resulted in a 62% and 57% decreases in maximal clot strength (from 10,334.0 ± 3,599.3 to 3,914.1 ± 691.1 and 4,423.1 ± 450.0 dynes/sec, respectively) with a 0 and 1.9% lysis 60 minutes after maximal clot strength was reached. Increasing plasmin to 84 U/ml resulted in a 77% decrease (2,388.2 ± 476.1 dynes/sec)

from the untreated sample with 8.2% lysis. Strength of rFI-based clots decreased 49%, 41%, and 92% with the addition of 8.4, 17, and 84 U/ml (from 5,632.3 ± 1,151.4 to 2,896.6 ± 729.8, 3,315.6 ± 1,682.3 and 474.4 ± 105.5 dynes/sec, respectively) with subsequent lysis of 31.4%, 59.7% and 94.1% 60 minutes after maximal clot strength was reached. Addition of 842 mU/ml resulted in no clot formation.

Table 4.1. Effects of plasmin on clotting parameters of Tisseel®, pdFI- and rFI-based clots by TEG. Zero to 842 mU/ml of plasmin were added to solutions containing pdFI- (Tisseel and Enzyme Research) and rFI-based LFS components. Values listed are means ± standard deviation.

Sample		Time to Clot Initiation (sec)	Maximal Clot Strength (dynes/sec)	Lysis (%)
Tisseel®	0 mU/ml plasmin	8.3 ± 2.9	26,374.6 ± 6,242.6	0 ± 0
	8.4 mU/ml plasmin	10.0 ± 0	19,381.7 ± 1,185.9	0 ± 0
	84 mU/ml plasmin	10.0 ± 0	23,486.9 ± 1,771.9	0 ± 0
pdFI-based LFS	0 mU/ml plasmin	10.0 ± 0	10,334.0 ± 3,599.3	0 ± 0
	8.4 mU/ml plasmin	13.3 ± 2.9	3,914.1 ± 691.5	0 ± 0
	17 mU/ml plasmin	11.7 ± 2.9	4,423.1 ± 450.0	1.9 ± 1.8
	84 mU/ml plasmin	15.0 ± 0	2,388.2 ± 476.1	8.2 ± 7.7
rFI-based LFS	0 mU/ml plasmin	10.0 ± 0	5,632.3 ± 1,151.4	0 ± 0
	8.4 mU/ml plasmin	10.0 ± 0	2,896.6 ± 729.8	31.4 ± 4.8
	17 mU/ml plasmin	10.0 ± 0	3,315.6 ± 1,683.2	59.7 ± 7.9
	84 mU/ml plasmin	15.0 ± 3.2	474.4 ± 105.5	94.1 ± 3.6
	842 mU/ml plasmin	No clot	No clot	No clot

Discussion

The objective of the research presented in this chapter was to optimize the components of and identify the importance of FXIII in a LFS. Fibrinogen is the key factor that provides FS their adhesive[6, 14, 50] and hemostatic abilities and tensile strength.[14] All research concurs regarding the import of fibrinogen in FS. Our data supported earlier

findings that increases in fibrinogen result in stronger clots;[23] however, we observed diminishing returns while increasing FI concentration. Increasing FI from 3 to 6 mg/ml resulted in a 2.4-fold increase in maximal clot strength; however, increasing from 12 to 15 mg/ml did not yield significantly different maximum clot strengths ($p = 0.110$). Thus, the extremely high FI levels in many FS, like Tisseel® which contains up to 53 mg/ml, may not be necessary unless the protein's preparation lowers FI clotability.

Thrombin is also a key factor in FS. Previous research found that FIIa significantly increases the rate of fibrin formation[14, 23, 51] and also plays a role in tensile strength.[11, 14] The ratio of FI to FIIa is important.[52] Our results support these findings. The increase of FIIa sped clot formation and kinetics and also significantly increased maximum clot strength (Figure 4.4); however, excess FIIa can deleteriously affect clotting. Researchers found that if FIIa is too high, inhomogeneous clots are formed.[52] We found that high levels of thrombin could reduce maximum clot strength (data not shown) probably due to the rapid increase in viscosity lowering the diffusion of FXIII required to create a strong clot; however, more research needs to be conducted to clarify this phenomenon.

The import of FXIII is debated. Some researchers found that the ratio of FI to FXIII was important[52] while others did not see differences when FXIII was added to FS.[11, 53] Biochemical studies indicate that α-α and γ-γ crosslinking by FXIIIa increases clot strength 3.5-fold;[18] therefore, FXIII should be included in FS if clot strength is desired. Researchers found that the rate of fibrin crosslinking was faster in FS containing more FXIII[46] and thereby increased the clot's resistance to fibrinolysis.[46, 54] In addition, research found that FXIII was critical in FS for fibroblast migration.[12] In

challenging situations where blood flow was not easily disrupted requiring FS to clot and adhere to tissue quickly, sealants that included FXIII had significantly better results than those without FXIII.[46]

Most FS on the market contain FI and FIIa in similar amounts; however, FXIII content ranges.[46] The ratio of FXIII to FI in human plasma is approximately 0.4 U/mg; however, some commercial products contain no FXIII or 0.1 U/mg except for Beriplast P which contains approximately 0.44 to 0.89 U/mg.[46] Dickneite et al. found that a FXIII to FI ratio of 0.78 U/mg (70 U/ml FXIII) resulted in a slightly greater tensile strength than concentrations above or below this range.[46] They concluded that the addition of FXIII hastens crosslinking and increases clot strength.[46] Their research suggested 40 to 80 U/ml (0.44 to 0.89 U/mg) FXIII concentration in FS.[46]

We added multiple levels of rFXIIIa to our LFS and found even our lowest addition of 23.13 U rFXIIIa per mg FI (208 U/ml) yielded a significantly higher maximal clot strength than rLFS without rFXIIIa (Figure 4.5). This lowest treatment is almost 24-fold greater than the highest levels added to commercial FS. Our optimal rLFS contains 274 U rFXIIIa per mg FI (2,464 U/ml) which is 308-fold greater than commercial FS. Previous research has not added FXIII to the levels that we have because this requires a production source that can create abundant amounts of rFXIIIa. Thromboelastography indicates that the addition of FXIII prolongs fibrinolysis,[54] reduces time to clot initiation and increases clotting kinetics and viscoelastic strength.[55, 56] While our results supported the increase in clot strength, kinetics and time to clot initiation were not greatly affected.

Byrne et al. varied FS components FI (23 to 58 g/l), FXIII (1 to 12.5 U/ml, FXIII/FI ratio: 0.16 to 0.24) and FIIa (50 to 1000 U/ml) to identify the optimal mixture. This research found that FS with 39 mg/ml FI, no added FXIII and 200 to 600 U/ml FIIa yielded the best viscoelastic properties.[53] Higher FI and FIIa concentrations inhibited wound healing and lower levels were not effective sealants.[11, 53] Our optimal FI and FIIa levels are significantly lower than the published optimal mixture and commercially available products.

Our optimal LFS contains 9 mg/ml FI, 0.36 mg/ml FXIIIa (FXIIIa/FI molar ratio of 0.16), 105.6 U/ml FIIa (FIIa/FI molar ratio of 0.18) and 12 mM $CaCl_2$. While 15 mg/ml rFI yielded slightly higher clot strength, it was not statistically significant (Figure 4.3); therefore, we selected 9 mg/ml rFI for our optimal rLFS. The optimal ratio of FXIIIa to FI (0.16) was selected to provide the highest viscoelastic strength (Figure 4.4 and 4.8). The optimal ratio of FIIa to FI (0.18) was selected to provide the fastest initiation of clot formation and clotting kinetics. rFI concentrations were selected to provide the necessary clot strength while minimizing material use. 12 mM $CaCl_2$ was selected to ensure that when applied to a wound an ample amount of the required component was available to both exogenous and endogenous proteins. Our results indicate that rLFS is unaffected by increases in calcium concentration greater than 3 mM (slightly above physiological levels of ~2 mM) which contradicts previous research that indicated that reducing calcium below 10 mM resulted in reduction in viscoelastic strength.[11] Fibrin clots made with rFI, rFXIII and FIIa yielded 5.0-fold greater shear elastic modulus strength than clots formed from NHB alone. The clotting kinetics and viscoelastic strength of our optimized LFS was equivalent to those of a commercially

available LFS; however, it uses approximately 75% less fibrinogen and thrombin. Initial preclinical testing indicates that this optimal rLFS is effective as a sealant alone and in combination with a dressing on multiple liver and femoral arteriotomy models.

Acknowledgements

This work was supported by a grant from the Department of Defense titled "Production and Purification of Fibrinogen Components for the Production of a Fibrin Sealant Hemostatic Dressing."

References

1. Stewart, R.M. et al. Seven hundred fifty-three consecutive deaths in a level I trauma center: the argument for injury prevention. *J Trauma* **54**, 66-70; discussion 70-61 (2003).
2. Bellamy, R.F., Maningas, P.A. & Vayer, J.S. Epidemiology of trauma: military experience. *Ann Emerg Med* **15**, 1384-1388 (1986).
3. Anderson, R.N. & Smith, B.L. Deaths: leading causes for 2001. *Natl Vital Stat Rep* **52**, 1-85 (2003).
4. Holcomb, J. et al. Efficacy of a dry fibrin sealant dressing for hemorrhage control after ballistic injury. *Arch.Surg.* **133**, 32-35 (1998).
5. Pusateri, A.E. et al. Effect of a chitosan-based hemostatic dressing on blood loss and survival in a model of severe venous hemorrhage and hepatic injury in swine. *J Trauma* **54**, 177-182 (2003).
6. Jackson, M.R. Fibrin sealants in surgical practice: An overview. *Am.J.Surg.* **182**, 1S (2001).
7. Mankad, P.S. & Codispoti, M. The role of fibrin sealants in hemostasis. *Am.J.Surg.* **182**, 21S (2001).
8. Alam, H.B. et al. Application of a zeolite hemostatic agent achieves 100% survival in a lethal model of complex groin injury in Swine. *J Trauma* **56**, 974-983 (2004).
9. Rhee, P. et al. QuikClot use in trauma for hemorrhage control: case series of 103 documented uses. *J Trauma* **64**, 1093-1099 (2008).
10. Gibble, J.W. & Ness, P.M. Fibrin glue: the perfect operative sealant? *Transfusion* **30**, 741-747 (1990).
11. Sierra, D.H. Fibrin sealant adhesive systems: a review of their chemistry, material properties and clinical applications. *J.Biomater.Appl.* **7**, 309 (1993).
12. Amrani, D.L., Diorio, J.P. & Delmotte, Y. Wound healing: Role of commercial fibrin sealants. *Ann.N.Y.Acad.Sci.* **936**, 566 (2001).
13. Laurens, N., Koolwijk, P. & De Maat, M.P.M. Fibrin structure and wound healing. *Journal of Thrombosis and Haemostasis* **4**, 932 (2006).
14. Lee, M.-G.M. & Jones, D. Applications of fibrin sealant in surgery. *Surg Innov* **12**, 203 (2005).
15. Schwartz, M.L., Pizzo, S.V., Hill, R.L. & McKee, P.A. Human factor XIII from plasma and platelets. Molecular weights, and subunit structures, proteolytic activation, and crosslinking of fibrinogen and fibrin. *J.Biol.Chem.* **248**, 1395 (1973).
16. Folk, J.E. & Finlayson, J.S. The e-(g-glutamyl)lysine crosslink and the catalytic role of transglutaminases. *Adv.Protein Chem.* **31**, 1 (1977).
17. McDonagh, J.M. in Hemostasis and Thrombosis: Basic Principles and Clinical Practice, Edn. Third Edition. (eds. R.W. Colman, J. Hirsh, V.J. Marder & E.W. Salzman) 301 (J.B. Lippincott Company, Philadelphia; 1994).
18. Standeven, K.F. et al. Functional analysis of fibrin g-chain cross-linking by activated factor XIII: determination of a cross-linking pattern that maximizes clot stiffness. *Blood* **110**, 902 (2007).

19. Greenberg, C.S. & Shuman, M.A. Specific binding of blood coagulation factor XIIIa to thrombin-stimulated platelets. *J.Biol.Chem.* **259**, 14721 (1984).
20. Chandler, W.L. et al. Factor XIIIA and clot strength after cardiopulmonary bypass. *Blood Coagulation Fibrinol.* **12**, 101 (2001).
21. Crawley, J.T.B., Zanardelli, S., Chion, C.K.N.K. & Lane, D.A. The central role of thrombin in hemostasis. *Journal of Thrombosis and Haemostasis* **5**, 95 (2007).
22. Cronkite, E., Lozner, E. & Deaver, J. Use of thrombin and fibrinogen in skin grafting. *Journal of the American Medical Association* **124**, 976 (194).
23. Spotnitz, W.D. & Prabhu, R. Fibrin sealant tissue adhesive--review and update. *J.Long.Term.Eff.Med.* **15**, 245 (2005).
24. Jackson, M.R. Tissue sealants: current status, future potential. *Nat Med* **2**, 637-638 (1996).
25. Albala, D.M. & Lawson, J.H. Recent clinical and investigational applications of fibrin sealant in selected surgical specialties. *J.Am.Coll.Surg.* **202**, 685 (2006).
26. Kjaergard, H.K. & Trumbull, H.R. Bleeding from the sternal marrow can be stopped using vivostat patient-derived fibrin sealant. *Ann Thorac Surg* **69**, 1173-1175 (2000).
27. Taylor, L.M., Jr. et al. Prospective randomized multicenter trial of fibrin sealant versus thrombin-soaked gelatin sponge for suture- or needle-hole bleeding from polytetrafluoroethylene femoral artery grafts. *Journal of vascular surgery official publication, the Society for Vascular Surgery [and] International Society for Cardiovascular Surgery, North American Chapter* **38**, 766-771 (2003).
28. Fabian, T., Federico John, A. & Ponn Ronald, B. Fibrin glue in pulmonary resection: a prospective, randomized, blinded study. *Ann Thorac Surg* **75**, 1587-1592 (2003).
29. Miyamoto, H. et al. Fibrin glue and bioabsorbable felt patch for intraoperative intractable air leaks. *Jpn J Thorac Cardiovasc Surg* **51**, 232-236 (2003).
30. Oliver, D.W., Hamilton, S.A., Figle, A.A., Wood, S.H. & Lamberty, B.G. A prospective, randomized, double-blind trial of the use of fibrin sealant for face lifts. *Plast Reconstr Surg* **108**, 2101-2105, discussion 2106-2107 (2001).
31. Jeschke Marc, G. et al. Development of new reconstructive techniques: use of Integra in combination with fibrin glue and negative-pressure therapy for reconstruction of acute and chronic wounds. *Plast Reconstr Surg* **113**, 525-530 (2004).
32. Evans, L.A., Ferguson, K.H., Foley, J.P., Rozanski, T.A. & Morey, A.F. Fibrin Sealant for the Management of Genitourinary Injuries, Fistulas and Surgical Complications. *J. Urol. (Hagerstown, MD, U. S.)* **169**, 1360-1362 (2003).
33. Finley, D.S. et al. Fibrin glue-oxidized cellulose sandwich for laparoscopic wedge resection of small renal lesions. *J. Urol. (Hagerstown, MD, U. S.)* **173**, 1477-1481 (2005).
34. Cappabianca, P. et al. Easy sellar reconstruction in endoscopic endonasal transsphenoidal surgery with polyester-silicone dural substitute and fibrin glue: technical note. *Neurosurgery* **49**, 473-475; discussion 475-476 (2001).
35. Nakamura, H. et al. The effect of autologous fibrin tissue adhesive on postoperative cerebrospinal fluid leak in spinal cord surgery: a randomized controlled trial. *Spine (Phila Pa 1976)* **30**, E347-351 (2005).

36. MacGillivray, T.E. Fibrin sealants and glues. *J.Card.Surg.* **18**, 480 (2003).
37. Carless, P.A., Henry, D.A. & Anthony, D.M. Fibrin sealant use for minimising peri-operative allogeneic blood transfusion. *Cochrane Database Syst Rev*, CD004171 (2003).
38. Alving, B.M., Weinstein, M.J., Finlayson, J.S., Menitove, J.E. & Fratantoni, J.C. Fibrin sealant: summary of a conference on characteristics and clinical uses. *Transfusion* **35**, 783 (1995).
39. Schlag, M.G., Hopf, R. & Redl, H. Convulsive seizures following subdural application of fibrin sealant containing tranexamic acid in a rat model. *Neurosurgery* **47**, 1463-1467 (2000).
40. Key, N.S. & Negrier, C. Coagulation factor concentrates: past, present, and future. *Lancet* **370**, 439-448 (2007).
41. Lubon, H., Paleyanda, R.K., Velander, W.H. & Drohan, W.N. Blood proteins from transgenic animal bioreactors. *Transfus Med Rev* **10**, 131-143 (1996).
42. Drohan, W.N. The past, present, and future of transgenic bioreactors. *Thromb.Haemost.* **78**, 543 (1997).
43. Bishop, P. & Lawson, J. Recombinant biologics for treatment of bleeding disorders. *Nature Reviews Drug Discovery* **3**, 684 (2004).
44. Velander, W.H., Lubon, H. & Drohan, W.N. Transgenic livestock as drug factories. *Sci.Am.* **276**, 70 (1997).
45. Butler, S.P., Van Cott, K., Subrumanian, A., Gwazduaskas, F.C. & Velander, W.H. Current progress in the production of recombinant human fibrinogen in the milk of transgenic animals. *Thromb.Haemost.* **78**, 537 (1997).
46. Dickneite, G., Metzner, H.J., Kroez, M., Hein, B. & Nicolay, U. The Importance of Factor XIII as a Component of Fibrin Sealants. *J.Surg.Res.* **107**, 186 (2002).
47. Inan, M. et al. Saturation of the secretory pathway by overexpression of a hookworm (Necator americanus) protein (Na-ASP1). *Methods in Molecular Biology (Totowa, NJ, United States)* **389**, 65 (2007).
48. Zhang, W., Inan, M. & Meagher, M.M. Rational design and optimization of fed-batch and continuous fermentations. *Methods in Molecular Biology (Totowa, NJ, United States)* **389**, 43 (2007).
49. Gorkun, O.V., Veklich, Y.I., Weisel, J.W. & Lord, S.T. The conversion of fibrinogen to fibrin: recombinant fibrinogen typifies plasma fibrinogen. *Blood* **89**, 4407-4414 (1997).
50. Marx, G. & Mou, X. Characterizing fibrin glue performance as modulated by heparin, aprotinin, and factor XIII. *J Lab Clin Med* **140**, 152-160 (2002).
51. Boyles, P.W., Ferguson, J.H. & Muehlke, P.H. Mechanisms involved in fibrin formation. *J Gen Physiol* **34**, 493-513 (1951).
52. Lewis, K.B., Teller, D.C., Fry, J., Lasser, G.W. & Bishop, P.D. Crosslinking kinetics of the human transglutaminase, factor XIII A2 , acting on fibrin gels and gamma-chain peptides. *Biochemistry* **36**, 995 (1997).
53. Byrne, D.J., Hardy, J., Wood, R.A., McIntosh, R. & Cuschieri, A. Effect of fibrin glues on the mechanical properties of healing wounds. *Br J Surg* **78**, 841-843 (1991).

54. Nielsen, V.G., Steenwyk, B.L. & Gurley, W.Q. Contact activation prolongs clot lysis time in human plasma: role of thrombin-activatable fibrinolysis inhibitor and Factor XIII. *J.Heart Lung Transplant.* **25**, 1247 (2006).
55. Nielsen, V.G., Gurley, W.Q., Jr. & Burch, T.M. The impact of factor XIII on coagulation kinetics and clot strength determined by thrombelastography. *Anesth.Analg.* **99**, 120 (2004).
56. Nielsen, V.G., Kirklin, J.K., Hoogendoorn, H., Ellis, T.C. & Holman, W.L. Thrombelastographic method to quantify the contribution of factor XIII to coagulation kinetics. *Blood Coagul.Fibrinolysis* **18**, 145 (2007).

Chapter 5

Ex vivo Evaluation of the Liquid Fibrin Sealant Components

Abstract

Commercial scale biosynthesis has been demonstrated for recombinant fibrinogen (rFI) in the milk of transgenic cows, thrombin (FIIa) by mammalian cell culture and Factor XIII by cell culture (rFXIII). These recent developments will enable the use of therapeutics that require abundant production schemes that could not previously be met by plasma sources. One possible use for these three proteins is as components in a recombinant liquid fibrin sealant (rLFS). The function of fibrin sealants is based on complicated interactions between other pro- and anticoagulant proteins, blood cells and vessel surface under flow and viscosity conditions; therefore, our optimized rLFS and its components needed to be tested *ex vivo*. Each individual component and all combinations of the LFS components were dosed into citrated normal human blood (NHB) and its respective platelet rich (PRP) and platelet poor plasma (PPP) fractions to analyze its effects on blood coagulation. Thromboelastographic analysis showed:

- rFI at near-hyperfibrinogenemic levels can increase clot strength when dosed into NHB, PRP and PPP. rFI alone or with rFXIII increases time to clot initiation when added to PRP or PPP.
- FIIa in combination with other components or alone significantly decreases the time to clot initiation for NHB, PRP and PPP. The addition of FIIa alone or with rFXIII to NHB, PRP or PPP significantly reduces clot strength; however, addition of rFI reverses the loss in clot strength.
- rFXIII alone or in combination with rFI increases clot strength when added to PPP but not when added to NHB and PRP indicating that blood-borne platelets

play a large role by providing FXIII. When added to NHB, rFXIII speeds time to clot initiation by a median of 24%.

With regard to therapeutic uses, both rFI and rFXIIIa have advantages. rFI dosed in NHB alone did not significantly alter time to clot initiation or coagulation time but did increase clot strength. Consequently, rFI may be useful for infusion therapy following haemodilution. rFXIIIa reduced time to clot initiation slightly but did not significantly change clot strength or kinetics; therefore, it may be an effective infusion therapy for FXIII deficiency. The research presented in this chapter is the first detailed evaluation of the effects of haemodilution on PRP and PPP coagulation parameters. In addition, it is also the first report of detailed *in vitro* effects of doping FI, FXIIIa and FIIa into NHB, PRP and PPP.

Introduction

Commercial scale biosynthesis has been demonstrated for recombinant fibrinogen (rFI) in the milk of transgenic cows, thrombin (FIIa) by mammalian cell culture and Factor XIII by cell culture (rFXIII). These recent developments will enable the use of therapeutics that require abundant production schemes that could not previously be met by plasma sources. One possible use for these three proteins is as components in a recombinant liquid fibrin sealant (rLFS). Fibrin sealants (FS) mimic natural clotting mechanisms thereby providing similar functions as endogenous plasma components such as creating hemostatic clots[1] and providing a scaffold for cellular infiltration needed to regenerate tissue.[1, 2] FS, which contain fibrinogen (FI), thrombin (FIIa) and calcium chloride and occasionally Factor XIII (FXIII), reproduce the final stage of the clotting cascade to aid hemostasis. FIIa catalyzes the conversion of FI to soluble fibrin monomer and FXIII to activated FXIII (FXIIIa).[3-6] FXIIIa then catalyzes the formation of the crosslinked, insoluble fibrin clot that is melded with the platelet-based, primary hemostatic plug.[5, 7-9] FS function is based on complicated interactions between other pro- and anticoagulant proteins, blood cells and vessel surface under flow and viscosity conditions;[10] therefore, our optimized rLFS and its components should be tested *ex vivo*.

Very little research has been performed on the effects of LFS components on hemostasis in *ex vivo* situations. Thromboelastographic (TEG) analysis of blood samples taken after rFXIII administration showed increased clot strength and decreased fibrinolysis with lesser effects on the speed of clot formation.[11] Detailed analysis of the impact of rFI dosing into blood (*in vitro* or *in vivo*) on clotting kinetics and viscoelastic strength requires gram amounts of rFI and thus has not been reported to date. The

objective of the research presented in this chapter was to evaluate our optimized rFI, rFXIIIa and rLFS *ex vivo*. In particular, rFI was evaluated as a replacement therapy following near exsanguination by examining the interaction of rFI with endogenous proteins. Each component of the rLFS was added individually and in combination with the others to normal human blood (NHB) and platelet rich (PRP) and platelet poor plasma (PPP) to evaluate interactions between exogenous and endogenous proteins and cellular components. The research presented in this chapter is the first detailed evaluation of the effects of haemodilution on PRP and PPP coagulation parameters. In addition, this is the first report of detailed testing of kinetics and viscoelastic strength of clots formed by endogenous and individual and combined exogenous components of a LFS.

Materials and Methods

Materials

Purified, plasma-derived prothrombin was bought from Enzyme Research Laboratories (South Bend, IN). Recombinant thrombin (Recothrom®) was purchased from Zymogenetics. Purified recombinant fibrinogen, expressed in the milk of transgenic Swiss Brown cows, was obtained from Pharming Group NV (Leiden, Netherlands). Materials for the thromboelastograph were purchased from Haemoscope (Niles, IL). Unless otherwise specified, reagents were purchased from Sigma (St. Louis, MO).

Vector construction, expression and purification of FXIIIA in Pichia pastoris

The human Ultimate ORF clone containing the human coagulation factor FXIIIA1 cDNA in the pENTR™221 vector was purchased from Invitrogen (Carlsbad

CA). The following primers were used to obtain FXIIIa gene to subclone in pPICZA intracellular Pichia expression vector. (Forward, 5'-CCAATTGATGCATCATCATCATCATTCAGAAACTTCCAGGACCGC-3'; Reverse, 5'-GCGGCCGCTCACATGGAAGGTCGTCTTTGAATC-3'). The forward primer introduced a methionine and 6 histidine amino acids at the N-terminus of mature FXIIIa peptide. The PCR product was digested with MfeI and NotI and subcloned into pPICZA which was digested with the same enzymes. The DNA sequence of the FXIIIA was confirmed by sequencing the insert fragment. One of the confirming plasmid pPICZAFXIIIa was linearized with PmeI and transformed into P. pastoris X-33 host strain and copy number of the clones was determined as described.[12] Varying copy number clones were screened in shake flask culture to confirm intracellular production of FXIIIa protein. The highest producing clone was scaled up to 5 L bench scale. A fed-batch fermentation protocol was followed to optimize FXIIIa production as described by Zhang et al., (2007).[13] At the end of fermentation process the cells were separated by centrifugation (6,000g) and pellet was stored at -80^{o}C.

Frozen cell paste was processed in 300 gram batches. Cells were lysed in three sets of 100 gram batches. 100 grams of cell paste was resuspended in 100 ml of cold lysis buffer (50 mM Tris-HCL, 10 mM $MgSO_4$, 1 mM EDTA, 10 mM potassium acetate, 1 mM DTT (DL-Dithiothreitol), 2 mM PMSF (phenylmethanesulphonylfluoride) in methanol, pH 9.5). 100 ml (250 g) of 0.5 mm glass beads (Biospec, Bartlesville, OK) were added and the cells. Surrounded by an ice bath, cells were lysed using a BeadBeater Blender (Biospec, Bartlesville, OK) with twenty 20 second on/off cycles. The cell lysate mixture was then centrifuged to remove cellular debris. The lysate from 300 grams of

cell paste was combined and purified using the HisBind Purification Kit (EMD Chemicals, Inc., San Diego, CA) with 40 ml of resin slurry. Following purification, rFXIII was dialyzed in 10 mM Tris-HCl, 0.1 mM EDTA, 60 µM polysorbate-20, pH 8.0 in snake-like dialysis membranes and the protein samples were filter-sterilized and concentrated using the Amicon tubes (Millipore, Billerica, MA). The purity of the sample was tested by SDS-PAGE (NuPAGE 12% Bis-Tris) (Invitrogen, Carlsbad, CA) and immunoblot. The concentration of rFXIII was determined by standard Bicinconic Acid (BCA) methods.

FIIa preparation

Frozen, plasma-derived human prothrombin (Enzyme Research Laboratories, South Bend, IN), was thawed at 37^{o}C. Plasma-derived thrombin (Enzyme Research Laboratories, South Bend, IN) was added at a 1/10 mass to mass thrombin/prothrombin ratio. 0.35 grams of sodium citrate per milliliter of solution was added (Lanchantin 1965). This solution was incubated at 37^{o}C on a rotating mixer for five hours. Sodium citrate was removed using PD-10 desalting columns (GE Healthcare, Giles, United Kingdom). Activation of prothrombin to thrombin was confirmed by reducing and nonreducing SDS-PAGE (12% Bis-Tris NuPAGE) (Invitrogen, Carlsbad, CA) stained with Colloidal Blue (Invitrogen, Carlsbad, CA). The concentration of the thrombin solution was determined by standard Bicinconic Acid (BCA) methods. The specific activity was determined by aPTT analysis.

Human blood sampling and processing

Fresh, normal whole human blood (NHB) from 20 healthy, medication-free individuals, collected in tubes containing 3.2% citrate, was obtained from Research Blood Components (Brighton, MA). Each individual NHB sample was divided in thirds. The NHB sample remained unprocessed while the other two were processed into platelet-rich plasma (PRP) and platelet-poor plasma (PPP). PRP was prepared by centrifuging NHB at 160xg for 8 minutes at 22^{o}C. NHB was centrifuged at 2300xg for 15 minutes at 22^{o}C to obtain PPP. All blood fractions were used within 36 hours of being drawn and were stored at 0^{o}C until analyzed at which time the samples were warmed to 37^{o}C.

Thromboelastography analysis of fibrin clot formation

TEG analysis was conducted on individual fresh, citrated NHB, and respectively derived PRP and PPP samples from 20 individuals. Aliquots of each NHB, PRP and PPP sample were dosed with purified rFI, rFXIII and/or pdFIIa alone or combination. All blood fractions were diluted to 1.3x to provide volume for addition of the biologics. Control samples were performed to determine the affects of diluting NHB, PRP and PPP on time to clot initiation (R), coagulation time (K, time to reach clot firmness of 20 mm) and maximal clot strength (MA) as evaluated by TEG. Each NHB and respective plasma samples (429.72 µl) were transferred to single-use TEG cups that had been enlarged by boring with a 0.406 inch bit (650 µl final volume). Combinations of solutions containing rFI (1.42 mg, 2.32 mg/ml rFI in cup), rFXIII (0.11 mg, 0.18 mg/ml rFXIIIa in cup, rFXIII/rFI molar ratio = 0.16), FIIa (0.08 mg, 0.13 mg/ml FIIa in cup, FIIa/rFI molar ratio = 0.25), and $CaCl_2$ (11 mM) were added to the TEG cups. Ringer's solution was used to normalize mixture volumes.

The TEG Analytical Software (version 4.2.2, Haemoscope, Niles, IL) collected the time to clot initiation (R), the time to achieve a clot firmness of 20mm (K) and the maximal clot strength (MA) for blood products collected from 20 donors. Samples were run until program termination to collect percent lysis 60 minutes after reaching maximum clot strength (LY60) on blood products from 3 of the 20 donors. Data was exported from the TEG Analytical Software to Microsoft Excel for analysis. ANOVA and two tail T test (equal variance) analyses were performed to identify statistical significance between treatment groups of raw data. An α of 0.05 was used for all statistical analyses. The percent change of TEG values resulting from treatment with biologics was normalized relative to the averaged respective sample (N = 20) treated with Ringer's solution alone.

The instrument was calibrated each day of use. All tests described above include three replicate samples in each treatment group. All NHB and respective plasma samples were tested within 36 hours of the blood draw of each individual donor.

NHB, PRP and PPP samples from 20 donors were tested untreated and treated with rFI alone, rFI and FIIa together, rFI and rFXIIIa together, rFI, rFXIIIa and FIIa together. NHB, PRP and PPP samples from 10 donors were tested when treated with FIIa alone, FXIIIa alone and FIIa and FXIIIa in combination.

Results

rFXIIIa and pdFIIa characterization

SDS-PAGE and N-terminal sequencing indicated that the purified protein from the yeast was rFXIIIa rather than rFXIII. These and immunoblots indicated rFXIIIa had a purity of greater than 98% (data not shown). The Pefakit® Factor XIII Incorporation

Assay (Pentapharm, CT) yielded a specific activity of almost 7,000 U/mg for rFXIIIa. The pdFIIa prepared by citrate activation was comprised of α-thrombin and fragments as per SDS-PAGE (Figure 5.2A, lane 10) and chromogenic assay yielded a specific activity of 528 U per mg.

Donor data

Blood was collected from 20 healthy, drug-free donors from 15 men and 5 women with a mean age of 29 (median: 26, maximum: 50, minimum: 20). 11 of the 20 were White, 7 Black, 1 Asian and 1 Hispanic.

TEG analysis of haemodilution

All blood fractions were diluted 1.3x so that 30% of the TEG cup volume was available for addition of the biologics. The effect of dilution by Ringer's solution on NHB, PRP and PPP was evaluated by thromboelastography for time to clot initiation (R), coagulation time (time to reach clot firmness of 20 mm, K) and maximal clot strength (MA). Dilution resulted in statistically significant changes in time to clot initiation for PRP and PPP when diluted with Ringer's solution ($p = 0.011$ and 0.014) but not for NHB ($p = 0.087$). Coagulation time was statistically different for NHB ($p = 0.002$) but not for PRP and PPP ($p = 0.626$ and 0.132). Maximal clot strength was statistically different for PPP ($p = 0.026$) but not for NHB and PRP ($p = 0.288$ and 0.245).

Although not statistically significant, in general, diluting with Ringer's solution reduced R, K and MA for NHB (Figure 5.1). Percent change in R was reduced in 17 of the 23 NHB samples ranging from a 38% reduction to almost 10% increase (Figure 5.1A). Similarly, coagulation time (K) was reduced in 19 of 22 with a range from a 52%

reduction to an 8% increase (Figure 5.1B). 14 of the 23 NHB samples also had reduced clot strength when diluted with Ringer's solution ranging from a 22% reduction to a 22% increase (Figure 5.1C).

As with NHB, dilution of PRP with Ringer's solution tended to reduce R, K and MA (Figure 5.2). When diluted with Ringer's solution, PRP was reduced in all 22 cases ranging from a just over 2% to a 33% reduction (Figure 5.2A). 15 of 22 diluted PRP samples had reduced coagulation time but ranged from a 47% reduction to 54% increase (Figure 5.2B). Percent changes in clot strength for diluted PRP ranged from a 23% reduction to 13% increase; however, 20 of 22 PRP samples had reductions in clot strength (Figure 5.2C).

Like NHB and PRP, R and MA were reduced when PPP was diluted with Ringer's solution; however, coagulation time tended to increase (Figure 5.3). All but 2 of the 22 PPP samples had reduced clot initiation time (R) when diluted with Ringer's solution. Percent change in R ranged from a 41% reduction to a 3% increase (Figure 5.3A). All 22 PPP samples had a reduction in clot strength from 14% to 35% when diluted (Figure 5.3C). Coagulation time of diluted PPP was the only measured parameter that showed primarily an increase after dilution (Figure 5.3B). The six PPP samples with zero percent change in K were samples that never reached 20 mm clot strength either before or after dilution. Four of the 22 samples (Donors R, X, Z and AA) reached 20 mm clot strength before dilution but not after. Only two samples showed a reduction in K when diluted. Percent changes of K ranged from a 34% reduction to a 539% increase.

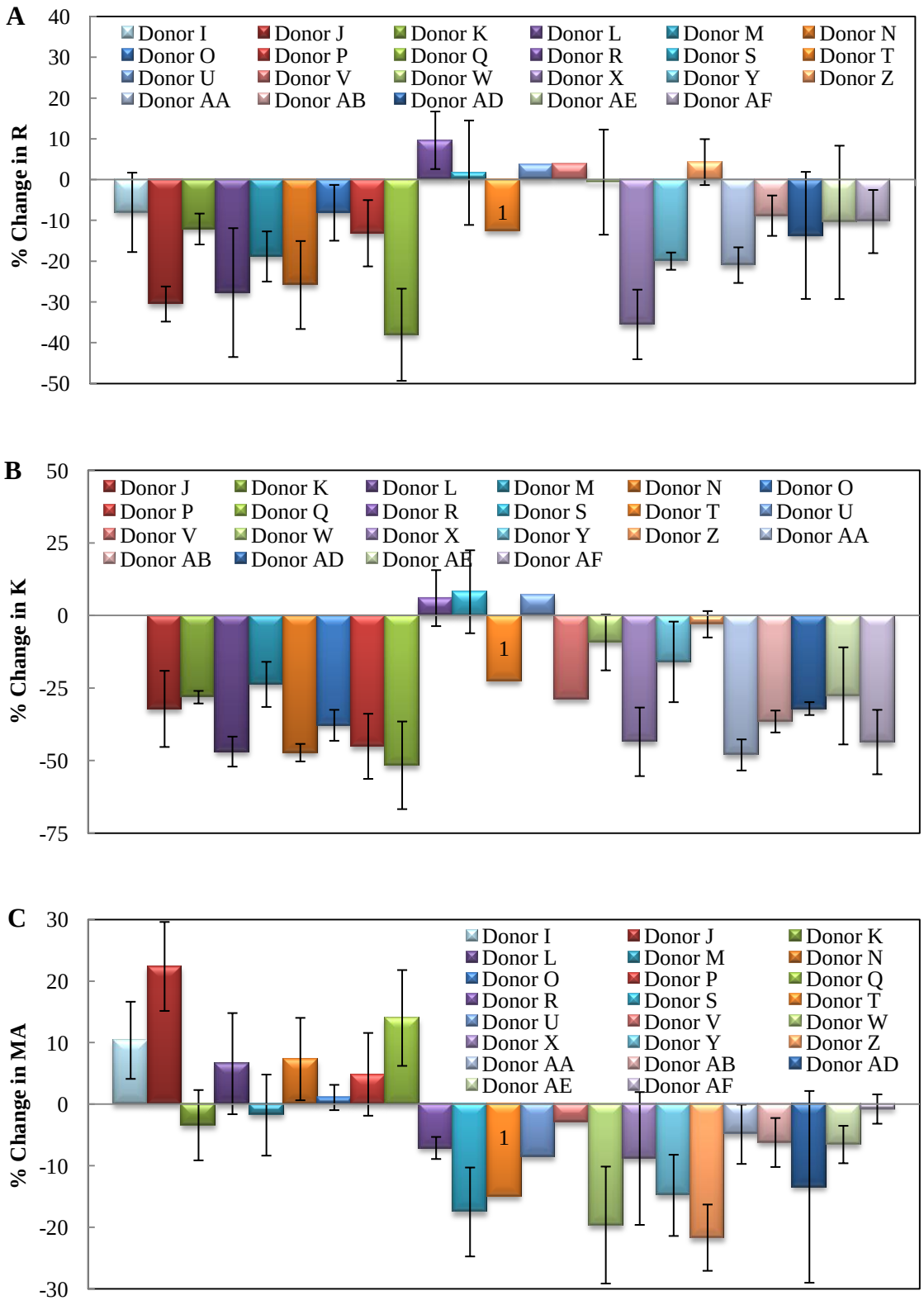

Figure 5.1. Percent change in time to clot initiation (R), clot coagulation time (K) and maximal clot strength (MA) when normal human blood (NHB) is diluted 30% with Ringer's solution. The bars represent average values and the brackets represent the standard deviation. N = 23 for R and MA, 22 for K.

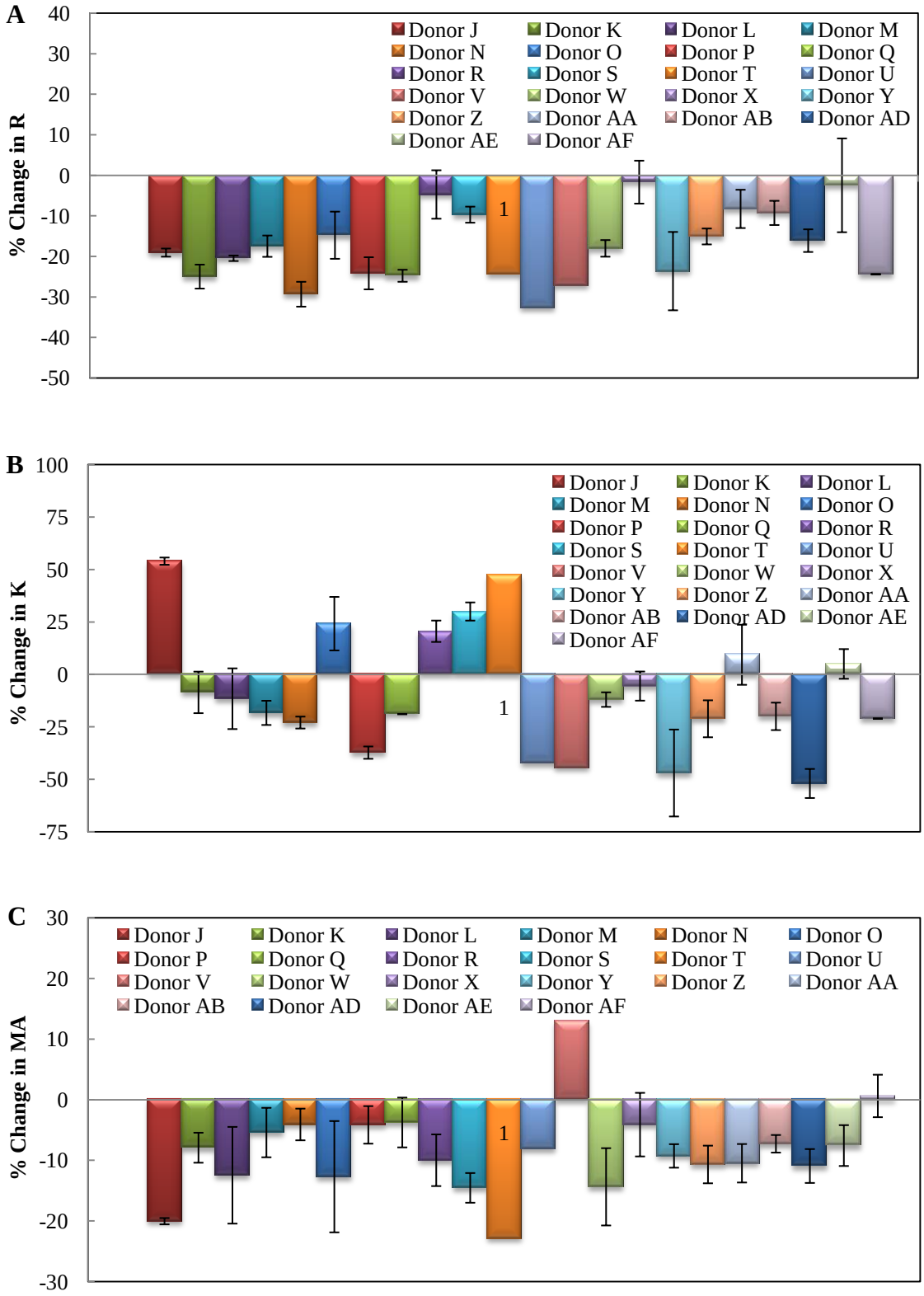

Figure 5.2. Percent change in time to clot initiation (R), clot coagulation time (K) and maximal clot strength (MA) when platelet rich plasma (PRP) is diluted 30% with Ringer's solution. The bars represent average values and the brackets represent the standard deviation. N = 22.

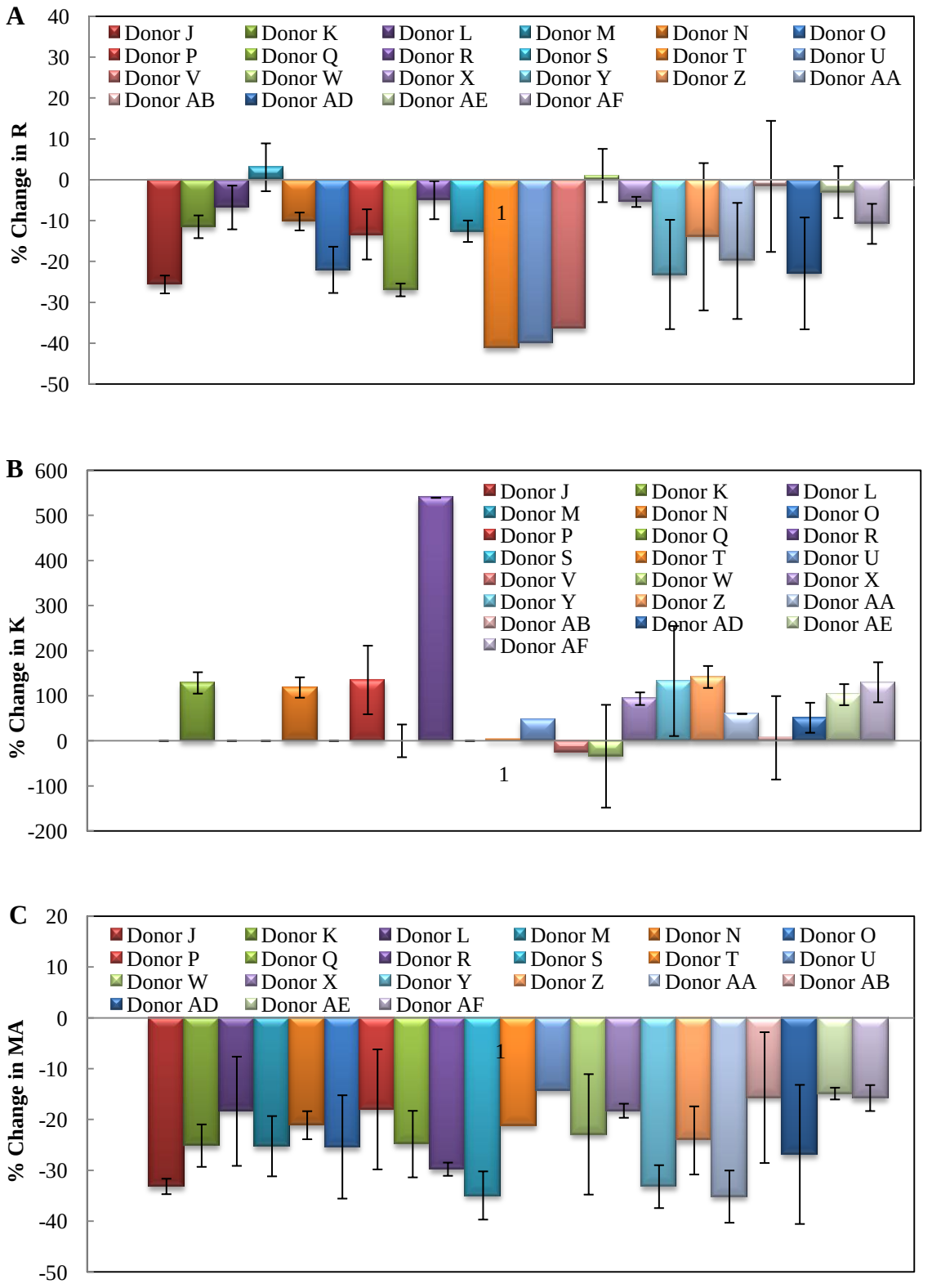

Figure 5.3. Percent change in time to clot initiation (R), clot coagulation time (K) and maximal clot strength (MA) when platelet poor plasma (PPP) is diluted 30% with Ringer's solution. The bars represent average values and the brackets represent the standard deviation. N = 22.

The three blood products, NHB, PRP and PPP, diluted by 30% were statistically compared. R, K and MA results for NHB, PRP and PPP were compared by t test if significant differences were identified by ANOVA (Table 5.1). With respect to clot initiation time, NHB was not statistically different form PRP or PPP; however, PRP and PPP were significantly different from each other. NHB, PRP and PPP were statistically different from each other with respect to both K and MA. These findings indicate that platelets and cellular components contribute to coagulation parameters.

Table 5.1. p values from t test comparisons of normal human blood (NHB), platelet rich plasma (PRP) and platelet poor plasma (PPP) on time to clot initiation (R), time to reach clot firmness of 20 mm (K) and maximal clot strength (MA).

Clotting Parameter	Time to clot initiation (R)	Coagulation time (K)	Maximum clot strength (MA)
NHB vs. PRP	0.572	< 0.001*	< 0.001*
NHB vs. PPP	0.062	< 0.001*	< 0.001*
PRP vs. PPP	0.014*	< 0.001*	< 0.001*

* statistical significance based on $\alpha = 0.05$

TEG analysis of protein doping into NHB, PRP and PPP

rFI (final concentration: 2.32 mg/ml), rFXIII (final concentration: 0.18 mg/ml), and/or FIIa (final concentration: 0.13 mg/ml, 52.9 U/ml) were dosed into purchased citrated, NHB and its respective PRP and PPP. Time to clot initiation (R), coagulation time (time to reach clot firmness of 20 mm, K) and maximal clot strength (MA) were evaluated by thromboelastograph (TEG). ANOVA analysis indicates that dosing NHB, PRP and PPP with proteins do result in statistically significant changes in clotting parameters (Table 5.2). t test analyses were performed to identify which proteins significantly altered clotting parameters. The percent change of TEG values resulting from treatment with biologics were normalized relative to the averaged respective sample (N = 20) treated with Ringer's solution alone.

Table 5.2. p values from ANOVA analyses on time to clot initiation (R), time to reach clot firmness of 20 mm (K) and maximal clot strength (MA) due to treatment with biologics.

Clotting Parameter	Normal Human Blood	Platelet Rich Plasma	Platelet Poor Plasma
Time to clot initiation (R)	< 0.0001	< 0.0001	< 0.0001
Coagulation time (K)	< 0.0001	< 0.0001	0.0001
Maximum Clot Strength (MA)	< 0.0001	< 0.0001	< 0.0001

* statistical significance based on $\alpha = 0.05$

TEG analysis of time to clot initiation

ANOVA analyses indicated that protein treatment significantly altered R for NHB, PRP and PPP (Table 5.2). t test analyses indicated that dosing any protein into PRP or PPP and all but rFI alone or rFI in combination with rFXIIIa results in a significant change in time to clot initiation (Table 5.3).

Table 5.3. p values from t test analyses on time to clot initiation (R) comparing diluted normal human blood (NHB), platelet rich plasma (PRP) and platelet poor plasma (PPP) to samples containing biologics.

Diluted sample vs.:	Normal Human Blood	Platelet Rich Plasma	Platelet Poor Plasma
rFI dosed sample	0.101	< 0.001*	< 0.001*
rFXIIIa dosed sample	0.003*	0.010*	0.001*
FIIa dosed sample	< 0.001*	< 0.001*	< 0.001*
rFI + FIIa dosed sample	< 0.001*	< 0.001*	< 0.001*
rFXIIIa + FIIa dosed sample	< 0.001*	< 0.001*	< 0.001*
rFI + rFXIIIa dosed sample	0.950	0.001*	< 0.001*
rFI + rFXIIIa + FIIa dosed sample	< 0.001*	< 0.001*	< 0.001*

* statistical significance based on $\alpha = 0.05$

Percent changes in R indicate that FIIa dominates clot speed (Figure 5.4). When examining percent changes, the addition of rFI alone increased clot initiation by 8%, 30%, and 39% for NHB, PRP and PPP, respectively. Individual sample values ranged from a 42% increase to a 13% decrease in time to clot initiation for NHB, 14% to 49% increase for PRP and 15% to 72% increase for PPP. The average standard deviations for each sample were 10, 5 and 8 for NHB, PRP and PPP, respectively.

The addition of rFXIII alone decreased R by 24%, 12%, and 13% for NHB, PRP and PPP, respectively. Individual sample values ranged from 2% to 40% decrease in time to clot initiation for NHB, 30% increase to 38% decrease in R for PRP and 2% increase to 21% decrease for PPP. The average standard deviations for each sample were 6, 4 and 6 for NHB, PRP and PPP, respectively.

Clot initiation time (R) was affected predominantly by FIIa which added alone decreased median clot initiation times by 74%, 91% and 91% for NHB, PRP and PPP, respectively. Individual sample values ranged from 68% to 83% decrease in time to clot initiation for NHB, 87% to 93% decrease for PRP and 67% to 95% decrease for PPP. The average standard deviations for each sample were 7, 5 and 5 for NHB, PRP and PPP, respectively.

When FIIa is added with rFI, time to clot initiation decrease by 86%, 95% and 96% for NHB, PRP and PPP, respectively. The average standard deviations for each sample were 2, 3 and 5 for NHB, PRP and PPP, respectively. Individual sample values ranged from 82% to 92% decrease in time to clot initiation for NHB, 91% to 96% decrease for PRP and 91% to 97% decrease for PPP. The average standard deviations for each sample were 6, 5 and 6 for NHB, PRP and PPP, respectively.

When FIIa is added with rFXIII, time to clot initiation decrease by 81%, 93% and 94% for NHB, PRP and PPP, respectively. Individual sample values ranged from 76% to 88% decrease in time to clot initiation for NHB, 87% to 95% decrease for PRP and 81% to 96% decrease for PPP. The average standard deviations for each sample were 5, 4 and 4 for NHB, PRP and PPP, respectively.

The addition of rFI with rFXIII did not affect the time to clot initiation for NHB but increased it for PRP and PPP by 33% and 25%, respectively. Individual sample values ranged from a 13% increase to 22% decrease in time to clot initiation for NHB, 14% to 72% increase for PRP and 11% to 49% increase for PPP. The average standard deviations for each sample were 8, 6 and 4 for NHB, PRP and PPP, respectively.

Addition of rFI, rFXIII and FIIa decreased clot initiation time by 88%, 94% and 96% for NHB, PRP and PPP, respectively. Individual sample values ranged from 82% to 92% decrease in time to clot initiation for NHB, 92% to 96% increase for PRP and 94% to 97% increase for PPP. The average standard deviations for each individual sample were 4, 5 and 6 for NHB, PRP and PPP, respectively.

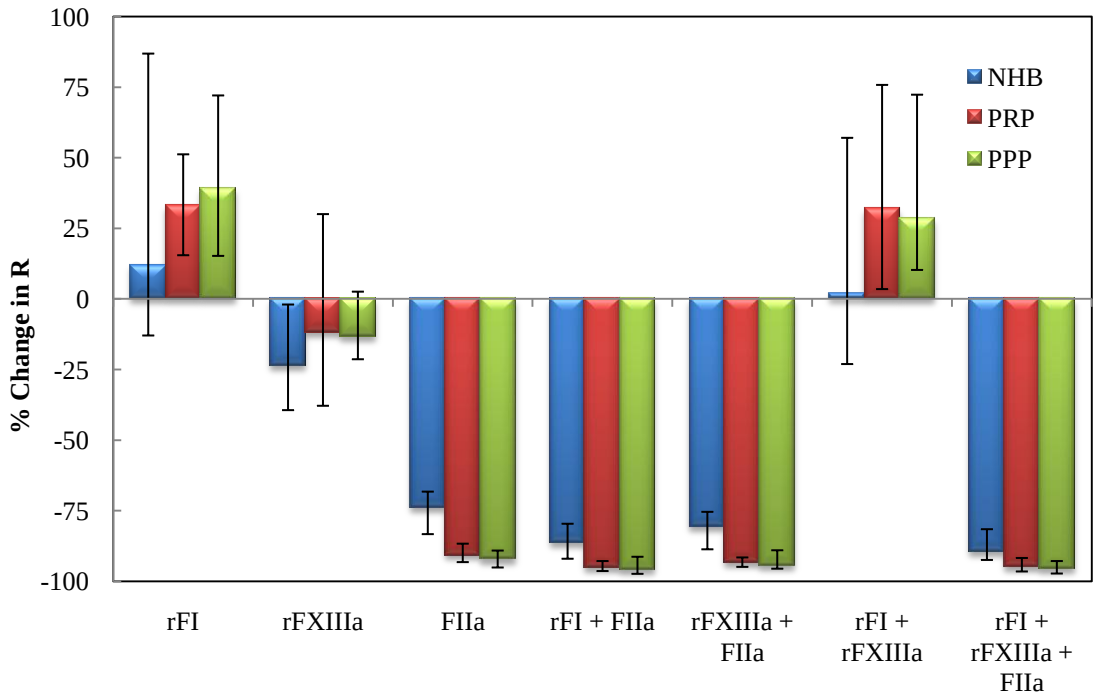

Figure 5.4. Percent change in time to clot initiation (R) with the addition of recombinant fibrinogen (rFI), plasma-derived thrombin (pdFIIa) and/or recombinant FXIIIa (rFXIIIa) to normal human blood (NHB), platelet rich plasma (PRP) and platelet poor plasma (PPP). The bars represent median values and the brackets represent the highest and lowest values for the 20 subjects.

TEG analysis of coagulation time

ANOVA analyses indicated that protein treatment significantly altered K for NHB, PRP and PPP (Table 5.2). t test analyses indicated that dosing rFI alone, FIIa alone, rFI and FIIa together, rFXIIIa and FIIa together, and rFI, rFXIIIa and FIIa together significantly changes maximal clot strength (Table 5.4). K of PRP was significantly altered with the addition of FIIa alone and rFXIIIa and FIIa in combination. K of PPP was significantly altered with the addition of rFI alone, rFI with rFXIIIa, and rFI with rFXIIIa, and rFI.

Table 5.4. p values from t test analyses on coagulation time (K) comparing diluted normal human blood (NHB), platelet rich plasma (PRP) and platelet poor plasma (PPP) to samples containing biologics.

Diluted sample vs.:	Normal Human Blood	Platelet Rich Plasma	Platelet Poor Plasma
rFI dosed sample	0.004*	0.954	0.025*
rFXIIIa dosed sample	0.568	0.137	0.077
FIIa dosed sample	< 0.001*	0.003*	
rFI + FIIa dosed sample	0.002*	0.064	0.370
rFXIIIa + FIIa dosed sample	< 0.001*	0.036*	
rFI + rFXIIIa dosed sample	0.318	0.790	< 0.001*
rFI + rFXIIIa + FIIa dosed sample	0.012*	0.117	0.016*

* statistical significance based on $\alpha = 0.05$, FIIa and rFXIIIa + FIIa dosed samples never achieved 20 mm clot strength.

Percent changes in K indicate that FIIa dominates coagulation time (Figure 5.5). Coagulation time (K) was reduced 24% and 54% for NHB and PPP, respectively, and increased 14% for PRP when rFI was added. Individual sample values ranged from a 1% increase to a 48% decrease in K time for NHB, a 60% increase and 21% decrease for PRP and 0% to 70% decrease for PPP.

When rFXIIIa was added, the K value was increased 5% for NHB and reduced 24% and 70% for PRP and PPP, respectively. Individual sample values ranged from a

52% increase to a 32% decrease in coagulation time for NHB, 0% to 43% decrease for PRP and 0% to 91% decrease for PPP.

When FIIa was added, coagulation time 111%, 125% and 0% for NHB, PRP and PPP, respectively. Individual sample values ranged from 48% to 165% increase in coagulation time for NHB, 59% to 269% increase for PRP and 0% to 199% increase for PPP. When FIIa was added with rFI, coagulation time increased by 35%, 46% and 0% for NHB, PRP and PPP, respectively. Individual sample values ranged from a 13% decrease and 72% increase in K value for NHB, a 126% increase to a 14% decrease for PRP and a 199% increase to 61% decrease for PPP. When FIIa is added with rFXIII, coagulation time increased by 90%, 64% and 0% for NHB, PRP and PPP, respectively. Individual sample values ranged from 62% to 233% increase in K for NHB, 30% to 144% increase for PRP and 0% to 199% increase for PPP.

The addition of rFI with rFXIII decreased NHB and PPP by 16% and 82%, respectively, and increased PRP by 17%. Individual sample values ranged from a 44% increase to 43% decrease in K for NHB, a 78% increase to 62% decrease in K for PRP, and 37% to 94% decrease for PPP.

Addition of rFI, rFXIII and FIIa increased coagulation time for NHB and PPP by 30% and 39%, respectively, and a 57% decrease for PPP. Individual sample values ranged from a 5% decrease to a 61% increase in K for NHB, a 29% decrease to a 113% increase in K for PRP and a 83% decrease to a 8% increase in K for PPP.

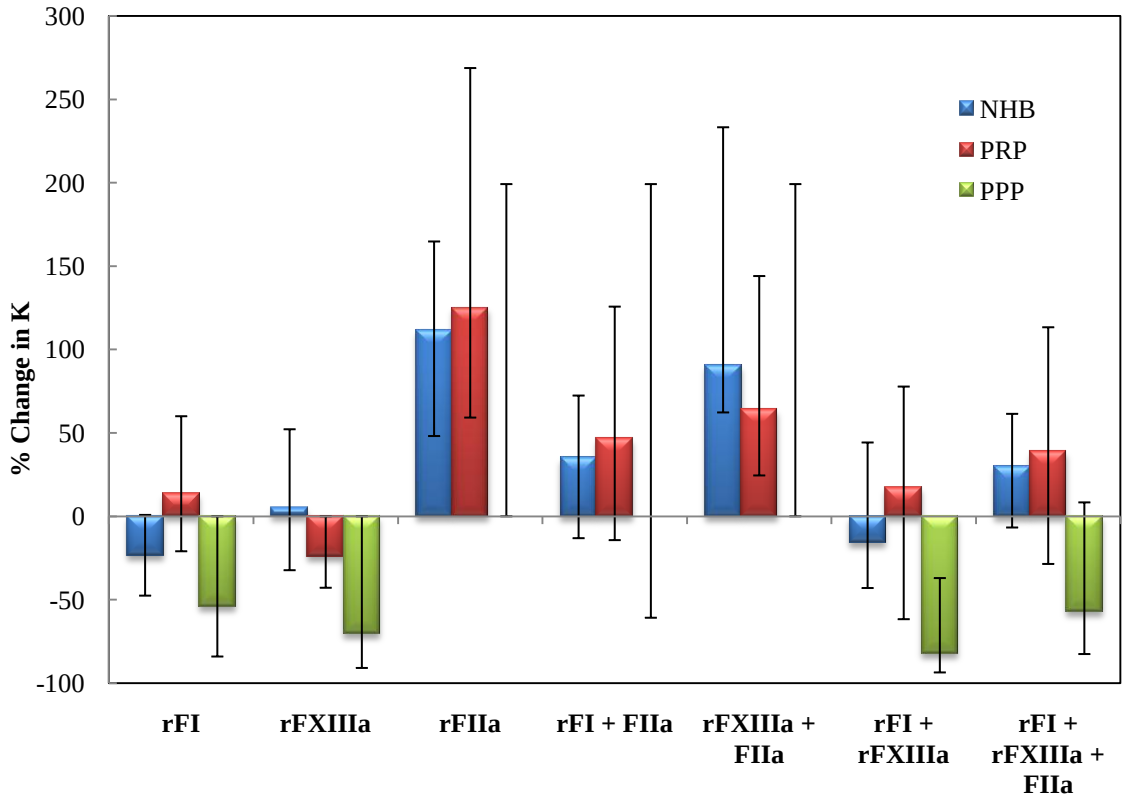

Figure 5.5. Percent change in coagulation time (K) with the addition of recombinant fibrinogen (rFI), plasma-derived thrombin (pdFIIa) and/or recombinant FXIIIa (rFXIIIa) to normal human blood (NHB), platelet rich plasma (PRP) and platelet poor plasma (PPP). The bars represent median values and the brackets represent the highest and lowest values for the 20 subjects.

TEG analysis of maximal clot strength

ANOVA analyses indicated that protein treatment significantly altered MA for NHB, PRP and PPP (Table 5.2). t test analyses indicated that dosing rFI alone, rFXIIIa alone, FIIa alone, rFXIIIa and FIIa together, and rFI and rFXIIIa together significantly changes maximal clot strength (Table 5.5). MA of PRP was significantly altered with the addition of FIIa alone and rFXIIIa and FIIa in combination. MA of PPP was significantly altered with the addition of FIIa alone, FIIa together with rFI or rFXIIIa, and rFI in combination with rFXIIIa.

Table 5.5. p values from t test analyses on maximal clot strength (MA) comparing diluted normal human blood (NHB), platelet rich plasma (PRP) and platelet poor plasma (PPP) to samples containing biologics.

Diluted sample vs.:	Normal Human Blood	Platelet Rich Plasma	Platelet Poor Plasma
rFI dosed sample	< 0.001*	0.935	0.802
rFXIIIa dosed sample	0.028*	0.212	0.852
FIIa dosed sample	< 0.001*	0.002*	< 0.001*
rFI + FIIa dosed sample	0.850	0.125	0.027*
rFXIIIa + FIIa dosed sample	< 0.001*	0.004*	< 0.001*
rFI + rFXIIIa dosed sample	0.047*	0.817	0.039*
rFI + rFXIIIa + FIIa dosed sample	0.647	0.452	0.881

* statistical significance based on $\alpha = 0.05$

rFI dominated the changes in clot strength as can be observed with percent change in MA (Figure 5.6). When added alone, rFI increased median clot strength by 27%, 6% and 26% for NHB, PRP and PPP, respectively. The individual sample values ranged from a 19% to 51% increase in clot strength for NHB, a 14% increase to 20% decrease for PRP and 5% to 103% increase in strength for PPP. The average standard deviations for each sample were 2, 2 and 1 for NHB, PRP and PPP, respectively.

rFXIII added alone did not greatly affect clot strength of NHB or PRP but increased strength of PPP clots by a median of 48%. The individual sample values ranged from a 6% increase to 57% decrease in clot strength for NHB, a 6% increase to 16% decrease for PRP and 17% to 95% increase for PPP. The average standard deviations for each sample were 3, 3 and 1 for NHB, PRP and PPP, respectively.

When FIIa was added alone to NHB, PRP and PPP, median clot strength for each sample decreased by 30%, 26%, 51%, respectively. The individual sample values ranged from 23% to 38% for NHB, 18% to 38% for PRP and 46% to 64% for PPP. The average standard deviations for each sample were 2, 2 and 1 for NHB, PRP and PPP, respectively.

When rFI was added with FIIa, rFI reversed the effects of FIIa resulting in clot strengths similar to NHB, PRP and PPP alone. Median clot strengths were increased

11% and 29% for NHB and PPP and decreased 3% for PRP. Individual sample values ranged from a 5% decrease to a 25% increase in clot strength for NHB, a 31% decrease to 5% increase for PRP and 18% decrease to 65% increase for PPP. The average standard deviations for each sample were 2, 2 and 1 for NHB, PRP and PPP, respectively.

When FIIa was combined with rFXIII to NHB, PRP and PPP, there were similar decreases in median clot strength of 32%, 19%, 39%, respectively. The individual sample values ranged from 25% to 47% for NHB, 13% to 33% for PRP and 17% to 57% for PPP. The average standard deviations for each sample were 2, 3 and 1 for NHB, PRP and PPP, respectively.

When added in combination with rFXIII, rFI increased median clot strength for NHB, PRP and PPP by 18%, 5% and 63%, respectively. The individual sample values ranged from 3% to 36% increase in clot strength for NHB, a 23% increase to 10% decrease for PRP and 5% to 161% for increase in strength for PPP. The average standard deviations for each sample were 3, 3 and 2 for NHB, PRP and PPP, respectively.

The addition of rFI, rFXIII and FIIa did not change PRP clot strength but increased median clot strengths of NHB and PPP by 6% and 61%, respectively. Individual sample values ranged from a 5% decrease to a 29% increase in clot strength for NHB, a 6% decrease to 14% increase for PRP and a 12% to 22% increase for PPP. The average standard deviations for each sample were 3, 4 and 2 for NHB, PRP and PPP, respectively.

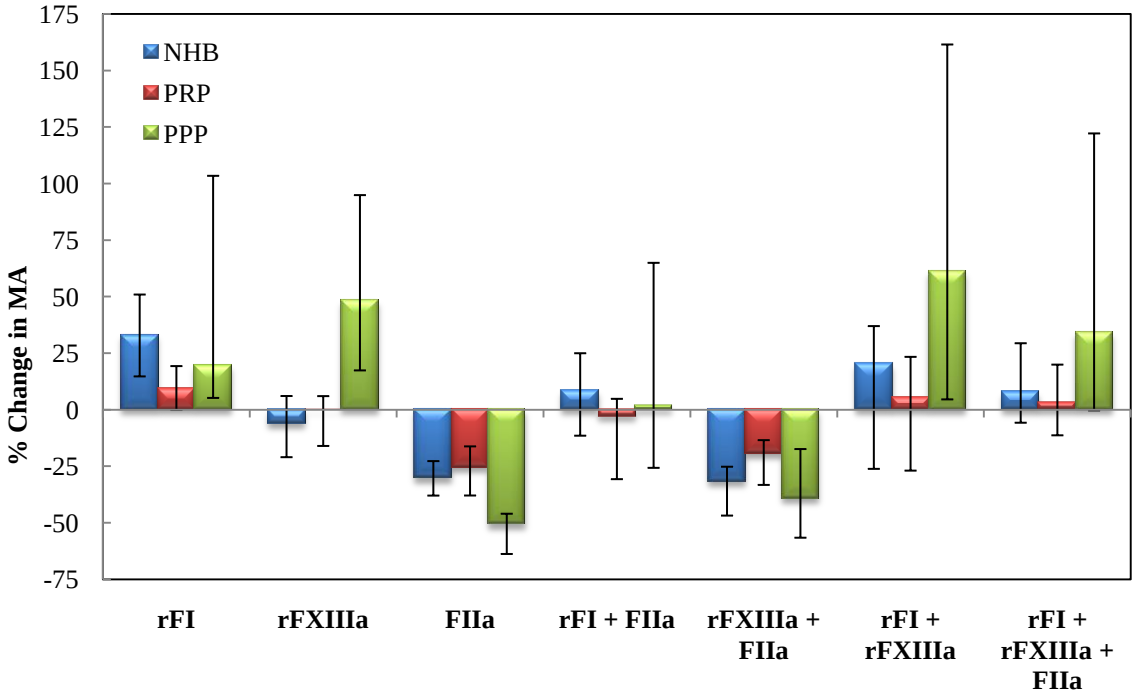

Figure 5.6. Percent change in maximal clot strength (MA) with the addition of recombinant fibrinogen (rFI), plasma-derived thrombin (pdFIIa) and/or recombinant FXIIIa (rFXIIIa) to normal human blood (NHB), platelet rich plasma (PRP) and platelet poor plasma (PPP). The bars represent median values and the brackets represent the highest and lowest values for the 20 subjects.

TEG analysis of lysis

The percent lysis 60 minutes after achieving maximal clot strength was measured by TEG (Figure 5.7). Undiluted NHB was lysed by 3.7% 60 minutes after achieving maximal clot strength with a range of 0% to 4.9%. Undiluted PRP was lysed by 6% ranging from 2.8% to 10.4%. Undiluted PPP was lysed by 0% ranging from 0% to 1%. Diluted NHB, PRP and PPP were lysed by 1.7%, 11.1% and 0%, respectively. The individual sample values ranged from 0.5% to 8.2% for NHB, 8.8% to 13.1% for PRP and 0% to 0.1% for PPP.

When rFI was added, NHB and PRP were lysed by 3.7% and 9.6%, respectively with ranges of 0.9% to 3.9% for NHB and 9.5% to 12.7% for PRP. When rFI and FIIa were added, NHB and PRP were lysed by 0% and 4.1%, respectively with ranges of 0%

to 5.2% for NHB and 0.3% to 6.5% for PRP. When rFI was in combination with rFXIIIa, NHB and PRP were lysed by 1.4% and 2.0%, respectively with ranges of 0.6% to 2.1% for NHB and 0% to 3.9% for PRP. When rFI, rFXIIIa and FIIa were added, NHB and PRP were lysed by 0% and 6.6%, respectively with no lysis for NHB and a range of 1.7% to 8.5% for PRP. PPP had no detectable lysis when rFI, rFXIIIa and/or FIIa were added.

ANOVA analyses indicated that treatment with proteins alone or in combination did not significantly alter lysis in NHB and PPP ($p = 0.620$ and 0.533); however, there were significant changes in PRP ($p = 0.025$). t test analyses indicated that PRP samples dosed with rFI with FIIa or rFI with rFXIIIa significantly increased the percent lysis ($p = 0.028$ and 0.025, respectively).

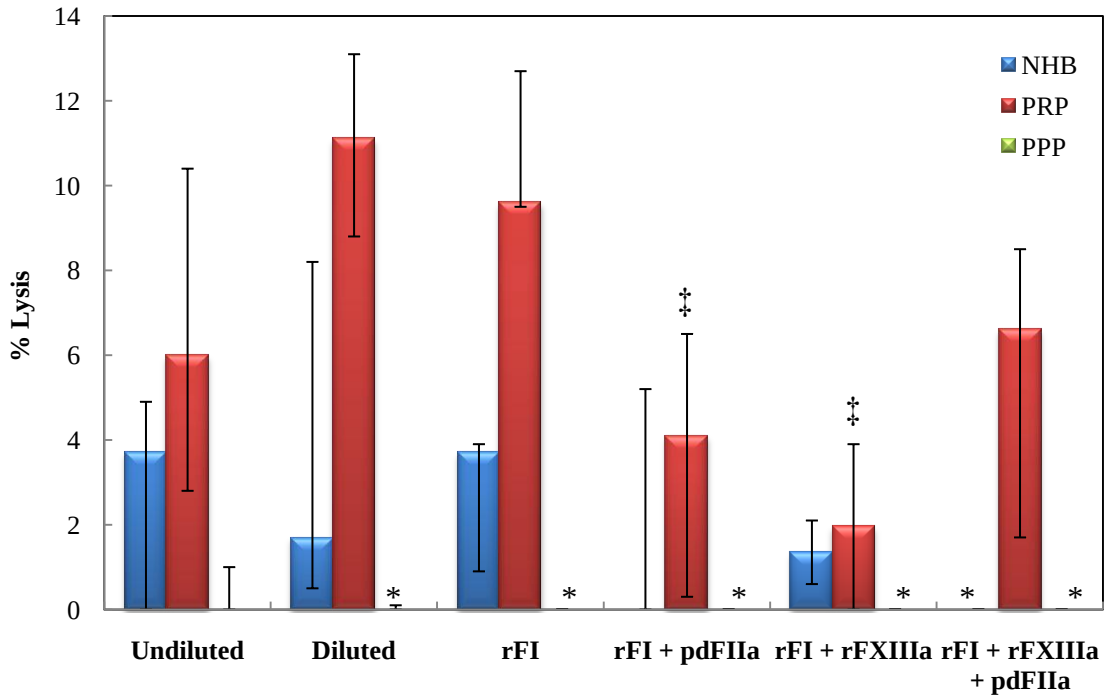

Figure 5.7. Percent lysis 60 minutes after reaching maximum clot strength of undiluted or diluted normal human blood (NHB), platelet rich plasma (PRP) and platelet poor plasma (PPP) alone or with the addition of recombinant fibrinogen (rFI), plasma-derived thrombin (pdFIIa) and/or recombinant FXIIIa (rFXIIIa). The bars represent median values and the brackets represent the highest and lowest values for 3 subjects. Samples with no detectable lysis are marked (*). Statistical significance is identified by ‡. P values were 0.028 for rFI + pdFIIa and 0.025 for rFI + rFXIIIa.

Discussion

The data presented in this chapter indicate that time to clot initiation (R) and maximal clot strength (MA) were not significantly altered by 30% haemodilution but coagulation time (K) was significantly reduced for NHB. These findings partially support previous research which showed that 29% dilution of citrated human blood with lactated Ringer's solution did not significantly alter time to clot initiation (R), coagulation time (K) and maximal clot strength (MA) as measured by TEG.[14] Both of these studies contradict findings that NHB diluted 33% with lactated Ringer's solution had significantly faster activated clot times but slightly slower clotting rates.[15] This is

the first report of a detailed analysis of results of dilution of PRP and PPP on clotting parameters. Dilution with Ringer's solution significantly reduced the time to clot initiation for PRP and PPP and maximum clot strength for PPP.

Coagulation time (K) was significantly altered by haemodilution in NHB only. Time to clot initiation (R) was significantly reduced for PRP and PPP and although it was not statistically significant, 17 of the 22 NHB samples showed reduced times to clot initiation (R). Dilution of NHB reduces the concentration of fibrinogen[15, 16] and other plasma proteins and also decreases platelet[16] and other cellular components in the blood. By reducing cellular components, the viscosity of blood should decrease thereby easing the diffusion of coagulation proteins to the clotting site. However, both PRP and PPP are free of red blood cells but neither are significantly different than NHB with regard to time to clot initiation. Consequently, cellular components may not interfere greatly with initiation of clots. Rather, the dilution of plasma proteins may play a greater role. While the reduction in fibrinogen would hinder clotting, dilution also lowers the concentrations of anticoagulant proteins which may interfere with the initiation and rate of clot formation. With respect to viscoelastic strength, dilution with Ringer's solution resulted in a significant reduction in PPP only. This indicates that platelets play an important role in creating clot strength. This could be due to their inclusion in the clot by providing surfaces for the fibrin clot but is also certainly related to their release of FXIII which crosslinks the fibrin clot creating viscoelastic strength. Platelets dispersed throughout the clot probably hasten[17] and further stabilize the clot[18] by releasing additional FXIII. Activated platelets play an essential role in the formation of the primary hemostatic plug and clot strength[1, 7, 9, 19-21] because they supply both dimeric FXIII and the majority of

FIIa to the wound surface[9, 21, 22] Research indicates that FXIII in the platelets is necessary to obtain optimal crosslinking.[23]

This study examines the effects of added rFI, rFXIIIa and pdFIIa on fibrin clot formation in NHB, PRP or PPP *ex vivo*. The fibrinogen concentration was increased by 50% in each sample to near hyperfibrinogenemic levels. rFXIIIa and pdFIIa were dosed at optimal LFS concentrations determined in the research in the previous chapter.

Thrombin played the most dominant role in altering time to clot initiation. Addition of pdFIIa alone or in combination with one or both of the other proteins to NHB, PRP and PPP resulted in significant reductions in clot initiation times (Figure 5.4). The coagulation cascade culminates in the activation of large amounts of prothrombin to thrombin which is responsible for activating both endogenous and exogenous fibrinogen into fibrin and FXIII into FXIIIa. The lag observed from the start of the test and the formation of a clot is related to the rate limiting activation of prothrombin to thrombin. By adding this key enzyme in the active form, the limiting step is removed resulting in near instantaneous clot formation. rFXIIIa added alone did not greatly affect time to clot initiation; whereas rFI alone or with rFXIIIa slowed time to clot initiation time in PRP and PPP but not NHB.

FIIa alone or in combination with rFXIIIa significantly prolonged coagulation time for NHB and PRP. rFXIIIa addition without FIIa resulted in slight decreases in coagulation time for PPP but not for NHB or PRP. This indicates that platelets provide enough FXIII to maintain normal coagulation kinetics and the absence of FXIII reduces the rate of formation of a crosslinked fibrin clot.

The addition of FIIa alone or with rFXIII to NHB, PRP or PPP significantly reduced clot strength; however, addition of rFI reversed the loss. FIIa addition results in fast initiation of clot formation resulting in a rapid increase in viscosity which reduces diffusivity of FXIIIa required to crosslink the fibrin aggregations creating a stronger clot. rFI added alone to yield near-hyperfibrinogenemic levels increased clot strength when dosed into NHB and PPP. However, when rFI was added in combination with rFXIIIa it only increased clot strength for PPP but not when added to NHB and PRP indicating that blood-borne platelets play a large role by providing FXIII.

The addition of any of the biologics alone or in combination with any of the others did not significantly alter clot lysis for NHB or PPP. Lysis of PRP was significantly reduced with the addition of rFI in combination with pdFIIa or rFXIIIa. The addition of excess rFXIIIa in combination with rFI reduces lysis compared to rFI added alone because it ensures ample crosslinking of endogenous and exogenous fibrin(ogen). The addition of pdFIIa seems to interfere with fibrinolysis components located in plasma.

These results suggest that rFI and rFXIII in combination with FIIa can be combined to create a LFS with equivalent or better kinetic and viscoelastic properties as currently available products. With regard to therapeutic uses, both rFI and rFXIIIa have advantages. rFI dosed in NHB alone did not significantly alter time to clot initiation or coagulation time but did increase clot strength. Consequently, rFI may be useful for infusion therapy following haemodilution. rFXIIIa reduced time to clot initiation slightly but did not significantly change clot strength or kinetics; therefore, it may be an effective infusion therapy for FXIII deficiency.

Acknowledgements

I am incredibly grateful to Leonard Akert who modified hundreds of TEG cups to increase their volumes. This work was supported by a grant from the Department of Defense titled “Production and Purification of Fibrinogen Components for the Production of a Fibrin Sealant Hemostatic Dressing.”

References

1. Laurens, N., Koolwijk, P. & De Maat, M.P.M. Fibrin structure and wound healing. *Journal of Thrombosis and Haemostasis* **4**, 932 (2006).
2. Lee, M.-G.M. & Jones, D. Applications of fibrin sealant in surgery. *Surg Innov* **12**, 203 (2005).
3. Schwartz, M.L., Pizzo, S.V., Hill, R.L. & McKee, P.A. Human factor XIII from plasma and platelets. Molecular weights, and subunit structures, proteolytic activation, and crosslinking of fibrinogen and fibrin. *J.Biol.Chem.* **248**, 1395 (1973).
4. Folk, J.E. & Finlayson, J.S. The e-(g-glutamyl)lysine crosslink and the catalytic role of transglutaminases. *Adv.Protein Chem.* **31**, 1 (1977).
5. McDonagh, J.M. in Hemostasis and Thrombosis: Basic Principles and Clinical Practice, Edn. Third Edition. (eds. R.W. Colman, J. Hirsh, V.J. Marder & E.W. Salzman) 301 (J.B. Lippincott Company, Philadelphia; 1994).
6. Standeven, K.F. et al. Functional analysis of fibrin g-chain cross-linking by activated factor XIII: determination of a cross-linking pattern that maximizes clot stiffness. *Blood* **110**, 902 (2007).
7. Greenberg, C.S. & Shuman, M.A. Specific binding of blood coagulation factor XIIIa to thrombin-stimulated platelets. *J.Biol.Chem.* **259**, 14721 (1984).
8. Chandler, W.L. et al. Factor XIIIA and clot strength after cardiopulmonary bypass. *Blood Coagulation Fibrinol.* **12**, 101 (2001).
9. Crawley, J.T.B., Zanardelli, S., Chion, C.K.N.K. & Lane, D.A. The central role of thrombin in hemostasis. *Journal of Thrombosis and Haemostasis* **5**, 95 (2007).
10. Mankad, P.S. & Codispoti, M. The role of fibrin sealants in hemostasis. *Am.J.Surg.* **182**, 21S (2001).
11. Ponce, R. et al. Safety of recombinant human factor XIII in a cynomolgus monkey model of extracorporeal blood circulation. *Toxicol.Pathol.* **33**, 702 (2005).
12. Inan, M. et al. Saturation of the secretory pathway by overexpression of a hookworm (Necator americanus) protein (Na-ASP1). *Methods in Molecular Biology (Totowa, NJ, United States)* **389**, 65 (2007).
13. Zhang, W., Inan, M. & Meagher, M.M. Rational design and optimization of fed-batch and continuous fermentations. *Methods in Molecular Biology (Totowa, NJ, United States)* **389**, 43 (2007).
14. Petroianu, G.A., Liu, J., Maleck, W.H., Mattinger, C. & Bergler, W.F. The effect of In vitro hemodilution with gelatin, dextran, hydroxyethyl starch, or Ringer's solution on Thrombelastograph. *Anesth Analg* **90**, 795-800 (2000).
15. Konrad, C., Markl, T., Schuepfer, G., Gerber, H. & Tschopp, M. The effects of in vitro hemodilution with gelatin, hydroxyethyl starch, and lactated Ringer's solution on markers of coagulation: an analysis using SONOCLOT. *Anesth Analg* **88**, 483-488 (1999).
16. Xiao, D., Jinbao, L., Ying, D. & Keming, Z. Effects of hemodilution with different artificial plasma substitutes on blood coagulation in vitro. *Chinese Journal of Anesthesiology* **23** (2003).

17. Devine, D.V., Andestad, G., Nugent, D. & Carter, C.J. Platelet-associated factor XIII as a marker of platelet activation in patients with peripheral vascular disease. *Arterioscler Thromb* **13**, 857-862 (1993).
18. Devine, D.V. & Bishop, P.D. Platelet-associated factor XIII in platelet activation, adhesion, and clot stabilization. *Semin Thromb Hemost* **22**, 409-413 (1996).
19. Jackson, S.P. The growing complexity of platelet aggregation. *Blood* **109**, 5087 (2007).
20. Ruggeri, Z.M. & Mendolicchio, G.L. Adhesion Mechanisms in Platelet Function. *Circ.Res.* **100**, 1673 (2007).
21. Ono, A. et al. Identification of a fibrin-independent platelet contractile mechanism regulating primary hemostasis and thrombus growth. *Blood* **112**, 90 (2008).
22. Wolberg, A.S. Thrombin generation and fibrin clot structure. *Blood Rev.* **21**, 131 (2007).
23. Francis, C.W. & Marder, V.J. Rapid formation of large molecular weight alpha-polymers in cross-linked fibrin induced by high factor XIII concentrations. Role of platelet factor XIII. *J Clin Invest* **80**, 1459-1465 (1987).

Chapter 6

Preliminary *in vivo* Testing of the Optimized Liquid Fibrin Sealant

Abstract

The research presented in this chapter evaluates the optimal liquid fibrin sealant (LFS) consisting of recombinant human fibrinogen (rFI) and recombinant Factor XIII (rFXIIIa) *in vivo* in multiple injury models. The rLFS was evaluated for its effectiveness in aiding hemostasis alone and in presence of a dressing as assessed in femoral arteriotomy and multiple liver models in swine. A 4 mm femoral arteriotomy model described previously was used to evaluate the ability of rLFS to aid in hemostasis when exposed to arterial pressure and blood flow. Three liver injury models were also used to test the rLFS: small wedge-shaped resections and Grade V X-shaped stelate liver lacerations and liver lobe resections. This is the first report of the use of a fully-recombinant LFS used alone or in combination with a bioresorbable dressing. We also designed and tested a prototype airbrush-based spray device for LFS application and compared it to a pressurized air canister and the typical dual syringe applicator. Stelate liver lacerations, major lobe resections and some of the larger wedge resections included extensive tissue and vascular damage; however, our optimal LFS successfully achieved hemostasis in a significant number of the wounds. LFS applied without the assistance of a dressing was able to stop bleeding of oozing wounds or those with small vessels; however, a scaffold was needed when wounds contained large vasculature. Although the results presented in this chapter are promising, more research needs to be conducted to develop the best LFS application device and dressing that optimizes hemostatic results but is not dependent on the experience of the applicator.

Introduction

Trauma deaths are a result of hemorrhage in 37% of civilians[1] and 47% military personnel[2] and are the primary cause of death for individuals under 44 years of age.[3] For the past 2000 years, the same techniques have been used to stop hemorrhage: packing with gauze, direct pressure and tourniquet.[4] This method is inadequate for treating severe hemorrhage. The Department of Defense Combat Casualty Care Research Program is focused on developing more effective options for treating hemorrhage[5] and especially desires a hemostatic dressing.[5]

Fibrin sealants (FS), also known as fibrin glues, are viewed as the best tissue sealant[6] because they are biocompatible,[7-9] biodegradable[9] and safe[7] and are not linked to excessive inflammation, immune responses or necrosis.[8, 9] Because they mimic natural clotting mechanisms, FS provide similar functions as endogenous components such as creating hemostatic clots[10] and providing a scaffold for cellular infiltration needed to regenerate tissue[10, 11] and dissolve the clot.[10] FS, which contain fibrinogen (FI), thrombin (FIIa) and calcium chloride and occasionally Factor XIII (FXIII), reproduce the final stage of the clotting cascade to aid hemostasis. FIIa catalyzes the conversion of FI to soluble fibrin monomer and FXIII to activated FXIII (FXIIIa).[12-15] FXIIIa then catalyzes the formation of the cross-linked, insoluble fibrin clot that is melded with the platelet-based, primary hemostatic plug.[14, 16-18] In addition to binding other fibrin molecules and creating the fibrin clot, fibrin adheres the clot to the wound by binding to collagen exposed at the site of tissue injury in addition to platelets, endothelial and other cells.[7]

To aid in hemostasis, FS can be used alone or in combination with a dressing to stop blood oozing which cannot be stopped by suturing.[19] FS are typically applied by a needle and syringe sequentially or simultaneously in a dual-syringe delivery device.[7, 20] Devices have also been designed to deliver FS in aerosol form.[7] While FS have proved useful in innumerable surgical procedures, they have their weakness. When applied to wounds with large vascular damage, FS can be diluted or swept away from the injury.[21] The use of a scaffold to provide mechanical support and a matrix on which to clot can aid hemostasis by FS. The composition of the dressing is important and the optimal FS-bandage will include a bioresorbable material that does not require a subsequent operation for its removal which may cause hemorrhage in an already over-taxed system. Dressings consisting of dry, lyophilized FI and FIIa on different backings (gauze,[22] silicone,[4, 23] and Vicryl[21, 24]) were evaluated in femoral arteriotomy,[22, 23, 25] ballistic injury[4] and Grade V liver injury[21] models. Under normal, hypothermic and coagulopathic conditions, these bandages were significantly better than control dressings with respect to minimizing blood loss[4, 22, 23, 25] and maintaining blood pressure.[4, 22] A liquid fibrin sealant (LFS) has also been tested in combination with a dressing. A resorbable polyglycolide felt dressing in combination with a commercial LFS successfully sealed air leaks following pulmonary surgery.[26]

FS function is based on complicated interactions between other pro- and anticoagulant proteins, blood cells and vessel surface under flow and viscosity conditions;[19] therefore, our optimized rLFS must be tested *in vivo*. Femoral arterial and liver injury models in swine are frequently used to evaluate FS efficacy. Both femoral and liver injuries mimic severe wounds that result in hemorrhagic death. The liver

provides a hemostatic challenge because the parenchymal tissue is highly vascularized[19] and the vessel is unable to be constricted.[27] Most hemorrhage requiring reoperation[28] and death from abdominal organ injury is due to liver injury.[29] Liver injuries that expose significant vascularity and extensive parenchymal tissue damage is considered a "Grade V" [30] and 50 to 90% result in death.[21] To date, these injuries are best treated by packing with gauze and closing the abdomen; however, another operative procedure is required to remove the gauze.[31-33] Consequently, a liver injury model is an excellent test of FS. While there is some research on FS use in liver, there is need for control trials testing FS in liver injury models that compare FS and compression results.[34]

The objective of the research presented in this chapter was to evaluate our optimized rLFS *in vivo* in multiple injury models. The rLFS was evaluated for its adherence to injured tissue and its effectiveness in aiding hemostasis alone and in presence of a bioresorbable dressing as assessed in femoral arteriotomy and multiple liver models in swine. A 4 mm femoral arteriotomy model described previously[23] was used to evaluate the ability of rLFS to aid in hemostasis when exposed to arterial pressure and blood flow. Three liver injury models were also used to test the rLFS: small wedge-shaped resections and Grade V X-shaped stelate liver lacerations and large lobe resections. This is the first report of the use of a fully-recombinant LFS used alone or in combination with a bioresorbable dressing. We also designed and tested a prototype airbrush-based spray device for LFS application and compared it to a pressurized air canister and the typical dual syringe applicator.

Materials and Methods

Materials

Purified, plasma-derived prothrombin was bought from Enzyme Research Laboratories (South Bend, IN). Recombinant thrombin (Recothrom®) was purchased from Zymogenetics. Purified recombinant fibrinogen, expressed in the milk of transgenic Swiss Brown cows, was obtained from Pharming Group NV (Leiden, Netherlands). Materials for the thromboelastograph were purchased from Haemoscope (Niles, IL). Unless otherwise specified, reagents were purchased from Sigma (St. Louis, MO).

Vector construction, expression and purification of FXIIIA in Pichia pastoris

The human Ultimate ORF clone containing the human coagulation factor FXIIIA1 cDNA in the pENTR™221 vector was purchased from Invitrogen (Carlsbad CA). The following primers were used to obtain FXIIIa gene to subclone in pPICZA intracellular Pichia expression vector. (Forward, 5'-CCAATTGATGCATCATCATCATCATCATTCAGAAACTTCCAGGACCGC-3'; Reverse, 5'-GCGGCCGCTCACATGGAAGGTCGTCTTTGAATC-3'). The forward primer introduced a methionine and 6 histidine amino acids at the N-terminus of mature FXIIIa peptide. The PCR product was digested with MfeI and NotI and subcloned into pPICZA which was digested with the same enzymes. The DNA sequence of the FXIIIA was confirmed by sequencing the insert fragment. One of the confirming plasmid pPICZAFXIIIa was linearized with PmeI and transformed into P. pastoris X-33 host strain and copy number of the clones was determined as described.[35] Varying copy number clones were screened in shake flask culture to confirm intracellular production of

FXIIIa protein. The highest producing clone was scaled up to 5 L bench scale. A fed-batch fermentation protocol was followed to optimize FXIIIa production as described by Zhang et al., (2007).[36] At the end of fermentation process the cells were separated by centrifugation (6,000g) and pellet was stored at -80^{o}C.

Frozen cell paste was processed in 300 gram batches. Cells were lysed in three sets of 100 gram batches. 100 grams of cell paste was resuspended in 100 mL of cold lysis buffer (50 mM Tris-HCL, 10 mM $MgSO_4$, 1 mM EDTA, 10 mM potassium acetate, 1 mM DTT (DL-Dithiothreitol), 2 mM PMSF (phenylmethanesulphonylfluoride) in methanol, pH 9.5). 100 ml (250 g) of 0.5 mm glass beads (Biospec, Bartlesville, OK) were added and the cells. Surrounded by an ice bath, cells were lysed using a BeadBeater Blender (Biospec, Bartlesville, OK) with twenty 20 second on/off cycles. The cell lysate mixture was then centrifuged to remove cellular debris. The lysate from 300 grams of cell paste was combined and purified using the HisBind Purification Kit (EMD Chemicals, Inc.,San Diego, CA) with 40 mL of resin slurry. Following purification, rFXIII was dialyzed in 10 mM Tris-HCl, 0.1 mM EDTA, 60 µM polysorbate-20, pH 8.0 in snake-like dialysis membranes and the protein samples were filter-sterilized and concentrated using the Amicon tubes (Millipore, Billerica, MA). The purity of the sample was tested by SDS-PAGE (NuPAGE 12% Bis-Tris) (Invitrogen, Carlsbad, CA) and immunoblot. The concentration of rFXIII was determined by standard Bicinconic Acid (BCA) methods.

FIIa preparation

Frozen, plasma-derived human prothrombin (Enzyme Research Laboratories, South Bend, IN), was thawed at 37^{o}C. Plasma-derived thrombin (Enzyme Research

Laboratories, South Bend, IN) was added at a 1/10 mass to mass thrombin/prothrombin ratio. 0.35 grams of sodium citrate per milliliter of solution was added (Lanchantin 1965). This solution was incubated at 37^{o}C on a rotating mixer for five hours. Sodium citrate was removed using PD-10 desalting columns (GE Healthcare, Giles, United Kingdom). Activation of prothrombin to thrombin was confirmed by reducing and nonreducing SDS-PAGE (12% Bis-Tris NuPAGE) (Invitrogen, Carlsbad, CA) stained with Colloidal Blue (Invitrogen, Carlsbad, CA). The concentration of the thrombin solution was determined by standard Bicinconic Acid (BCA) methods. The specific activity was determined by aPTT analysis.

Experimental dressings

Nanofiberous and macrofiberous made from a racemic poly(D,L-lactide) (PDLLA) was obtained from LNK Chemsolutions. The production process and treatment of the bandage are proprietary knowledge of LNK. The nanofiberous PDLLA has fiber diameters of approximately 100 nm and is produced as a 100 µm thick sheet. 8-ply bandages were created to yield better handling ability by stacking eight 100 µm layers. The smooth and hydrophobic unmodified PDLLA was evaluated. It was also tested after coating with a proprietary treatment to create a hydrophilic dressing. Both the hydrophobic and hydrophilic dressings were modified by adding macropores and corrugations to assist its hemostatic capability by allowing blood inflow. Macropores were created by punching several sets of holes using a bed of nails device (Figure 6.1). Corrugations were also created by wetting the bandage with water until damp and heating it between two plates at approximately 32^{o}C for 10 minutes to several hours (Figure 6.2).

In many of the experiments, these 8-ply modified bandages were stacked in layers with the corrugations laid perpendicular to each other (Figure 6.3).

.

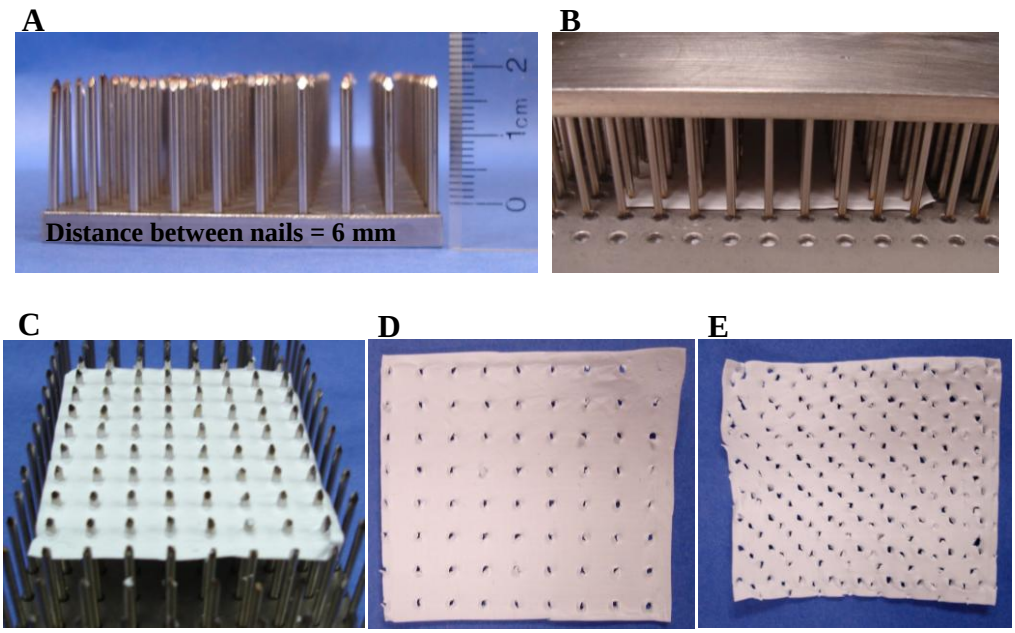

Figure 6.1. Device and method for perforating the PDLLA dressing. This bed of nails (A) was used to create macropores in the PDLLA. PDLLA was laid on a thin stainless steel plate containing holes matching the bed of nails (B) and the bed of nails was firmly pressed so that the nails transversed the PDLLA and embedded in a layer of styrofoam below the plate (C). After creating the first set of holes (D), the PDLLA was removed, placed back on the plate and the bed of nails carefully aligned to create another set of macropores. This device was used three times on each bandage creating a well perforated bandage (E).

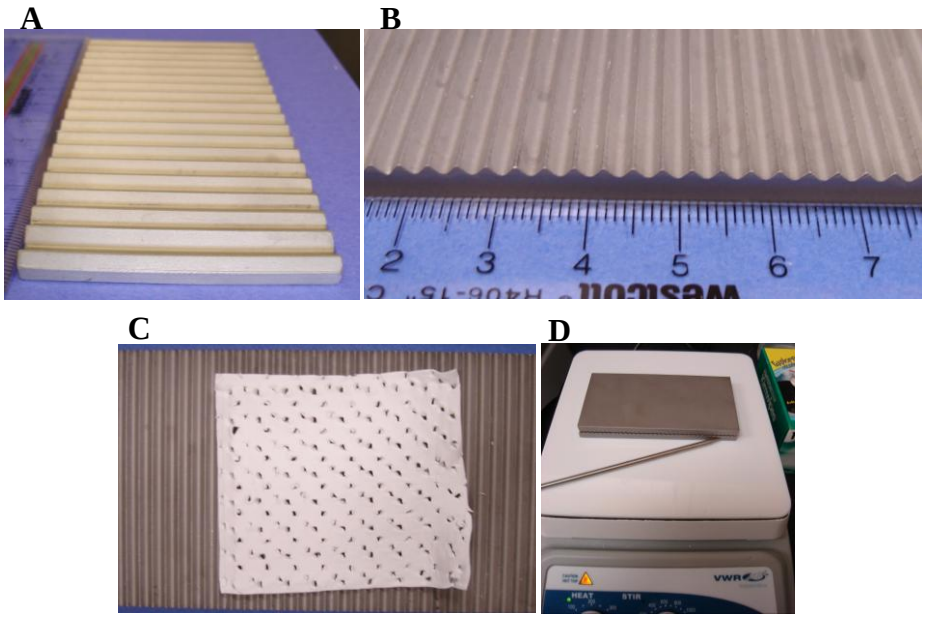

Figure 6.2. Plates and method employed to corrugate PDLLA. Two stainless steel plates were designed with peak heights of 1.5 mm and a 3 mm distance between peaks (A, B). These plates were heated to approximately 32°C and PDLLA dampened with deionized water was placed between the plates (C). The PDLLA was incubated between the heated plates for 10 minutes to several hours to create corrugations (D).

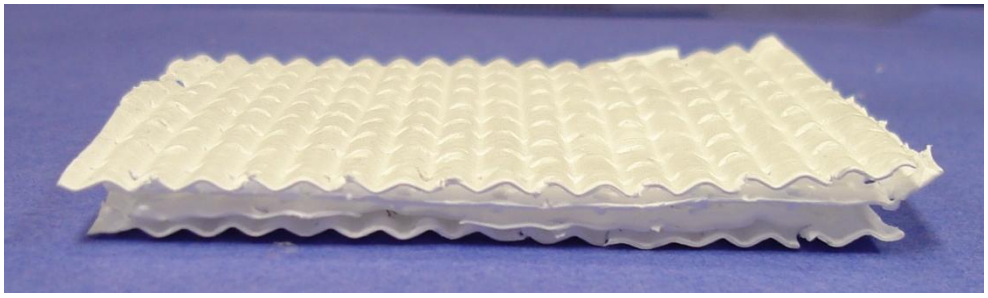

Figure 6.3. Final PDLLA bandage format. The perforated, corrugated PDLLA was layered so that the corrugations were perpendicular to those in adjacent layers.

LFS application devices

The LFS was tested alone in two liver injury models and with the aid of a scaffold (gauze or PDLLA) in a femoral arteriotomy and massive liver resection. LFS was applied to the wounds or the dressing by numerous methods (Figure 6.4). LFS was applied to the wedges by a dual-syringe system made in the operating room (Figure 6.4A)

and spray device predecessor to UNL's device (not shown). LFS was applied to the stelate liver lacerations by Tisseel's Duploject® system (Figure 6.4B) and the PTI spray device (Figure 6.4C). LFS was applied to dressings by pipette or UNL's airbrush-based spray device (Figure 6.4D and E).

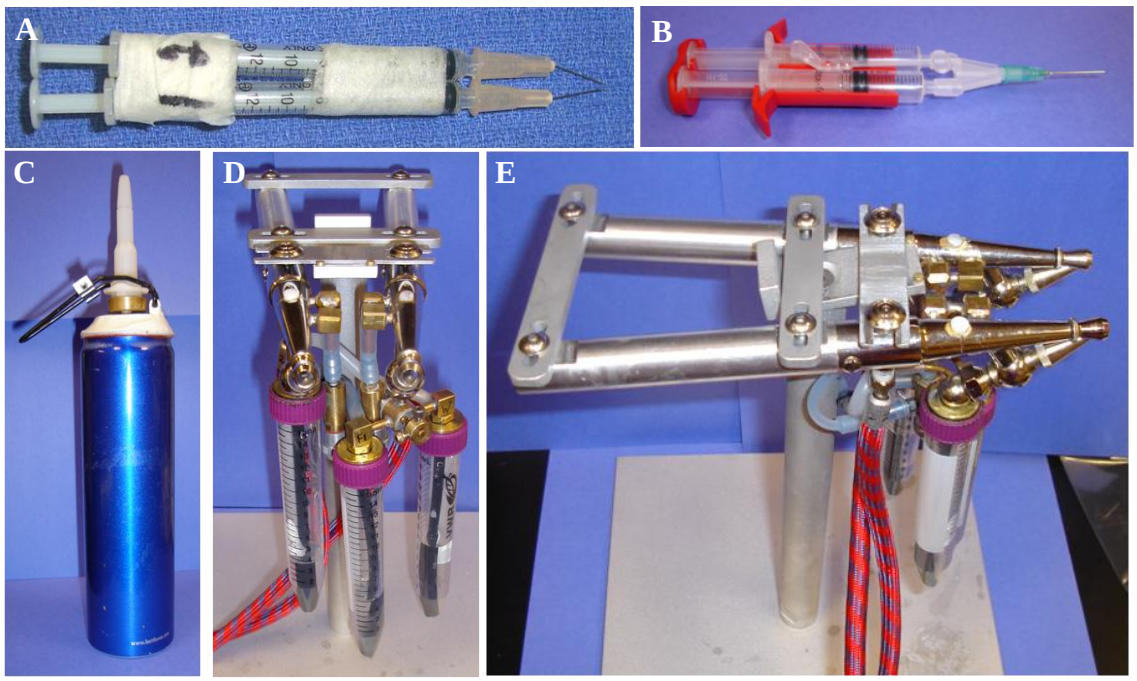

Figure 6.4. LFS application device used during *in vivo* experiments. LFS was applied by two syringes taped together with needles bent towards each other (A), Tisseel's® duploject system (B), PTI's spray device (C), frontal (D) and top (E) views of UNL's airbrush-based spray device.

A spray device was designed to deliver the rLFS in two atomized components at finely-adjustable flow rates over a narrow focus area. The device consists of two modified artist-grade airbrushes (single-action, external mix, Paasche airbrushes), a main pressure regulator and two fine control pressure regulators. The airbrushes were modified from delivering liquid by suction to a pressurized flow allowing the use of lower air flow. Both regulators pressurizing the solutions to each airbrush was set at 15 psi. Each spray device is equipped with adjustable nibs which control the spray pattern, flow rate and the amount of material delivered. The airbrushes were coupled together

and a single trigger bar created to synchronize spraying. The pressure adjustment module consists of a main pressure regulator that adjusts the air pressure from house air which is coupled to two fine control pressure regulators that modulate the air flow and pressure into each airbrush.

Animals

This research used crossbred commercial (domestic) swine obtained from UNL Agricultural Research and Development Center (Mead, NE). All procedures performed during this research were approved by the Institutional Animal Care and Use Committee of the Omaha VA Hospital. All animals were treated according to the *Guide for the Care and Use of Laboratory Animals* (National Institutes of Health publication 86-23, revised 1996).

TEG evaluation of blood samples throughout surgery

Multiple blood samples were drawn throughout surgery. Samples were drawn before surgery, after surgery and between procedures that resulted in significant blood loss. One to two milliliters of blood were drawn into tubes containing 3.2% sodium citrate and stored on ice until testing by thromboelastography (TEG) which occurred within five hours. 340 µl of each sample was loaded into a single-use TEG cup followed by 20 µl of 200 mM $CaCl_2$ (final concentration: 11.11 mM) to start the reaction. The TEG Analytical Software (version 4.2.2, Haemoscope, Niles, IL) collected the time to clot initiation (R), the time to achieve a clot firmness of 20mm (K) and the maximal clot strength (MA) for 30 minutes. Data was exported from the TEG Analytical Software to Microsoft Excel for analysis. t tests with an α of 0.05 were used to compare pre- and

post-surgical clotting parameters for statistical significance. The percent change of TEG values from the initial and final blood samples for each pig were calculated. The instrument was calibrated each day of use. All tests included three replicate samples in each treatment group.

In vivo evaluation of rLFS

In vivo experiments on the rLFS were performed on 44 male pigs three months of age and a mean weight of 32.1 ± 2.2 kg (range: 27.2 and 38.6 kg). Pigs were anesthetized by inhalation through an endotracheal tube. Under general anesthesia, a catheter was inserted into the right carotid artery and jugular vein of each swine for blood pressure monitoring and administration of fluid and medication. Animals were included in results only if their systolic blood pressures were greater than 100 mmHg. Depending on the planned experiments, the liver and/or the femoral arteries were exposed. The femoral artery injury model consisted of a 4 mm hole. A midline laparotomy was performed and the liver pulled up through the incision. Liver injuries included small wedge-shaped excisions, X-shaped stelate liver lacerations and large liver lobe resections. A Pringle maneuver was used on the stelate liver lacerations and several of the large liver resections to minimize blood loss. After creating the injury, the planned treatment was applied. The LFS was tested alone or in combination with the PDLLA dressing which was also evaluated alone and with various modifications. rLFS was tested alone on wedge-shaped liver resections and stelate liver wounds. rLFS combined with the PDLLA dressings was evaluated on femoral arteriotomy injuries and large liver lobe resections. Each swine underwent multiple procedures and were euthanized at the end of testing. ANOVA and two tail t test (equal variance) analyses were performed to identify

statistical significance between treatment groups of raw data. An α of 0.05 was used for all statistical analyses.

rLFS on hepatic wedge resections

For the small, wedge-shaped liver resections, a cauterization tool was utilized to draw the triangular wedge resections with a base of 1 cm and increasing heights of 0.5, 1.0, 1.5, 2.0, 2.5 and 3.0 cm (Figure 6.5). Each wedge was resected with scissors. rLFS (9 mg/ml rFI, 0.36 mg/ml rFXIII (2,463 U/ml, rFXIIIa/FI = 0.16), 105.6 U/ml rFIIa (FIIa/FI = 0.18), 12 mM $CaCl_2$) was applied by spray device or by two 3 ml syringes taped together with needles bent together to mix the solution approximately 2 cm from the tips. The rLFS was separated into two reservoirs: rFI/rFXIII into one and rFIIa/$CaCl_2$ in the other and applied at an approximate flow rate of 0.4 ml/sec. A total of 18 mg rFI, 0.72 mg rFXIIIa and 211.2 U rFIIa was applied to each wedge. Hemostasis was subsequently evaluated and given a score: 1 indicated complete hemostasis; 2 for mostly hemostatic with minor oozing; 3 for partially hemostatic with prominent oozing and 4 for minimal effect and complete failure. Ringer's solution was applied as a control.

Figure 6.5. Wedges marked on a liver lobe by a cauterization tool. Wedges with a base of 1.0 cm and increasing heights of 0.5 to 3.0 cm marked on a liver lobe by a cauterization tool for testing rLFS.

rLFS on hepatic stelate laceration

Grade V stelate liver lacerations were created by making one or two overlapping X-shaped wounds using a home-made device (Figure 6.6) with an arm length of ~38 cm and X-shaped blades ~8 cm in length. The injuries were treated in five pigs with rLFS (7.1 mg/ml rFI, 0.25 mg/ml rFXIII (1,735 U/ml, rFXIIIa/FI = 0.16), 84.64 U/ml rFIIa (FIIa/FI = 0.18), 12 mM $CaCl_2$). The solution was applied by Tisseel's Duploject® two-syringe system (Figure 6.4B). A total of 6 ml were used to treat four pigs and 10 ml to treat the other pig. With this system, the rLFS was applied over 30 seconds to several minutes.

The rLFS was also applied by Propulsion Technology, Inc.'s (PTI) delivery device (Figure 6.4C) in three pigs. The device separates the rLFS into two reservoirs (rFI/ $CaCl_2$ and rFXIIIa/rFIIa/$CaCl_2$) and utilizes air pressure for delivery. This system applied 60 ml of rLFS (9 mg/ml rFI, 0.36 mg/ml rFXIII (2,463 U/ml, rFXIIIa/FI = 0.16),

105.6 U/ml rFIIa (FIIa/FI = 0.18), 12 mM $CaCl_2$) in approximately 3 to 30 seconds. Each stelate liver laceration was treated with 540 mg rFI, 21.6 mg rFXIIIa and 6,336 U rFIIa. Hemostasis was subsequently evaluated.

In one pig, LFS (10.2 mg/ml rFI, 0.40 mg/ml rFXIII (2,791 U/ml, rFXIIIa/FI = 0.16), 119.7 U/ml rFIIa (FIIa/FI = 0.18), 12 mM $CaCl_2$) was applied by the initial spray device designed by LNK Chemsolutions. 5 ml LFS was applied intermittently over a couple of minutes. The laceration was treated with 51 mg rFI, 2 mg rFXIIIa and 598.5 U rFIIa. Hemostasis was subsequently evaluated.

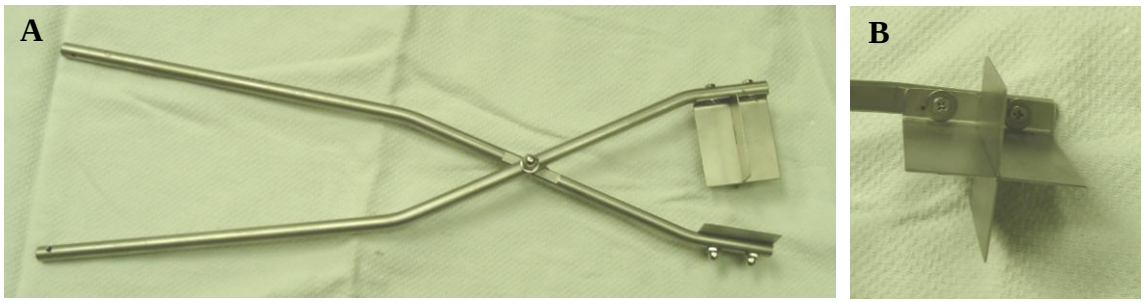

Figure 6.6. Device used to create stelate liver laceration. Home-made, stainless steel device designed with ~38 cm arms (A) and sharp X-shaped blades (B) to create a ~8 cm x ~8cm wound.

rLFS dressing on femoral arteriotomy model

rLFS coated nanofiberous and microfiberous PDLLA was evaluated in a femoral arteriotomy model. After exposing both femoral arteries, blood flow through the artery was controlled by applying vessel loops or arterial clamps proximal and distal from the site of injury. While blood flow was occluded, a femoral arteriotomy was created with a 4 mm aortic punch. The test dressing was carefully laid over the wound and the blood was allowed to flow through the artery. Manual pressure was held on the bandage for four to five minutes. The success of a dressing was evaluated by the level of hemostasis (complete hemostasis, oozing or uncontrolled flow) and adherence to the artery.

Bandages constructed of hydrophobic unaltered PDLLA nanofibers (typically 4 cm x 4 cm, 8-ply) were tested dry, wet with Ringer's solution or wet with rLFS (0.44 mg/cm^2 per ply rFI, 0.02 mg/cm^2 per ply rFXIIIa (rFXIIIa/rFI = 0.16), 5.07 U/cm^2 per ply FIIa (FIIa/rFI = 0.18), 12 mM $CaCl_2$). PDLLA coated with Ringer's solution and FIIa (9.32 mg/cm^2 pdFIIa, 7 mM $CaCl_2$) were also evaluated. Hydrophilic, modified PDLLA dressings were also tested alone and coated with rLFS at the same levels. Microfiberous PDLLA bandages (3 cm x 3 cm with a depth of 1 cm) were coated with rFI, rFXIII and pdFIIa (3.87 mg/cm^2 rFI, 0.15 mg/cm^2 rFXIII, 0.09 mg/cm^2 pdFIIa, 7 mM $CaCl_2$) or Ringers solution alone or with pdFIIa (0.09 mg/cm^2 pdFIIa, 7 mM $CaCl_2$). Liquids were applied to the dressings by pipette.

rLFS dressing on hepatic resections

The LFS was tested on hepatic resections of multiple sizes. Small resections excised the tip of the lobe exposing a parenchymal area of 5-7 cm by 2 cm. Excisions of medium resections exposed an area of 10-12 cm by 3 cm. Large resections exposed an area of 15-17 cm by 5-6 cm (25-33% of the liver mass). After removal of the lobe by scissors, blood flow was limited by manual pressure or a Pringle maneuver. Dressings were applied to the exposed tissue and held by manual pressure for three minutes. When released, the success was evaluated by the level of hemostasis (1 indicated complete hemostasis; 2 for mostly hemostatic with minor oozing; 3 for partially hemostatic with prominent oozing and 4 for minimal effect and complete failure).

Bandages constructed of hydrophilic, PDLLA nanofibers modified with macropores, corrugations and roughing of the wound-side (typically 5 cm x 5 cm, 8-ply) were tested dry, wet with Ringer's solution or wet with approximately 0.43 mg/cm^2 per

ply rFI, 0.02 mg/cm^2 per ply rFXIIIa (rFXIIIa/rFI = 0.16), 5.07 U/cm^2 per ply FIIa (FIIa/rFI = 0.18), 12 mM $CaCl_2$. rLFS was applied to the PDLLA by pipette or by UNL's spray device (Figure 6.4D and E). After being coated with rLFS, the bandages were placed on the wound within 2 to 4 seconds and a small amount of blood was allowed to flow through the macropores and infiltrate the bandage. A series of 5 cm x 5 cm bandages were coated and applied to the wound. Small resections typically required three or four bandages. Medium and large bandages typically needed five to seven coated dressings. Therefore, small resections used approximately 33 mg rFI, 1.3 mg rFXIIIa and 380 U rFIIa. Medium and large resections used approximately 78 mg rFI, 3 mg rFXIIIa and 887 U rFIIa.

Results

Evaluation of swine clotting factors

Blood samples for each swine were drawn before, during and after surgical procedures and evaluated within five hours by thromboelastography (TEG). This was used to identify pigs with abnormal clotting parameters and to monitor changes in endogenous coagulation parameters throughout the surgery due to blood loss or haemodilution (Table 6.1). t tests indicated that average pre- and post-surgical clotting parameters were not significantly different for time to clot initiation ($p = 0.242$), coagulation time ($p = 0.319$) or maximum clot strength ($p = 0.185$). Consequently, all procedures on each swine can typically be included; however, this was determined for each individual swine. A representative TEG tracing is shown (Figure 6.7). Even after

significant blood loss, few post-surgical TEG results differed significantly from initial samples.

Table 6.1. Average time to clot initiation (R), coagulation time (K) and maximum amplitude of pre-surgical and post-surgical blood samples and the subsequent percent change. Data presented as average ± standard deviation, N = 35 for pre-surigical, 33 for post-surgical and % change.

	Time to Clot Initiation (sec)	Coagulation Time (sec)	Maximum Amplitude (mm)
Pre-surgical blood sample	328.71 ± 93.03	100.98 ± 28.58	67.92 ± 4.82
Post-surgical blood samples	362.60 ± 140.31	109.32 ± 39.36	65.48 ± 9.58
% Change	0.12 ± 0.32	0.13 ± 0.36	-0.04 ± 0.14

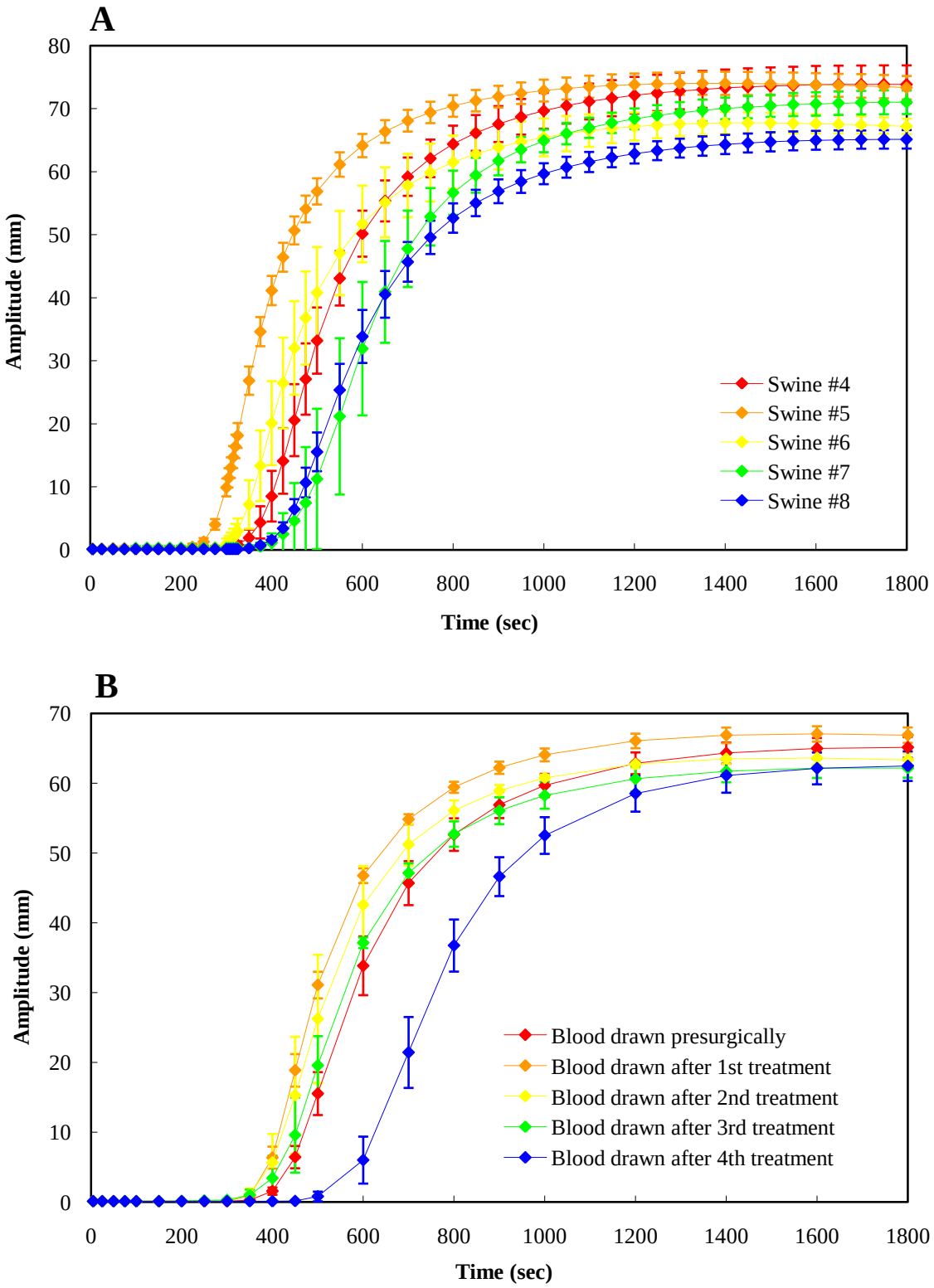

Figure 6.7. Representative TEG tracings of blood samples from a pig before, during and at the conclusion of the surgery. Thromboelastographic comparison of clotting parameters of presurgical blood samples from five swine (A); and comparisons of bloods drawn from the same swine throughout the surgical procedure (B).

LFS on hepatic wedge resections

The optimized rLFS was applied to wedge resections of the liver with a base of 1.0 cm and heights from 0.5 to 3.0 cm. Wedge resections were performed on 16 pigs and rLFS was applied by spray device (Figure 6.8) on 9 pigs and the two-syringe system (Figure 6.9) on the remaining 7 pigs.

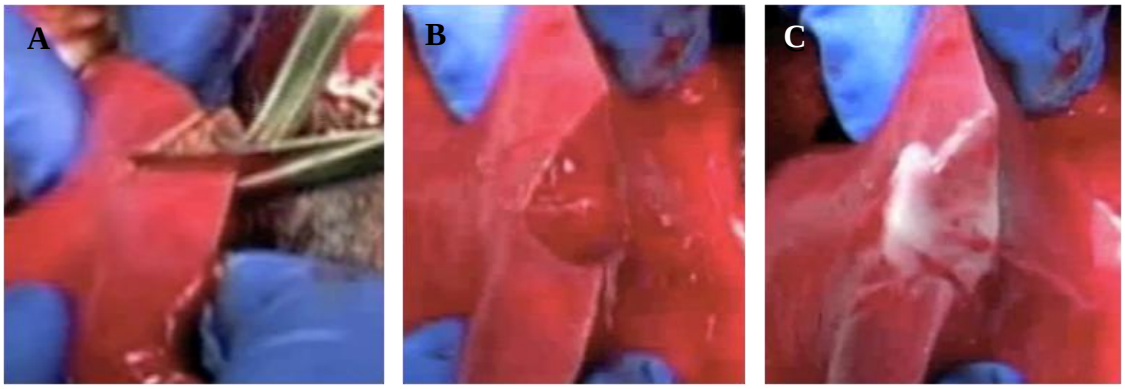

Figure 6.8. Wedge resection treated with rLFS applied by spray-device. Triangular-shaped wedges with bases of 1.0 cm and 0.5 to 3.0 cm heights were resected (A) resulting in profuse bleeding (B) which was treated with rLFS applied by a spray-device (C). This application resulted in complete hemostasis.

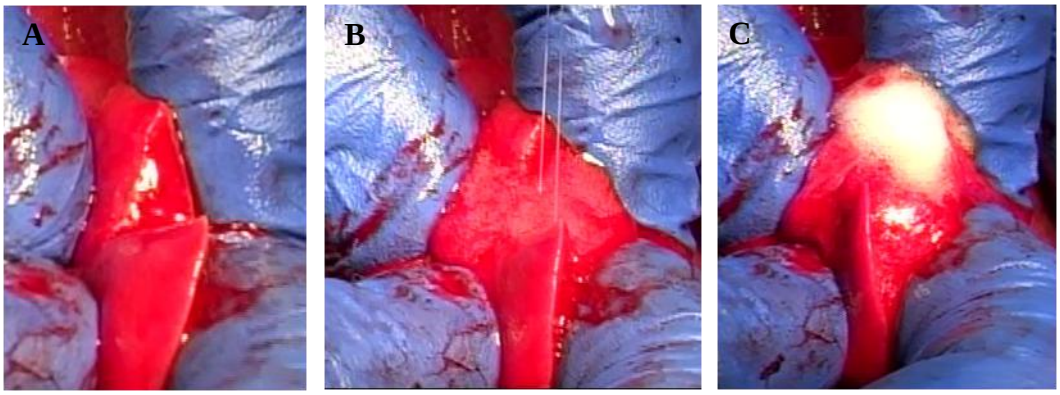

Figure 6.9. Wedge resection treated with rLFS applied by double barrel syringe. Triangular-shaped wedges with bases of 1.0 cm and 0.5 to 3.0 cm heights were resected resulting in profuse bleeding (A) which was treated with rLFS applied by a spray-device (B). The rLFS created a solid, white clot (C). This application resulted in complete hemostasis.

The two application techniques yielded similar results. ANOVA indicates that hemostatic results obtained at different depths are statistically different ($p < 0.001$).

Complete hemostasis was achieved most frequently in the smaller wedges (Figure 6.10, Table 6.2). 82% of the 0.5 cm height wedge cuts were completely hemostatic while the remaining two cuts were mostly hemostatic. 64% of the 1.0 cm height resections were mostly hemostatic with the other 5 being completely hemostatic. At a depth of 1.5 cm, 27% were completely hemostatic, 45% mostly hemostatic, 18% less hemostatic and 9% failed. At 2.0 cm, 9% were completely hemostatic, 45% were mostly hemostatic and 45% were less hemostatic. 9% were mostly hemostatic while 91% of 2.5 cm depths resulted in minimal hemostasis. At a depth of 3.0 cm, 75% were minimally hemostatic with the remaining 25% resulting in no hemostasis.

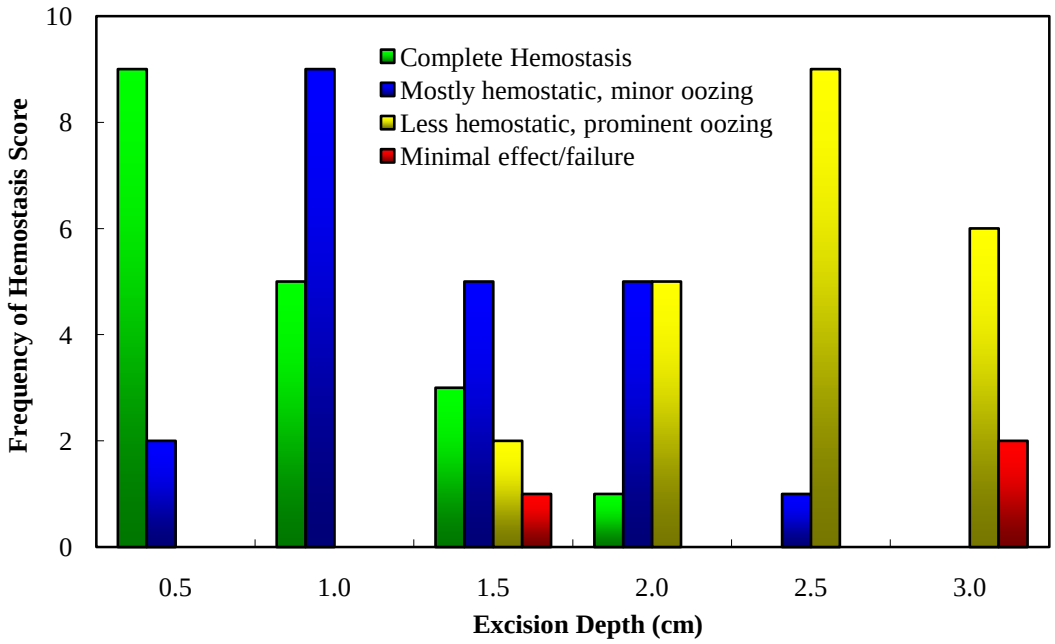

Figure 6.10. Frequency of hemostasis scores at each excision depth. The frequency of complete hemostasis (green), mostly hemostatic (blue), less hemostatic (yellow) and minimal effect (red) is shown at each excision depth.

Table 6.2. Average hemostasis scores for excision depths.
Data presented as average ± standard deviation.

Depth (cm)	N	Hemostasis Score
0.5	11	1.18 ± 0.40
1.0	14	1.64 ± 0.50
1.5	11	2.09 ± 0.94
2.0	11	2.36 ± 0.67
2.5	10	2.90 ± 0.32
3.0	8	3.25 ± 0.46

The approximate areas of the parenchymal tissue were estimated at each depth and volume of LFS needed to create hemostasis estimated (Table 6.3). This data was used to calculate the approximate volume of LFS needed per cm^2 of tissue injury. At wedge depths of 0.5, 1.0 and 1.5 cm, 5.0, 3.8 and 2.8 ml LFS per cm^2 is needed to typically yield complete hemostasis, respectively. Consequently, the average volume of LFS needed is 3.88 ± 1.09 ml/cm^2 using 34.9 mg/cm^2 rFI, 1.4 mg/cm^2 rFXIIIa and 409.7 U/cm^2 rFIIa. These values are true for wedges with a depth of 1.5 cm or less. Unlike the smaller wedges, the larger wounds contained large blood vessels up to 1 cm in diameter (Figure 6.11) that interfered with hemostasis. The LFS was unable to stop bleeding of large vessels. LFS formed a clot over the large vessels; however, the LFS was unable to adhere to the parenchymal tissue surrounding the vessel most likely due to the pressure of the blood pouring out of the vessel. This resulted in significant bleeding from under the clotted layer of LFS.

Table 6.3. Estimated areas of the wound created by the wedge excisions.

Depth (cm)	Approximate Thickness (cm)	Estimated Area (cm^2)	LFS needed for hemostasis (ml)	Estimated LFS (ml) per cm^2 needed
0.5	0.3	0.12	0.6	5
1.0	0.4	0.37	1.4	3.78
1.5	0.5	0.71	2.0	2.8
2.0	0.6	1.14	> 2.0	
2.5	0.7	1.68	> 2.0	
3.0	0.8	2.31	> 2.0	

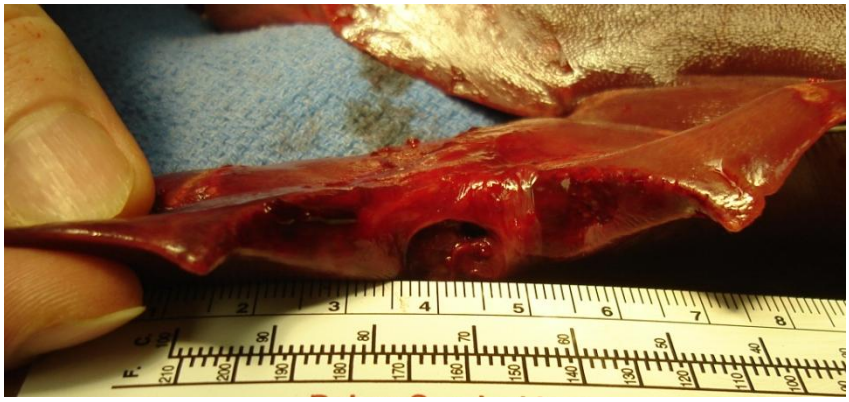

Figure 6.11. Sizeable vessel transected in larger wedge resections. The wedges with depths of 2.5 an 3.0 cm typically had sizeable vasculature at the apex of the wedge up to 1 cm in diameter.

rLFS on hepatic stelate laceration

The optimal LFS was tested on grade V stelate liver lacerations in nine pigs (Figure 6.12). The average hemostasis score was calculated based on the number of X-shaped wounds (Table 6.3). One X-shaped wound had an average hemostasis score of 1.50 ± 0.55. Two X-shaped wounds had an average hemostasis score of 1.67 ± 0.58. One X-shaped wound was created in the five pigs treated with LFS applied by Tisseel's Duploject® system. Three of the five resulted in complete hemostasis. The last two were mostly hemostatic with minor oozing that was subsequently stopped by packing with gauze and pressure. Two overlapping X-shaped wounds were created in two of the three stelate lacerations treated by PTI's application device. The last pig had only one X-shaped wound created. After the four to five minute hold, all three were mostly hemostatic with minor oozing that was stopped by gauze and pressure. The one pig treated with LFS applied by LNK's spray device had two overlapping X-shaped wounds that was completely hemostatic.

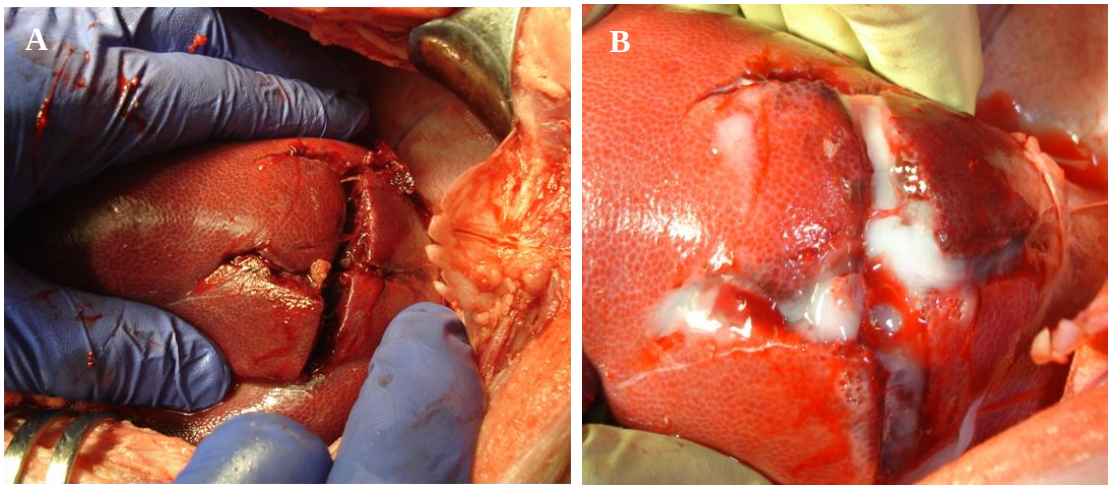

Figure 6.12. Grade 5 stelate liver injury treated with LFS. Stelate liver laceration before (A) and after (B) treatment with 7.05 mg/ml rFI, 0.28 mg/ml rFXIII, 0.16 mg/ml pdFIIa (84.5 U/ml), 6 mM $CaCl_2$ applied by Duploject system (see Figure 6.5).

Table 6.3. Average hemostasis scores for number X-shaped wounds. Data presented as average ± standard deviation.

# X-shaped Wounds	N	Hemostasis Score
1	6	1.50 ± 0.55
2	3	1.67 ± 0.58

rLFS dressing on femoral arteriotomy model

Numerous versions of the PDLLA bandage and gauze were tested alone, wet with Ringer's solution and coated in various components of LFS on a 4 mm femoral arteriotomy (Figure 6.13) in 13 pigs. Two forms of PDLLA were tested: nanofiberous (Figure 6.13B) and microfiberous (Figure 6.13C). The nanofiberous PDLLA was tested in its original smooth, hydrophobic form (Figure 6.13B) and in a hydrophilic, modified form (Figure 6.3). Only 14.7% of nanofiberous PDLLA were hemostatic (Figure 6.13D); however, 60% of treatments with the microfiberous PDLLA were hemostatic (Figure 6.13E, Table 6.4). Four of the five successful nanofiberous PDLLA dressings were coated with all of the components of the LFS and were modified with corrugations; however, a majority of those treatments failed. A significantly larger percentage of the

microfiberous PDLLA dressings were successful and the best results were observed when treated with rFXIIIa and FIIa and with all components of the LFS.

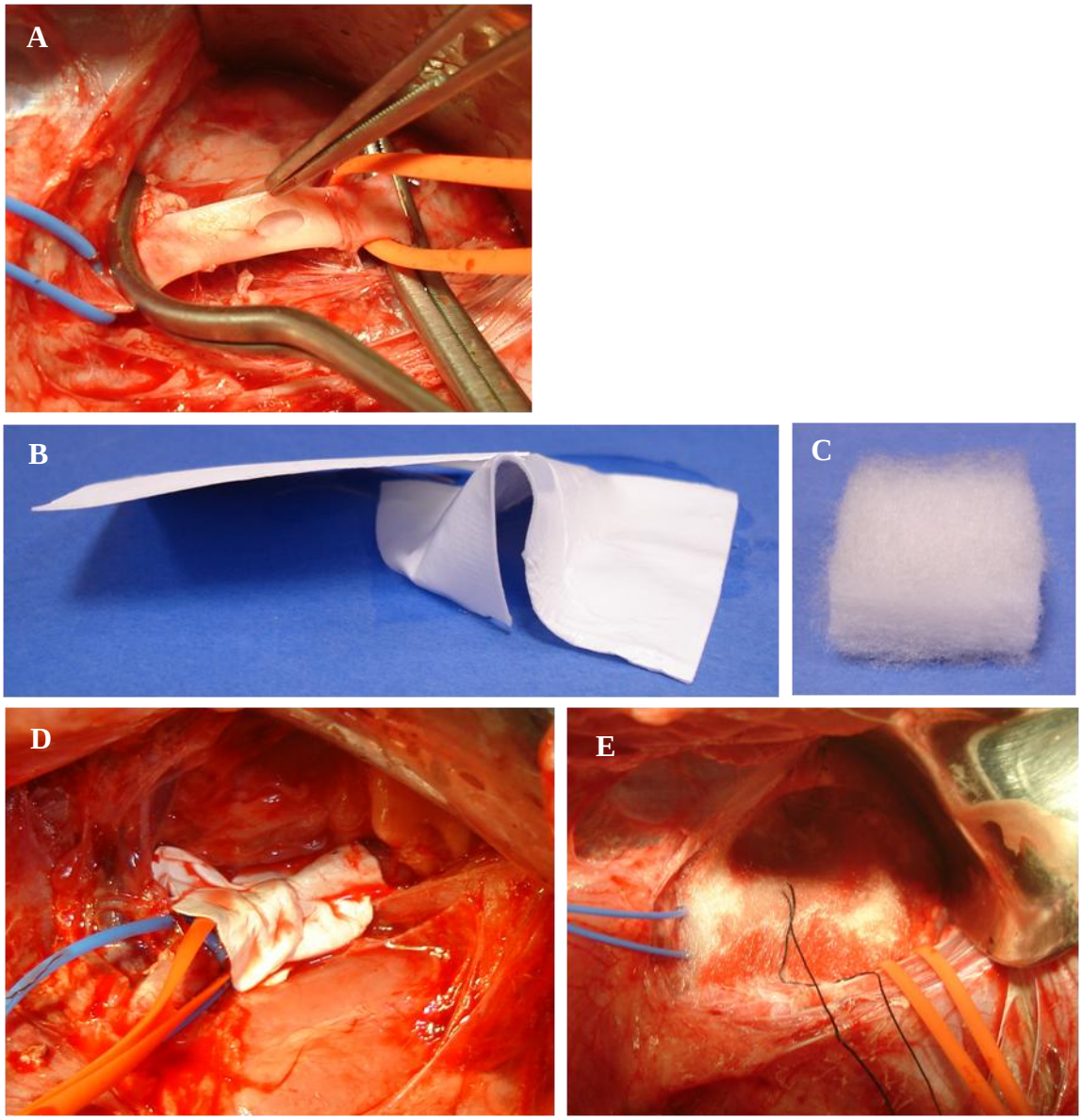

Figure 6.13. 4 mm arteriotomy treated with bandages soaked in LFS. A 4 mm hole was made in the femoral artery (A) and treated with bandages constructed of PDLLA nanofibers (B) and microfibers (C). Nanofiberous bandages (4 cm x 4 cm, 8-ply) were coated with rFI, rFXIII and pdFIIa (0.44 mg/cm^2 per ply rFI, 0.02 mg/cm^2 per ply rFXIII, 0.004 mg/cm^2 per ply pdFIIa, 7 mM $CaCl_2$) (D). Microfiberous bandages (3 cm x 3 cm with a depth of 1 cm) were coated with rFI, rFXIII and pdFIIa (3.87 mg/cm^2 rFI, 0.15 mg/cm^2 rFXIII, 0.09 mg/cm^2 pdFIIa, 7 mM $CaCl_2$) (E).

Table 6.4. Hemostatic results of PDLLA treated with Ringer's or various components of LFS applied to femoral arteriotomies.

PDLLA form	Modifications	Treatment	N	% hemostatic
Microfiberous	None	None	10	50
Microfiberous	None	Ringer's	11	64
Microfiberous	None	FIIa	4	50
Microfiberous	None	rFXIIIa + FIIa	1	100
Microfiberous	None	rFI + rFXIIIa + FIIa	4	75
Nanofiberous	None	Ringer's	7	0
Nanofiberous	None	FIIa	1	0
Nanofiberous	None	rFXIIIa	1	0
Nanofiberous	None	rFXIIIa + FIIa	2	0
Nanofiberous	None	rFI + rFXIIIa + FIIa	4	0
Nanofiberous	corrugation	rFXIII + FIIa	4	0
Nanofiberous	corrugation	rFI + rFXIIIa + FIIa	4	50
Nanofiberous	macropores, corrugation	None	1	0
Nanofiberous	macropores, corrugation, surface roughing	None	1	0
Nanofiberous	macropores, corrugation, surface roughing	rFI	2	50
Nanofiberous	macropores, corrugation, surface roughing	rFI + rFXIIIa + FIIa	7	29

rLFS dressing on hepatic resections

Three large hepatic resections were made, covered with gauze and sprayed with LFS (Figure 6.14). All three were completely hemostatic. Three small, one medium and 35 large resections were treated with PDLLA alone or coated with LFS (Table 6.5). Once the lobe was resected, 5 cm x 5 cm dressings coated with LFS were applied one by one to the wound surface. 53.3% of the LFS coated dressings were completely hemostatic (Figure 6.15) while 43.3% were mostly hemostatic and the remaining 3.3% were less hemostatic. Some applications successfully adhered to the entire wound surface and were not affected by the large vessels (Figure 6.15C); however, pockets frequently formed over the largest vessels apparently due to the pressure from the blood flow. The cases that were not completely hemostatic oozed from under the dressing apparently from these large vessels. These had less adhesion then those resulting in complete hemostasis. The method of application of the LFS to the PDLLA did not appear to affect the success.

Figure 6.14. Treatment of large hepatic resection with gauze coated with rLFS. A fatal injury was created by removing an ~12 cm long section (A) which was covered with gauze (B) and then rLFS (C).

Table 6.5. Hemostatic results of PDLLA treated with LFS applied to hepatic resections. All bandages were modified by adding macropores, corrugations and roughing the surface.

PDLLA form	Size of Resection	Hydrophobicity	N	Completely Hemostatic	Mostly Hemostatic	Less Hemostatic	Failed
Nanofiberous	Small	Hydrophobic	1	1	0	0	0
Nanofiberous	Small	Hydrophilic	2	2	0	0	0
Nanofiberous	Medium	Hydrophobic	1	1	0	0	0
Nanofiberous	Large	Hydrophobic	1	1	0	0	0
Nanofiberous	Large	Hydrophilic	30	16	13	1	0

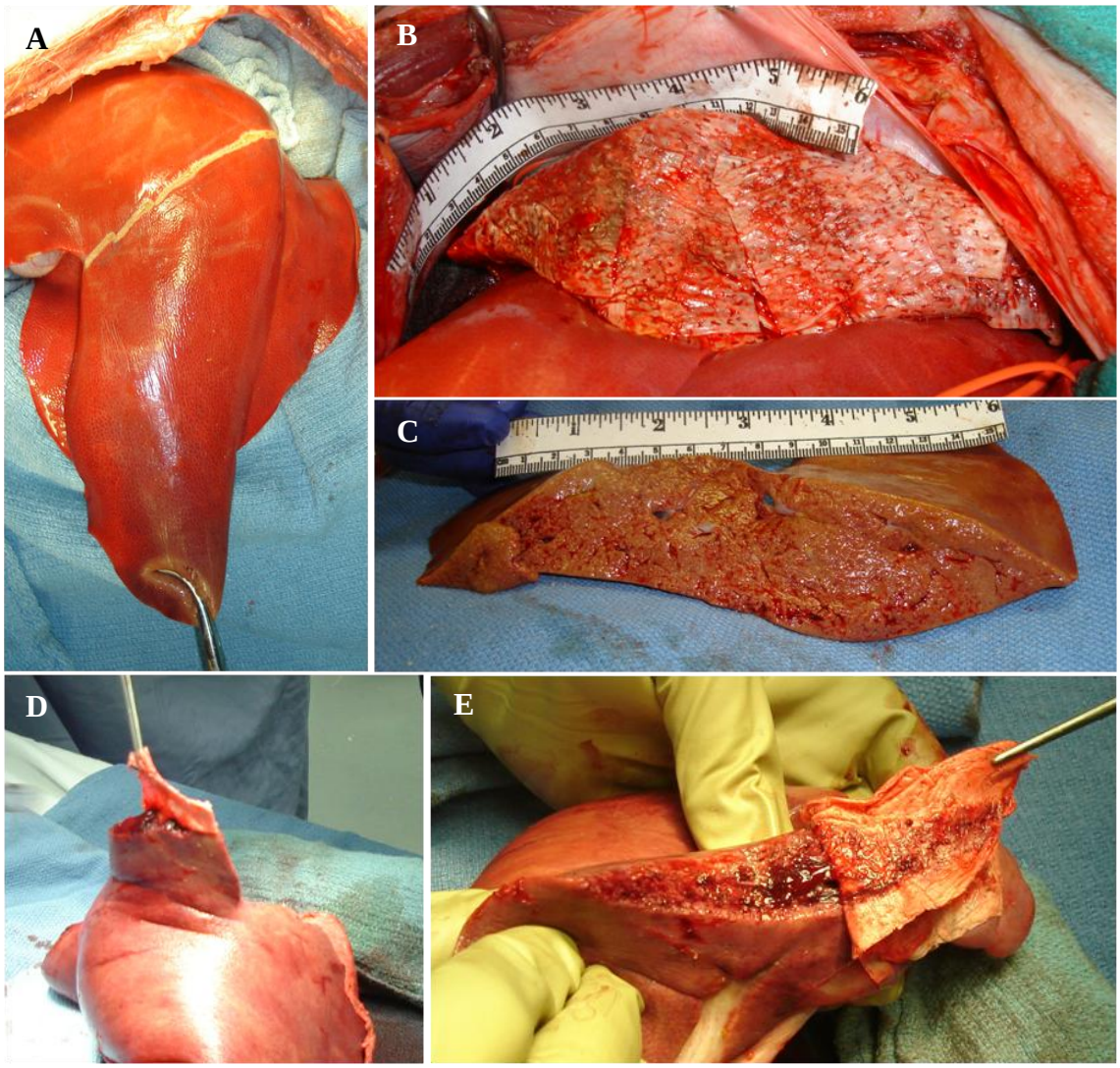

Figure 6.15. Treatment of a large hepatic resection with nanofiberous PDLLA coated with rLFS. The planned resection, consisting of ~25% of the liver mass, was marked by a cauterization tool (A). Following removal, 5 cm x 5 cm nanofiberous PDLLA dressings coated with rLFS were applied to the wound and held for 3 minutes under pressure. When the pressure was removed, the wound was hemostatic (B) despite the presence of large vasculature as visualized in the removed portion of the liver (C). After the surgery, the bandage was removed and the level of adherence evaluated. The adherence was strong enough to lift the liver by the bandage (D). Clot is clearly visible on the surface of the dressing (E).

Dry PDLLA without LFS was also applied to three liver resections resulting in complete hemostasis in one and minor oozing in another. Although these results are similar to that achieved with LFS coated PDLLA, the dressings alone were not as adhered to the wound as those treated with LFS. We also applied larger (10 cm x 5 cm) rather than multiple small dressings coated with LFS; however, both attempts resulted in

minimal hemostasis. The large bandages tended to have creases and were difficult to lay flat on the wound resulting in tunneling of blood under the dressing. Consequently, the dressings failed to adhere to the tissue.

Discussion

Our optimal LFS was tested alone and in combination with a PDLLA dressing on multiple injury models. The LFS was effective in stopping bleeding in wedge resections with shallow depths but failed in deeper cuts. Depths of 2.0 or more centimeters typically had large vasculature at the apex of the wedge (Figure 6.11). The LFS successfully formed a clot over the large vessels; however, the LFS was unable to adhere to the parenchymal tissue surrounding the vessel most likely due to the pressure of the blood pouring out of the vessel. This resulted in significant bleeding from under the clotted layer of LFS. Consequently, LFS can effectively treat oozing tissue and wounds containing small vasculature; however, requires a scaffold when large vessels are present.

Research indicates that the fibrinogen in FS is critical for adhesion and the best results are attained at 40 to 70 mg/ml;[8] however, we achieved good hemostasis with 9 mg/ml as seen in the stelate liver laceration model (Figure 6.12). All of the grade V stelate lacerations resulted in complete hemostasis or only slight oozing which was subsequently stopped by pressure and gauze. Although all of the treatments were considered successful, the best results were achieved with the minimal amount of sealant implying that application is the key. Three of the five resulting in complete hemostasis were treated with 6 ml LFS and the one with two X-shaped wounds that ended in complete hemostasis was treated with 5 ml LFS. Three of the four treatments resulting in

slight oozing were treated with 60 ml of LFS. Hence, the Duploject® and spray device applicators were significantly better than PTI's device which mixed large volumes of FS in a nozzle.

Application with the spray device appears to lower the amount of LFS required to achieve hemostasis. This is probably true because the device focuses the application to a targeted area, judiciously supplies the proteins, and better mixes the two components of the LFS. The spray device was designed for possible uses such as:

1. treating wounds not containing major blood vessels;
2. coating the PDLLA dressing with LFS immediately prior to application;
3. applying LFS to the top of a wound already covered with PDLLA;
4. precoating the wound prior to mesh application.

The spray device has two chambers that keep the rFI/rFXIIIa solution separate from the rFIIa solution until application and can administer as little as 0.5 ml volumes of LFS. Its efficiency is a result of the spray pattern which focuses the spray to a 1 to 3 cm diameter target area without spurious atomization and thoroughly mixes the clotting factors for immediate clot formation.

Our bioengineering paradigm for bandage design focuses on the use of a resorbable mesh to efficiently deliver expensive clotting factors. The use of a dressing in combination with the LFS shifts the burden of the mechanical stabilization of the wound surface to the mesh. Hence, the dressing material withstands the pressure from blood flow while exogenous and endogenous clotting factors need only adhere the dressing to the wound. Macropores, corrugations and roughing of the surface of the PDLLA

dressing were performed in an attempt to enlist endogenous factors in the blood as additional support for the LFS by allowing it to intercolate into the bandage material.

The modifications to the PDLLA are designed to mimic the ability of surgical cotton gauze to intercolate endogenous blood to gain adhesion. This was done by imparting a corrugated and perforated structure to the PDLLA nanofibrous mesh which resulted in the necessary macroporous interstitial space for sufficient blood clot intercolation to achieve adhesion. This was done without increasing the mass of PDLLA mesh. Cotton gauze macroporosity arises from microfilamentous structure and not only has the deficiency of not being resorbable, but has a material mass that is not affordable when translated directly to a PDLLA microfibrous equivalent.

A dressing consisting of dry, lyophilized FI and FIIa on a different backings was evaluated in a femoral arteriotomy (6 mg/cm^2 pdFI, 50 U/cm^2 pdFIIa),[22] ballistic injury (10.29 mg/cm^2 pdFI, 28.57 U/cm^2 pdFIIa, 2.5 mg/cm^2)[4] and Grade V liver injury (15 mg/cm^2 pdFI, 37.5 U/cm^2 pdFIIa, 117 µg/cm^2)[21] models. Under normal, hypothermic and coagulopathic conditions, this bandage was significantly better than gauze with respect to minimizing blood loss and maintaining blood pressure.[4, 22] We have significantly reduced the protein levels on the PDLLA making the dressing more economically feasible. Compared to the grade V liver injury, our LFS contains 97% less FI (0.43 mg/cm^2) and 90% less FIIa (5.07 U/cm^2). Despite significantly reducing the protein content, our LFS successfully aided hemostasis in grade V liver injuries.

Jackson et al. coated a silicone backing with a lyophilized FS which proved significantly more successful in creating hemostasis than the control dressing in a 4 mm femoral arteriotomy model in pigs. Five of six wounds resulted in complete hemostasis

in 15 minutes compared to none of the controls after 60 minutes.[23] Our LFS coated dressing failed to achieve this success. The modified nanofiberous PDLLA succeeded in only 29% of the treatments; however, the microfiberous PDLLA successfully resulted in hemostasis in 75% of treatments. These results were achieved after a five minute hold compared to the 15 minutes in the previous study. We believe our low success rate is due to the limited cross-sectional area for adhesion of bandage. This was supported by our success in achieving hemostasis in large liver resections.

Our success rate significantly increased when treating larger surface areas with LFS coated nanofiberous PDLLA despite the existence of vessels up to 1 cm in diameter. 53.3% of treatments were completely hemostatic and 43.3% mostly hemostatic after a 3 minute hold; however, if pressure was held for 15 minutes, many of the mostly hemostatic results may have been upgraded. The success appeared to be highly dependent on the application technique in large liver laceration. The best results were achieved when a slight amount of blood was allowed to flow through the bandage and pressure was held over the entire length of the wound to ensure adhesion especially around the large blood vessels. Practice typically resulted in better results. When pressure was not held directly over the wound, pockets of blood would form under the bandage. These pockets were frequently hemostatic; however, they typically resulted in lower adhesion of the bandage to the wound. The treatments that continued to ooze were frequently linked to the lifting of the bandage by the blood flow from a major vessel.

Our aim is to create a FS dressing that works under various conditions by untrained personnel; therefore, more work needs to be done to lessen the effect of

application technique. Despite the unreliable performance, 97% of the applications yielded complete or mostly hemostatic results on a lethal injury. Those rated as mostly hemostatic were rendered completely hemostatic by applying pressure and gauze or a second application of LFS coated PDLLA. One application of LFS coated PDLLA on a large resection resulted in complete hemostasis without holding pressure.

Previous research indicates that efficacy of FS depend on the surgical situation and the method and speed of application is critical for success.[37] Our research supports these conclusions. While our LFS alone could successfully achieve hemostasis in some wounds, it required a scaffold in wounds with major vasculature. Our LFS coated dressings were extremely successful in treating grade V hepatic resections; however, was less effective when treating 4 mm femoral arteriotomies. As previously described, the application technique significantly affects results and once the PDLLA is coated with the mixed solutions it must be applied quickly before the LFS clots. Our future objective is to minimize these limitations.

Like the LFS, the PDLLA bandage is early in its design stage. The dressing was designed to provide a strong matrix so that for larger wounds the bandage provides the necessary strength to withstand blood pressure while the LFS stops bleeding through the pores of the bandage and glues the bandage to the wound. It was also designed to encourage tissue regeneration with respect to cell migration and proliferation. Details regarding the design of the bandage including manufacturing process, fiber features, pore sizes and pre-treatments of the material to make it more hydrophilic are proprietary knowledge of LNK Chemsolutions. The degradation rate of the matrix after implantation has not yet been determined; however, it is estimated to be removed within 30 to 60 days.

Future studies will include detailed evaluation of (1) the interaction of the LFS and bandage fibers at the molecular level; (2) the degradation/dissolution rate of the bandage material *in vivo* and effects of byproducts which are anticipated as being minimal; and (3) the rate of remodeling of tissue on the LFS/PDLLA matrix.

The research presented in this chapter is the first report of the use of a fully-recombinant LFS used alone or in combination with a bioresorbable dressing. We also designed and tested a prototype airbrush-based spray device for LFS application and compared it to a pressurized air canister and the typical dual syringe applicator. Stelate liver lacerations, major lobe resections and some of the larger wedge resections included extensive tissue and vascular damage; however, our optimal LFS successfully achieved hemostasis in a significant number of the wounds. LFS applied without the assistance of a dressing was able to stop bleeding of oozing wounds or those with small vessels; however, a scaffold was needed when wounds contained large vasculature. Although the results presented in this chapter are promising, more research needs to be conducted to develop the best LFS application device and dressing that optimizes hemostatic results but is not dependent on the experience of the applicator.

Acknowledgements

I am incredibly grateful to Dr. Mark Carlson, Dr. Iraklis Pipinos, Dr. John Cavanaugh and Dr. Jason Johanning who performed all of the surgeries. I would also like to thank Chris Hansen, Dr. Crystal Cordes and Dr. Dean Heimann for all of their help during surgical procedures. I appreciate all of Dr. Carlson's work in scoring hemostasis and compiling surgical results. I would also like to thank Dr. Gustavo Larsen,

Dr. Ruben Spretz and Dr. Sandra Noriega from LNK Chemsolutions for providing all of the bandage material and early versions of a LFS spray device. Leonard Akert and Mostafa Fatemi designed and built the airbrush-based spray device. Leonard Akert also made the bed of nails and corrugated plates used to alter the bandage material. Dr. Wilson Burgess and PTI Technologies provided us with the can spray device. This work was supported by a grant from the Department of Defense titled "Production and Purification of Fibrinogen Components for the Production of a Fibrin Sealant Hemostatic Dressing."

References

1. Stewart, R.M. et al. Seven hundred fifty-three consecutive deaths in a level I trauma center: the argument for injury prevention. *J Trauma* **54**, 66-70; discussion 70-61 (2003).
2. Bellamy, R.F., Maningas, P.A. & Vayer, J.S. Epidemiology of trauma: military experience. *Ann Emerg Med* **15**, 1384-1388 (1986).
3. Anderson, R.N. & Smith, B.L. Deaths: leading causes for 2001. *Natl Vital Stat Rep* **52**, 1-85 (2003).
4. Holcomb, J. et al. Efficacy of a dry fibrin sealant dressing for hemorrhage control after ballistic injury. *Arch.Surg.* **133**, 32-35 (1998).
5. Pusateri, A.E. et al. Effect of a chitosan-based hemostatic dressing on blood loss and survival in a model of severe venous hemorrhage and hepatic injury in swine. *J Trauma* **54**, 177-182 (2003).
6. Gibble, J.W. & Ness, P.M. Fibrin glue: the perfect operative sealant? *Transfusion* **30**, 741-747 (1990).
7. Sierra, D.H. Fibrin sealant adhesive systems: a review of their chemistry, material properties and clinical applications. *J.Biomater.Appl.* **7**, 309 (1993).
8. Amrani, D.L., Diorio, J.P. & Delmotte, Y. Wound healing: Role of commercial fibrin sealants. *Ann.N.Y.Acad.Sci.* **936**, 566 (2001).
9. Jackson, M.R. Fibrin sealants in surgical practice: An overview. *Am.J.Surg.* **182**, 1S (2001).
10. Laurens, N., Koolwijk, P. & De Maat, M.P.M. Fibrin structure and wound healing. *Journal of Thrombosis and Haemostasis* **4**, 932 (2006).
11. Lee, M.-G.M. & Jones, D. Applications of fibrin sealant in surgery. *Surg Innov* **12**, 203 (2005).
12. Schwartz, M.L., Pizzo, S.V., Hill, R.L. & McKee, P.A. Human factor XIII from plasma and platelets. Molecular weights, and subunit structures, proteolytic activation, and crosslinking of fibrinogen and fibrin. *J.Biol.Chem.* **248**, 1395 (1973).
13. Folk, J.E. & Finlayson, J.S. The e-(g-glutamyl)lysine crosslink and the catalytic role of transglutaminases. *Adv.Protein Chem.* **31**, 1 (1977).
14. McDonagh, J.M. in Hemostasis and Thrombosis: Basic Principles and Clinical Practice, Edn. Third Edition. (eds. R.W. Colman, J. Hirsh, V.J. Marder & E.W. Salzman) 301 (J.B. Lippincott Company, Philadelphia; 1994).
15. Standeven, K.F. et al. Functional analysis of fibrin g-chain cross-linking by activated factor XIII: determination of a cross-linking pattern that maximizes clot stiffness. *Blood* **110**, 902 (2007).
16. Greenberg, C.S. & Shuman, M.A. Specific binding of blood coagulation factor XIIIa to thrombin-stimulated platelets. *J.Biol.Chem.* **259**, 14721 (1984).
17. Chandler, W.L. et al. Factor XIIIA and clot strength after cardiopulmonary bypass. *Blood Coagulation Fibrinol.* **12**, 101 (2001).
18. Crawley, J.T.B., Zanardelli, S., Chion, C.K.N.K. & Lane, D.A. The central role of thrombin in hemostasis. *Journal of Thrombosis and Haemostasis* **5**, 95 (2007).
19. Mankad, P.S. & Codispoti, M. The role of fibrin sealants in hemostasis. *Am.J.Surg.* **182**, 21S (2001).

20. MacGillivray, T.E. Fibrin sealants and glues. *J.Card.Surg.* **18**, 480 (2003).
21. Holcomb, J.B. et al. Effect of dry fibrin sealant dressings versus gauze packing on blood loss in grade V liver injuries in resuscitated swine. *J Trauma* **46**, 49-57 (1999).
22. Larson, M.J., Bowersox, J.C., Lim, R.C., Jr. & Hess, J.R. Efficacy of a fibrin hemostatic bandage in controlling hemorrhage from experimental arterial injuries. *Arch.Surg.* **130**, 420 (1995).
23. Jackson, M.R. et al. Hemostatic efficacy of a fibrin sealant-based topical agent in a femoral artery injury model: a randomized, blinded, placebo-controlled study. *J.Vasc.Surg.* **26**, 274 (1997).
24. Holcomb, J.B. et al. Dry fibrin sealant dressings reduce blood loss, resuscitation volume, and improve survival in hypothermic coagulopathic swine with grade V liver injuries. *J Trauma* **47**, 233-240; discussion 240-232 (1999).
25. Jackson, M.R. Tissue sealants: current status, future potential. *Nat Med* **2**, 637-638 (1996).
26. Miyamoto, H. et al. Fibrin glue and bioabsorbable felt patch for intraoperative intractable air leaks. *Jpn J Thorac Cardiovasc Surg* **51**, 232-236 (2003).
27. Clark, W.R., Jr. & Leather, R.P. Hemostasis during liver resections. *Surgery* **67**, 556-557 (1970).
28. Hirshberg, A., Wall, M.J., Jr., Ramchandani, M.K. & Mattox, K.L. Reoperation for bleeding in trauma. *Arch.Surg.* **128**, 1163-1167 (1993).
29. Hoyt, D.B. et al. Death in the operating room: an analysis of a multi-center experience. *J Trauma* **37**, 426-432 (1994).
30. Moore, E.E. et al. Organ injury scaling: spleen and liver (1994 revision). *J Trauma* **38**, 323-324 (1995).
31. Cue, J.I., Cryer, H.G., Miller, F.B., Richardson, J.D. & Polk, H.C., Jr. Packing and planned reexploration for hepatic and retroperitoneal hemorrhage: critical refinements of a useful technique. *J Trauma* **30**, 1007-1011; discussion 1011-1003 (1990).
32. Feliciano, D.V., Mattox, K.L., Burch, J.M., Bitondo, C.G. & Jordan, G.L., Jr. Packing for control of hepatic hemorrhage. *J Trauma* **26**, 738-743 (1986).
33. Hirshberg, A. & Walden, R. Damage control for abdominal trauma. *Surg Clin North Am* **77**, 813-820 (1997).
34. Berrevoet, F. & de Hemptinne, B. Use of Topical Hemostatic Agents during Liver Resection. *Dig.Surg.* **24**, 288 (2007).
35. Inan, M. et al. Saturation of the secretory pathway by overexpression of a hookworm (Necator americanus) protein (Na-ASP1). *Methods in Molecular Biology (Totowa, NJ, United States)* **389**, 65 (2007).
36. Zhang, W., Inan, M. & Meagher, M.M. Rational design and optimization of fed-batch and continuous fermentations. *Methods in Molecular Biology (Totowa, NJ, United States)* **389**, 43 (2007).
37. Clark, R.A.F. Fibrin glue for wound repair: Facts and fancy. *Thromb.Haemost.* **90**, 1003 (2003).

Chapter 7

Biologically Active Single Chain Recombinant Human FVIII:von Willebrand Factor Complexes Made Abundantly in Transgenic Milk

Steven W. Pipe,[1] Hongzhi Miao,[1] Stephen P. Butler,[2] Jennifer Calcaterra,[3] and William H.Velander[3]

[1] Department of Pediatrics, University of Michigan, Ann Arbor, MI
[2] Department of Dairy Science, Virginia Polytechnic Institute and State University, Blacksburg, VA
[3] Department of Chemical & Biomolecular Engineering, University of Nebraska – Lincoln

Abstract

Recombinant factor VIII (rFVIII) therapy for Hemophilia A has proven to be safe and efficacious. However, rFVIII is produced by mammalian cell culture at low levels similar to blood plasma which cannot satisfy the future global demand for prophylactic and other optimal therapies. The milk of transgenic livestock may be the most cost effective and prodigious production vehicle for achieving that future goal. Prior to this study, FVIII expressed in mouse, rabbit, and pig milks was largely inactive. For the first time, we report the expression of a bioengineered FVIII together with von Willebrand Factor (vWF) in milk (FVIII-tg). FVIII-tg was produced by the mammary gland at >600-fold higher activity levels than human plasma and >450-fold higher than reported for cell culture. FVIII-tg had biological activity similar to commercial rFVIII and showed similar binding avidity to plasma-derived vWF which is a prerequisite for stability when in circulation. The intravenous infusion of immunopurified FVIII-tg rendered normal hemostasis to hemophilia A mice in response to tail transection. Importantly, this work in transgenic mice serves as a basis for the translational development of rFVIII produced by transgenic pigs.

Introduction

Hemophilia A is an X-linked, inherited disorder of blood coagulation primarily caused by deficiency or dysfunction of factor VIII (FVIII) that affects approximately one in every 5,000-10,000 males.[1-3] Currently, hemophilic patients are treated with intravenous infusion of highly purified FVIII concentrates derived from donor human plasma or a variety of recombinantly-derived FVIII (rFVIII) produced by animal cells such as Chinese hamster ovary (CHO) cells in large scale bioreactors.[4-6] Aggressive prophylactic FVIII replacement therapy reduces hemarthroses[7] and this has become the standard of care for the management of pediatric patients with severe hemophilia and is now also showing benefits in adult patients. However, to achieve this level of prophylactic replacement therapy requires greater than $100,000 USD per patient per year.[8] Despite the clear benefits of prophylactic therapy in this population, 80% of the world hemophilia population does not receive adequate access to replacement therapy. Many factors contribute to this, but a lack of abundance and associated costs of current production of plasma-derived FVIII and rFVIII concentrates, preclude the application of universal prophylactic treatment of hemophilia A in even the most economically developed countries and routine access in developing countries.[1, 4, 5]

The commercial manufacturing of FVIII from blood plasma and rFVIII from animal cell culture are both greatly and similarly inefficient. This is primarily due to limitations in the biosynthetic pathway of rFVIII which have been well detailed in mammalian expression systems.[9-11] This pathway is inhibited at transcription,[12-14] post-translational modification and translocation from the endoplasmic reticulum to the Golgi apparatus.[9, 15] While wild-type (WT)-FVIII is expressed in animal cell culture at <1

unit/ml, the co-expression of von Willebrand Factor (vWF) greatly stabilizes and increases the accumulation of secreted WT-FVIII activity and is commercially used to produce rFVIII. Alternatively, we and others have previously reported on the ability of the mammary gland to express rFVIII in the milk of transgenic mice,[16] rabbits,[17, 18] sheep[19] and pigs[20] (Table 7.1). Using milk avails the mammary gland's high cell density of about 10^9 epithelial cells per ml of luminal volume relative to the much lower 5×10^6 animal cells per ml of the classical bioreactor [21]. However, while WT-FVIII was made in milk at 600-fold greater concentration than blood plasma or animal cell culture, the specific activity of the rFVIII was very low at about 2 to 10% of expected.[16, 17, 20] Analysis suggests that the markedly reduced specific activity was a consequence of the instability of rFVIII expressed in milk, especially in the absence of vWF.

Table 7.1. A comparison of expression levels and activity of WT-FVIII made in plasma, cell culture and milk of transgenic animals.

Source*	WT-FVIII Concentration (µg/ml)	Activity Level (IU/ml)	Specific Activity (IU/mg)
Human plasma[3]	0.2	1	5,000
COS-1 in cell culture[10]	0.026	0.125	4,800
Dual vWF/FVIII transfected CHO cell culture	N/A	1.397[9]	>4,000[22]
Milk of Transgenic Mice[16]	50.21	13.41	267
Milk of Transgenic Rabbits[17]	117	0.521	4.5
Milk of Transgenic Pigs[20]	2.66	0.62	233
Milk of Transgenic Sheep[19]	0.006	N/A	N/A

* The highest expression levels of WT-FVIII reported from references provided. N/A: not available.

As a fundamental precursor to large-scale production in transgenic livestock, we show for the first time that fully biologically active, single chain rFVIII can be secreted into the milk of transgenic mice while at >450-fold activity levels than previously reported with WT-FVIII in animal cell culture. First, we utilized a novel bioengineered

form of rFVIII with demonstrated high secretion efficiency (226/N6) yielding >10-fold improved expression over B domain-deleted FVIII and WT-FVIII.[15]. This particular form of rFVIII is expressed in mammalian cells as a single chain molecule with high efficiency due to improved mRNA expression, improved ER-Golgi transport, and reduced cellular ER stress.[23] Secondly, we further enhanced the stability of FVIII within the milk environment by co-expression of vWF and alpha-1 antitrypsin (AAT). This is the first report of FVIII and vWF coexpression in transgenic animals.

Materials and Methods

DNA constructs

The WAP7FVIII 226/N6 construct was assembled by altering the Kpn I site of pUCWAP6[24] by the addition of linkers that introduced a Sal I site immediately downstream of the 4.1 kbp WAP (whey acidic protein) promoter and in front of 1.7 kbp of mouse WAP 3' UTR that contains the coding of the polyadenylation signal to produce pUCWAP7. The sequence for 226/N6 was removed by restriction enzyme digest using Sal I and Xho I from $pMT_2$226/N6 described previously.[15] This fragment was introduced into the Sal I site of pUCWAP7 and ligated. The resulting plasmid, pUCWAP7FVIII-226/N6, was digested with Not I to release the expression construct (WAP7FVIII-226/N6) that was separated by agarose gel electrophoresis.

The plasmid pUCWAP6vWF containing the WAP6vWF expression construct was a gift from Dr. Henryk Lubon, (American Red Cross, Rockville, MD). This plasmid contained the cDNA for vWF placed between the 4.1 kbp WAP promoter and the 1.7 kbp 3'UTR. Removal of the WAP6vWF expression construct was achieved by digesting the

plasmid with Not I and Sfi I followed by agarose gel electrophoresis. The plasmid designated PPL456 containing the BLG (beta lactoglobulin) driven AAT construct was a kind gift from Dr. David Ayares (Revivicor, Blacksburg, Virginia). This construct has been previously described in detail.[25] The expression construct (BLG-AAT) was removed from plasmid elements by digest with restriction enzymes Not I and Sal I followed by agarose gel electrophoresis. All released fragments were purified by extraction prior to microinjection using a Nucleospin Extract kit (Clonetech Laboratories, Inc. Palo Alto, CA).

Generation and identification of transgenic mice

Transgenic mice were generated by pronuclear microinjection of purified DNA constructs through the Transgenic Core facility at the University of Michigan. Briefly, purified DNA was microinjected into fertilized eggs obtained by mating (C57BL/6 x SJL)F1 or C57BL/6 female mice with (C57BL/6 x SJL)F1 male mice. Pronuclear microinjection was performed as previously described.[26] PCR primer pairs were: for WAP7FVIII-226/N6, WAPS2 (ctgtgtggccaagaaggaagtttg)/FVIIIA2 (ccttggcttagcgatgttga); for WAP6vWF, WAP150 (gctctctctgtgtggccaag)/vWFA1 (ttccttctgcacaaagggtc); for AAT construct, BLG-S1 (ctggctctgacctgtccttg)/AATa1 (atcgtgagtgtcagccttgg).

Southern analysis was performed on select mice to confirm PCR results and evaluate transgene ratio and copy number. Mouse DNA (10 μg) was digested with EcoRI and Hind III and subjected to agarose gel electrophoresis. Probes were produced by biotin incorporation via PCR using the KPL Detector DNA biotinylation kit (KPL, Inc. Gaithersburg, Maryland). PCR primers are as follows: for WAP, WAPprobeS1

(gcatgctcacactcaacagg)/ WAPprobeA1 (taagagtgtggaggcgcttg); for AAT, same primers as for PCR, BLG-S1/AAT-A1. Size of each probe is approximately 500 bp. Blocking and detection was performed per manufacturer's instructions using a KPL Detector AP chemiluminescent blotting kit followed by exposure to film.

Mouse milk collection and preparation

Milk collection was done as previously described[26]. Briefly, naturally lactating females were separated from their pups for a period of 1 to 3 hours, then anesthetized with 0.2 to 0.4 ml of Avertin given IP. After becoming anesthetized, animals were then given 2 IU of oxytocin IM in the hind leg. After 30 seconds each gland was massaged to express milk then milk was collected into a 1.5 ml microcentrifuge tube by vacuum aspiration through a small heat-polished glass capillary tube. Samples were stored at -70^{o}C.

Factor VIII Biochemical Analysis

Samples were thawed at 37 ^{0}C, immediately placed on ice, diluted 1:10 using PBS buffer and centrifuged at 10,000 rpm for 10 minutes. The upper lipid layer was removed and the supernatant analyzed. FVIII ELISA was purchased from Affinity Biologicals Inc. (Ancaster, ON, Canada). FVIII deficient plasmas and FACT (normal human pooled plasma) were purchased from George King Bio-Medical Inc. (Overland Park, Kansas). FVIII activity was measured by 1) one-stage aPTT clotting assay on an MLA Electra 750 fibrinometer by reconstitution of human FVIII-deficient plasma or 2) by modified two-stage assay utilizing the COAMATIC Factor VIII (Chromogenix, Milano, Italy) according to the manufacturer's instructions. The ELISA activity assay standard curves

assumed a FVIII concentration of 200 ng/mL antigen (1 IU/mL) of activity. The ELISA assays on milk samples were sensitive to 0.02 μg FVIII/ml. Chromogenic FVIII activity measurements were sensitive to 0.05 IU/ml in milk.

Immunoaffinity chromatography purification of FVIII from transgenic mouse milk

Supernatant of pretreated milk samples were pooled and passed through a 0.2 um filter. After incubating transgenic mouse milk (diluted to 50 ml with TBS) with F8-conjugated sepharose beads overnight, the sample and beads were packed into a 50 ml/1.5 cm diameter column. The purification procedure was carried out according to the protocol described previously.[27] 226/N6-CHO protein was purified from stably-transfected Chinese hamster ovary (CHO) cell lines as described previously.[15]

Western Blots

Nonreduced and reduced samples were evaluated by sodium dodecyl sulfate polyacrylamide (SDS-PAGE) gel electrophoresis on 4-12% NuPage® Bis-Tris gels (Invitrogen Carlsbad, CA). Blots were probed for FVIII with a sheep anti-human FVIII polyclonal antibody (USBiological, F0016-10, Swampscott, MA) primary antibody and a donkey anti-sheep IgG peroxidase conjugate secondary antibody (Sigma, A3415, St. Louis, MO). Blots were probed for vWF with a goat anti-human vWF peroxidase conjugated polyclonal antibody (USBiological, V2700-04B, Swampscott, MA). Blots were probed for AAT with a rabbit anti-human α1-antitrypsin polyclonal antibody (USBiological, A2298-27H, Swampscott, MA) primary antibody and a goat anti-rabbit IgG peroxidase conjugate secondary antibody (Sigma, A9169, St. Louis, MO).

FVIII-vWF binding ELISA

Immulon 4HBX plates (Fisher Scientific, Pittsburgh, PA) were coated with anti-FVIII antibody (F8C-EIA-C, Affinity Biologicals) overnight at 4^0C diluted 1:100 in 0.05 M sodium carbonate/bicarbonate, pH 9.6. Protein samples were diluted in TBST (50 mM Tris-HCl, pH 7.6, 150 mM NaCl, 0.05% Tween 20), 3% BSA, 1% FVIII-deficient human plasma(George King Bio-Medical) in 1.5 mL microcentrifuge tubes, and incubated for 2 hours at 37^0C. Wells were washed with TBST containing 10mM $CaCl_2$ four times. Samples were loaded into wells and incubated for 2 hours. Wells were washed four times, and anti-vWF antibody conjugated with HRP (p0266, Dako, Carpenteria, CA) was diluted 1:1000 with TBST, and incubated for 2 hours at 37^0C or overnight at 4^0C. After four washes with TBST with 10mM $CaCl_2$, O-phenylenediamine dihydrochloride substrate (SIGMAFAST OPD, Sigma) was added and the reaction was stopped by 2.5 M H_2SO_4. Absorbance was read at 490 nm.

In vivo tail clip assay in the hemophilia A mouse

Hemophilia A mice (exon 16 knockout)[28] were subjected to a tail clip bleeding assay. Mice of at least 10 weeks age were injected with purified FVIII proteins 226/N6-tg or 226/N6-CHO-FVIII. C57BL/6 and hemophilia A mice littermates were used as controls for injection with lactated Ringer's solution. Mice were injected with 80IU/kg body weight of the FVIII proteins in 100 μl lactated Ringer's solution via tail vein. Ketamine 85 mg/kg with xylazine 5 mg/kg was injected IP to induce anesthesia. After 5 minutes, the tails of mice were cut 1.5 mm from tail tips. The tails were then immediately submerged into 14 ml conical tubes filled with saline at 37^0C. Blood from the tail was

collected 10 minutes. Weights of the tubes at time 0 and 10 minutes were measured and the difference used to quantify blood lost. Mice were euthanized after the procedure.

Results

Identification and expansion of transgenic lineages

The aim of this study was to characterize the properties of single chain rFVIII made in the milk of the highest expressing lineages prior to trialing in transgenic pigs. In particular, we have assessed the secretion limitations, biological activity and stability of 226/N6 in milk. We focused our lineage expansion on a single trigenic and two bigenic lineages which expressed 226/N6-tg at 100-fold higher levels than other lineages: bigenic for 226/N6 and AAT (875 and 406) and trigenic for 226/N6, AAT and vWF (415). Transgenic mouse lineages were detected by Southern analysis after screening DNA isolated from tail biopsy using PCR. Figure 7.1A shows the schematics for the three constructs used: WAP7FVIII-226/N6, WAP6vWF, and BLG-AAT. The PCR 5' and 3' oligonucleotide primer sites and restriction endonuclease cleavage sites used for Southern analysis are indicated. Most mono-, bi- and trigenic lineages contained multiple copies of the FVIII, and/or VWF, and/or AAT transgenes, respectively. A typical Southern Blot used to simultaneously detect and ascertain the copy number of the WAP7FVIII-226/N6 and WAPvWF transgenes is shown in Figure 7.1B. The probe DNA was derived from the mouse WAP promoter and was designed to detect not only the FVIII and vWF transgenes but also the endogenous WAP gene as an internal standard present at two copies per mouse genome. For example, band sizes were present in the DNA of trigenic 415 mice (Lane 3) corresponding to 10 copies of the 2.4 kbp WAP72FVIII-226/N6, and 3

copies of the 4.5 kbp WAP6vWF relative to the 7.2 kbp endogenous WAP gene. The presence of the BLG-AAT transgene was confirmed by the use of the BLG-AAT cross junction probe (separate Southern analysis, data not shown). All lineages studied contained greater than one copy of BLG-AAT transgene per genome. The estimated copy numbers for the highest 226/N6-tg expressers of bigenic mouse lineages were: 2 and 4 copies of WAP7FVIII-226/N6 for Line 406 (Lane 1) and Line 875 (Lane 3), respectively and >1 copy for BLG-AAT. In each lineage, the BLG-AAT transgene was likely co-integrated into the same chromosomal loci along with WAP7FVIII-226/N6 as evidenced by the Mendelian co-transmission of both transgenes through F1 and F2 generations that were made by out breeding with wild-type mice (data not shown).

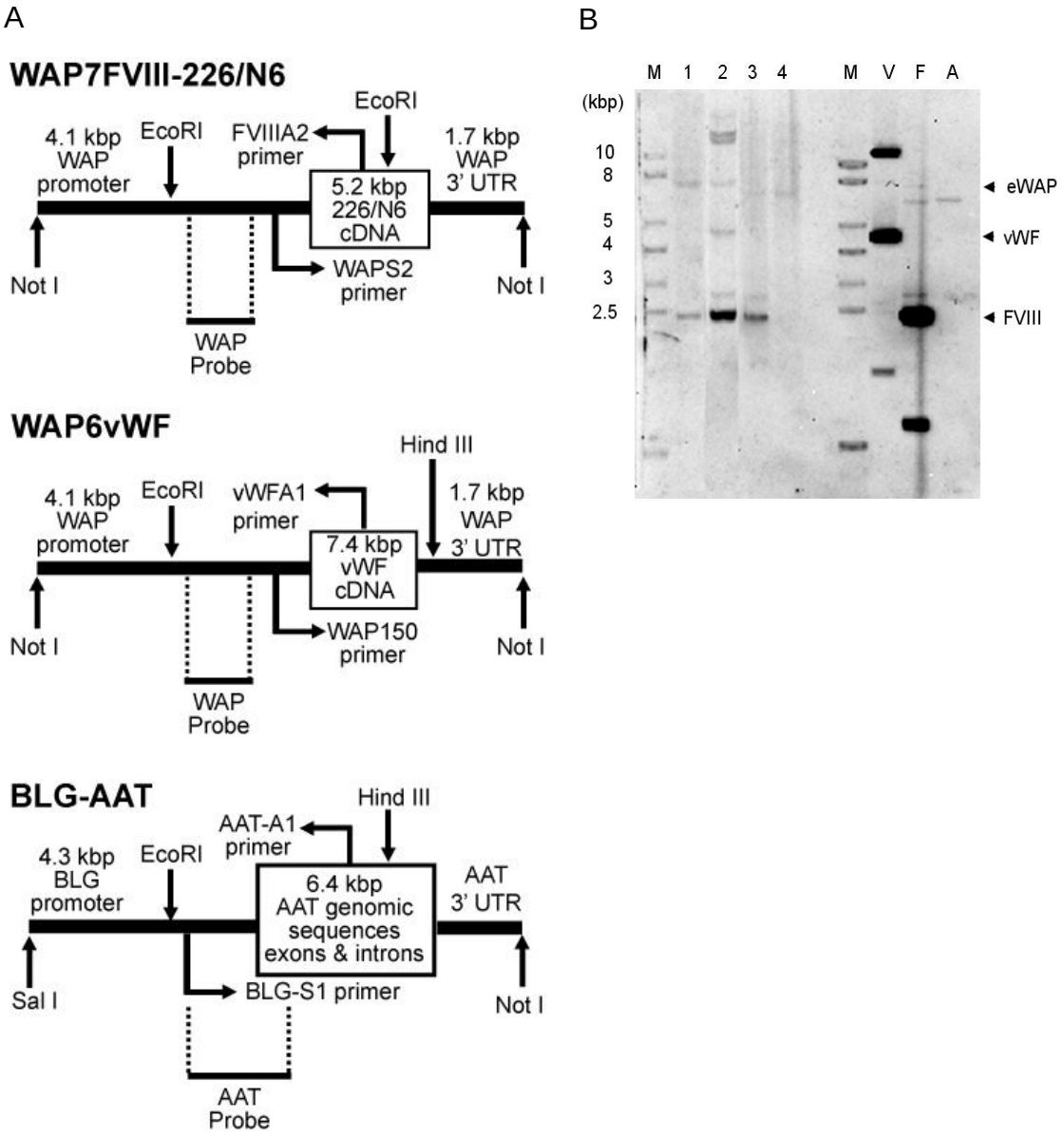

Figure 7.1. Transgene construction schematics and Southern analysis for 226/N6, vWF, and AAT. (A) Schematics for transgenic constructs WAP7FVIII-226/N6, WAP6vWF and BLG-AAT are presented. Restriction sites (vertical arrows) used for Southern analysis and oligomeric DNA primer binding hybridization sites (horizontal lines and arrows) used for PCR detection of the transgenes are shown. (B) Isolated genomic mouse DNA from three highest 226/N6 expressing lineages was digested with EcoRI/Hind III and probed with a WAP promoter probe. Expected fragments sizes are: WAP7FVIII-226/N6: 2.4 kbp; WAP6vWF: 4.5 kbp; and endogenous mouse WAP gene: 7.2 kbp. Sample loading is as follows: M = molecular weight marker, lane 1-4, 406 mouse (bigenic for 226/N6 and AAT), 415 mouse (trigenic for 226/N6, vWF and AAT), 875 mouse (bigenic for 226/N6 and AAT) and non-transgenic control. Reference DNAs: column V = 50 copies/genome WAP6vWF, column F = 50 copies of WAP7FVIII 226/N6 and column A = 50 copies of BLG-AAT. Molecular weight markers are listed on the left and restriction digest product band designation is on the right: band eWAP = endogenous mouse WAP gene; vWF = WAP6vWF; FVIII = WAP7FVIII-226/N6.

Coexpression of 226/N6-tg, vWF-tg and AAT-tg in trigenic mouse milk

We used comparative Western blot analysis of SDS-PAGE under non- and reducing conditions to determine the extent of complexation and underlying proteolysis, respectively. Reducing conditions disrupt both FVIII-vWF complexes and the disulfide bridges linking vWF subunits. Reduced Western blots probed with anti-human FVIII polyclonal antibody are shown in Figure 7.2A. Commercial rFVIII (Recombinate, Baxter, Deerfield, IL) (Lane 2) shows typical heterogeneity due to proteolytic fragmentation of the B domain resulting in variably sized heavy chains of M_r 120 to 180 kDa. In contrast, plasma-derived FVIII-vWF complex (CSL Behring, King of Prussia, PA) (Lane 3) shows less FVIII proteolysis and has a predominant species of M_r 280 kDa. A sample pool from milks collected on different days from the highest expressing trigenic mouse lineage (415; Lane 4) shows a predominant species at M_r 190 kDa and lesser species at about M_r 140 kDa. The theoretical molecular weight of 226/N6 is about 190 kDa. Samples from the highest expressing bigenic 226/N6-tg:AAT-tg mice showed a similar profile to Lane 4 (data not shown). The non-transgenic mouse milk pool (Lane 5) shows no signal.

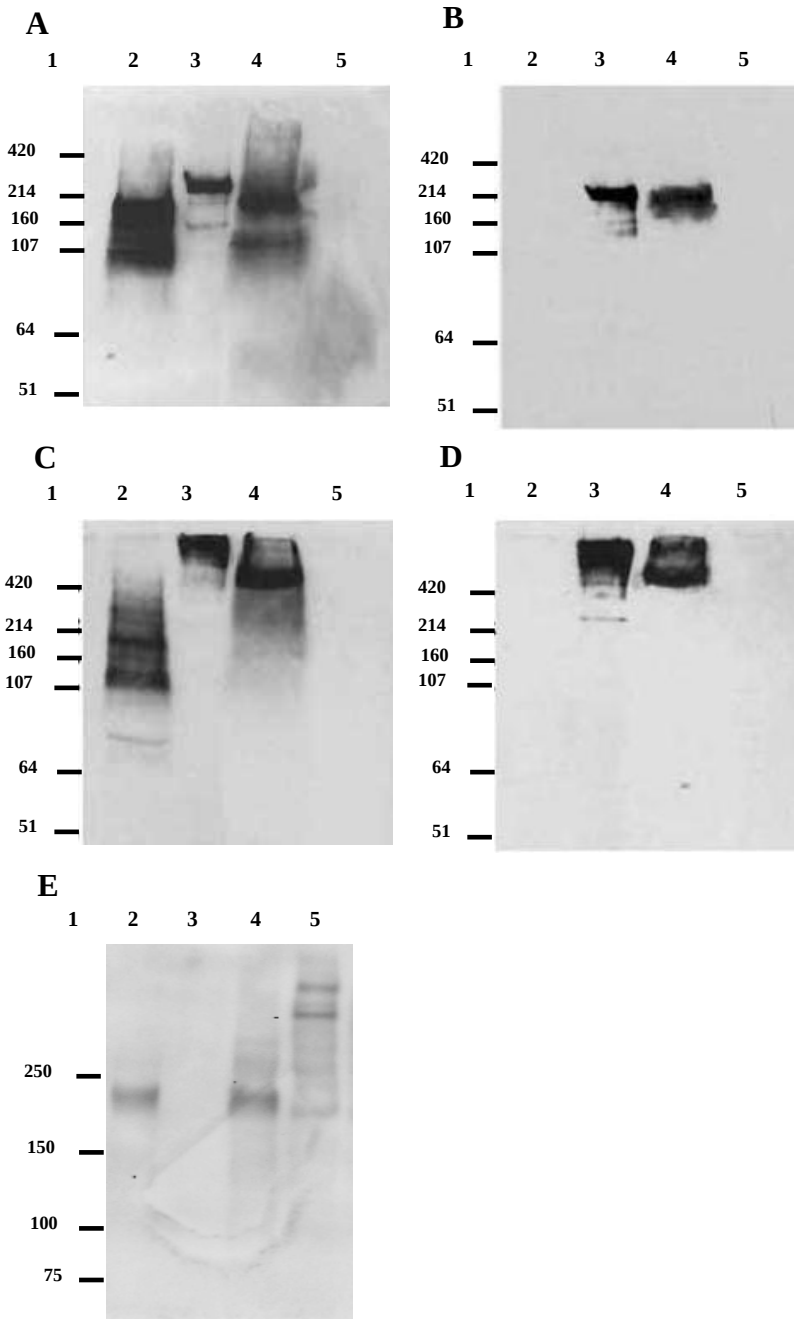

Figure 7.2. 226/N6-tg is complexed with vWF-tg in transgenic mouse milk. Assessment of vWF binding by analyzing (A) reduced anti-FVIII, (B) reduced anti-vWF, (C) non-reduced anti-FVIII, and (D) non-reduced anti-vWF Western Blots. All blots contain a molecular weight marker (lane 1), Commercial rFVIII (lane 2), commercial pd-FVIII:vWF concentrate (lane 3), 226/N6-tg mouse milk (lane 4), non-transgenic mouse milk (lane 5). A non-reduced anti-FVIII Western Blot was performed to analyze nonspecific binding of mouse milk proteins to 226/N6-tg and immunopurified 226/N6-CHO (E): molecular weight marker (lane 1), 226/N6-CHO (lane 2), non-transgenic mouse milk (lane 3), 226/N6-CHO added to non-transgenic mouse milk (lane 4), and 226/N6-tg:vWF-tg trigenic mouse milk (lane 5).

Anti-vWF Western analysis under reducing conditions is shown in Figure 7.2B. No vWF signal is observed in the rFVIII and non-transgenic mouse milk pool (Lanes 2 and 5, respectively). The reference plasma-derived FVIII-vWF concentrate shows a sharp, single band signal at about M_r 270 kDa (Lane 3) consistent with all VWF species existing as monomeric units that are disassociated from FVIII under reducing conditions. The trigenic milk pool sample shows a similarly strong band at about M_r 270 kDa (Lane 4). The approximate stoichiometric ratio of 226/N6-tg to vWF-tg subunits in the milk of trigenic lineage 415, as evidenced by Western blot, was estimated to be about 1:1. This in turn was further corroborated by FVIII (Table 7.2) and vWF ELISA (data not shown) quantitation.

Table 7.2. ELISA, 2-stage activity assay, and specific activity data on mono-, bi- and trigenic mice.

226/N6 Source	Mouse ID	226/N6 Concentration (μg/ml)	Activity Level (IU/ml)	Specific Activity (IU/mg)
Monogenic mice: 226/N6				
	1960-1702	0.144	0.621	4,313
	1926-1742	0.093	0.121	1,301
	46-1247	0.066	0.392	5,939
Bigenic mice: 226/N6-AAT				
	875-234	34	25	735
	875-233	6.2	44	7,097
	516-45	7.3	13	1,781
	406-128-10	83	122	1,470
Trigenic mice: 226/N6-vWF-AAT				
	415-101-2	183	678	3,705
	415-101-1-2	14.5	555	4,549

Presence of FVIII-vWF complexes in trigenic mouse milk.

This is the first report of vWF being co-expressed with FVIII in milk and also the first study of vWF complexation with 226/N6. Based upon the stability introduced to rFVIII by rvWF in cell culture,[29] we sought a similar effect on FVIII in milk. We found that native, plasma-derived FVIII:VWF complexes exist within monomeric and higher

molecular weight vWF species under non-reducing, SDS-treatment conditions. Similar to plasma-derived vWF, vWF-tg is expressed in milk as monomers and also higher molecular weight species that likely represent multimers consisting of monomers linked by disulfide bridges. For example, Western analysis for FVIII-VWF concentrate shows FVIII and vWF band signals within a similar M_r range that are both >420 kDa (Figure 7.2, lanes 3 of Panels C and D, respectively) due to co-migration caused by the complexes. Conversely, the reference commercial rFVIII that is devoid of vWF has a similarly broad pattern as occurs under reducing conditions with an upper M_r limit less than 280 kDa (Figure 7.2, Panel C, Lane 2). Congruently, rFVIII shows no signal for vWF (Figure 7.2, Panel D, Lane 2). The trigenic mouse milk pool shows a predominant band near M_r 420 kDa and another minor band at a much higher M_r (Figure 7.2, Panel D, Lane 4) that is similar to the reference plasma-derived FVIII-vWF concentrate (Figure 7.2, Panel D, Lane 3). This is consistent with a major population of 226/N6-tg complexed with monomeric vWF-tg at M_r 450 kDa and a higher band due to complexing with multimeric vWF-tg species. The high avidity of this complex is underscored by the apparent absence of free 226/N6-tg under these conditions.

We did not observe nonspecific binding of milk proteins with 226/N6-tg in transgenic milk or with 226/N6-CHO added to control mouse milk by using non-reduced Western analysis (Figure 7.2, Panel E). Immunopurified 226/N6-CHO was made in CHO cells without co-expression of vWF and it migrates as a single band at M_r 190 kDa (Lane 2). When incubated with non-transgenic mouse milk, 226/N6-CHO still consisted of a single band at 190 kDa (Lane 4). This suggests that it does not form strong complexes

with endogenous mouse milk proteins as does 226/N6-tg with coexpressed vWF (Lane 5).

Coexpression of AAT

The presence of serine proteases in milk such as plasmin and trypsin has been well documented [39,40]. This BLG-AAT transgene was chosen because biologically active rAAT has been previously and consistently produced at greater than 1000 μg/ml in the milk of transgenic mice and sheep. Figure 7.3 shows the nonreduced, Western Blot analysis of SDS-PAGE using detection by a polyclonal anti-AAT antibody. The AAT-tg was expressed at much higher levels than either 226/N6-tg or vWF-tg and estimated to be >1000 μg/ml.

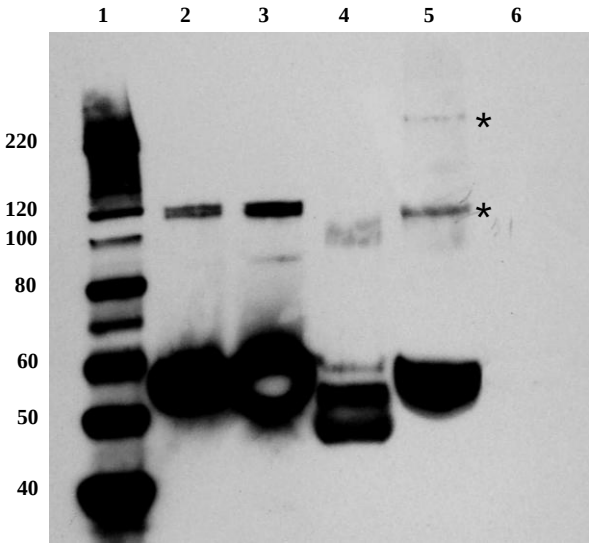

Figure 7.3. AAT is coexpressed in transgenic mouse milk. The non-reduced anti-AAT Western blot contains a molecular weight marker (lane 1), 2 μg (lane 2) and 5 μg (lane 3) recombinant AAT, plasma-derived AAT (lane 4), transgenic mouse milk (lane 5), and non-transgenic mouse milk (lane 6). * - denotes putative AAT-serine protease inhibitor covalent complex (SERPIN). The recombinant AAT (lanes 2 and 3) and plasma-derived AAT references (Lane 4) as well as transgenic milk samples (Lane 5) have bands present at about 54 kDa and >100 kDa. The putative AAT- SERPIN complexes indicate that the AAT was biologically active.

Quantitative analysis of rFVIII biological activity

Biochemical analysis of FVIII within the milk of mono-, bi- and trigenic mice is presented in Table 7.2. Chromogenic FVIII activity and antigen as determined by a FVIII-specific ELISA are shown. Milk was collected from F1 and F2 lineages during three different days over a 17 day lactation. Three different F0 bigenic 226/N6-tg/vWF-tg founders all expressed less than 0.02 μg/ml of FVIII by ELISA and so were not chosen for expansion (data not shown).

One stage FVIII (aPTT) and two stage chromogenic activities were measured in each of the expanded lineage specific milk pools. For aPTT coagulation measurements, dilutions of milk of >1:200 were required to minimize nonlinear effects caused by milk calcium and lipid. For those milks having greater than about 1 IU/ml, the aPTT and chromogenic activities were comparable. Table 7.2 shows the highest chromogenic activity and ELISA antigen values over the course of lactation within these milk samples and their respective specific activities. The specific activities of commercial rFVIII ranged from 1100 to 5000 IU/mg. The highest FVIII antigen and FVIII activity levels occurred in the milk of one trigenic lineage (415), at 183 μg/ml and 678 IU/ml respectively, yielding a specific activity of 3,705 IU/mg. In addition, high concentration levels of 226/N6-tg activity and antigen were also measured in three of four 226/N6-tg:AAT-tg bigenic lineages.

Notably, the range of 226/N6-tg specific activities was similar for all mouse milks and expression levels. However, the lowest detectable levels of antigen and activities occurred within monogenic 226/N6-tg mice: <0.15 μg/ml rFVIII antigen and <0.62 IU/ml activity. The maximum and mean specific activity levels present in milk were

between 1,000 and 6,000 IU/mg for 226/N6-tg monogenic, 1,000 and 7,000 IU/mg for bigenic 226/N6-tg:AAT-tg, 3700 and 4500 IU/mg in the trigenic 226/N6-tg:AAT-tg:vWF-tg milks. Thus, the biochemical quality of 226/N6-tg was consistent in the milk over a wide range of throughput by the mammary epithelia.

Immunopurification of rFVIII from trigenic mouse milk pools using an anti-A2 monoclonal immunosorbent (R8B12)[30] resulted in a vWF-tg free product (data not shown). The specific activity was 2838 IU/mg which compared favorably to 226/N6 that was immunopurifed from CHO cells at 2892 IU/mg. Importantly, the specific activity of 226/N6-tg immunopurified from milk was consistent with that measured directly in the trigenic mouse milk. ELISA detection of the binding of this vWF-free 226/N6-tg to plasma-derived vWF (Figure 7.4) indicates that 226/N6-CHO, commercial rFVIII and 226/N6-tg have similar affinity to vWF.

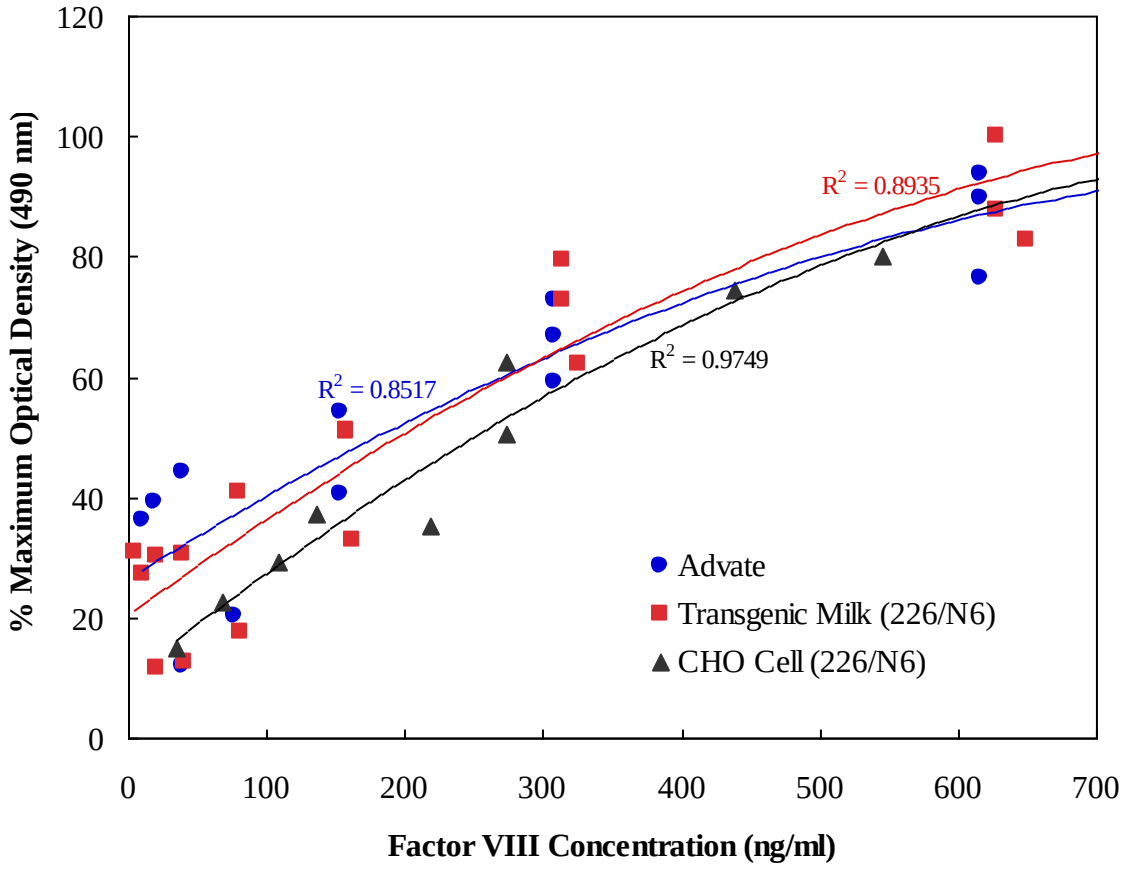

Figure 7.4. 226/N6-tg binds pd-vWF similarly to rFVIII. The relative affinity of plasma-derived vWF for 226/N6-tg immunopurified from milk pools made from highest expressing trigenic mice (415), commercial rFVIII, and 226/N6-CHO immunoaffinity purified protein were compared. Assessment of vWF binding to various FVIII molecules by ELISA: commercial rFVIII (●), 226/N6-tg (■), 226/N6-CHO (▲). Polynomial trend lines are shown for the reference rFVIII (solid line), 226/N6-tg (dashed line), 226/N6-CHO (dotted line) with R^2 values of 0.85, 0.89 and 0.97, respectively. The plasma-derived vWF was found to similarly bind each of the FVIII species over a concentration range that approximates the linear FVIII-vWF binding curve.

In vivo tail clip assay in the hemophilia A mouse

Total blood loss in mg was observed for normal C57/BL mice and FVIII knockout hemophilia A (HA) mice resulting from a terminal tail transection (Figure 7.5). The HA mice were infused with either lactated Ringer's, immunopurified 226/N6-CHO or immunopurified 226/N6-tg. The 226/N6-CHO and 226/N6-tg proteins were each infused at 80 IU/kg body weight. The normal C57/BL mice typically showed a cessation of bleeding (4 of 4) at about 2 to 5 minutes (data not shown) with a total weight of blood

loss over 10 minutes ranging from 80 to 175 mg. The HA mice infused with lactated Ringer's typically did not show a cessation of bleeding (10 of 12) with a total weight of blood loss that ranged from 110 to 700 mg. The HA mice infused with 226/N6-CHO showed a cessation of bleeding (5 of 5) typically at about 2 to 5 minutes with a total weight of blood loss ranging from 50 to 225 mg. The HA mice infused with 226/N6-tg showed a cessation of bleeding (5 of 6) typically at about 2 to 5 minutes with most mice having a total weight of blood loss ranging from 50 to 225 mg. One HA mouse infused with 226/N6-tg showed a total blood loss weight of 500 mg. An analysis of variance indicated that the effect of treatment was significant ($p < 0.001$). Post hoc analysis determined that only saline treated hemophilic A mice were significantly different from control mice treated with saline ($p = 0.002$). An α of 0.05 was used as a significance criterion for all statistics.

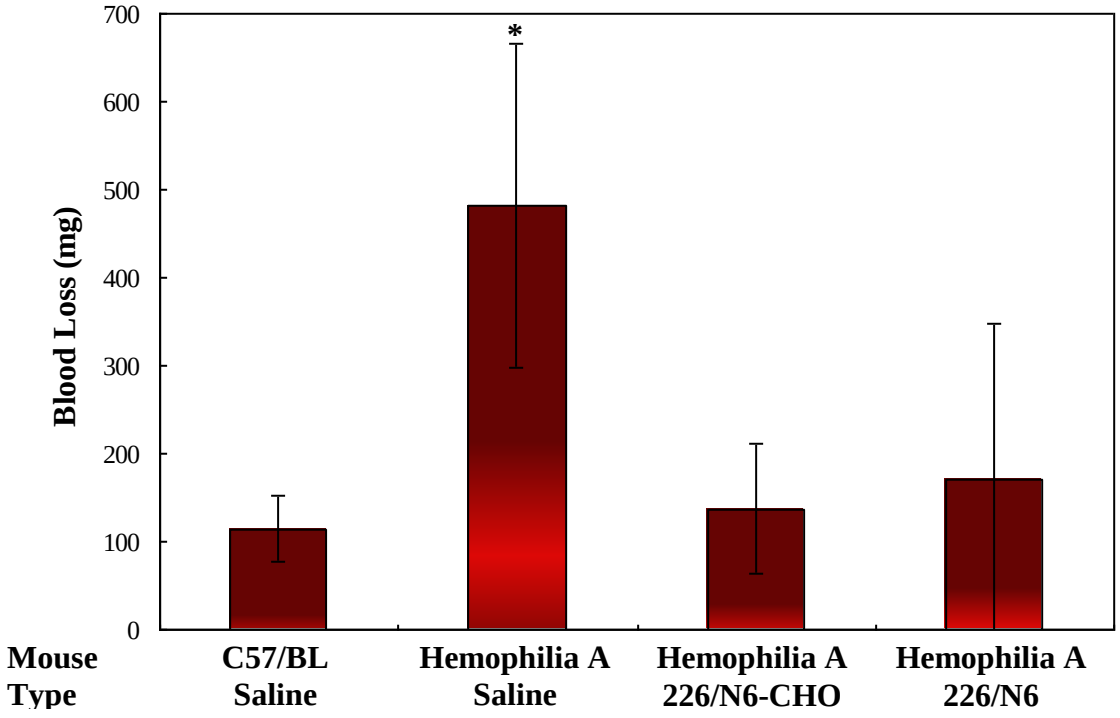

*** p = 0.002 ($\alpha_{0.05}$)**

Figure 7.5. Hemostatic efficacy *in* vivo of 226/N6-tg and 226/N6–CHO within the hemophilia A mouse model. Total blood loss in mg was observed for normal C57/BL mice and FVIII knockout hemophilia A (HA) mice resulting from a terminal tail transection. The HA mice were infused with either lactated Ringer's, immunopurified 226/N6-CHO or immunopurified 226/N6-tg. Bars represent the mean ($n \geq 4$) and the error bars the standard deviation.

Discussion

By expressing rFVIII variant with high secretion efficiency in the milk of transgenic mice, we have generated >450-fold higher levels of FVIII activity over that reported for the animal cell culture expression of WT-FVIII. The highest reported levels of FVIII made in animal cell culture have been those using co-expression of vWF to stabilize the secreted FVIII (Table 7.1). To overcome the previously low expression of FVIII activity in milk, our bioengineering strategy combined the advantages of the high cell density of the mammary gland with high secretory efficiency, single chain stability of 226/N6, the stabilizing complexation of co-expressed vWF, and decreased milk-borne

proteolysis through co-expression of AAT. In addition, the gene design of 226/N6 not only imparted increased transcriptional efficiency but also benefited from decreased transcriptional silencing provided by the co-integration of the highly active BLG-AAT transgene. This is the first proof of principle that biologically active FVIII can be made in milk at similarly high levels to that already demonstrated for other complex coagulation proteins. While this study used mice, where typically only a few milk samples spanning a 17 day lactation can be collected, it was a necessary step used to assess the gross expression levels and general biochemical characteristics of the recombinant protein before attempting to translate these concepts to livestock. Further optimization of mammary expression of 226/N6 such as screening for lineages having still higher expression levels due to more transcriptionally active chromosomal integration sites is best done in a livestock species that is a candidate for commercial production. Thus, the full delineation of our bioengineering effort to stabilize FVIII activity by co-expression of VWF and AAT will be best assessed and realized in the >100 liter per year lactations produced in animals such as pigs.

Our studies show that the single chain structure of 226/N6-tg retains its procoagulant activity in milk where its specific activity is similar to commercial grade, plasma-derived and recombinant FVIII (Table 7.2) in contrast to the proteolytically fragmented, low activity WT-FVIII previously observed in the milk of mice,[16] rabbits,[17, 18] sheep[19] and pigs[20] (Table 7.1). The robustness of 226/N6-tg activity was reflected by the similar specific activities of immunopurified and milk-borne 226/N6-tg as measured by both one and two stage clotting assays. Importantly, the immunopurified 226/N6-tg rendered normal hemostasis to FVIII knockout mice in response to a post-infusion, tail

transection trauma challenge. In contrast to 226/N6, heterodimeric WT-FVIII has proven to be unstable and therefore not suitable for production in milk. Importantly, our work suggests that other FVIII variants that use covalent structure similar to 226/N6 which stabilize the association of heavy and light chains[15, 31, 32] may be appropriate candidates for abundant production in the milk of transgenic livestock.

The co-expression of vWF in cell culture[33] has been shown to stabilize the heavy and light chains of WT-FVIII. Ours is the first report of FVIII co-expressed in milk along with vWF. We have shown that essentially all of 226/N6-tg was strongly associated with vWF-tg. The functionality of these complexes was reflected by the similarly high specific coagulation activity measured by one and two stage assays. This activity indicates that the vWF-tg is released upon thrombin cleavage of 226/N6 to form FVIIIa as occurs in plasma-derived FVIII that is complexed by vWF.[34, 35] In addition, 226/N6-tg was greater than 90% separated from vWF-tg by immunopurification in a similar manner used to purify plasma-derived FVIII from vWF (data not shown). The immunopurified 226/N6-tg was subsequently shown to recombine *in vitro* with plasma-derived vWF in a similar way as WT-FVIII. Importantly, complexation of FVIII with vWF is a prerequisite for stability in circulation after infusion,[9, 29, 36] The highest concentration of 226/N6-tg in milk occurred with the presence of vWF-tg at an estimated 1:1 ratio of 226/N6-tg to vWF-tg subunits. The native binding behavior of the 226/N6-tg with either vWF-tg or vWF indirectly shows that the proper post-translational sulfation of tyrosine 1680 in the A3 domain of 226/N6 likely occurred, as it is required for complexation.[37] The detailed characterization of the post-translational modification of 226/N6-tg such as detection of

sulfation and also its multiple sites of glycosylation will be done on material produced from the milk of transgenic pigs.

While the FVIII activity levels reported here were very high, we believe that still higher levels are possible in livestock. Mammary specific expression in transgenic mice is typically more subject to transcriptional silencing than has been observed in transgenic pigs. Transgene silencing and attenuation of mammary specific expression occurs in >60% of mouse lineages[38] and is thought to be primarily due to random transgene insertion into transcriptionally dormant chromosomal locations.[38] Using the same WAP regulatory elements employed here for 226/N6-tg in mice, our past experiences with the expression of other complex coagulation proteins such as human protein C typically obtained levels of 500 to 1000 μg/ml in mice but 1000 to 5000 μg/ml in pigs. It is noteworthy that the inclusion of the A1-A2 domain needed for FVIII functionality means that some transcriptional limitations will be also inherent as is still present in the bioengineered 226/N6 gene and not associated with the B domain.[12-14] The consistently very low rFVIII levels in monogenic 226/N6 or bigenic vWF:226/N6 mice were likely due to the combination of FVIII transcriptional and chromosomal insertion transgene silencing. It is also noted that co-expression of vWF and WT-FVIII in CHO cells does not result in higher transcriptional efficiency for either protein. In contrast, we believe that the high levels of FVIII and vWF expressed in bigenic 226/N6-AAT and trigenic 226/N6-vWF-AAT mice (Table 7.2) benefited from transcriptional rescue by co-integration of the BLG-AAT minigene. In a prior study, co-integration into the same chromosomal site of the BLG-AAT with a BLG-human Factor IX transgene resulted in increased expression in mouse milk.[39, 40]

The AAT-tg was efficiently made at >1 g/l in the majority of the mouse milks studied here. This is consistent with its previously reported mammary specific expression behavior in mice[16] and sheep.[41, 42] The presence of AAT antigen reactive bands at about 90 to 100 kDa M_r is consistent with the formation of stable, AAT-serine protease complexes reflecting the presence of serine proteases such as plasmin in milk and the SERPIN-biological activity of the milk borne AAT. While it is not known exactly how much protection from proteolysis[36] and or metal chelation[43] was provided to 226/N6-tg, the highest concentration of biological activity occurred in mice having both by AAT-tg and/or vWF-tg. While we used co-microinjection of the three transgenes to make trigenic mice, we will use somatic cell cloning to make trigenic pigs with special attention to the preselection of cell lines having both equal stoichiometric and same site co-integration and therefore more predictable expression efficiency for each of the transgenes. The co-expression of other protease inhibitors more specific to plasmin such as alpha-2 plasmin inhibitor is also another potential extension of this work.

Pigs are the most likely choice of transgenic livestock for future production of FVIII because they combine the advantages of milk volume and hepatocyte-like post-translational biochemistry such as glycosylation [67]. While ruminants also provide ample milk volume, their mammary biochemistry produces higher mannose, low sialic acid glycoforms which may affect circulation residence times due to interactions with asialyo receptors found in the human liver.[67] Pigs have 100 days of lactation and produce 100 to 200 liters of milk per year.[16,17,68] Hence, the number of pigs needed to meet the current global FVIII demand is only about 400 if 226/N6 expression reported here in mice is translated into the milk of sows (Table 7.3).The advantage of pig milk over other FVIII

sources such as cell culture bioreactors and human plasma is evident in the greater than two orders of magnitude reduction in source volume estimated to meet global FVIII demand.[16] In the case when infrastructure must be expanded to increase capacity, the capital investment costs for classical cell culture become significant. In contrast, transgenic production yields high concentration of biopharmaceutical in milk which reduces capital investment because adding additional pigs does not require significant changes in expanding infrastructure.[44] This will become important when developing countries begin routine access to FVIII therapy including that needed for inhibitor patients to facilitate immune tolerance strategies. It is noted that perhaps 25% or more of FVIII used in most developed countries is consumed by inhibitor patients.[45-47]

Table 7.3. Potential volumes of source materials needed for current global FVIII consumption.

Source	Volume of Source Material (liters/year)
Plasma	27,400,000
Production Bioreactor Supernatant	13,700,000
Milk of Transgenic Pig	40,000

Potential volumes of source materials for Factor VIII required to meet the needs for current global consumption.[48] The estimated amount of FVIII in each source: plasma (1 IU/ml); CHO cell bioreactor (2 IU/ml), and transgenic pig milk (678 IU/ml). A 20% purification yield for each source is assumed. The milk of 400 pigs (100 liters/year/pig) could supply the entire amount of FVIII currently needed for global consumption.[48]

The safety and efficacy of transgenic milk derived products has crossed an important threshold as the US FDA and EMEA has approved recombinant anti-thrombin III made in goat milk (ATRYN^{R}). The large scale processing renders the anti-thrombin product to 99.99% purity. The high levels of FVIII biological activity reported here in mouse milk bodes well for the development of transgenic livestock and an accompanying purification process that will provide an abundant, cost effective source of FVIII. This source would help to enable prophylactic intravenous therapy and also the development

of alternative routes of administration including its use in longer lasting replacement product designs. For example, using PEGylation[5] to make longer lasting 226/N6-tg as well as application to non-intravenous methods of delivery by intratracheal[10] or oral[5,11,12] administration will be facilitated by the abundance of FVIII provided by transgenic milk.

Authorship

Contribution: H.Z.M., S.P.B., and J.C. performed experiments, analyzed results and made the figures; S.W.P. and W.H.V. designed the research and wrote the paper. Conflict-of-interest disclosure: The academic institutions of S.W.P. and W.H.V. have licensed recombinant 226/N6 technology (University of Michigan) to Inspiration Biopharmaceuticals and transgenic Factor VIII technology (Virginia Tech) to GTC Biotherapeutics and Progenetics, LLC. Both S.W.P. and W.H.V. have financial interest in Inspiration Biopharmaceuticals. W.H.V. has financial interest in Progenetics, LLC. S.P.B. is an employee of Progenetics, LLC.

Acknowledgements

The authors gratefully acknowledge the Transgenic Animal Model Core of the University of Michigan's Biomedical Research Core Facilities for their contributions to the preparation of the transgenic mice and the Michigan Economic Development Corporation and the Michigan Technology Tri-Corridor for support for this research program (Grant 085P1000815).

References

1. Kasper, C.K. et al. Haemophilia in the 1990s: report of a joint meeting of the World Health Organization and World Federation of Hemophilia. *Vox Sang* **61**, 221-224 (1991).
2. Rosendaal, F.R. & Briet, E. The increasing prevalence of haemophilia. *Thromb Haemost* **63**, 145 (1990).
3. Hoyer, L.W. Hemophilia A. *N Engl J Med* **330**, 38-47 (1994).
4. Pipe, S.W., Saint-Remy, J.-M. & Walsh, C.E. New High-technology Products for the Treatment of Haemophilia. *Haemophilia* **10**, 55-63 (2004).
5. Pipe, S.W., High, K.A., Ohashi, K., Ural, A.U. & Lillicrap, D. Progress in the molecular biology of inherited bleeding disorders. *Haemophilia* **14 Suppl 3**, 130-137 (2008).
6. Jankowski, M.A. et al. Defining 'full-length' recombinant factor VIII: a comparative structural analysis. *Haemophilia* **13**, 30-37 (2007).
7. Manco-Johnson, M.J. et al. Prophylaxis versus episodic treatment to prevent joint disease in boys with severe hemophilia. *N Engl J Med* **357**, 535-544 (2007).
8. Globe, D.R., Curtis, R.G. & Koerper, M.A. Utilization of care in haemophilia: a resource-based method for cost analysis from the Haemophilia Utilization Group Study (HUGS). *Haemophilia* **10 Suppl 1**, 63-70 (2004).
9. Kaufman, R.J., Wasley, L.C. & Dorner, A.J. Synthesis, processing, and secretion of recombinant human factor VIII expressed in mammalian cells. *J. Biol. Chem.* **263**, 6352-6362 (1988).
10. Pipe, S.W. & Kaufman, R.J. Factor VIII C2 domain missense mutations exhibit defective trafficking of biologically functional proteins. *J. Biol. Chem.* **271**, 25671-25676 (1996).
11. Pittman, D.D., Millenson, M., Marquette, K., Bauer, K. & Kaufman, R.J. A2 domain of human recombinant-derived factor VIII is required for procoagulant activity but not for thrombin cleavage. *Blood* **79**, 389-397 (1992).
12. Lynch, C.M., Israel, D.I., Kaufman, R.J. & Miller, A.D. Sequences in the coding region of clotting factor VIII act as dominant inhibitors of RNA accumulation and protein production. *Hum. Gene Ther.* **4**, 259-272 (1993).
13. Koeberl, D.D., Halbert, C.L., Krumm, A. & Miller, A.D. Sequences within the coding regions of clotting factor VIII and CFTR block transcriptional elongation. *Hum. Gene Ther.* **6**, 469-479 (1995).
14. Hoeben, R.C. et al. Expression of the blood-clotting factor-VIII cDNA is repressed by a transcriptional silencer located in its coding region. *Blood* **85**, 2447-2454 (1995).
15. Miao, H.Z. et al. Bioengineering of Coagulation Factor VIII for Improved Secretion. *Blood* **103**, 3412-3419 (2004).
16. Chen, C.-M., Wang, C.-H., Wu, S.-C., Lin, C.-C., Lin, S.-H., Cheng, W. T. K. Temporal and Spatial Expression of Bilogically Active Human Factor VIII in the Milk of Transgenic Mice Driven by Mammary-Specific Bovine Lactalbumin Regulation Sequences. *Transgenic Res.* **11**, 257-268 (2002).

17. Cherenek, P., Ryban, L., Vetr, H., Makarevich, A. V., Uhrin, P., Paleyanda, R. K., Binder, B. R. Expression of Recombinant Human Factor VIII in Milk of Several Generations of Transgenic Rabbits. *Transgenic Res.* **16**, 353-361 (2007).
18. Chrenek, P. et al. Increased transgene integration efficiency upon microinjection of DNA into both pronuclei of rabbit embryos. *Transgenic Res.* **14**, 417-428 (2005).
19. Niemann, H. et al. Expression of Human Blood Clotting Factor VIII in the Mammary Gland of Transgenic Sheep. *Transgenic Res.* **8**, 237-247 (1999).
20. Paleyanda, R.K. et al. Transgenic Pig Produce Functional Human Factor VIII in Milk. *Nat. Biotechnol.* **15**, 971-975 (1997).
21. Morcol, T. et al. The porcine mammary gland as a bioreactor for complex proteins. *Ann. N. Y. Acad. Sci.* **721**, 218-233 (1994).
22. (Baxter Healthcare Corporation, Westlake Village; 2007).
23. Malhotra, J.D. et al. Antioxidants reduce endoplasmic reticulum stress and improve protein secretion. *Proc. Natl. Acad. Sci. U. S. A.* **105**, 18525-18530, S18525/18521-S18525/18510 (2008).
24. Chauhan, M.S. et al. Bovine follicular dynamics, oocyte recovery, and development of oocytes microinjected with a green fluorescent protein construct. *J. Dairy Sci.* **82**, 918-926 (1999).
25. Archibald, A.L., McClenaghan, M., Hornsey, V., Simons, J.P. & Clark, A.J. High-level expression of biologically active human alpha 1-antitrypsin in the milk of transgenic mice. *Proc. Natl. Acad. Sci. U. S. A.* **87**, 5178-5182 (1990).
26. Velander, W.H. et al. Production of biologically active human protein C in the milk of transgenic mice. *Ann. N. Y. Acad. Sci.* **665**, 391-403 (1992).
27. Michnick, D.A., Pittman, D.D., Wise, R.J. & Kaufman, R.J. Identification of individual tyrosine sulfation sites within factor VIII required for optimal activity and efficient thrombin cleavage. *J. Biol. Chem.* **269**, 20095-20102 (1994).
28. Bi, L. et al. Further characterization of factor VIII-deficient mice created by gene targeting: RNA and protein studies. *Blood* **88**, 3446-3450 (1996).
29. Kaufman, R.J. et al. Effect of von Willebrand factor coexpression on the synthesis and secretion of factor VIII in Chinese hamster ovary cells. *Mol. Cell. Biol.* **9**, 1233-1242 (1989).
30. Fay, P.J., Haidaris, P.J. & Smudzin, T.M. Human factor VIIIa subunit structure. Reconstitution of factor VIIIa from the isolated A1/A3-C1-C2 dimer and A2 subunit. *J. Biol. Chem.* **266**, 8957-8962 (1991).
31. Pittman, D.D. et al. Biochemical, Immunological, and In Vivo Functional Characterization of B-Domain - Deleted Factor VIII. *Blood* **81**, 2925-2935 (1993).
32. Gale, A.J. & Pellequer, J.L. An engineered interdomain disulfide bond stabilizes human blood coagulation factor VIIIa. *J. Thromb. Haemostasis* **1**, 1966-1971 (2003).
33. Wise, R.J., Dorner, A.J., Krane, M., Pittman, D.D. & Kaufman, R.J. The Role of von Willebrand Factor Multimers and Propeptide Cleavage in Binding and Stabilization of Factor VIII. *J Biol Chem* **266**, 21948-21955 (1991).
34. Lollar, P., Hill-Eubanks, D.C. & Parker, C.G. Association of the Factor VIII Light Chain with von Willebrand Factor. *J Biol Chem* **263**, 10451-10455 (1988).

35. Hill-Eubanks, D.C., Parker, C.G. & Lollar, P. Differential proteolytic activation of factor VIII-von Willebrand factor complex by thrombin. *Proc. Natl. Acad. Sci. U. S. A.* **86**, 6508-6512 (1989).
36. Weiss, H.J., Sussman, I.I. & Hoyer, L.W. Stabilization of factor VIII in plasma by the von Willebrand factor. Studies on posttransfusion and dissociated factor VIII and in patients with von Willebrand's disease. *J. Clin. Invest.* **60**, 390-404 (1977).
37. Leyte, A. et al. Sulfation of Tyr1680 of human blood coagulation factor VIII is essential for the interaction of factor VIII with von Willebrand factor. *J. Biol. Chem.* **266**, 740-746 (1991).
38. Clark, A.J., Harold, G., Yull, F.E. Mammalian cDNA and Prokaryotic Reporter Sequences Silence Adjacent Transgenes in Transgenic Mice. *The Oxford Journals, Nucleic Acids Research* **25**, 1009-1014 (1997).
39. Clark, A.J., Cowper, A., Wallace, R., Wright, G., Simons, J. P. Rescuing Transgene Expression by Co-Integration. *J Biotechnol.* **10**, 1450-1454 (1992).
40. Yull, F., Binas, B., Harold, G., Wallace, R. & Clark, A.J. Transgene Rescue in the Mammary Gland is Associated with Transcription but does not Require Translation of BLG Transgenes. *Transgenic Res.* **6**, 11-17 (1997).
41. Wright, G. et al. High Level Expression of Active Human Alpha-1-Antitrypsin in the Milk of Transgenic Sheep. *Bio/Technology* **9**, 830-834 (1991).
42. Carver, A.S. et al. Transgenic livestock as bioreactors: stable expression of human alpha-1-antitrypsin by a flock of sheep. *Bio/Technology* **11**, 1263-1270 (1993).
43. Tagliavacca, L., Moon, N., Dunham, W.R. & Kaufman, R.J. Identification and functional requirement of Cu(I) and its ligands within coagulation factor VIII. *J. Biol. Chem.* **272**, 27428-27434 (1997).
44. Echelard, Y., Ziomek, C.A. & Meade, H.M. Production of recombinant therapeutic proteins in the milk of transgenic animals. *BioPharm Int.* **19**, 36-40, 42, 44, 46 (2006).
45. Bohn, R.L. et al. The economic impact of factor VIII inhibitors in patients with haemophilia. *Haemophilia* **10**, 63-68 (2004).
46. Gautier, P. et al. Cost related to replacement therapy during hospitalization in haemophiliacs with or without inhibitors: experience of six French haemophilia centres. *Haemophilia* **8**, 674-679 (2002).
47. Ullman, M. & Hoots, W.K. Assessing the costs for clinical care of patients with high-responding factor VIII and IX inhibitors. *Haemophilia* **12 Suppl 6**, 74-79; discussion 79-80 (2006).
48. Hemophilia, W.F.o. 1-34 (World Federation of Hemophilia, Montreal; 2009).

Chapter 8

Future Works

Citrate activation of prothrombin

Chapter 2 was the first detailed analysis of the sequence of activation of prothrombin by sodium citrate. Activation fragments were identified by N-terminal sequencing. Unfortunately, this research was unable to answer several questions which could be elucidated by the following:

1. *FII activation in the absence of citrate: autocatalytic or reciprocal proenzyme activation*: Long-term incubation of FII results in activation despite inhibition of FXa and FIIa. This proteolysis could be due to either autocatalytic activation, reciprocal proenzyme activation (activation by FX) or by FXa which is autoactivated. Purified plasma-derived material contains trace amounts of other proteins; therefore, it is difficult to completely isolate individual proteins to identify their roles in activation.[1] Consequently, recombinant prothrombin preparations are needed that do not have trace amounts of plasma proteins to test certain hypotheses. Once purified, recombinant FII will be incubated alone and with purified FX to test Teng and Seegers'[2] theory that they coactivate.
2. *Separate bands from citrate activation and analyze more thoroughly*: The primary bands formed after citrate activation appear to be composed of thrombin, α-thrombin and β-thrombin. These bands could be separated by size exclusion chromatography and analyzed to ensure their identities and to determine more accurate activity levels for each thrombin species.

Recombinant factor XIIIa

Chapter 3 characterized rFXIIIa expressed in *Pichia pastoris*. These results indicate that rFXIIIa expressed in yeast closely mimic plasma-derived FXIII and may be a good alternative for therapeutic uses; however, further research will further elucidate the efficacy of rFXIIIa as a therapeutic:

1. *Further evaluation of FXIIIa molecule*: In this chapter, I propose that the rFXIIIa molecule has an equivalent molecular weight as FXIII because of the addition of the His-tag and myc epitope which is removed by incubation with thrombin. These hypotheses could be confirmed by anti-His and/or anti-c-myc epitope immunoblot analysis.
2. *rFXIIIa as an infusion therapy*: pdFXIII is used as an infusion therapy to treat into individuals with FXIII deficiency.[3] Yeast can produce ample amounts of rFXIIIa for use in infusion therapies; however, the feasibility, efficacy, safety and tolerability of rFXIIIa as an infusion therapy must be tested. FXIII can crosslink substrates; however, FXIIIa crosslinks at a faster rate.[4] Infusing the active form may be detrimental and therefore needs to be evaluated.
    a. *rFXIIIa interaction with plasma proteins:* If used as an infusion therapy, rFXIIIa will need to be evaluated with regard to its interactions with the plasma proteins. Deleterious effects with regard to being FXIIIa rather than FXIII will need to be evaluated.
    b. *rFXIIIa ability to bind to fibrin's αC-domain:* Once activated, FXIIIa binds to residues 241 to 476 in the αC-domain of fibrin[5] which brings

fibrin protofibrils into close proximity. This interaction is important for rapid crosslinking thereby creating a strong clot resistant to lysis.

c. *Pharmacokinetics*: The time rFXIIIa lasts in circulation and the rate at which it is utilized, metabolized, and removed needs to be evaluated. Methods used to evaluate the rFXIII expressed in *Saccharomyces cerevisiae* could be mimicked.[6]

d. *Immune response*: This yeast produced protein will need to be evaluated for its immunogenicity. This will need to be tested *in vivo*.

Optimization of a liquid fibrin sealant

Chapter 4 identified the optimal ratio of components for a rLFS and identified FXIIIa as an important factor in clot strength. The clotting kinetics and viscoelastic strength of our optimized LFS was equivalent to those of a commercially available LFS; however, it uses approximately 75% less fibrinogen and thrombin. While these results are promising, more research needs to be performed to better characterize the clot that is formed:

1. *Examine clot structure created by optimal rLFS:* The structure of the matrix produced by a FS is altered by altering concentrations of any of the components or the pH or temperature. Such changes can alter the function and adhesive nature of the FS.[7] In addition, the fiber diameter, porosity, branching and permeability of a clot and fibrin(ogen)'s ability to bind platelets, endothelial cells, smooth muscle cells and other cells play an important role in wound healing.[8] For example, high FIIa concentrations reduce "gelation time" which results in the

production of small fiber diameters and pores.[7] Research also indicates that the rate of clot lysis is related to fiber diameter: thinner fibers lyse at a slower rate than thicker fibers.[9] Fiber diameter of clots created by rFI-based LFS should be compared to those produced by pdFI-based LFS *in vitro*. Mullin et al. incubated FI with FIIa, monitored protofibril formation and fibrinolysis by turbidity, and evaluated fiber size by scanning electron microscopy (SEM).[9] This research optimized the speed and strength of the clot formed by our rLFS; however, we have not yet analyzed the structure of the clot. Microscopy and other techniques can be utilized to determine fibrin fiber thickness.[10]

2. *Identify rheological properties*: The rheological properties of clots created by our rLFS should be evaluated with and without FXIII and compared to other commercial FS as described previously.[11]
3. *Model diffusion effects due to increases in thrombin*: Increasing thrombin can result in reductions in clot strength. This is probably due to an increase in viscosity created by aggregation of fibrin which minimizes the diffusion of FXIII need for crosslinking and creating a strong clot. This effect should be modeled.
4. *Evaluate importance of extra FXIII activity in tissue adhesion:* Marx and Mou[12] found that the native transglutaminase activity in tissue (rat skin) is enough to crosslink fibrin clots created by FS. The same methods described in this study can be used to determine if the significantly greater FXIII activity (approximately 36-fold higher) assists in adhesion to multiple tissues (not just rat skin).

5. *rLFS affects on cell migration and proliferation and wound healing*: In addition to cessation of bleeding, the fibrin clot plays a key role in wound healing by serving as a scaffold for and trapping growth factors and other ingredients necessary for tissue regeneration.[13, 14] The clot binds proteins and extracellular matrix which directly contributes to wound healing[15] and binds fibronectin creating cellular adhesion.[16-18] The fiber diameter, porosity, branching and permeability of a fibrin clot is important for these functions.[8] Fibrinolysis is also controlled by fiber size and by binding plasminogen,[19, 20] tissue plasminogen activator (tPA)[19, 20] and α_2-antiplasmin (A2AP).[19, 21] Interactions with these molecules promote cell migration and encourage tissue regeneration.[13] Several studies can be performed to predict rLFS' effect on wound healing:

    a. *Detailed analysis of clot porosity, fiber branching and permeability of clot:* Compare the porosity, branching and permeability of clots generated by rFI to those created by pdFI so the effect on wound healing can be predicted.

    b. *rFI-based clot retraction*: Test the ability of a rFI-based clot to undergo clot retraction which is necessary for wound healing.[22]

    c. *rLFS interaction with endothelial cells*: Evaluate the ability of endothelial cells to bind to and proliferate and migrate on rFI-based clots. Endothelial cells infiltrate the clot and regenerate vascular tissue;[8] therefore, the ability of these cells to thrive on the recombinant fibrin clot is critical.

***In vivo* testing of rLFS**

Chapter 6 details the efficacy of our rLFS in initial *in vivo* models. Research on specific uses and long-term use must be completed.

1. *Long-term hemostasis, wound healing and LFS degradation*: All of our *in vivo* experiments have been nonsurvival; therefore, the ability of the rLFS with or without the bandage to maintain hemostasis and allow functional tissue regeneration without serious complications is unknown. Kroez, Lang and Dickneite[23] evaluated immune response, wound healing and degradation kinetics of a commercially available FS in a partial liver resection rabbit model. These same methods could be used in our model. The thickness of the FS and tissue regeneration is evaluated by histology. Antibody development to human proteins were measured by ELISA.[23] Survival studies on Grade V liver injuries could be modeled after Holcomb et al.'s methods.[24, 25]
2. *rLFS feasibility, tolerability, efficacy and safety for specific uses:* Commercial LFS' are used in a variety of surgeries including cardiovascular,[7, 26] vascular,[27] thoracic,[28, 29] plastic,[7, 30] reconstructive,[31] oncologic,[32] ophthalmologic,[32] dental,[32] orthopedic,[7, 32] hepatic[33] and urologic surgeries,[34, 35] microsurgical procedures[7] and neurosurgery.[7, 36, 37] We need to determine whether our rLFS can be used successfully under the same circumstances in the pig model.
3. *rLFS as a capable delivery vehicle*: Previous research indicates that LFS' can be used as a delivery vehicle for fibroblasts;[38] however, not all sealants can be utilized in this manner.[39] Determine whether our rLFS can be reliably and

successfully used as a delivery vehicle for fibroblasts and other possible drugs/factors.

4. *Perfect spray delivery device*: It is critical to develop a delivery device that is convenient and easy to use for medical care personnel[7] while applying the optimal amount of each of the FS components. We have had difficulties in fitting off-the-shelf spray devices to our needs. Our primary issue is finding a device that has fine control over flow rates while aerosolizing the solutions. A device needs to be designed that meets all of our needs.

References

1. Seegers, W.H., Mc, C.R.I. & Fahey, J.L. Some properties of purified prothrombin and its activation with sodium citrate. *Blood* **5**, 421-433 (1950).
2. Teng, C.-M. & Seegers, W.H. Activation of factor X and thrombin zymogens in 25% sodium citrate solution. *Thromb.Res.* **22**, 203-212 (1981).
3. Gootenberg, J.E. Factor concentrates for the treatment of factor XIII deficiency. *Curr Opin Hematol* **5**, 372-375 (1998).
4. Siebenlist, K.R., Meh, D.A. & Mosesson, M.W. Protransglutaminase (factor XIII) mediated crosslinking of fibrinogen and fibrin. *Thromb.Haemost.* **86**, 1221-1228 (2001).
5. Procyk, R., Bishop, P.D. & Kudryk, B. Fibrin--recombinant human factor XIII a-subunit association. *Thromb Res* **71**, 127-138 (1993).
6. Ponce, R.A. et al. Preclinical safety and pharmacokinetics of recombinant human factor XIII. *Toxicol.Pathol.* **33**, 495 (2005).
7. Sierra, D.H. Fibrin sealant adhesive systems: a review of their chemistry, material properties and clinical applications. *J.Biomater.Appl.* **7**, 309 (1993).
8. Laurens, N., Koolwijk, P. & De Maat, M.P.M. Fibrin structure and wound healing. *Journal of Thrombosis and Haemostasis* **4**, 932 (2006).
9. Mullin, J.L., Norfolk, S.E., Weisel, J.W. & Lord, S.T. Clot lysis of variant recombinant fibrinogens confirms that fiber diameter is a major determinant of lysis rate. *Ann N Y Acad Sci* **936**, 331-334 (2001).
10. Wolberg, A.S. Thrombin generation and fibrin clot structure. *Blood Rev.* **21**, 131 (2007).
11. Glover, C.J., McIntire, L.V., Brown, C.H., 3rd & Natelson, E.A. Rheological properties of fibrin clots. Effects of fibrinogen concentration, Factor XIII deficiency, and Factor XIII inhibition. *J Lab Clin Med* **86**, 644-656 (1975).
12. Marx, G. & Mou, X. Characterizing fibrin glue performance as modulated by heparin, aprotinin, and factor XIII. *J Lab Clin Med* **140**, 152-160 (2002).
13. Clark, R.A. Fibrin is a many splendored thing. *J Invest Dermatol* **121**, xxi-xxii (2003).
14. Greiling, D. & Clark, R.A. Fibronectin provides a conduit for fibroblast transmigration from collagenous stroma into fibrin clot provisional matrix. *J Cell Sci* **110 (Pt 7)**, 861-870 (1997).
15. Clark, R.A. Fibrin and wound healing. *Ann N Y Acad Sci* **936**, 355-367 (2001).
16. Cheresh, D.A., Berliner, S.A., Vicente, V. & Ruggeri, Z.M. Recognition of distinct adhesive sites on fibrinogen by related integrins on platelets and endothelial cells. *Cell* **58**, 945-953 (1989).
17. Corbett, S.A., Lee, L., Wilson, C.L. & Schwarzbauer, J.E. Covalent cross-linking of fibronectin to fibrin is required for maximal cell adhesion to a fibronectin-fibrin matrix. *J Biol Chem* **272**, 24999-25005 (1997).
18. Corbett, S.A. & Schwarzbauer, J.E. Fibronectin-fibrin cross-linking: a regulator of cell behavior. *Trends Cardiovasc Med* **8**, 357-362 (1998).
19. Collet, J.P. et al. The alphaC domains of fibrinogen affect the structure of the fibrin clot, its physical properties, and its susceptibility to fibrinolysis. *Blood* **106**, 3824-3830 (2005).

20. Tsurupa, G. & Medved, L. Identification and characterization of novel tPA- and plasminogen-binding sites within fibrin(ogen) alpha C-domains. *Biochemistry (N.Y.)* **40**, 801-808 (2001).
21. Sakata, Y. & Aoki, N. Cross-linking of alpha 2-plasmin inhibitor to fibrin by fibrin-stabilizing factor. *J Clin Invest* **65**, 290-297 (1980).
22. Bennett, J.S. & Kolodziej, M.A. Disorders of platelet function. *Dis Mon* **38**, 577-631 (1992).
23. Kroez, M., Lang, W. & Dickneite, G. Wound healing and degradation of the fibrin sealant Beriplast P following partial liver resection in rabbits. *Wound Repair Regen* **13**, 318-323 (2005).
24. Holcomb, J.B. et al. Effect of dry fibrin sealant dressings versus gauze packing on blood loss in grade V liver injuries in resuscitated swine. *J Trauma* **46**, 49-57 (1999).
25. Holcomb, J.B. et al. Dry fibrin sealant dressings reduce blood loss, resuscitation volume, and improve survival in hypothermic coagulopathic swine with grade V liver injuries. *J Trauma* **47**, 233-240; discussion 240-232 (1999).
26. Kjaergard, H.K. & Trumbull, H.R. Bleeding from the sternal marrow can be stopped using vivostat patient-derived fibrin sealant. *Ann Thorac Surg* **69**, 1173-1175 (2000).
27. Taylor, L.M., Jr. et al. Prospective randomized multicenter trial of fibrin sealant versus thrombin-soaked gelatin sponge for suture- or needle-hole bleeding from polytetrafluoroethylene femoral artery grafts. *Journal of vascular surgery official publication, the Society for Vascular Surgery [and] International Society for Cardiovascular Surgery, North American Chapter* **38**, 766-771 (2003).
28. Fabian, T., Federico John, A. & Ponn Ronald, B. Fibrin glue in pulmonary resection: a prospective, randomized, blinded study. *Ann Thorac Surg* **75**, 1587-1592 (2003).
29. Miyamoto, H. et al. Fibrin glue and bioabsorbable felt patch for intraoperative intractable air leaks. *Jpn J Thorac Cardiovasc Surg* **51**, 232-236 (2003).
30. Oliver, D.W., Hamilton, S.A., Figle, A.A., Wood, S.H. & Lamberty, B.G. A prospective, randomized, double-blind trial of the use of fibrin sealant for face lifts. *Plast Reconstr Surg* **108**, 2101-2105, discussion 2106-2107 (2001).
31. Jeschke Marc, G. et al. Development of new reconstructive techniques: use of Integra in combination with fibrin glue and negative-pressure therapy for reconstruction of acute and chronic wounds. *Plast Reconstr Surg* **113**, 525-530 (2004).
32. Spotnitz, W.D. & Prabhu, R. Fibrin sealant tissue adhesive--review and update. *J.Long.Term.Eff.Med.* **15**, 245 (2005).
33. Mankad, P.S. & Codispoti, M. The role of fibrin sealants in hemostasis. *Am.J.Surg.* **182**, 21S (2001).
34. Evans, L.A., Ferguson, K.H., Foley, J.P., Rozanski, T.A. & Morey, A.F. Fibrin Sealant for the Management of Genitourinary Injuries, Fistulas and Surgical Complications. *J. Urol. (Hagerstown, MD, U. S.)* **169**, 1360-1362 (2003).
35. Finley, D.S. et al. Fibrin glue-oxidized cellulose sandwich for laparoscopic wedge resection of small renal lesions. *J. Urol. (Hagerstown, MD, U. S.)* **173**, 1477-1481 (2005).

36. Cappabianca, P. et al. Easy sellar reconstruction in endoscopic endonasal transsphenoidal surgery with polyester-silicone dural substitute and fibrin glue: technical note. *Neurosurgery* **49**, 473-475; discussion 475-476 (2001).
37. Nakamura, H. et al. The effect of autologous fibrin tissue adhesive on postoperative cerebrospinal fluid leak in spinal cord surgery: a randomized controlled trial. *Spine (Phila Pa 1976)* **30**, E347-351 (2005).
38. Horch, R.E., Bannasch, H. & Stark, G.B. Transplantation of cultured autologous keratinocytes in fibrin sealant biomatrix to resurface chronic wounds. *Transplant Proc* **33**, 642-644 (2001).
39. Clark, R.A. Fibrin glue for wound repair: facts and fancy. *Thromb Haemost* **90**, 1003-1006 (2003).